UNIVERSITY OF EDINBURGH

College of Science and Engineering

School of Chemistry

Palladium Chemistry in Chemical Biology

By

Rahimi M. Yusop

Doctor of Philosophy

May 2011

UNIVERSITY OF EDINBURGH

College of Science and Engineering

School of Chemistry

ABSTRACT

PALLADIUM CHEMISTRY IN CHEMICAL BIOLOGY

By

Rahimi M. Yusop

A range of fluorescein derivatives were synthesised via Pd^0-mediated cross-coupling chemistry of the mono triflate of fluorescein with a variety of boronic acids and the optical properties of each dye was studied. Among these derivatives, a new multicolour pH–dependant anthofluorescein which was highly sensitive to pH changes and viscosity changes was identified.

Work was carried out to explore intracellular catalysis based on the immobilisation of Pd^0 nanoparticles on microspheres. The entrapped Pd^0 nanoparticles were rapidly taken up by cells, stay harmlessly within the cytoplasm for days and were shown to carry out novel cell-based chemistry. This included an allylcarbamate cleavage and a Suzuki-Miyaura cross-coupling reaction for the *in situ* generation of a mitochondria-localized "switch-on" fluorophore.

Declaration of Authorship

The research work described in this thesis was carried out under the supervision of Professor Mark Bradley at the University of Edinburgh (February 2008 – May 2011).

No part of this thesis has been previously submitted at this or any other university for any other degree or a professional qualification. Part of this work has been published in the scientific literature and part of it is protected under patent:

Patent:

Novel fluorescein-derived pH sensors (**P16245GB**)

Articles:

"A fluorescein-derived anthocyanidin-inspired pH sensor", Asier Unciti-Broceta, Rahimi M. Yusop, Patricia R. Richardson, Jeffrey G.A. Walton and Mark Bradley. *Tetrahedron Letters* **2009,** 50, (26), 3713-3715.

"Palladium-Mediated Intracellular Chemistry**",** Rahimi M. Yusop, Asier Unciti-Broceta, Emma M. V. Johansson, Rosario M. Sanchez-Martin and Mark Bradley. *Nature Chemistry,* **2011,** 3, (3), 241-245.

"Palladium-Mediated Intracellular Chemistry**",** Rahimi M. Yusop, Asier Unciti-Broceta, Emma M. V. Johansson, Rosario M. Sanchez-Martin and Mark Bradley. *Synform,* **2011/06** (A48).

Signed: ……

Date: ……

Acknowledgements

My utmost gratitude goes to my supervisor, Professor Mark Bradley for his enormous support, opportunities and trust he placed in me throughout my research project in his group.

A big thanks goes to Malaysia Government and my employer, Universiti Kebangsaan Malaysia who were sponsored my study as well as University of Edinburgh for studentship.

A million "thank yous" goes to Dr. Asier who has been inspirational, enthusiastic and widely contributed ideas and proof read this thesis. Many thanks to Dr. Rosario who was very kind and taught me biology from my early day in the group. A special thanks goes to Dr. Emma for her infinite patience and guidance since she was joining the group.

These acknowledgments would not be completed without thanking Dr. Jeff and Dr. Sunay for their fruitful discussion on chemistry, Dr. Patricia for teaching me about fluorescent measurement, Dr. David Kelly who was very helpful during confocal microscopy study and Dr. Kev for *in vivo* study. I particularly thank to Dr. JuanJo, Dr. Salvo, Dr. Adam, Dr. Firdaus, Dr. Nicos, Dr. Rong, Dr. Mazen, Dr. Frank B., Dr. Gouher, Dr. Juanma, Thing, Mei and Martin for great friendship. Of course I have to thank ALL members (past and present) of the Bradley Research Group, who have made this experience so valuable and enjoyable.

I would like to thank my family in Malaysia and Malaysian friends in Edinburgh for their support throughout my study. A very special thanks goes to my beloved wife Norly, for her massive support until the very end of this thesis. Last, but far being least, I would like to give a 'big kisses' to my son Irfan and daughter Arissa for giving me an opportunity to be the happiest daddy in the world!!

Rahimi M. Yusop, 2011

Abbreviations

^{13}C-NMR	Carbon-13 Nuclear Magnetic Resonance
^{1}H-NMR	Proton Nuclear Magnetic Resonance
3D	Three dimensions
δ	Chemical Shift
Φ	Quantum yield
η	Viscosity
∈	Dielectric constant
Ac	Acetyl
Alloc	Allyloxycarbonyl
AM	Acetoxylmethyl
ASTM	American Society of Testing and Materials
BCECF	2′,7′-bis-(2-carboxyethyl)-5-(and-6-)carboxyfluorescein
BCFCF	2′,7′-bis-(2-carboxypropyl)-5-(and-6-)-carboxyfluorescein
BODIPY	Boron-dipyrromethene
C-C	Carbon-carbon
cps	Centipoise
d	Doublet
dd	Double doublet
DCM	Dichloromethane
DilC 18	1,1′-dioctadecyl-3, 3, 3′, 3′- tetramethylindocarbocyanine perchlorate
DMEM	Dubelcco's modified Eagle's medium
DMF	N,N-Dimethylformamide
DMSO	Dimethyl sulfoxide
DNA	Deoxyribonucleic acid
DIPEA	Diisopropylethylamine
EDTA	Ethylenediaminetetraacetic acid
ES	Electrospray
E_x	Emission maximum
E_m	Excitation maximum

FACS	Fluorescence-activated cell sorting
FBS	Fetal bovine serum
FCS	Foetal calf serum
FDP	3,6-fluorescein diphosphatase
FITC	Fluorescein isothiocyanate
GFP	Green Fluorescent Protein
GSH	Glutathione
HBSS	Hank's Buffered Salt solution
HeLa	Helacyton Gartleri (Cervical Tumor Cells from Henrietta Lacks)
Hoechst 33342	(2'-[4-Ethoxyphenyl]-5-[4-methyl-1-piperazinyl]-2,5'-bi-1*H*-benzimidazole trihydrochloride trihydrate)
HPLC	High Performance Liquid Chromatography
Hz	Hertz
ICP-OES	Inductively coupled plasma-atomic emission spectroscopy
J	Coupling Constant
LDR	Low dose radiation
LRMS	Low Resolution Mass Spectrometry
m/z	Mass-to-charge ratio
MeOH	Methanol
MHz	Mega Hertz
mPas	milipascal second
MRI	Magnetic resonance imaging
mRNA	Messenger ribonucleic acid
MS	mass spectrometry
MTT	(3-(4,5-Dimethylthiazol-2-yl)-2,5-diphenyltetrazolium bromide
Mw	Molecular Weight
nm	nanometer
NMR	Nuclear magnetic resonance
OTf	Triflate
PBS	Phosphate Buffered Saline

PdNP	Palladium nanoparticles
PEG	poly(ethylene glycol)
PGM	Platinum Group Metal
PhSH	Thiophenol
PPTase	Phosphatase
Rf	Retention Factor
RNA	Ribonucleic acid
PI	Propidium iodide
ppm	Parts per million
rpm	Revolutions per minute
RPMI	Roswell Park Memorial Institute Medium
s	Singlet
SC	Solid Content
SEM	Scanning Electron Microscopy
TEM	Transmission Electron Microscope
TICT	Twisted intramolecular charge transfer
TLC	Thin layer chromatography
XL-RC Pd	Cross-linked resin captured palladium
XRD	X-ray diffraction

Contents

CHAPTER 1:
INTRODUCTION

1.1 Palladium as a Catalyst

Over recent years, palladium-catalysed coupling reactions have become a key method in organic synthesis, the so-called cross-coupling reaction becoming a very powerful method for the creation of new C-C bonds.[1, 2] Pd-catalyzed cross-couplings are used worldwide on both a laboratory scale as well as in the commercial production[3] of pharmaceuticals[4] and molecules used in the electronics industry.[5] For their work in demonstrating the versatility of the catalyst in synthetic chemistry, Richard F. Heck, Ei-ichi Negishi and Akira Suzuki were awarded the 2010 Nobel Prize in chemistry for the development of ''Palladium-catalyzed cross-couplings in organic synthesis''.[5]

1.2 Palladium and its Applications

Palladium plays an important role in chemical transformations and is a catalyst in the synthesis of a range of molecules.[3, 4, 6] Palladium is often mixed with other platinum group metals ruthenium, rhodium, osmium, iridium, and platinum and has strong catalytic activity for reactions such as hydrogenation, dehydrogenation, oxidation and hydrogenolysis. Palladium catalysts are used for example for the acetoxylation of ethylene to vinyl acetate and in the manufacture of sulfuric acid and methanol. Due to its lower cost, palladium is also used in telecommunication and electric equipment as Pd-based contact materials to replace gold.[7] In addition, Pd has also been widely used to prepare dental filling materials and produce fine jewellery. For many years, automobiles have been equipped with Pd-based catalysts to minimise the emission of carbon monoxide, nitrogen oxides and hydrocarbons from fuel combustion.[8] In biomedical applications, Pd-103 is widely used in permanent low dose radiation (LDR) brachytherapy as a prostate cancer treatment. Palladium emits higher levels of radiation over a shorter period of time than iodine-125.[9, 10]

Meanwhile, Pd(II) complexes are able to intercalate in the double helix of DNA and subsequently kill cancerous cells.[11]

1.3 Problems with Palladium Catalysts

There is no longer doubt that the development of sustainable chemistry will motivate the emergence of efficient processes to solve current environmental issues for generations to come.[12] Limitation of natural resources, reduction of wastes, maximising renewability, and development of environmentally benign reagents are the next challenges for the chemical sciences. Therefore, environmentally benign processes for the recovery of Pd are of high interest.

Recovery of waste Pd is therefore of prime importance. It is generally pointed out that heterogeneous Pd systems have a catalytic activity lower than the homogeneous form while Pd often leaches out from the heterogeneous support contaminating the product and complicating recycling.[13-15] In addition, its use is often complicated by issues surrounding the separation of the palladium and ligands from the desired product while recovery and recycling becomes a major practical and economic issue with respect to large-scale applications.[16] Current techniques include costly and non-ecologically friendly processes, such as pyrometallurgy (processes used in the separation and concentration to enable recovery of valuable metals), solvent extraction and electrochemical recovery.[17]

1.4 Solving the Problem

Many studies have been performed aimed at improving the drawbacks previously described. One promising solution to this problem is the immobilisation of Pd on a solid support.[16, 18] In recent years there have been growing efforts in the area of Pd immobilisation, focusing on the development of insoluble supports to address the concerns of catalyst recovery and reusability.

1.4.1 General Methods

Over the past few years, a number of groups have immobilized a variety of Pd catalysts onto a range of other insoluble supports, most notably polymers. The most generally utilized methods for immobilization are physical adsorption of Pd nanoparticles (PdNPs) onto a solid support. Pd nanoparticles supported on insoluble solids are materials of considerable current interest in fundamental scientific fields as well as in environment-friendly recyclable catalytic applications.[19, 20] Advantages of PdNPs, includes the versatility of Pd as a catalyst and the extremely large surface-to-volume ratio.[2, 21-23] PdNPs so far have been immobilized on a many of solid supports, such as charcoal,[24] clay,[14] metal oxides, including silica,[25, 26] alumina,[27, 28] zeolites,[29] and also polymers.[30] The palladium nanoparticles are also able to be generated by bioabsorption in bacteria.[12]

1.4.2 Modern Methods

Kobayashi demonstrated a technique for immobilising catalysts into polymers in order to address recovery and recycling issues. This was based on physical envelopment by the polymers and also on electronic interactions between the electrons of the aryl rings of polystyrene-based polymers and vacant orbitals onto the catalysts. For example, he developed polymer-supported catalysts such as microencapsulated scandinium trifluoromethanesulfonate ($MCSc(OTf)_3$)[31] and osmium tetraoxide ($MCOsO_4$).[32] This method was successfully applied to immobilising palladium catalysts which were used for allylic substitution and Suzuki cross-coupling reactions.[33] Another success was heterogeneous palladium catalyst generated using polymer incarceration methods based on microencapsulation and cross-linking. The Pd catalyst showed high activity in hydrogenation, carbon−carbon, and carbon−oxygen bond-forming reactions as well as good recovery and reuse.[33, 34] Most recently, this technique was used to developed a polymer-incarcerated bimetallic (Au-Pd) nanoclusters as a catalyst for the sequential oxidation-addition reaction of 1,3-dicarbonyl compounds with allylic alcohols, with good catalytic activity.[35]

Another method was reported by Ley in 2002.[36] Polyurea was believed to be a appropriate encapsulation matrix because of the capability of the urea functionality to ligate and retain metal species such as $Pd(OAc)_2$. An interfacial polymerisation approach was used to encapsulate $Pd(OAc)_2$ and PdNPs in polyurea microcapsules for used in catalysis such as Suzuki cross-coupling,[36, 37] hydrogenolysis epoxide[38] and hydrogenation.[39] In addition, osmium tetroxide has been microencapsulated in a polyurea matrix through an in situ interfacial polymerization approach. This has been used as a catalyst in the dihydroxylation of olefins as well as excellent activity when the catalyst is reused.[40]

Meanwhile, Bradley demonstrated that palladium particles could be permanently immobilised in PS-PEG resins[16,18] using an amide molecular 'band', which minimises palladium particle leaching. These supported catalysts were used to perform Suzuki–Miyaura, Sonogashira–Hagihara and Heck–Mizoroki cross-coupling reactions and were heterogeneous in nature and the materials could be recycled without loss of activity. In this technique, palladium acetate ($Pd(OAc)_2$) was used as a precursor to the Pd^0 catalyst. Soluble $Pd(OAc)_2$ was adsorbed by the support. The cross-linked captured palladium (XLPd) was prepared by treating a mixture of solid support with $Pd(OAc)_2$ in toluene at 80 °C for 10 min and then room temperature for 2 hours to afford brown colored resin-captured. The resin was filtered and then treated with 10% hydrazine hydrate in methanol to give a black resin due to the trapped Pd^0 nanoparticles. Subsequently, the amino groups on the supports were "fixed and tangled" by cross-linking ensuring permanent capture of the PdNPs on the resin with succinyl chloride (**Figure 1.1**).

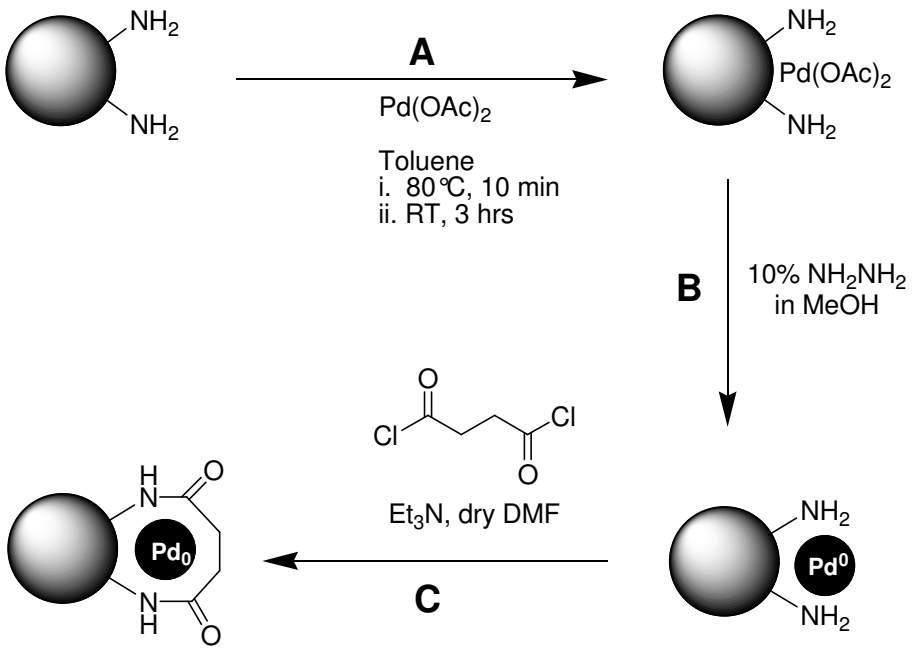

Figure 1.1 *Preparation of entrapped and entanglement Pd^0 nanoparticles. (**A**) TentaGel resin was treated with $Pd(OAc)_2$, (**B**) Hydrazine in methanol was used to reduce Pd^{2+} to Pd^0 and (**C**) subsequently trapped by cross-linking with succinyl chloride.*

1.5 Catalysts: A Brief Clasification

For many years, catalysts have played very important roles to make our lives easier. Catalysts must be able to increase reaction rates by reducing the activation energy and satisfy three criteria; Firstly, the chemical composition of the catalytic agents need to be unchanged upon completion of the reaction, secondly, minimal amounts of catalyst should be enough for the transformation of the reacting substances of course a catalyst cannot affect the final state equilibrium.[41]

There are 2 distinct group of catalyst, homogeneous and heterogeneous (**Figure 1.2**).[41] In heterogeneous catalysis the reactants and the catalyst are in different phases, while homogeneous catalysis the reactants and the catalyst are in same phase.

Enzymes are the representative biocatalysts known to catalyse metabolic reactions in living organisms. The main benefits offered by enzymes are their highl activities (10–10,000 s^{-1}) compared with chemocatalysts (1–10 s^{-1}), selectivity and

greenness as well as lack of cytotoxicity.[42] Chemocatalysts also can be divided into three categories, inorganic, organometallic and organocatalysts. Generally, heterogeneous catalysts are inorganic solids such as metals, metal oxides and metal sulfides, whereas organometallic compounds are widely used in homogeneous catalysis. Organocatalysis includes all metal-free organic catalysts of both low and high molecular weight but are inefficient compared to the enzyme systems.[43] Interestingly, chemocatalysts are becoming more biocompatible by mimicking biocatalysts both in size and mechanism. For example, Brunner synthesised organometallic catalysts that were enlarged by anchoring to dendrimers (dendrizymes)[44] or soluble polymers (chemzymes).[45]

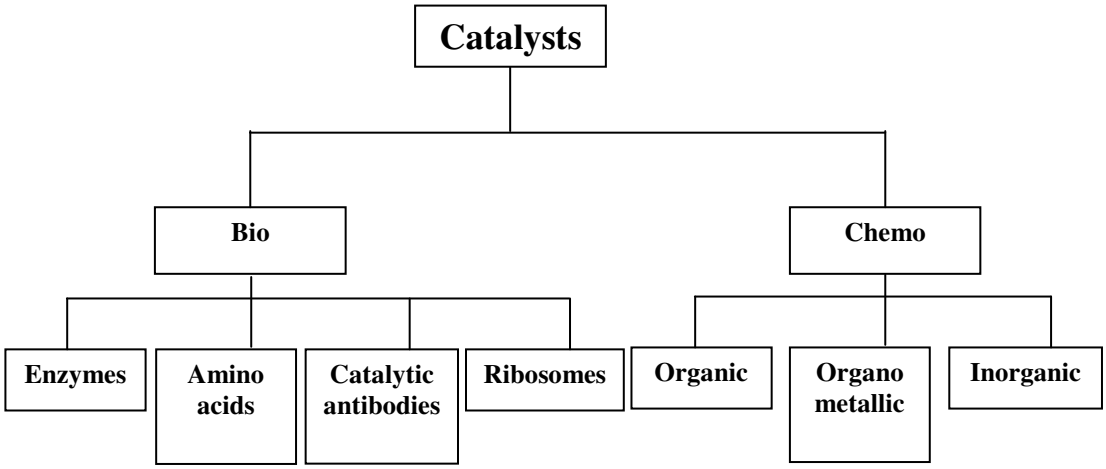

Figure 1.2 *Catalyst families.*[41]

1.6 Transition Metals in Chemical Biology

Transition metals have been used in biological systems because of their remarkable catalytic activity. Cells acquire a range of transition metals (sometime referred as trace elements) and frequently utilize them in proteins, where they can carry out catalytic activity. These are often required cofactors in biological systems, but due to the reactivity they can also be cytotoxic reactions even at low concentrations.[46, 47] Many important transformations in living systems rely on transition metals.[48]

Transition metals ions such as zinc, copper, iron are essential for many biological processes.[49, 50] For example, zinc is the second most abundant metal in the

human body (2-3g) with its highest concentrations occuring in the brain. Zinc is required in numerous metallo-enzymes which are involved in metabolism, maintain the immune system that protects the body against disease, as well as to support normal growth and development during pregnancy, childhood, and adolescence.[50, 51] Other transition metal such as iron and copper, which can exist in multiple oxidation states are very important for the cascades of electron transfer reactions that are characteristic of cellular processes. In fact, it is the answer to oxygen transportation, photosynthesis, nitrogen fixation, and respiration in most organisms.[46, 51-53] Small alterations in iron concentration have been implicated in many diseases including microbial infections, cancer and neurodegenerative disorders.[51]

However, much still remains to be revealed about the importance of metal ions in biological systems.[49] Recently, developments in small-molecule fluorescent probes for metal ions detection in living cells have been reported in order to understand the role of metal ions in living system including zinc,[54] copper,[55] iron and heavy metals (mercury, lead and cadmium).[51]

1.7 Fluorescence: A Brief History

The first fluorescent molecule reported was the natural product quinine, an important chemical for medical and organic chemistry (**Figure 1.3**).[56] Stokes explained how quinine was capable of absorbing energy from external sources and then emitting the light (emission). He introduced the term "fluorescence" to describe this phenomenon.[57]

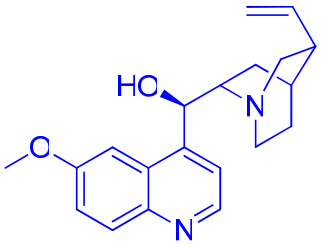

Figure 1.3 *Structure of quinine.*

The well-known xanthene dye fluorescein (**1**) was first reported by Baeyer in 1871, and its remains one of the most broadly utilized probes in modern biochemical, biological, and medicinal research.[58, 59] It was prepared from phthalic anhydride and resorcinol in the presence of zinc chloride via a Friedel-Crafts reaction (**Scheme 1.1**).

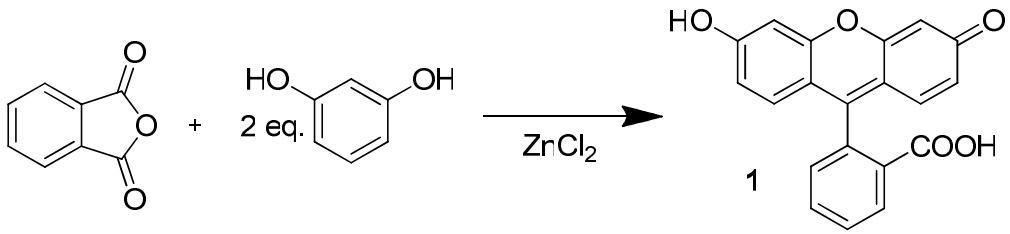

Scheme 1.1 *The preparation of fluorescein (**1**) by the condensation of resorcinol with phthalic anhydride catalyzed with zinc chloride.*

1.8 Fluorescence

The fluorescence phenomenon was first described in 1852.[57] Fluorescent molecules can be excited, by absorption of light and electron excitation to a higher energy state (excited state) (**Figure 1.4**). The energy of the excited state, which cannot be maintained for long, subsequently "decays" or decreases resulting in the emission of light energy. This process is called fluorescence.

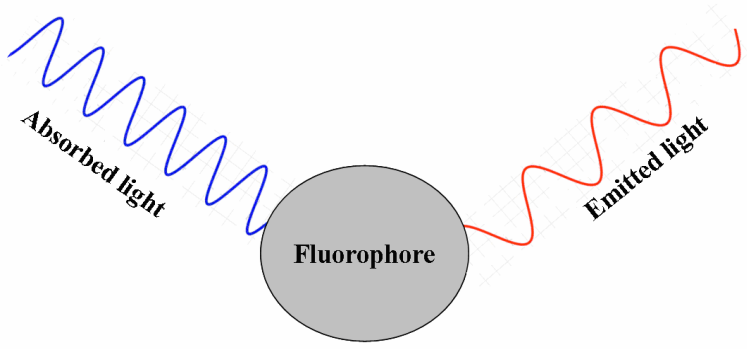

Figure 1.4 *Fluorophore molecules capable to absorb and emit energy as visible light.*

A fluorophore is a molecule that is able to fluorescence. This process can be explained by the Jablonski diagram in **Figure 1.5**. In its ground state level, the fluorophore molecules are in a low-energy, stable configuration. When a fluorophore

absorbs light energy, it is usually excited to a higher vibrational energy level in the highest excited state (**1**). At this point, the fluorophore is now in an unstable state (high energy), rapidly relaxing to the lowest energy level (lowest excited state) which is semi-stable state (**2**). Transition from the upper to lower excited state is termed vibrational relaxation and occurs in about a picosecond or less. Next, the fluorophore molecule rearranges from the lowest-excited state back to the ground state (more stable), consequently the excess energy is released and emitted as light (**3**). The emitted light has lower energy (longer wavelength) compared with the energy absorbed. The fluorophore which was in a ground state can absorb light energy again and go through the entire process repeatedly.

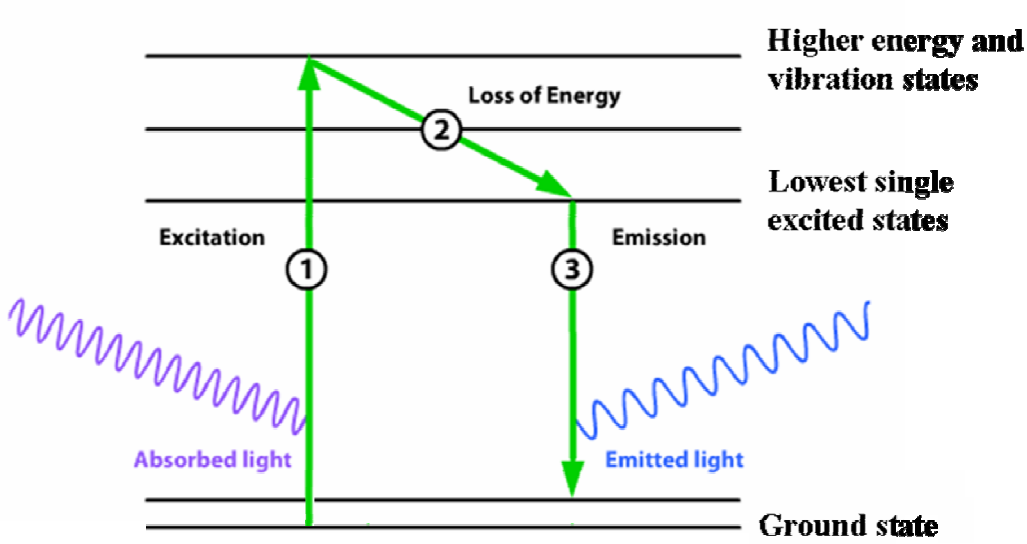

Figure 1.5 *The Jablonski diagram: (**1**) Excitation of a fluorophore through the absorption of light. (**2**) A short-lived excited lifetime undergoes vibrational energy loss with a little loss of energy. (**3**) The fluorophore reverts back to its ground state, and emits visible light. The light emitted is always of a longer wavelength (low energy) than the light energy absorbed, because energy is lost in the transient excited state lifetime in Step (**2**).*

Nowadays, fluorescence is used by many scientists in many disciplines. In fact, modern fluorescence is now a dominant methodology used in biotechnology, medical diagnostics, DNA sequencing, forensics, and genetic analysis.[60] Some dyes which are commercially used are shown in **Figure 1.6**.

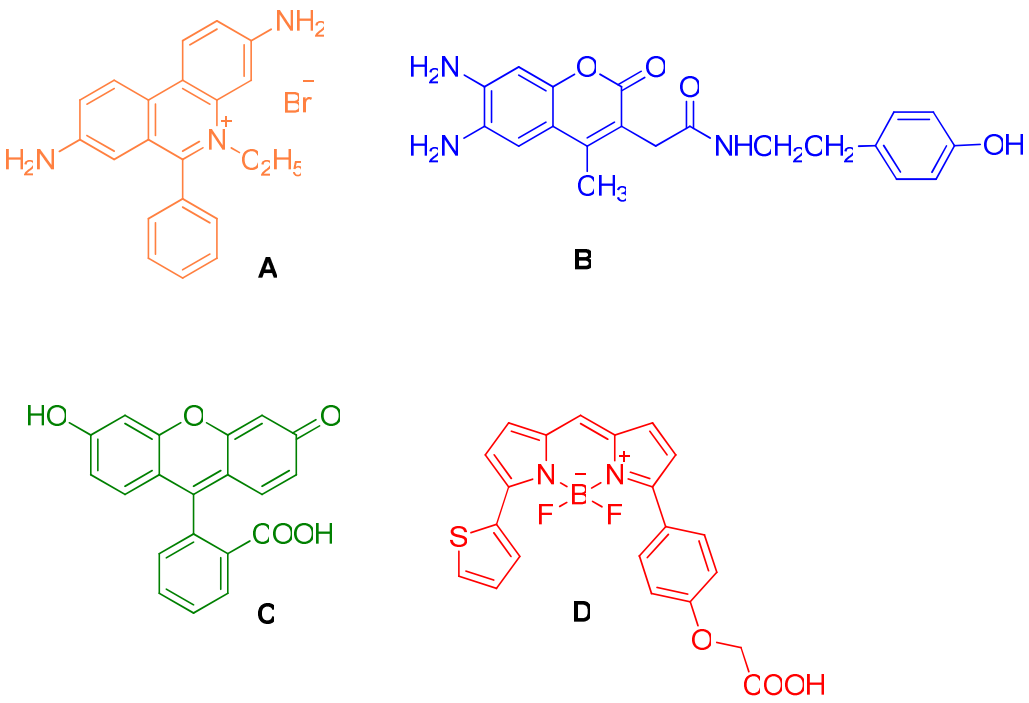

Figure 1.6 *Examples of some widely used fluorescent dyes (**A**) ethidium bromide, (**B**) Alexa Fluor dyes, (**C**) fluorescein and (**D**) BODIPY.*

1.9 Fluorescence and a few Applications

Fluorescence is powerful method currently available for observation of dynamic intracellular processes in living cells.[61] This methods allows high sensitivity and great versatility while minimally perturbing cell function.[62]

Fluorescence-based methods also include assays for biomolecules, metabolic enzymes, DNA sequencing, research into biomolecule dynamics, cell signalling and adaptation, and fluorescence *in situ* hybridisation to identify specific DNA and/or RNA sequences in tissues.[63, 64] Green fluorescent protein (GFP) is the most popular tagging agent for cellular imaging.[64-66] GFP was first isolated from the jellyfish *Aequorea victoria* and widely used as a reporter for gene expression and as a marker for biomolecules.[62, 64, 65, 67, 68] GFP is genetically encoded and requires no cofactors, and can be applied to analyze protein expression and localization in living systems. In addition, one advantage of fluorescent proteins is that they can be targeted to specific organelles such as the cytosol, nucleus, mitochondria, trans-Golgi, and

endoplasmic reticulum by expressing them in conjugation with appropriate targeting peptides or proteins.[69] Disadvantages of using GFP are that it requires significant amounts of work to express these proteins and the range of fluorescence wavelengths available is limited.[70] In the case of GFP, these relatively large proteins can perturb the protein structure and may influence the expression, localization or function of the protein to which they are attached.

1.9.1 Advantages

Over the years, fluorescein along with microscopy instrumentation has frequently been used in cell biology to measure important biochemical species or monitor biochemical pathways in living cells, tissues and organisms.[67, 71] A wide variety of fluorescein derivatives have been prepared and used as fluorescent derivatisation reagents. For example (**Figure 1.7**), 5(6)-carboxyfluorescein (**B**), 5(6)-carboxyfluorescein succinimidyl ester (**C**), 5-iodoacetamidofluorescein (**D**), and fluorescein isothiocyanate (**E**), which make them particularly suitable for biological evaluation in which fluorescein is covalently attached to molecules such as peptides, proteins antibodies, nucleotides, oligonucleotides, drugs, hormones, lipids, and other biomolecules.[72]

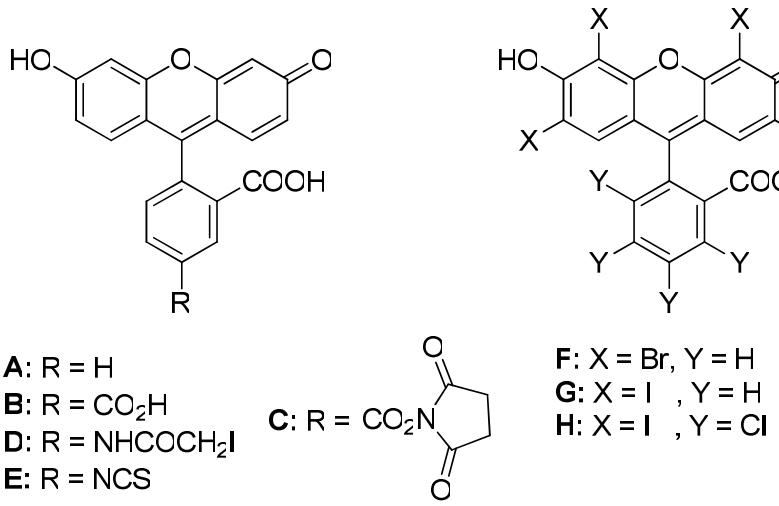

Figure 1.7 *Fluorescein derivatives.*

1.9.2 Challenges with Fluorescein

The application of fluorescence techniques to living specimens presents many challenges. For example, the fluorescence of fluorescein is pH dependant (between 5 and 8.5), and its maximum intensity occurs at a pH > 8.5. Moreover, many fluorescein conjugates are unstable with respect to the illumination produced in most fluorescence instrumentation.[72] The result is irreversible photobleaching, which typically results in a rapid decrease in the fluorescence. In aqueous solution (**Figure 1.8**) it can exist in cationic (**I**), neutral (**A**), anionic (**J**), and dianionic (**K**) forms, making its absorption and fluorescence properties strongly pH dependent. The p*K*a of fluorescein (**A**) in water is approximately 6.4; at the physiological pH range a considerable population of fluorescein is in the protonated, nonfluorescent form **L** and **M**.

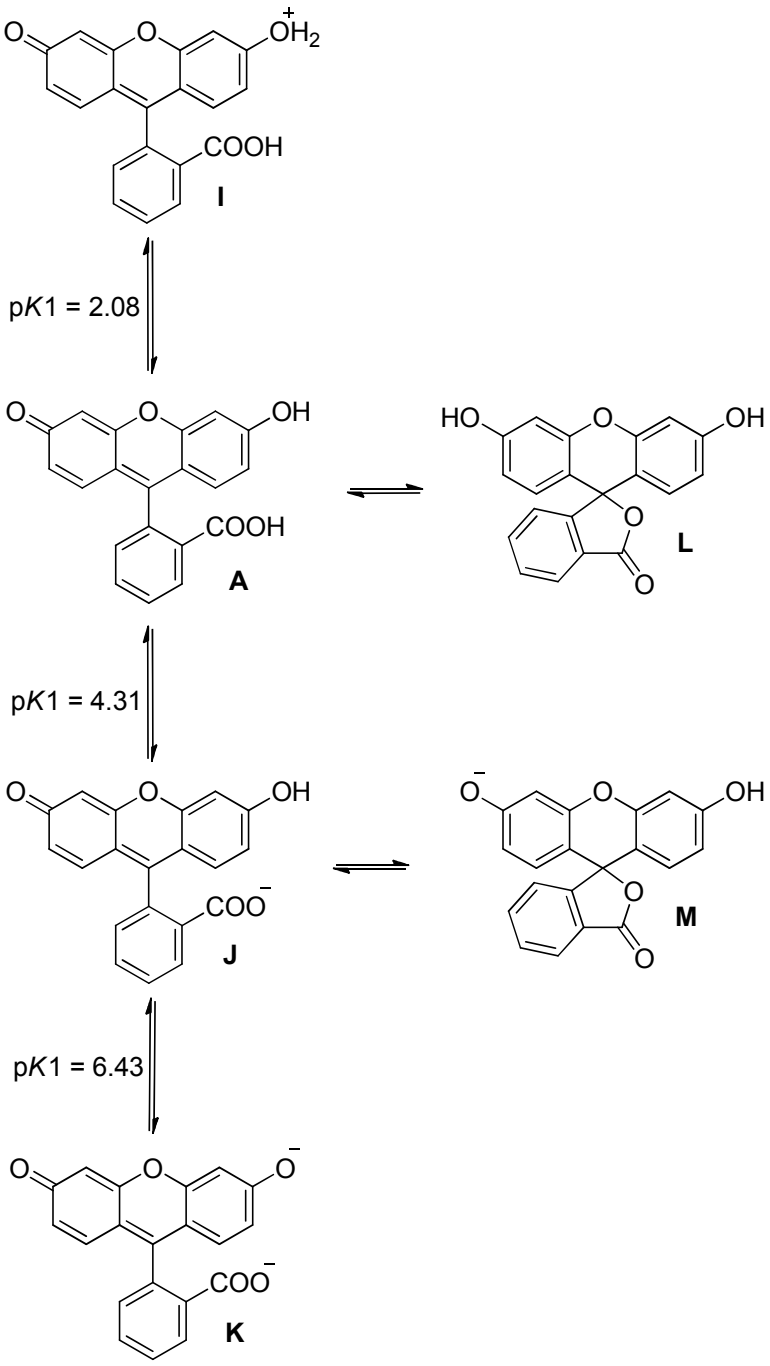

Figure 1.8 *pH dependence of fluorescein equilibria.*[72]

1.10 Aim of the Thesis

The goal of this thesis was to explore the use of Pd(0) catalysis in the generation of fluorophores. This included using Pd^0 to perform intracellular catalysis. Heterogeneous catalysts were chosen due to their stability and non-toxic nature. Pd^0-mediated intracellular chemistry was initiated with deprotection chemistry before moving to a challenging reaction, the formation of a C-C bond. This also involved the design of a new switch-on profile fluorophore used for quantification of catalytic activity. This effort initiates a new approach to the use of transition-metal catalysis as a tool for biological chemistry.

Another objective was to use Pd(0) catalysis to functionalise fluorescein by Suzuki cross-coupling in order to enhance its optical properties. A library of fluorescein analogues was generated and studied. Among these derivatives, it was hoped there would be a new dye useful for particular studies in chemical biology.

CHAPTER 2:
BREAKING OUT FROM THE FLUORESCEIN STRUCTURE

This chapter is divided into two sub-chapters:

A. A fluorescein-inspired Anthocyanidin pH Sensor[73]

B. Synthesis of Novel Anthofluorescein Derivatives: Study of the Influence of Conjugation Expanders on the Fluorescent Properties

2.1 Background and Significance

Fluorescent moieties are of tremendous value as probes in cell biology due to their fast- response, high sensitivity, and the ability to afford good spatial resolution through microscopic imaging.[61] Fluorescein is one of the most commonly used labels in biological assays because of its ready availability, solubility in aqueous buffers, high fluorescence quantum yield, stability and because variants, such as carboxyfluorescein allow ease of conjugation of target molecules.[59, 61] Additionally its excitation maximum (488nm) matches the argon-ion laser.[61]

Many of the typical cellular fluorescent probes for pH measurements are based on fluorescein and its derivatives since fluorescein exhibits multiple pH-dependent equilibria. Many fluorescein-based pH probes have been generated including fluorescein-derivatised polythiophene, fluorescein sulfonic acids and seminaphthofluorescein derivatives.

Significantly, fluorescein remains one of the most broadly utilized fluorophores in modern biochemical, biological, and medicinal research. Due to the particular needs of each and every study, fluorescent dyes and probes with a myriad of defined optical, chemical, and biological properties are in high demand. In order to fulfil the needs in biology, chemistry and materials science, scientists have

recently created numerous fluorescent probes and sensors for *in vitro* and *in vivo* studies such as imaging in cell biology,[67] including sensors for studying intracellular pH,[70] fluorescent sensors for study intracellular viscosity[74] and fluorescent sensors for studying the cell biology of metals.[51, 75]

2.2 pH Sensors

Great effort has been focused on the development of fluorescent pH chemosensors.[76-80] Hence, specific attention has been paid to the synthesis of highly sensitive indicators within the physiological pH range.[81, 82] In this area fluorescein and its derivatives are perhaps the most widely used fluorescent pH probes due in part to their excellent spectral and physical properties and their ease of modification.[83, 84]

2.2.1 Intracellular pH

Cells need to maintain their physiological pH in a controlled manner in order to continue viable cellular functions.[70] Small changes in pH affect many different types of cellular behaviours.[85] Intracellular pH[86, 87] plays very important roles in cellular, enzymatic, tissue activity, in proliferation and apoptosis,[88, 89] ion transport[90-92] endocytosis[88] and muscle contraction.[93] Monitoring pH changes inside living cells is important for investigating cellular internalization pathways, such as phagocytosis and endocytosis.[94] Abnormal pH is often associated with cellular dysfunction and is observed in diseases such as cancer[95, 96] and Alzheimer's.[97] However our understanding of how these changes affects physiological systems is limited. To address this issue, groups have begun to analyse the interactions between cell function and pH.[70]

2.2.2 Fluorescent pH Indicators

Compared to other methods such as absorbance spectroscopy, microelectrodes and NMR, fluorescence cellular analysis has many positive attributes in allowing the measurement of cellular pH changes. Moreover, it has high sensitivity, while the probes are easy to handle and importantly are non-cytotoxic.[70] Measurements of pH

qualitatively can be attained by using fluorescent probes that switch on or off at spectra pH ranges. However, such measurements can be influenced by numerous factors, including temperature and even excitation intensities. This problem can be resolved by the use of "ratiometric analysis", a method that uses fluorescent sensors that can be analysed at two distinct wavelengths often dynamically.[70, 98, 99]

The main benefit when using ratiometric methods is accuracy because they are not influenced by parameters such as local probe concentration, optical path length and leakage from the cells, since both signals come from the same environment.[70]

2.2.3 Fluorescein-Based pH Sensors

Tsien first introduced 2′,7′-bis-(2-carboxyethyl)-5-(and-6-)carboxyfluorescein (known as BCECF) which is the most widely used pH indicator for measuring cytoplasmic pH (**Figure 2.1**).[100]

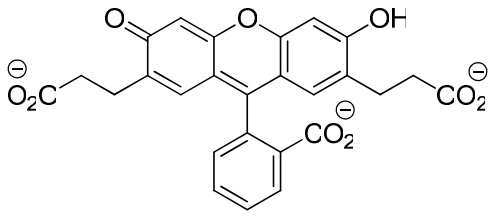

Figure 2.1 *BCECF, Φ=0.84 (0.1 M NaOH),* $\lambda_{max\ abs}$ *503nm,* $\lambda_{max\ em}$ *525nm.*

Since then it has been widely used in mammalian cells,[101, 102] living tissues,[103] and individual organelles,[104] such as the endoplasmic reticulum.[101] Like fluorescein, carboxyfluorescein, and fluorescein sulfonic acid, the absorbance of BCECF is sensitive to the pH changes but in the case of BCECF especially from pH 3.6 to 9.2.[105]

A homolog of BCECF named 2′,7′-bis-(2-carboxypropyl)-5-(and-6-)-carboxyfluorescein (BCPCF) has been synthesised (**Figure 2.2**) which has 2-

carboxypropyl substituents at the 2′- and 7′-xanthene positions. BCPCF has better excitation-ratiometric pH properties than BCECF.[106]

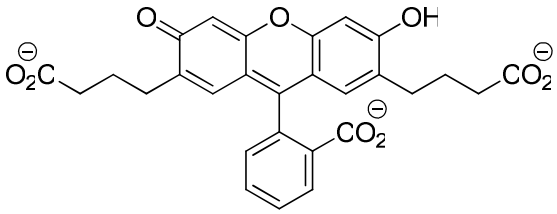

Figure 2.2 *BCPCF, Φ=0.83 (0.1 M NaOH), $\lambda_{max\ abs}$ 505nm, $\lambda_{max\ em}$ 527nm.*

Although BCECF and BCPCF are favoured for intracellular pH measurements, fluorescein sulfonic acid, and particularly carboxyfluorescein (**Figure 2.3**) are still widely used for pH studies because they are inexpensive to synthesise on a large scale.[107]

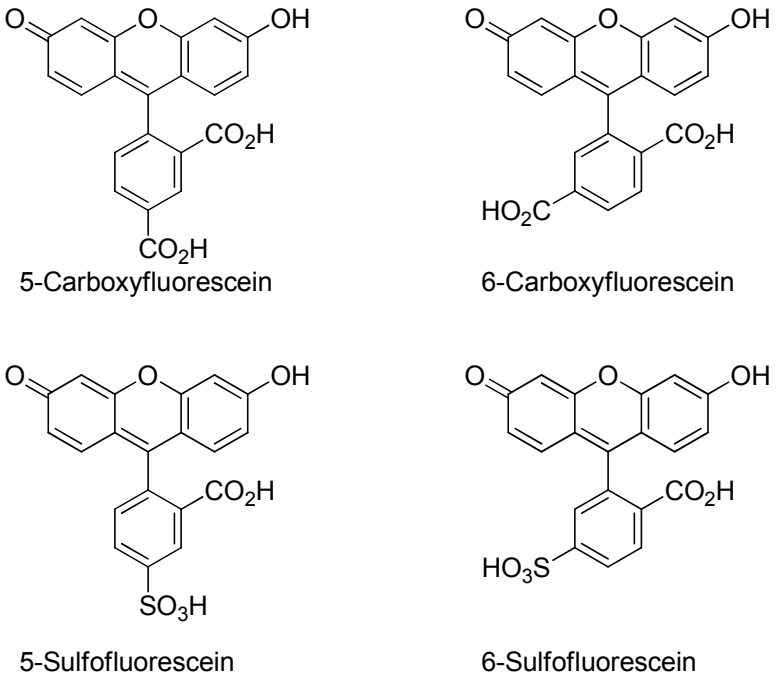

Figure 2.3 *Structure of fluorescein derivatives such as fluorescein sulfonic acid and carboxyfluorescein that have been used for pH cellular studies.*[70]

Another probe used for measuring pH values is fluorescein diacetate (**Figure 2.4**). This liberates fluorescein via cellular hydrolysis but since it leaches out from

the cells, it is difficult to determine if fluorescence intensity decreases are due to leakage, lack of acetate hydrolysis or pH changes.[108]

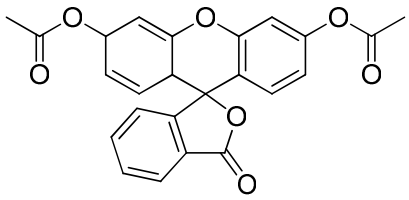

Figure 2.4 *Structure of fluorescein diacetate.*

To address the leaking problem the more highly charged derivatives, 5- and 6-carboxyfluorescein are preferred (**Figure 2.5**).

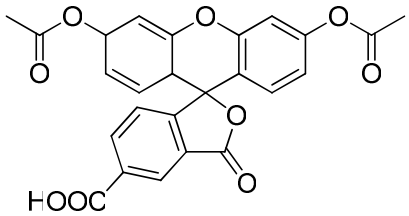

Figure 2.5 *Structure of 5-carboxyfluorescein diacetate.*

The 5- and 6-sulfofluoresceins (**Figure 2.3**) are even more water-soluble and even better retained inside cells compared with carboxyfluorescein. Unfortunately, these sulfonic acid derivatives are not favourable as intracellular pH indicators since their diacetate forms hardly diffuse into cells.[100] Some other fluorescein derivatives such as dimethylcarboxyfluorescein can be used as intracellular pH indicators, but many of these are not photostable or well retained in living cells.[109]

2.3 Viscosity Sensors

2.3.1 Conventional Viscometer

Viscosity is usually measured on a large volume of a fluid. The most typical instruments are a falling- ball viscometer but cone-and-plate viscometers are also available. In all cases these mechanical methods require relatively large amounts of fluid.[110]

2.3.2 Fluorescent Viscosity Sensors

In order to study intracellular viscosity, accurate measurements of viscosity and in particular real-time measurements of viscosity changes on a microscopic scale require of the development of methods that are appropriate at the molecular level.[111]

This has been accomplished through the use of molecular rotors. Molecular rotors are a group of fluorescent molecules that were characterized in the 1970s to 1980s.[112] Their most important property is that the molecule has two modes of relaxation either by photon emission (fluorescence) or by intermolecular rotation which will decrease fluorescent intensity due to the loss of energy. The rotation can be reduced if the molecule is in a highly viscous solvent. Consequently, the quantum yield and fluorescent intensity of the fluorophore is related to the viscosity of the fluid. Haidekker has shown that increased viscosity leads to increased quantum yield and therefore increases in fluorescence intensity.[113]

For many years molecular rotors have been successfully used as viscosity probes in polymerization processes,[114] phospholipid bilayers,[115] and also as probes for cell membranes.[116] Molecular rotors have been used in cell mechanotransduction research for observing changes in the fluidity of the cell membrane and shown good potential as fluorescent probes in biological studies.[113]

2.4 Molecular Strategies of Modifying Fluorescence

The fluorescein structure can be divided into two parts, the benzene and the xanthene moiety (**Figure 2.6**). In 2005 Urano reported that the carboxylic group actually is not important for the fluorescent properties of fluorescein, its just keeps the benzene and xanthane moieties orthogonal to each other[117] because there are no groundstate interaction between these moieties. In other words, modification of the benzene moiety will not be able to enhance the optical properties of fluorescein. Thus modification on xanthane moiety is favourable.

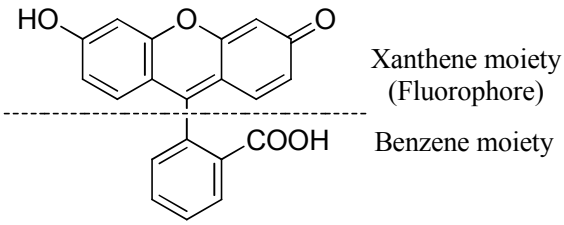

Figure 2.6 *The fluorescein structure divided into two parts, the aryl moiety and the fluorophore.*

Modification strategies have comprised extension of double-bond conjugation and decoration with additional rings, electron donating/withdrawing or charged substituents such as sulfonates.[118, 119] A range of fluorescein derivatives have been synthesized that utilize the electron-withdrawing groups on xanthenes such as chlorine[120, 121] or fluorine[122] substituents to shift the phenolic p*K*a to a lower value.[123] On the other hand, installation of an electron-donating group such as an alkyl group ortho to the phenol groups increases their p*Ka*. Acylation or alkylation of the phenolic groups of fluorescence forces this platform to adopt a closed, colorless and nonfluorecent lactone ring and serves as the basis for a variety of fluorogenic substrates for phosphatases, glycosylases, esterases, and other enzymes.[124, 125] For example, 3,6-fluorescein diphosphate (FDP) has been widely used for monitoring phosphatase (PTPase) activity (**Scheme 2.1**), the hydrolysis of the two phosphate by a PTPase leads to the formation of fluorescein.[124, 126]

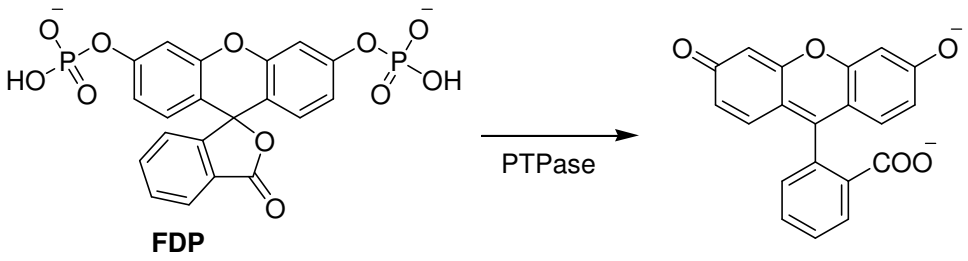

FDP

Scheme 2.1 *PTPase-catalysed hydrolysis of FDP.*

2.5 Aim of the Research

Encouraged by the vast opportunities and demand for fluorescein-based sensors, research was carried out to synthesize a range of fluorescein derivatives. The modifications were designed to utilize palladium catalysis with Suzuki cross-coupling chemistry. Fluorescein derivatives were screened, characterized and their spectroscopic properties studied. This straightforward modification via a simple reaction would contribute to a flexible method for fluorescence probe synthesis.

2.6 A fluorescein- inspired Anthocyanidin- pH Sensor[73]

2.6.1 Introduction

Anthocyanidins are the chromophores of a well-known family of natural dyes and are characterized by their broad spectral window, which is controlled by the various substituents on the benzopyrylium core and pH.[127] Inspired by the general structures of the anthocyanidins (**Figure 2.7**), work focused on the modification of fluorescein via substitution of one of its phenolic groups with *p*-hydroxyphenyl, a feature found in many anthocyanidins.[127]

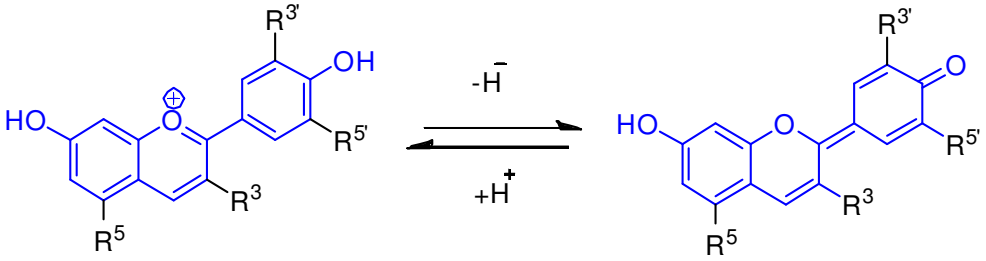

Figure 2.7 *General structures of anthocyanidins.*

This simple modification consisted of two reactions, triflation and Suzuki cross-coupling. The first step introduced the triflate group via microwave-assisted mono-triflation (**2**) of fluorescein (**1**) using one equivalent of phenylbis(trifluoromethanesulfonimide)[128] (a mild triflation reagent) (**Scheme 2.2**). This triflate protected fluorescein had reduced fluorescent properties (background) due to the less effective electron conjugation on the fluorophore.[73]

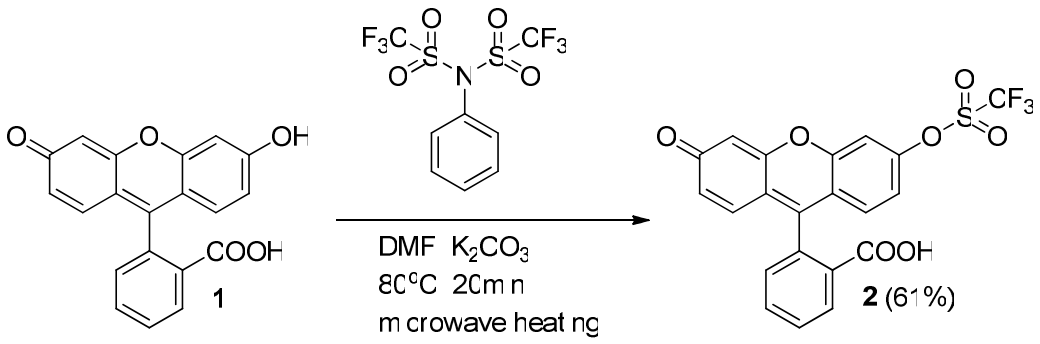

Scheme 2.2 *Synthesis of fluorescein mono-triflate* ***2****.*[73]

The second step was a Suzuki reaction between the fluorescein mono-triflate (**2**) and a boronic acid. The palladium-catalyzed cross-coupling of aryl halides (or triflates) with boronic acids is one of the most versatile and commonly utilized reactions for the construction of carbon-carbon bonds, in particular for the formation of biaryls.[129, 130] In this case, *p*-hydroxyphenylboronic acid was selected to be coupled with fluorescein mono-triflate (**2**). Suzuki aryl palladium-catalyzed cross-coupling of fluorescein mono-triflate with *p*-hydroxyphenylboronic acid give the fluorescein derivative (**Scheme 2.3**). The product, named anthofluorescein (**3**) was expected to have an extra electron conjugation due to the additional aryl ring.

Heterogeneous catalysis using polystyrene resin captured palladium (XL-RC Pd)[16] or palladium acetate ($Pd(OAc)_2$) were used for this reaction and gave yields of **3** of 41% and 78%, respectively.[127, 131]

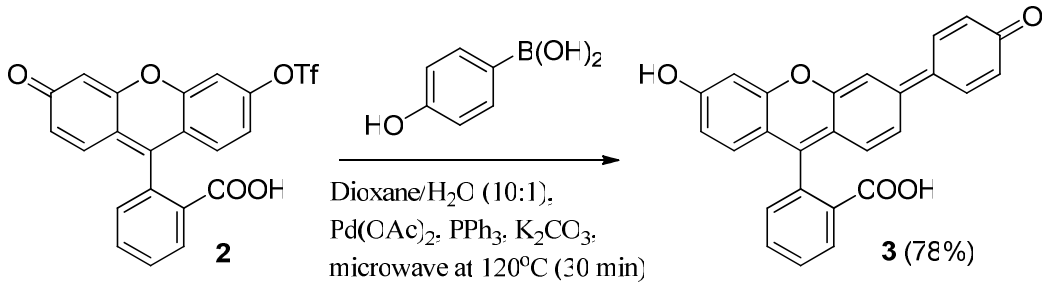

Scheme 2.3 *Suzuki cross-coupling between fluorescein mono-triflate,* ***2****, and p-hydroxyphenylboronic acid to give anthofluorescein,* ***3****.*[73]

2.6.2 Optical Properties of Anthofluorescein (3)

2.6.2.1 pH dependence

The solution of 50 μM anthofluorescein was placed in different buffers (pH 1-13). This simple experiment clearly shows that anthofluorescein has distinct optical properties from pH 7 to pH 13 turning from yellow to red (**Figure 2.8**).

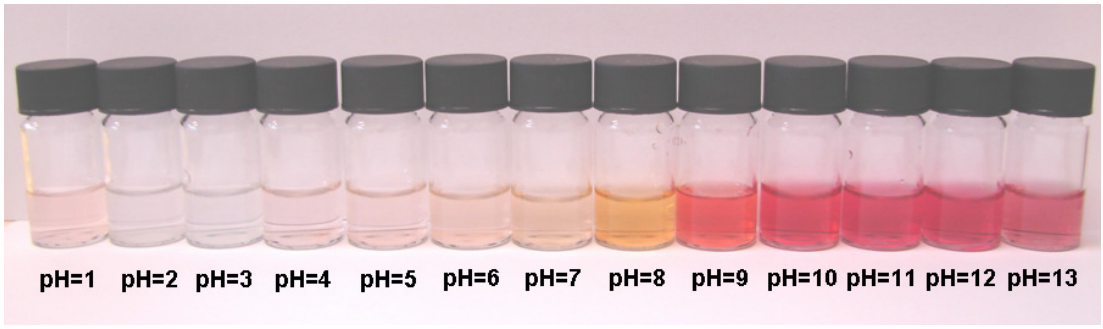

Figure 2.8 *50μM solutions of anthofluorescein in a set of pH buffers ranged from 1 to 13.*

2.6.2.2 Absorptivity study

A study of the absorptivity and the fluorescent properties of the novel dye confirmed that the optical properties of anthofluorescein were quite different from those of fluorescein, with both the absorption and emission spectra highly influenced by pH (as is also observed for the anthocyanidins). Spectrophotometric analysis of anthofluorescein solutions (50 μM) at distinct pH values showed that absorbance increased with pH, with the largest impact being observed between pH 7 and 10 (**Figure 2.9**).

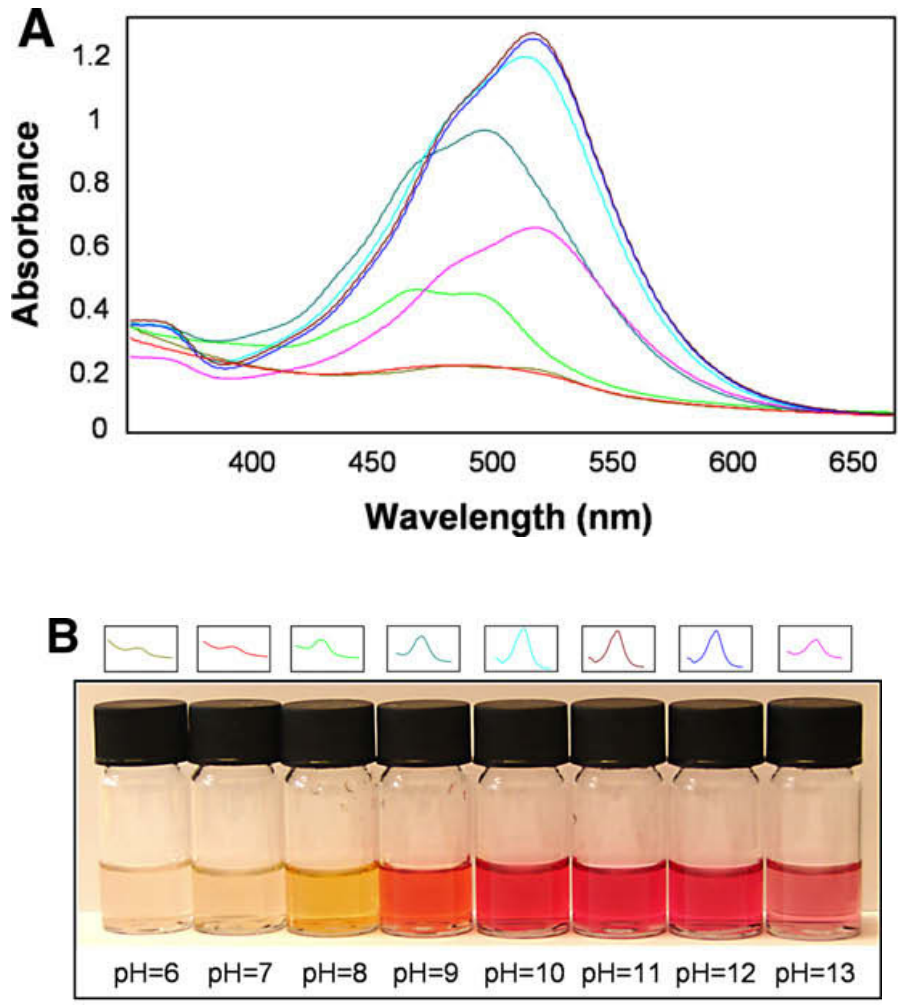

Figure 2.9 *(**A**) Absorption spectra of 50 μM solutions of anthofluorescein at pH 6–13. (**B**) Images of the dye solutions at various pH values and its emission.*

Absorptivity greatly decayed at pH 13, indicating a large change in the composition of the aromatic forms. The changes seen in the fluorescence emission spectra between pH 7 and pH 13 most probably being due to the prototropic equilibrium existing between the two dianionic forms of the molecule (**Figure 2.10**).

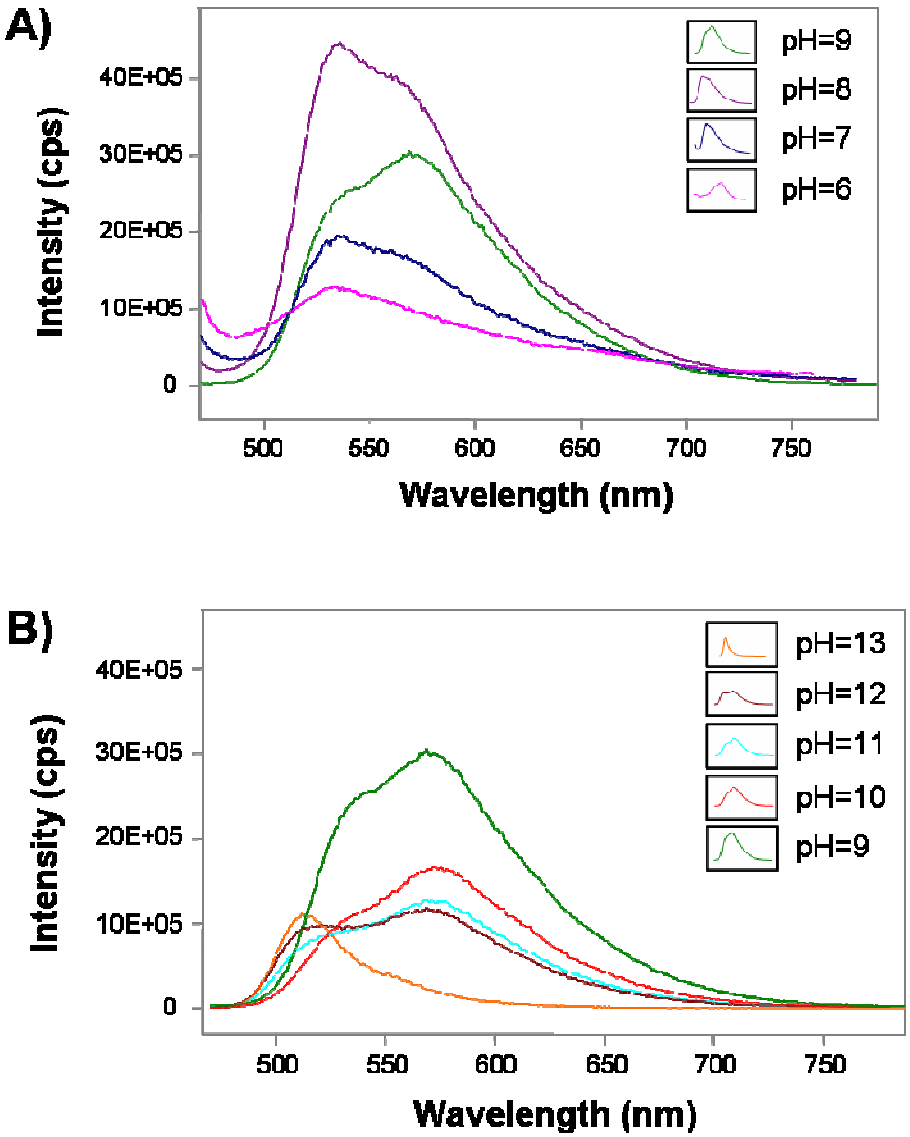

Figure 2.10 *Emission spectra of anthofluorescein, with excitation at 450 nm: (**A**) pH 6–9 and (**B**) pH 9–13.*

2.6.2.3 Excitation/emission analysis

At pH 6 the dominant band in the emission spectrum occurred at 535nm. A shoulder at 570nm appears on this band at pH 7 and pH 8, which at pH 9 becomes the dominant band. Above pH 9 a blue shifted shoulder, at 510nm, begins to appear until at pH 13 the emission spectrum becomes identical to that of fluorescein (**Figure 2.11**). The normalised emission spectra show clearly how the composition of the anthofluorescein solution changes with pH (**Figure 2.12**).

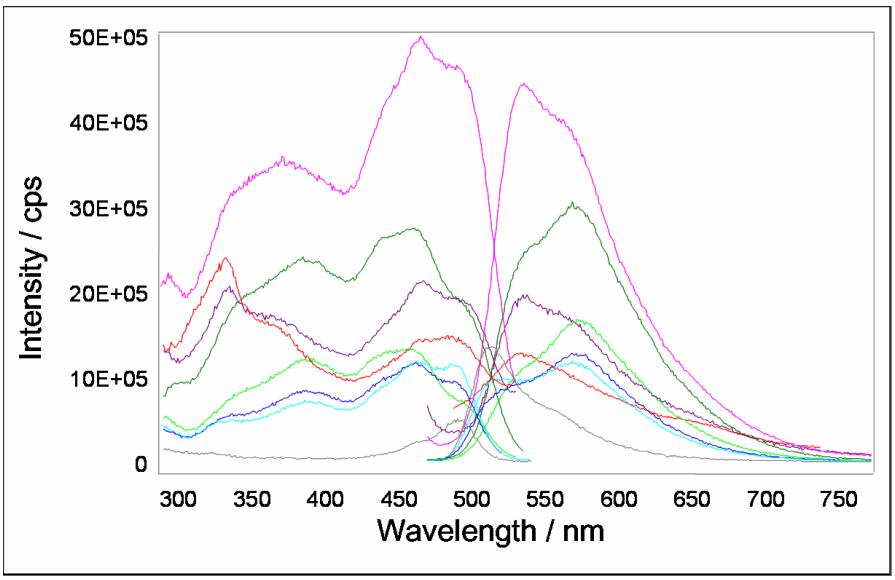

Figure 2.11 *Excitation spectra, on the left, recorded at an emission wavelength of 550nm, and emission spectra, on the right hand side, recorded at an excitation wavelength of 450nm, of anthofluorescein at pH 13 (grey), pH 12 (light blue), pH 11 (dark blue), pH 10 (light green), pH 9 (dark green), pH 8 (pink), pH 7 (purple), and pH 6 (red).*

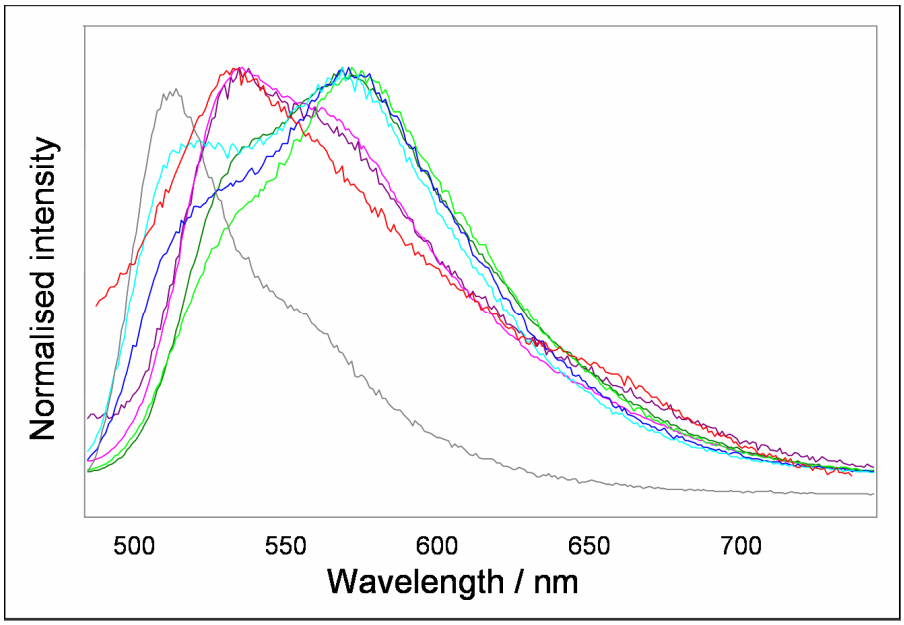

Figure 2.12 *Normalised emission spectra (with an excitation wavelength of 450nm) of anthofluorescein at pH 13 (grey), pH 12 (light blue), pH 11 (dark blue), pH 10 (light green), pH 9 (dark green), pH 8 (pink), pH 7 (purple), and pH 6 (red).*

2.6.2.4 Quantum yield study

The experimental quantum yield[132] of anthofluorescein at pH 8, where maximal emission was observed, was very low (0.02), which in practice would limit applicability for cell assays. However, further analysis indicated that the quantum yield was highly influenced by the viscosity of the solution, with the quantum yield rising to 0.3 at pH 8 in 20% glycerol (viscosity cells cytoplasma),[133] presumably due to a decrease in the rate of internal conversion mediated by the *p*-hydroxyphenyl group torsional motion.[134] It would be expected that the changes in emission intensity and quantum yield would be mirrored by changes in fluorescence lifetime and, as such, the molecule could find application as a, potentially, very sensitive probe of local temperature and viscosity in fluorescence lifetime imaging microscopy.

2.6.3 Cell Labelling/Viability Assay

The classic example of pro-drugging dyes is the application of nonfluorescent acetoxylmethyl (AM) or acetate esters.

A non-fluorescent derivative of anthofluorescein, 3´-acetyloxy-6´-(*p*-acetyloxyphenyl)fluoran, **4**, (AM anthofluorescein) was synthesized (**Scheme 2.4**) in order to enhance the cellular penetrability of anthofluorescein and also to eliminate extracellular background.

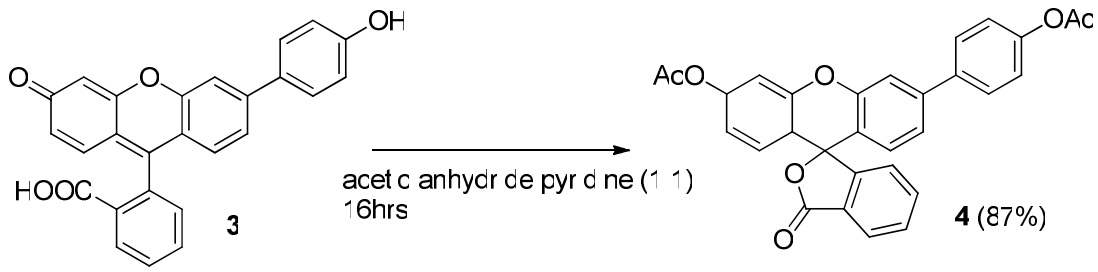

Scheme 2.4 *Synthesis of nonfluorescent bis-acetoxylmethyl of anthofluorescein (**4**).*

Acetoxymethyl anthofluorescein was incubated with HeLa cells for 2 h and then imaged using a 488/20 excitation filter. As expected, intracellular deacetylation led to the formation of anthofluorescein, which was identified by bright fluorescent yellow cells (**Figure 2.13**). Due to the higher viscosity of the cell cytoplasm

(expected to be more akin to glycerol than water)[133] the anthofluorescein dye was strongly emissive within the cells, confirming the previous viscosity observations. A diacetylated derivative of anthofluorescein **4** has been demonstrated to be cell permeable and to successfully label living cells.

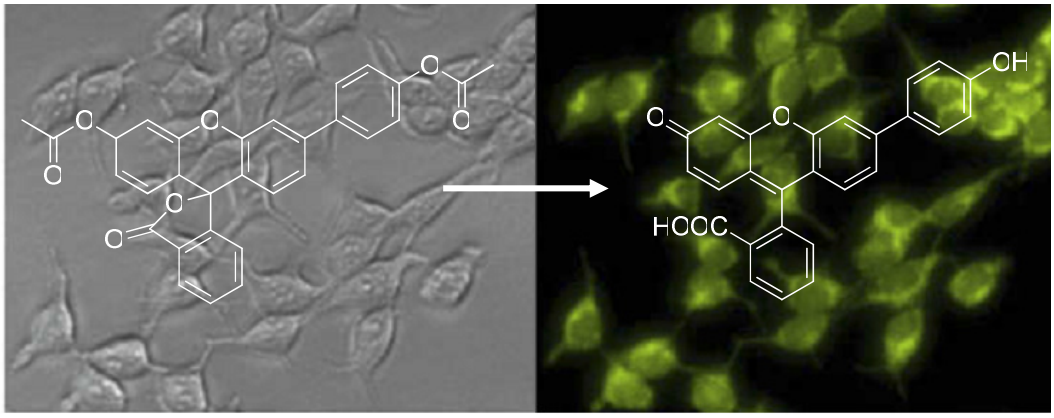

Figure 2.13 *HeLa cells were incubated for 2 h with a 25 μM solution of diacetylated anthofluorescein. Intracellular deacetylation to give anthofluorescein. Brightfield (left), Fluorescent image with 488nm excitation and no emission filter (right).*

2.6.4 Cytotoxicity of Anthofluorescein

The fluorescent dyes can localize in any cellular compartment, and the fluorescent compounds may tend to accumulate in organelles having high concentrations of esterases. The acetoxylmethyl ester and liberated dye could also be cytotoxic. Cytotoxicity of the anthofluorescein was therefore tested on HeLa cell using an MTT assay (**Figure 2.14**).

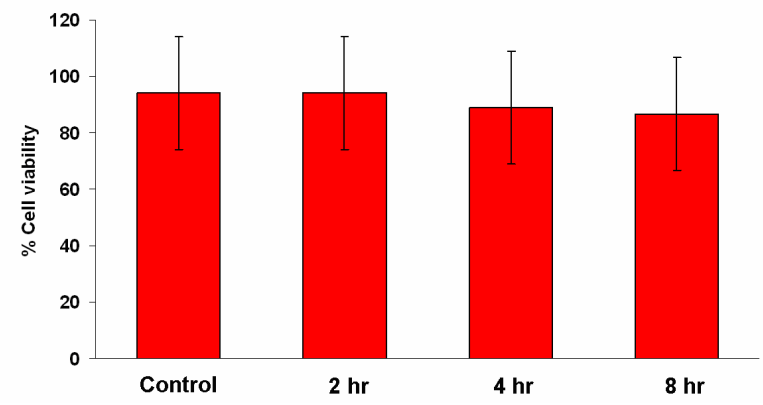

Figure 2.14 *Cytotoxicity analysis of bis-acetoxylmethyl of anthofluorescein,* ***4*** *(25 μM) on HeLa cells.*

The results suggested anthofluorescein was non-cytotoxic and did not perturb cell physiology after 8 hours. Based on microscopy analysis there was no significant leakage from cell (due to the presence of negative charges on the dye), therefore, anthofluorescein is a valuable candidate as a intracellular pH sensor.

2.6.5 Advantages of Anthofluorescein Compared to the Traditional Fluoresceins

Anthofluorescein is highly sensitive to pH changes between 7 and 10 and displays a green to red fluorescence shift in the physiological pH range, making it a candidate for biological studies. Its relatively cheap simple synthetic method makes the development of further multicolour fluorescence dyes from yellow to far-red practical. In addition, acetoxymethyl anthofluorescein has a low extracellular fluorescent background, giving excellent signal to noise ratios.

2.6.6 Conclusion

In conclusion a new pH-sensitive dye synthesized from fluorescein using a straightforward microwave-assisted two-step procedure consisting of mono-triflation and subsequent Suzuki aryl cross-coupling with *p*-hydroxyphenylboronic acid has been developed. The anthofluorescein was characterized by a highly pH sensitive absorption and fluorescence emission particularly in the pH range from 7 to 10 and good quantum yield in the physiological environment.

A diacetylated derivative of anthofluorescein (**4**) successfully labelled living HeLa cells with no obvious cytotoxycity observed. This indicates that might become a tool for cell labelling and viability studies. The synthetic method provides a facile route to the development of new multicolor fluorescence dyes with red-shifted absorption and emission, which are in high demand as fluorescence probes.

2.7 Synthesis of Novel Anthofluorescein Derivatives: The Influence of Conjugation Expanders on Fluorescent Properties

2.7.1 Introduction

Encouraged by the properties of anthofluorescein, research was focused on the modification of **2** using various boronic acids. A range of anthofluorescein derivatives were synthesised using different aryl and heteroaryl moieties decorated with electron donating/withdrawing groups as conjugation expanders.

2.7.2 Synthesise of Anthofluorescein Derivatives

The synthetic procedure of anthofluorescein derivative is outlined in **Scheme 2.5**.

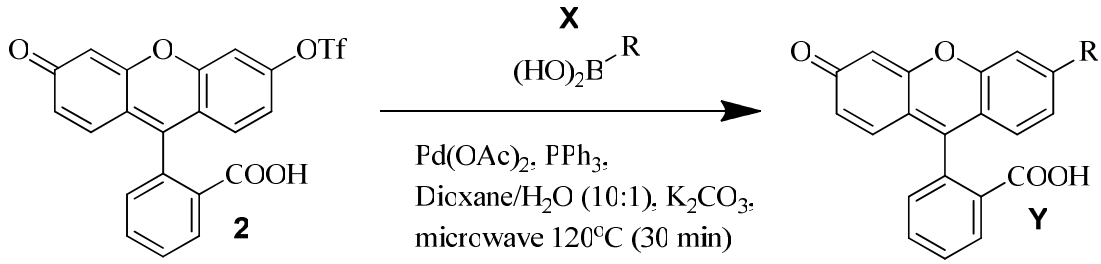

Scheme 2.5 *Suzuki cross-coupling between compound fluorescein-monotriflate (**2**) and boronic acids (**X**).*

Suzuki cross-coupling between fluorescein-monotriflate (**2**) with heteroaryl and aryl boronic acids (**X**) and its biaryl compound (**Y**) are summarised in **Table 2.1**.

2.7.2.1 Optical properties study

The excitation and emission maximum (E_x/E_m) of each derivative were recorded (**Table 2.1**).

2.7.2.2 Quantum yield study

The quantum yield measurement was made in ethanol at room temperature. The fluorescent standard was fluorescein with the quantum yield reported as 0.97.[135]

Table 2.1 *Heteroaryl boronic acid (entry 1-9) and aryl boronic acid (entry 10-22).*

Entry	Boronic acid X	Y	Yield (%)	E_x/E_m (nm)	Quantum yield (Φ)
A	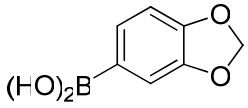	**5**	78	480/532	0.51
B	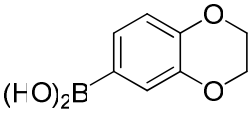	**6**	73	480/536	0.50
C	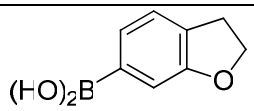	**7**	75	482/528	0.49
D	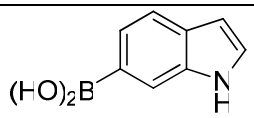	**8**	70	480/531	0.47
E	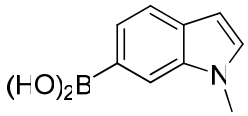	**9**	78	480/537	0.56
F	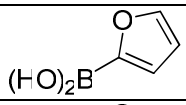	**10**	63	482/533	0.45
G	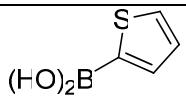	**11**	88	477/528	0.46
H	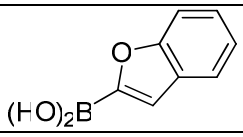	**12**	80	480/536	0.42
I	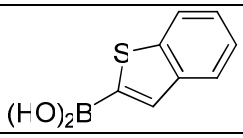	**13**	78	479/538	0.40
J	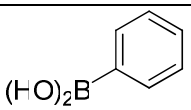	**14**	68	470/535	0.30
K	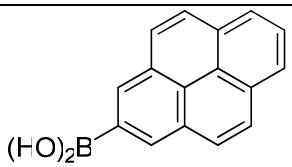	**15**	63	477/525	0.32
L	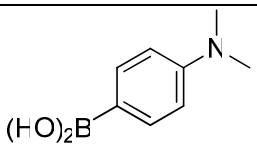	**16**	75	475/530	0.30

M	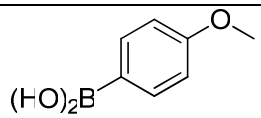	**17**	83	470/532	0.23
N	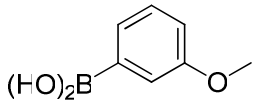	**18**	78	478/533	0.22
O	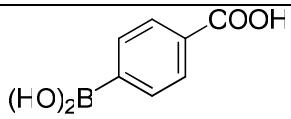	**19**	85	480/532	0.29
P	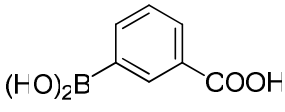	**20**	80	480/530	0.29
Q	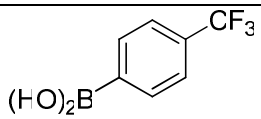	**21**	68	480/533	0.19
R	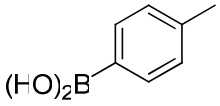	**22**	78	478/529	0.27
S	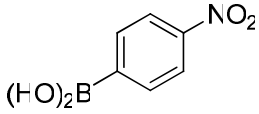	**23**	80	482/531	0.21
T	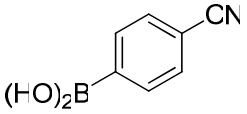	**24**	75	480/534	0.18
U	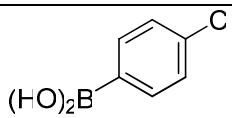	**25**	65	470/535	0.13
V	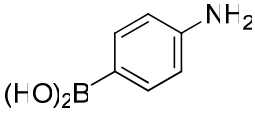	**26**	73	476/532	0.26

2.7.3 Further Investigation on 2-(3-(1-methyl-1H-indol-5-yl)-6-oxo-6H-xanthen-9-yl) benzoate (9)

Further investigation of **9** (**Figure 2.15**) which had highest quantum yield was carried out; specifically the behaviour of the optical properties in solvents of different viscosity.

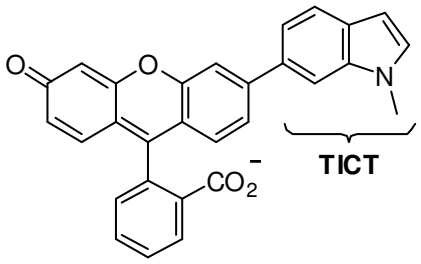

Figure 2.15 *Molecular structures of* ***9*** *containing twisted intramolecular charge transfer complexes (****TICT****).*[136]

The study was on the behaviour of the dye in different viscosity solution and polarity of the solvent. The viscosity sensitivity of **9** was tested by measuring its fluorescent intensity in mixtures of ethylene glycol and glycerol. Mixtures of ethylene glycol and glycerol were prepared to afford solutions of different viscosity with a constant dye concentration.

2.7.3.1 Effect of solvent viscosity on the fluorescent properties

The relationship between viscosity η and quantum yield is shown by the Föster-Hoffmann-equation[137] (**Equation 1**),

$$\log \Phi = C + x \log \eta \quad \textbf{(1)}$$

Where ***C*** is a temperature-dependant constant and ***x*** is a dye dependant-constant. To illustrate this relationship, the emission spectra of **9** (5 μM) in a mixture of ethylene glycol and glycerol with different viscosities were determined (**Table 2.1**), (increasing glycerol content is known to increase viscosity with only minimal changes of solvent polarity).[111]

Table 2.2 *Solution with different viscosity.*[111, 112]

Ethylene glycol / glycerol	100:0	20:80	40:60	50:50	60:40	70:30	80:20	100: 0
Viscosity (mPas)	13.5	36	72	109	165	248	374	945

Figure 2.16 shows the fluorescence intensity significantly increased with higher solvent viscosity. A higher glycerol content corresponds to a higher viscosity of the solvent which leads to increase emission intensity and suggested that **9** is strongly viscosity-dependant. A high viscosity environment means molecules **9** do not lose their energy via intermolecular rotation, therefore the energy was released by photon emission and leads to higher fluorescent intensity.

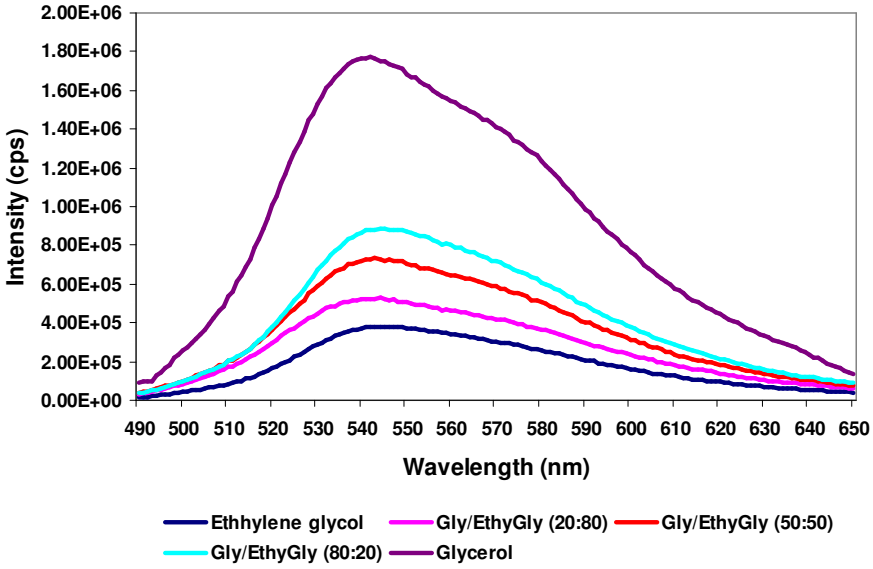

Figure 2.16 *Effect of solvent viscosity on the fluorescent intensity of* ***9*** *recorded with an excitation wavelength of 480nm.*

2.7.3.2 Effect of dye concentration on the fluorescent properties

The emission intensity of **9** increased not only with increased of solvent viscosity but also with increased dye concentration. **Figure 2.17** shows that the emission intensity of **5** depends on both solvent viscosity and dye concentration.

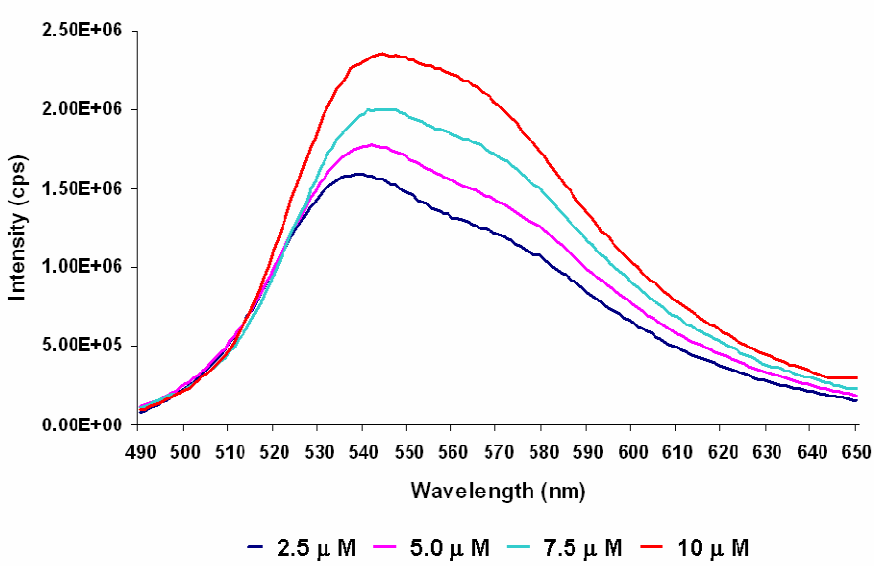

Figure 2.17 *Different concentration of* ***9*** *ranging from 2.5-10µM in glycerol/ethylene glycol (20:80), recorded with an excitation wavelength of 480nm.*

2.7.3.3 Effect of solvent viscosity and dye concentration

The effects of solvent viscosity and dye concentration were further investigated. The experiment was carried out using four different concentrations of **9** (2.5, 5.0, 7.5 and 10 μM) a five different viscosities (72, 109, 165, 248 and 374 mPas). The result shows linear relationship between fluorescent intensity versus viscosity of solvent (**Figure 2.18**), as per equation **1**.

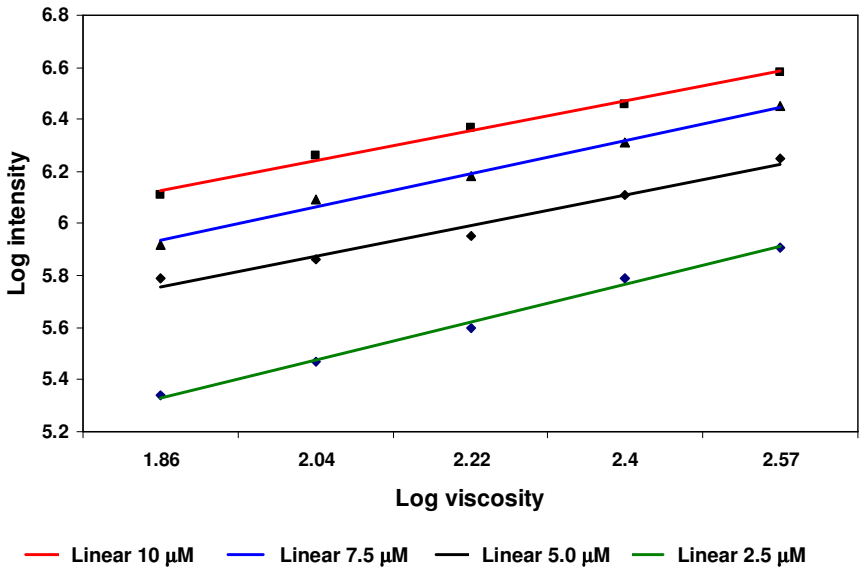

Figure 2.18 *Effect of concentration* ***9*** *over viscosity of solvent, recorded with an excitation wavelength of 480nm.*

2.7.3.4 Effect of solvent polarity on fluorescent intensity

In this study, the influence of solvent polarity **9** was examined. The dielectric constant ϵ of the solvents was used as an index of its polarity.[138] Four different solvents were used ethylene glycol, glycerol, DMSO, and benzene with dielectric constant values of 37.7, 42.5, 48.9 and 2.27 respectively. **Figure 2.19** shows the fluorescent peak intensity was influenced strongly by increased solvent polarity.

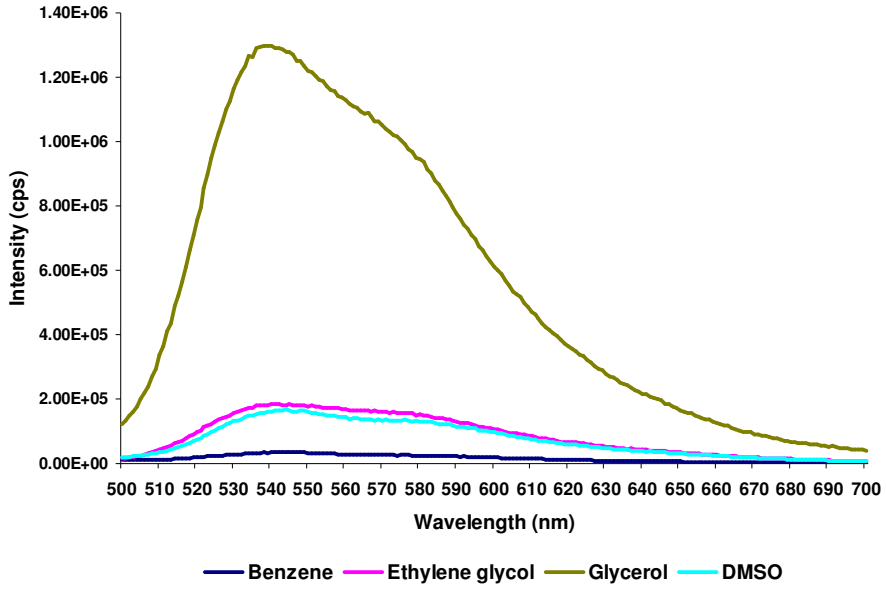

Figure 2.19 *Emission spectra of* ***9*** *(2.5μM) in selected solvents. Emission intensity increased in the moderately viscous ethylene glycol and in the highly viscous glycerol. The spectra recorded at excitation wavelength of 480nm.*

2.7.4 Cell Labelling/Viability Assay

The cell viability assay of dye **9** was tested on HeLa cells by direct staining for 2 hours. After the incubation time, the cells were washed, fixed using 4% paraformaldehyde and imaged using a 488/20 excitation filter (**Figure 2.20**).

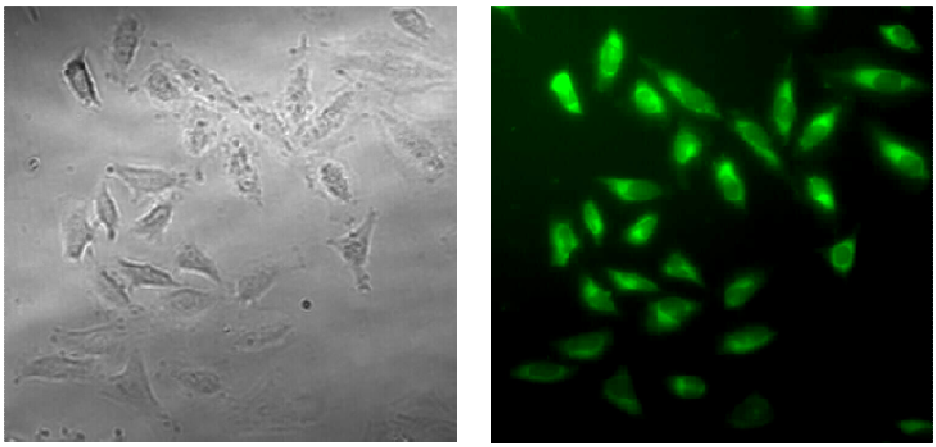

A **B**

Figure 2.20 *HeLa cells were incubated with a 5 μM solution of* ***9*** *for 2 h (**A**) Brightfield. (**B**) Fluorescent image with 488nm excitation and no emission filter.*

2.7.5 Conclusion

A series of anthofluorescein derivatives were synthesised via Suzuki cross-coupling and their spectroscopic properties studied. Emission spectra (**Appendix I**) showed all derivatives have a broad and slightly red-shift emission compared with fluorescein, due to the expanded electron conjugation on fluorophore skeleton. Among these derivatives, **9**, which was synthesised by coupling between fluorescein-monotriflate and 1-methyl-1H-indole-5-boronic acid showed the fluorescent intensity was highly dependent on viscosity of the solvent. The fluorescent intensity was dramatically increased with the increase of viscosity ranges from 13.5 to 945 mPas. The effect of solvent polarity and concentration of dye on optical properties were further investigated. The results showed the emission intensity increased in the moderately viscous ethylene glycol and in the highly viscous glycerol as well as higher concentration of **9**. Meanwhile, the cell viability assay test showed **9** was cell permeable and successfully labelled HeLa cells. These results strongly suggest **9** behaves as a molecular rotor where its emission intensity depends on both viscosity and polarity of the solvents. It is believed that compound **9** can be used as a micro-viscosity sensor, making it a valuable candidate for biological studies.

CHAPTER 3: INTRACELLULAR CATALYSIS WITH UNNATURAL METALS

3.1 Background and Significance[139]

Cellular biochemistry is governed by a wide range of enzymatic entities, with the complex cellular machinery engineered to perform numerous diverse chemical reactions.[140, 141] Many of these reactions are catalyzed by transition metals, typically in the form of metalloproteins,[142] which modulate a variety of transformations, ranging from highly selective oxidations to the efficient formation, lysis or isomerisation of multifarious chemical bonds.[140, 141] Many groups have exploited the singular properties of these proteins with the generation of bio-inspired devices, based on coordination complexes aimed at mimicking biological function.[143]

Much of our understanding of reactions in living cells has been drawn from established biochemistry.[144] Although many well-known *in vitro* assays are extremely effective, it is known that the setting of the cell is completely different from a test tube in a number of ways: (i) Many mRNA molecules, DNA and enzymes exist in low numbers and participate in random reaction events in the cell that are hidden in test tubes with large numbers of molecules. (ii) Reactions are regularly at nonequilibrium steady state in the cell. (iii) Many reactions are coupled in the cell, resulting in networks of complex interactions. (iv) Many proteins are in complex equilibria with each other. Consequently, a biochemical reaction in a single cell could have different properties from the same biochemical reaction *in vitro*.[144, 145]

A growing area of reaction methodology is focused on the development of chemical transformations with the selectivity, kinetics and biocompatibility required to proceed in living systems with minimal interference with the cell. As such, some

metal-catalized reactions have been attempted inside living cell such as copper-mediated click chemistry.[146, 147] Unfortunately, this reaction is not, at the moment, compatible with living systems due to the strict requirement for copper, a metal that is toxic to cells and organisms.[148, 149] In recent years, chemists and biologists have begun to share a common interest developing techniques to study biomolecules in their physiological environment. They have begun to shift away from the artificial confines of test tubes to investigate biological processes in the context of living cells and whole organisms.[64, 144] This requires the challenging process of designing biocompatible catalysts and reagent/s which work under physiological conditions.[64, 150] In this context both advances in instrumentation and also the design of new fluorophores are very important.[151] As such bioorganometallic chemistry has evolved as a fascinating field, full of possibilities and creative applications, ranging from highly-selective chemistries to the manipulation and *in situ* interrogation of a myriad of biological processes.[152]

3.2 Chemical Reactions in Cells

Among the numerous synthetic methods that chemists have developed, only a small number of them can be carried out under physiological conditions. The ability to carry out selective transformations inside a cell would allow researchers to manipulate or interrogate innumerable biological processes. For example, such catalysts could eventually be used to amplify signals by turning over a substrate multiple times,[150] catalytically labelling or deactivating target biomolecules, activation of prodrugs and also intracellular synthesis of impermeable drug.[139] Biomolecules within cells could be covalently labelled with probes using bioorthogonal reactions. Fast chemical methods have been elegantly developed to detect DNA biosynthesis during cell proliferation via Click chemistry which does not require sample fixation or DNA denaturation and permits good structural preservation.[147] Recently, Rao elegantly presented an approach for the constructing of large molecules within living cells via condensation reaction between 1,2-aminothiol and 2-cyanobenzothiazole that occurs *in vitro* and in living cells.[153]

3.3 Challenges in Developing Artificial Intracellular Catalysts

Nature has evolved to create extremely selective enzymes that allow for substrate recognition and subsequent reaction of functional groups with high efficiency and specificity. While this patient process has worked amazingly for nature, it is almost impossible for scientists to design and make new enzymatic entities to facilitate new selective covalent reactions such as the tagging of particular biomolecules.[64] Designing unnatural catalysts which work under physiological conditions, while very challenging due to their inherent toxicity,[154, 155] offers an ideal alternative to this purpose.

The mode of action of any unnatural metal, and palladium in particular, in biological systems remains unclear. Due to their ability to form strong complexes with both inorganic and organic ligands, they have the potential not only to disturb cellular equilibria or replace other essential ions but also to interact with functional groups of macromolecules, thereby disturbing a variety of cellular processes.[156-158] Its ability to cross-link DNA inside the nucleus is probably the most important drawback of using metals of the platinum group such as palladium inside cells.

In addition, intracellular catalysis must first take away any reaction that is sensitive to water. Designing metal-based catalysts which work under physiological conditions means the biocompatibility of the catalysts is crucial as it must have minimal or no reaction with biomolecules. The reaction desired should proceed with reasonable rate even when the concentration of the reactants are low. Most importantly, the reaction should only proceed inside the cells or even only at specific locations within the cells. All reagents used have to be cell-permeable and be retained within the cell while reaction products need to stay too to perform their function. Considering the abundant supply of thiols and amines in the cell, all reagents that are prone to nucleophilic attack might also need to be ruled out. Reactions that are sensitive to redox chemistry might be ineffective too due to the environment in the cell. Any reaction requiring heat (above 37 °C), high pressure, or

high concentrations to work will not be applicable. In addition, it needs to be considered that some reagent functionalities can be metabolized by cellular enzymes (*e.g.*, esterases, phosphatases, sulfatases, proteases, *etc*.). Last but not least, toxicity and localization of reagent, product and by-product are one of the main challenges for metal-based intracellular catalysis.

3.4 The Important Benefits of the Research

For many years now, palladium has been among the most popular transition metals in modern organic/industrial synthesis and is widely used for a significant number of synthetic transformations.[2, 140] However, the exceptional ability of palladium to catalyze a wide variety of chemical transformations has not yet been exploited *in vivo* in chemical biology.[159]

Based on these facts and the massive opportunities palladium could offer in a living context, the presented research focuses on designing unique biocompatible heterogeneous catalyst based on the idea of immobilising palladium nanoparticles onto microspheres that "travel and stay" in the cytoplasm of cells.[16] Such a truly heterogeneous catalyst would allow palladium chemistry to be performed within cells such as allylcarbamate cleavage and Suzuki-Miyaura chemistry.

3.5 Designing a Biocompatible Heterogeneous Catalyst

Encouraged by the vast possibilities and applications of palladium chemistry[1] the preparation of a "bio-friendly" internalisable Pd^0–based heterogeneous catalyst was undertaken. This was achieved by the application of two technologies. Firstly, the use of microsphere (500nm) mediated cellular delivery that has previously been used in both cellular labelling and intracellular delivery of biomaterials, showing remarkable cellular biocompatibility and exonuclear localization.[160-164] Secondly, the application of palladium nanoparticles entrapped within cross-linked resin beads that have been shown to operate in a truly heterogeneous manner.[16]

3.5.1 Synthesis of Pd^0-microspheres[139]

This catalyst-loaded delivery system was synthesized as shown in **Figure 3.1**. Amino-functionalized polystyrene microspheres (500nm, loading 0.08mmol) were used as a solid support as well as a delivery agent.[161] The amino-functionalised the microspheres were treated with $Pd(OAc)_2$ in toluene at 80°C for 10 min followed by 3 hours at room temperature to ensure maximum uptake and interaction with microspheres. The electron-rich microsphere network binds Pd^{2+} ions of $Pd(OAc)_2$ by coordination to the free amino groups and aromatic rings. The coordinated Pd^{2+} was subsequently trapped by extensive cross-linking with the bis acid chloride of racemic Fmoc-Glutamate (generated *in situ)* (**section 4.3.1**). Subsequent, reduction of Pd^{2+} to Pd^0 with 10% hydrazine hydrate in methanol gave black beads (due to the trapped Pd^0 nanoparticles). The final heterogeneous catalyst are, in this thesis, named Pd^0-microspheres.

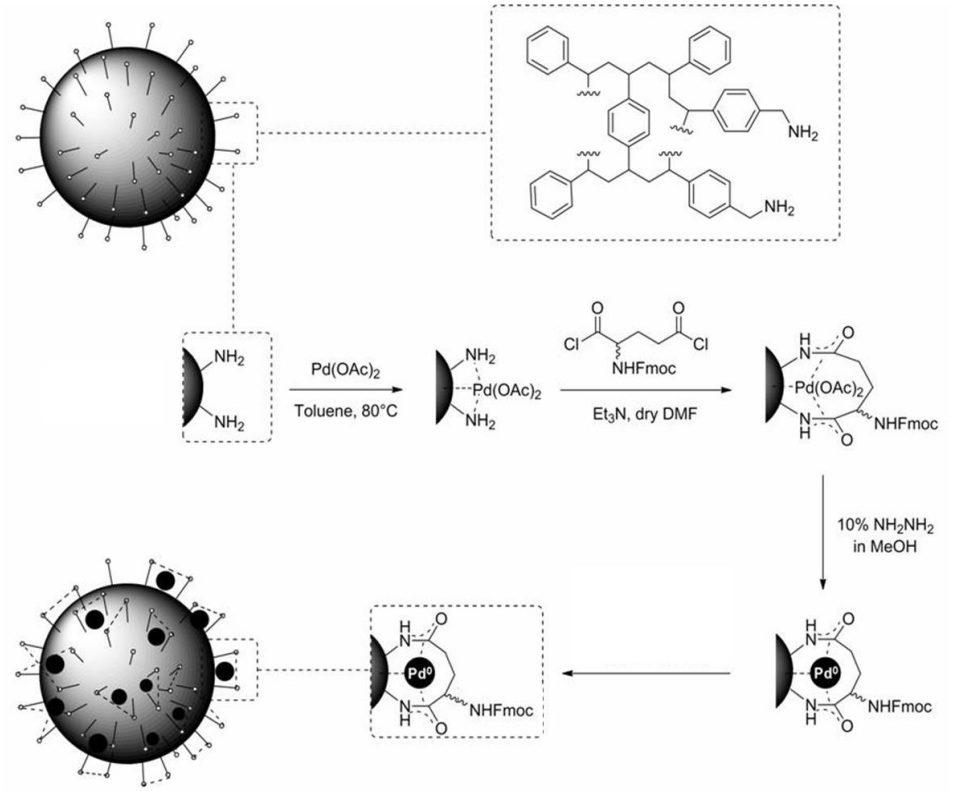

Figure 3.1 *Synthesis of Pd^0-microspheres via immobilisation of palladium nanoparticles on microspheres followed by extensive cross-linking.*

The Pd^0-microspheres were kept in water and stored at 4°C as a grey suspension (**Figure 3.2**), and were characterised and tested for catalytic activity, cytotoxicity and cellular uptake.

Figure 3.2 *Pd^0-microspheres. Left: Naked amino-functionalised microspheres (milky-white solution) and Right: Pd^0-microspheres (grey suspension).*

3.5.2 Characterisation of the Pd^0-microspheres

3.5.2.1 Scanning Electron Microscopy (SEM)

The morphology of the dried Pd^0-microspheres was determined using SEM (Philips XL30CP0) with gold coating by sputtering. The images of the Pd^0-microspheres showed there was no physical change in terms of size, shape and surface following entrapment (**Figure 3.3**).

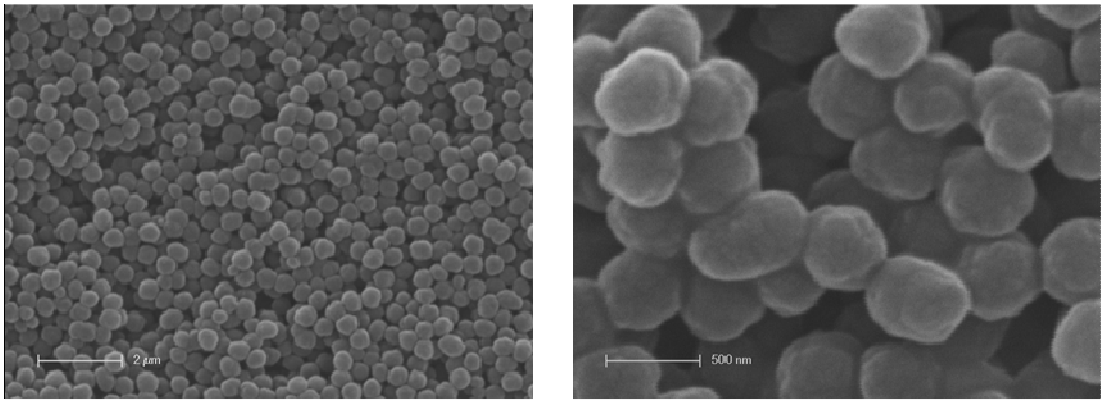

Figure 3.3 *SEM images of Pd^0-microspheres (0.5 µm) at different magnifications. Scale bar = 2µm (left) and 500µm (right).*

3.5.2.2 HR-Tranmission Electron Microscopy (TEM)

The size and distribution of the Pd^0 nanoparticles on microspheres was analysed using TEM (JEM-2011), and the TEM images of the Pd^0-microspheres (**Figure 3.4**) were compared with naked-microspheres. Analysis showed the Pd^0 nanoparticles to be evenly distributed with an average diameter of 5 ± 2.5 nm.

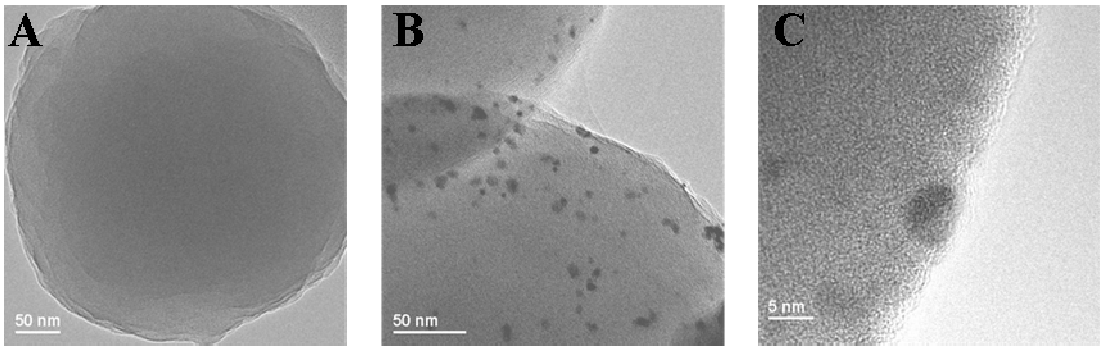

Figure 3.4 *Transmission Electron Microscopy (TEM) of Pd^0-microsphere at two different magnifications: (**A**) naked microspheres, (**B**) Pd^0 nanoparticles are observed physically captured and entrapped on the microspheres, (**C**) Image of a single microsphere-captured Pd^0 nanoparticles.*

3.5.3 Palladium Analysis

3.5.3.1 Quantitative palladium analysis: Inductively Coupled Plasma-Optical Emission Spectrometer (ICP-OES)

The presence of Pd^0 in the Pd^0-microspheres was measured by ICP-OES. Dried Pd^0-microspheres (50 mg) were dissolved in DCM and shaken for 24 hours. Due to the "solubilization" of the microspheres, the palladium nanoparticles were released from the support and collected by centrifugation. The supernatant was collected and this procedure repeated to ensure all Pd^0 nanoparticles were collected. After washing several times with DCM, palladium analysis was carried out by using ICP-OES with calibration against standard palladium solutions. Analysis gave a blank value of 0.30 ppm. The levels of Pd^0 obtained from 50 mg dried Pd^0-microspheres was determined as 22.35 ppm, which equates to 4.2×10^{-6} moles of Pd^0 per g of beads (0.45 mg of Pd^0 in 1 g of beads). Assuming there are 1.52×10^{13} beads/g,[161] one single bead contains $0.45 / 1.52 \times 10^{13} = 2.96 \times 10^{-14}$ mg Pd^0 (2.78×10^{-16} moles or about 20 millions atoms).

3.5.3.2 Qualitative Palladium Analysis: Powder X-Ray diffraction (XRD)

Qualitative Pd^0 analysis was carried out by powder X-ray diffraction (XRD). X-ray powder diffraction is most widely used for the identification of unknown crystalline materials (e.g. minerals and inorganic compounds). XRD is a rapid analytical technique primarily used for phase identification of a crystalline material. Dried Pd^0-microspheres (50 mg) were analysed on a Philips PW1800. The spectra were compared with Pd^0 standard (commercially available) and microspheres alone. The reflection peaks seen in an XRD pattern (**Figure 3.5**) at 2θ around 40.1, 46.6 and 68.3° corresponds to the (111), (200) and (220) planes of an fcc (face-centered cubic) lattice respectively. All data matches the data for Pd^0 provided by the ASTM (American Society for Testing and Materials) and previous work performed by Shen *et al.*[165]

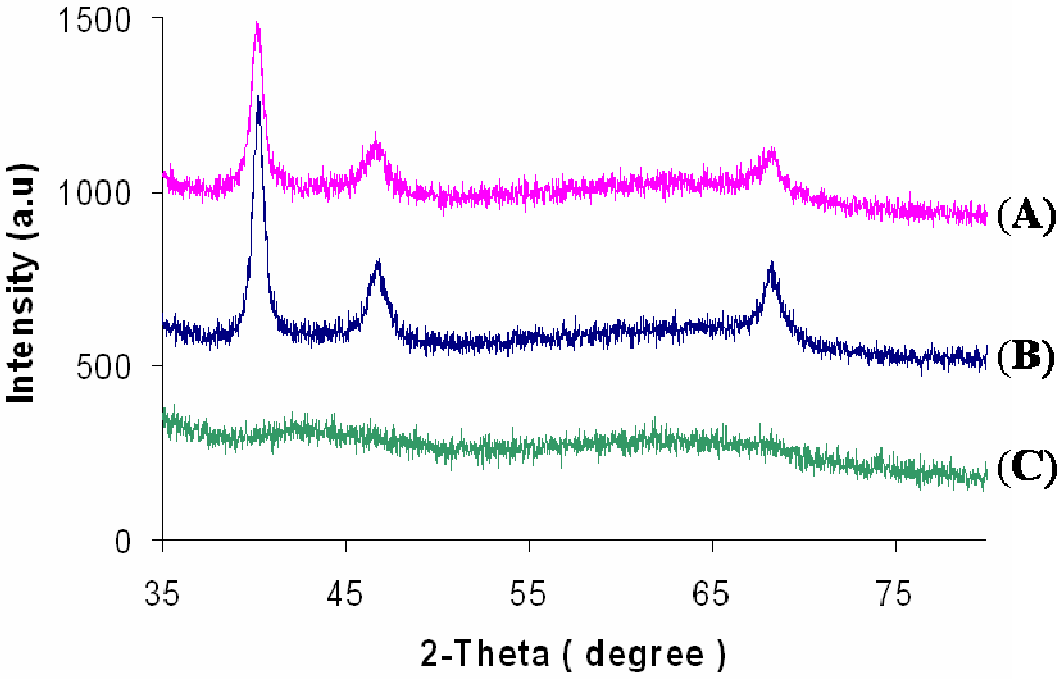

Figure 3.5 *Powder X-ray diffraction patterns of (**A**) Pd^0-microspheres, (**B**) commercial Pd^0 powder, and (**C**) naked microspheres.*

3.6 Investigating Catalytic Activity of Pd^0-Microspheres

The allyloxycarbonyl (Alloc) protecting group is often used to protect a hydroxyl or amino group when an orthogonal deprotection is required. To demonstrate the catalytic activity of the Pd^0-microspheres, the bis-allyloxycarbonyl rhodamine 110 (**28**), used by Meggers was synthesised.[150] Protection on both sides forces the molecule to adopt a closed, colorless and nonfluorecent lactone (**Scheme 3.1**).

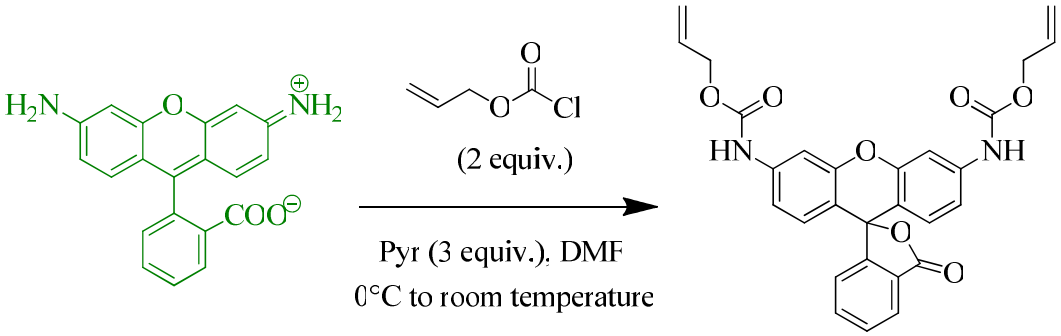

27
Fluorescent

28
Non-Fluorescent

Scheme 3.1 *Synthesis of bis-allyloxycarbonyl rhodamine 110 (**28**).*[150]

3.6.1 Alloc Deprotection in Solution

The catalytic activity of the Pd^0-microspheres were tested in solution under different conditions using bis-allyloxycarbonyl rhodamine 110 (**28**). This fluorophore is non-fluorescent, however upon allylcarbamate deprotection, strong green-fluorescent rhodamine 110 (**27**) is released (**Scheme 3.2**).

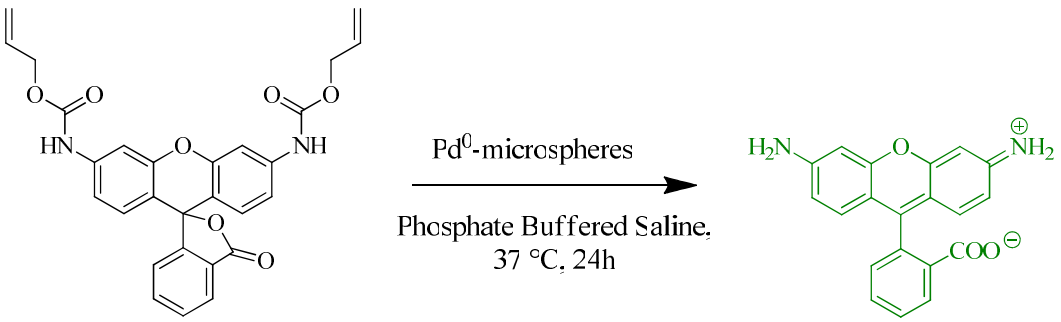

28
Non-Fluorescent

27
Fluorescent

Scheme 3.2 *Pd^0-microsphere induced allylcarbamate cleavage.*

The reaction progress was monitored with TLC and LCMS to confirm conversion of **27**. This experiment was the important test to evaluate catalytic activity of Pd^0-microspheres before its use for intracellular catalysis. As shown in **Figure 3.6**, after 24 hours reaction, green fluorescence (indicating the presence of uncaged rhodamine 110, **27**) was clearly observed from the reactions containing Pd^0-microspheres, while no fluorescence was observed from the negative control and in the absence of Pd^0-microspheres. Surprisingly, the reaction also occurred without presence of thiophenol which is known to be harmful to the living cell.[150] This suggested the deprotection only occurred with presence of Pd(0) as well as evidence of catalytic activity.

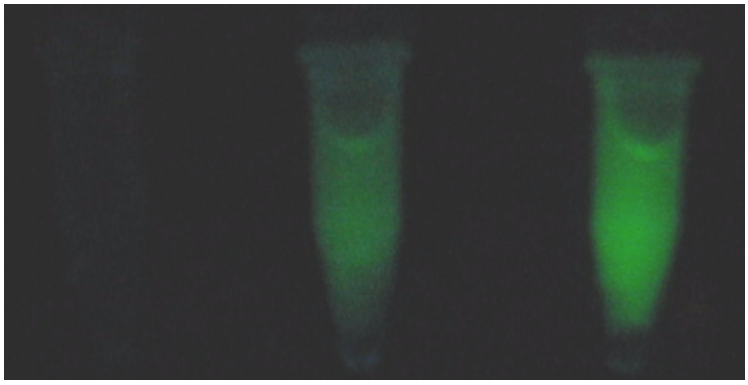

A **B** **C**

Figure 3.6 *Pd^0-microsphere were used for allylcarbamate cleavage of compound **28**. The images was taken under UV illumination shows (**A**) negative control, (**B**) reaction containing Pd^0-microspheres and (**C**) reaction containing thiophenol as a co-factor and Pd^0-microspheres.*

3.7 Cellular Uptake Study

Although the microspheres have shown remarkable cellular compatibility and have been widely used as a highly efficient cellular delivery vehicle for a variety of materials,[160, 162-164] the presence of Pd^0 on the beads required an investigation of their biological compatibility. Cellular uptake of Pd^0-microspheres was tested on HeLa cells (human cervical cancer) for 24 hours and analysed by flow cytometry analysis and confocal microscopy. In order to track Pd^0-microspheres inside the cell, Pd^0-microspheres were labelled with dyes through the free amino group. Labelling of the Pd^0-microspheres was realized by deprotection of the Fmoc group and subsequent

treatment with an ''activated dye" under basic conditions (**Scheme 3.3**). Two different dyes were used for analytical reasons: Cy5.5 for flow cytometry analysis and Texas Red for confocal analysis.

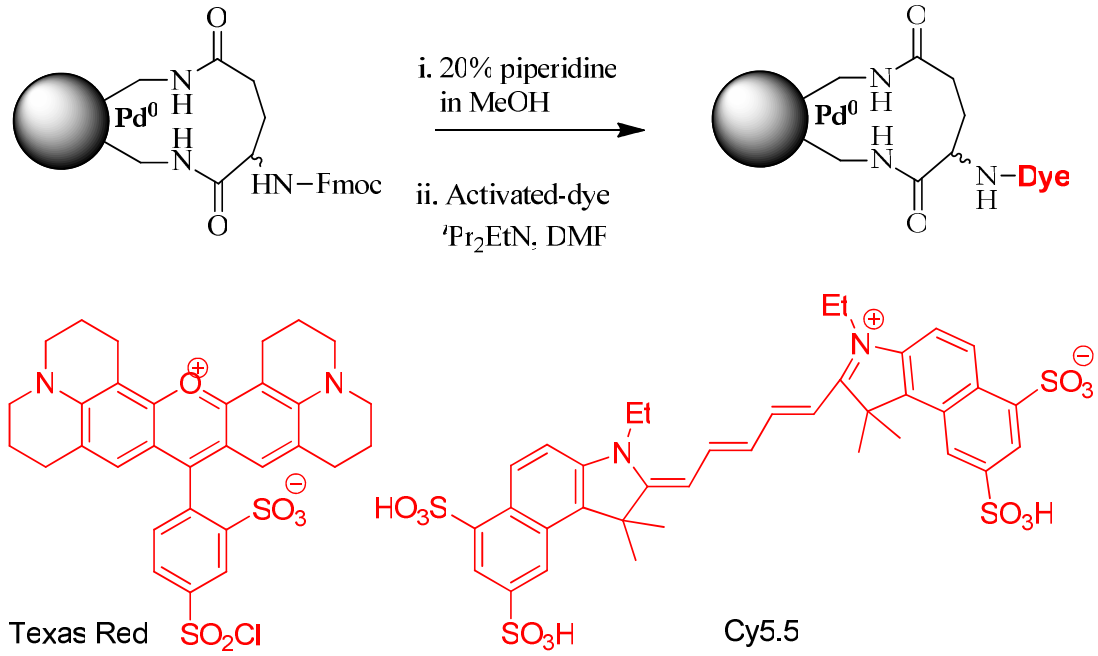

Scheme 3.3 *Synthesis of fluorescently Pd^0-microspheres labelled with dyes.*

3.7.1 Flow Cytometry Analysis.

Flow cytometric techniques allow quantification of cellular fluorescence. After incubation with beads, cells were washed twice with PBS, harvested with trypsin/EDTA and resuspended in 2% FCS in PBS. The internalization of labelled-microspheres was analyzed by flow cytometry. In order to distinguish between internalized Pd^0-microspheres and those on the extracellular membrane of cells, flow cytometry was performed in the solution in the presence of trypan blue (E_x/E_m = 520/650nm) which quenches fluorescence and labeled beads (fluorescence/rhodamine 110). Quantification by flow cytometry showed the clear presence of Texas Red (610/20 band pass filter) (**Figure 3.7**) and Cy5.5 (**Figure 3.8**) signal under the 780/60 band pass filter.

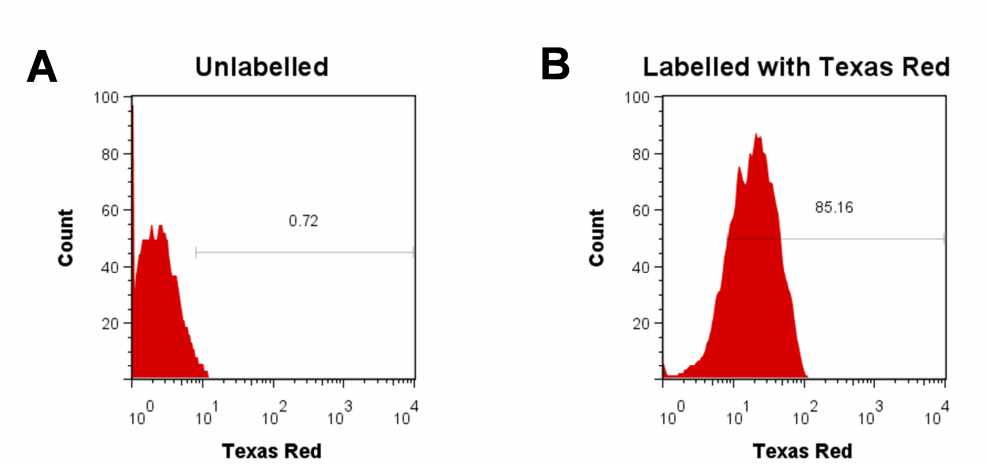

Figure 3.7 *Flow cytometry analysis of (**A**) unlabelled Pd^0-microspheres and (**B**) Texas Red-labelled Pd^0-microspheres.*

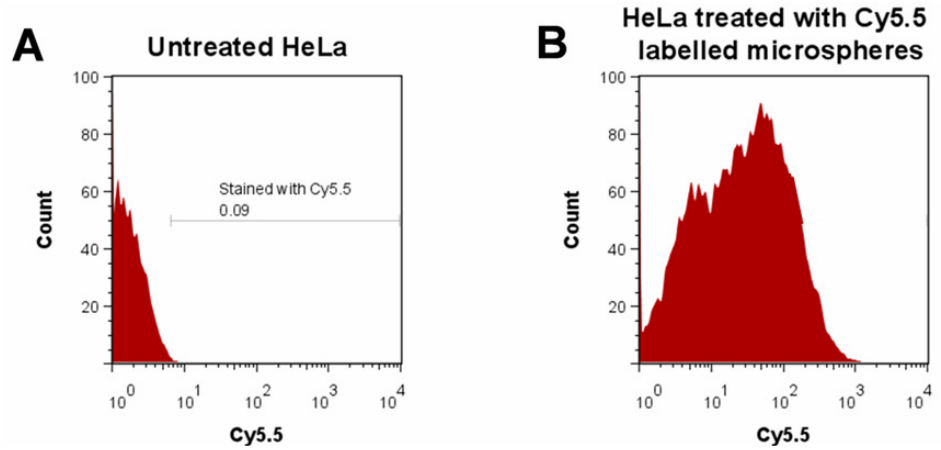

Figure 3.8 *Flow cytometry analysis of (**A**) untreated HeLa cells and (**B**) HeLa cells incubated with Cy5.5 labelled Pd^0-microspheres.*

3.7.2 Confocal Microscopy Studies

Confocal microscopy has the ability to collect a series of optical sections from thick specimens and analyse them in a 3D manner. Cellular uptake of Texas Red-labelled Pd^0-microspheres was further corroborated by confocal imaging. The presence of Texas Red labelled Pd^0-microspheres showed that Pd^0-microspheres were indeed within the cell (**Figure 3.9**).

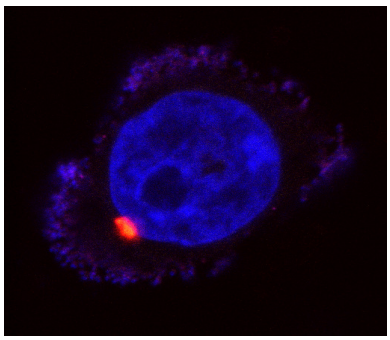

Figure 3.9 *HeLa cells containing Texas Red-labelled Pd^0-microspheres (in red) as viewed under a confocal microscope. The nucleus is shown in blue and the membrane in purple.*

3.8 Cytoxicity of Pd^0-Microspheres

The possibility of Pd^0-microsphere cytotoxicity was evaluated. This is perhaps the most important test to investigate if the Pd^0-microspheres are truly heterogeneous or not. Pd not trapped on the microspheres may leach out from the solid support and be toxic to the cells. However, extensive cross-linking should prevent leakage. Cytotoxicity associated with the Pd^0-microspheres was determined using both MTT (3-(4,5-dimethylthiozol-2-yl)2,5-diphenyl tetrazolium bromide) and propidium iodide assays.

3.8.1 MTT Assay

Cytotoxicity of Pd^0-microspheres was assessed by the use of an MTT assay[166] which is a quantitative colorimetric method that determines cell viability. It is based on cellular metabolism and reduction of the tetrazolium salt (MTT) to form an insoluble formazan dye mediated by cellular microsomal enzymes only produced by live cells (**Scheme 3.4**).

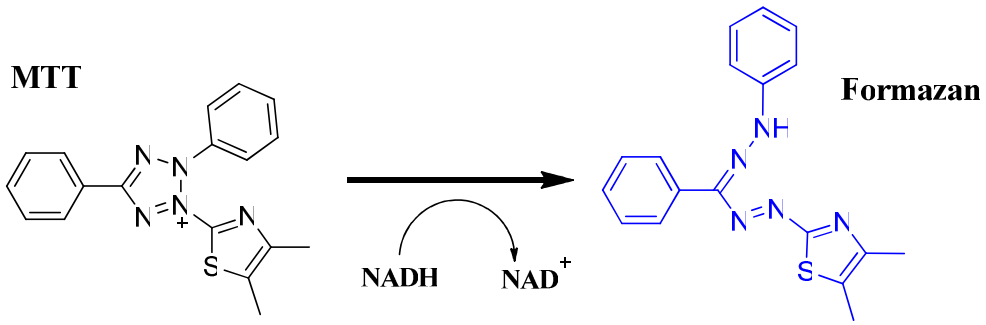

Scheme 3.4 *Metabolism of the "succinate-tetrazolium reductase".*

Cytotoxicity tests were carried out on the cell line HeLa. Cells were plated in a 96-well plate with a density of 5,000 cells/well and left to grow for 24 hours. Two concentrations of Pd^0-microspheres were studied (0.25 µL/100 µL (C1, $0.19x10^{10}$ beads/mL) and 0.5 µL/100 µL (C2 $0.38x10^{10}$ beads/mL)). Pd^0-microspheres were added to the well and incubated with the cells for 48 hours. Each condition was carried out in triplicate, with cells growth monitored under a microscope. After incubation, the general protocol for the cytotoxicity test was carried out and results compared to untreated cells. **Figure 3.10** shows the cell viability of HeLa cells treated with Pd^0-microspheres at two concentrations with no substantial cytotoxicity noted within error.

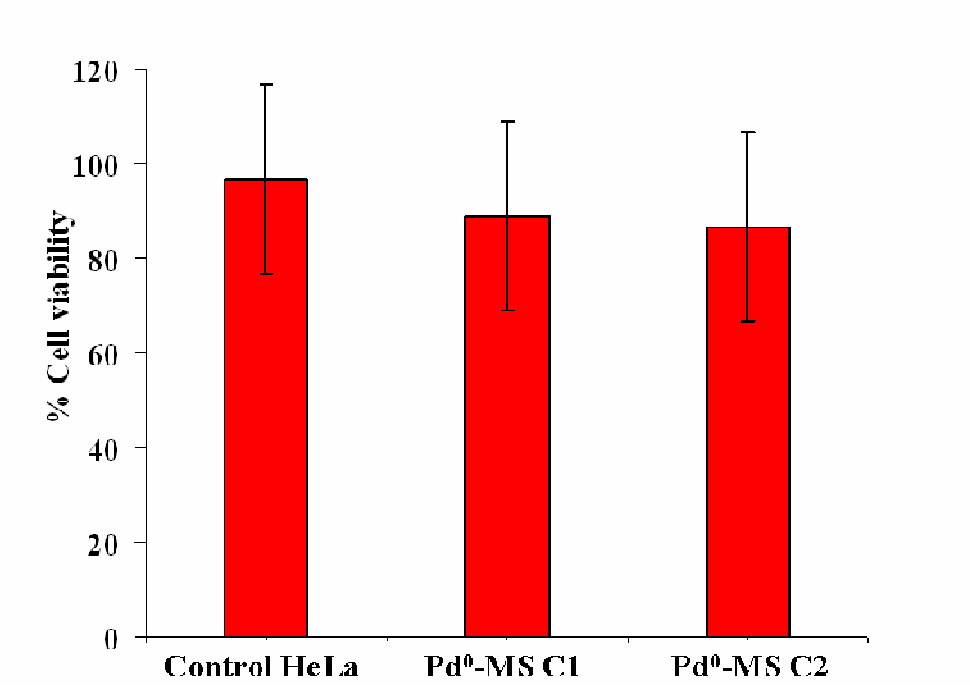

Figure 3.10 *Cytotoxicity of the Pd^0-microspheres ((**C1** $0.19x10^{10}$ beads/mL), (**C2** $0.38x10^{10}$ beads/mL)) on HeLa cells.*

3.8.2 Counting and Replating

This experiment was carried out to investigate the behaviour of cells containing Pd^0-microspheres after detachment from the well surface by trypsination. The ability of the cells to reattach was observed and used as a cell viability study (modified cell viability assay by Rossignol et al.).[167] HeLa cells were diluted in RPMI-CM (1 mL) with a density of 40,000 cells/well, plated in a 12 well plate and grown for 24 hours. Pd^0-microspheres (Texas red and Cy5.5 labelled) in media (1 µL/1 mL RPMI-CM,

0.76 x 10^{10} beads/mL) were added to the well plates and incubated for another 24 hours. The media was removed, the cells were washed with PBS (10 mM) and then detached with trypsin (2.5% in EDTA) for 5 min at 37°C. The cells were diluted with 1 mL of media, counted by phase contrast microscopy using trypan blue, and then replated for 1 hour. The number of cells in suspension after 1 hour was quantified by phase contrast microscopy using trypan blue for extracellular quenching (in triplicate). **Table 3.1** showed the viability for cells containing Pd^0-microspheres was good.

Table 3.1 *Cell viability after 36 hours treatment with Pd^0-microspheres. [a.]Number of cells at the beginning of the experiment. [b.]Number of cells after 36 hours of treatment with Pd^0-microspheres. [c.]Number of cells in the suspension after 1 hour of replating. Viable cells should have reattached.*

	Cells plated[a]	No. of Cells 36 h[b]	No. of cells in suspension[c]
Control	$4x10^4$	$31.5x10^4 \pm 4.8 x10^4$	$9.7x10^4 \pm 1.5 x10^4$
Pd^0-Tex Red	$4x10^4$	$38.0x10^4 \pm 3.6 x10^4$	$4.5x10^4 \pm 1.3 x10^4$
Pd^0-Cy5.5	$4x10^4$	$24.3x10^4 \pm 5.0 x10^4$	$6.4x10^4 \pm 1.4 x10^4$

3.9 Pd^0-mediated Allyl-carbamate Cleavage in Living Cells

In 2006, Meggers described a water-soluble ruthenium complex that rapidly entered cells and performed an allylcarbamate cleavage of bis-*N*-allyloxycarbonyl rhodamine 110 (**28**), which were non-toxic to cells during the short duration (minutes) of the experiment.[150] The use of a purely heterogeneous catalyst in the form of an "artificial organelle" would allow the long-term cytoplasmic presence of metals without toxicity (many transition metals; including palladium;[155] trigger cell death). [154] The non-cytotoxicity of Pd^0-microspheres, would allow the exploration of challenging metal-catalyzed reactions inside a cell.

3.9.1 Allylcarbamate Cleavage in HeLa Cells

In order to assess allylcarbamate cleavage, cells were loaded with fluorescently-labelled Pd^0-microspheres for 24 hours and subsequently washed to eliminate extracellular Pd^0-microspheres. Fresh media containing 30μM bis-allyloxycarbonyl rhodamine 110 (**28**) was incubated with the cells. The lipophilic nature of the non-fluorescent compound **28** allows its cellular internalization (**Scheme 3.5**), while allylcarbamate cleavage results in the liberation of the strongly fluorescent rhodamine 110 (**27**, Φ= 0.91, E_x/E_m: 498/521nm).

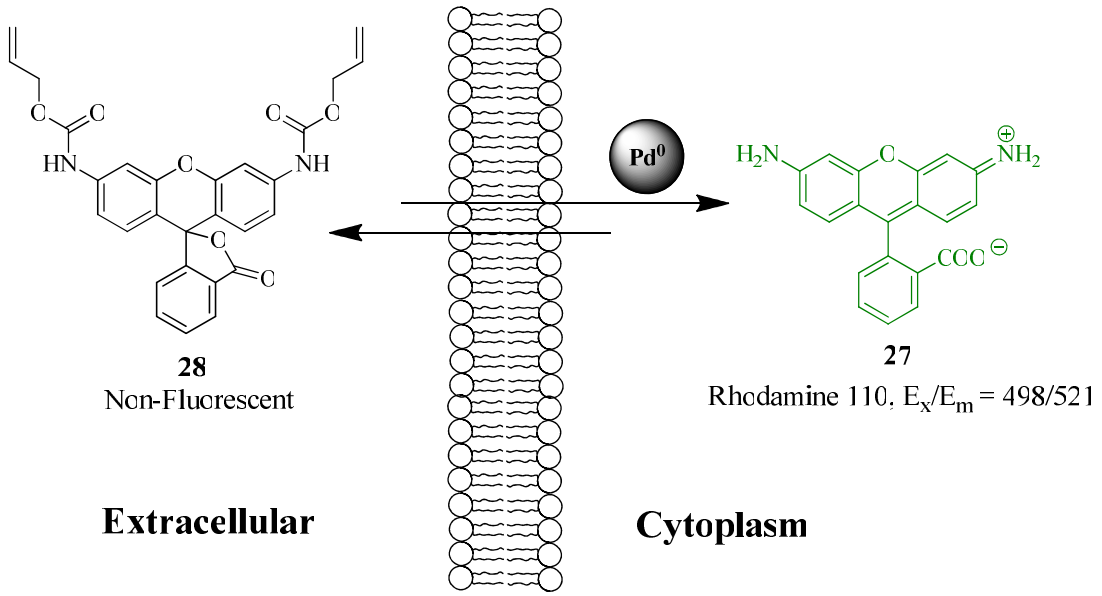

Scheme 3.5 *Intracellular Pd^0-mediated allylcarbamate cleavage in HeLa cells.*

3.9.2 Analysis by Flow Cytometry

In this experiment, Cy5.5 labelled-Pd^0-microspheres were used. The intracellular presence of Cy5.5 labelled-Pd^0-microspheres and fluorescent compound **27** were determined by flow cytometry (with appropriate control) using different band pass emission filters (780/60 and 530/30, respectively).

Figure 3.11 showed cytograms of Pd^0 catalysis of allylcarbamate cleavage. Untreated cells, a control treated with only the Pd^0-microspheres or incubated just with reagent **28**, showed no fluorescence under the FITC emission filter (530/35nm).

In contrast, Pd^0-microsphere loaded HeLa cells incubated with reagent **28** showed fluorescence emission under both Cy5.5 (indicating the presence of the Pd^0-microspheres) and FITC-like band pass filters (associated with the deprotection of dye **27**), showing for the first time Pd^0-mediated catalysis inside a cell. It is noteworthy that the Pd^0-microspheres did not require any exogenous co-factor (e.g. thiophenol which is know to be toxic to living cells) to assist catalysis of the reaction, but of course cells contain the thiol gluthatione, which would be an ideal co-factor.

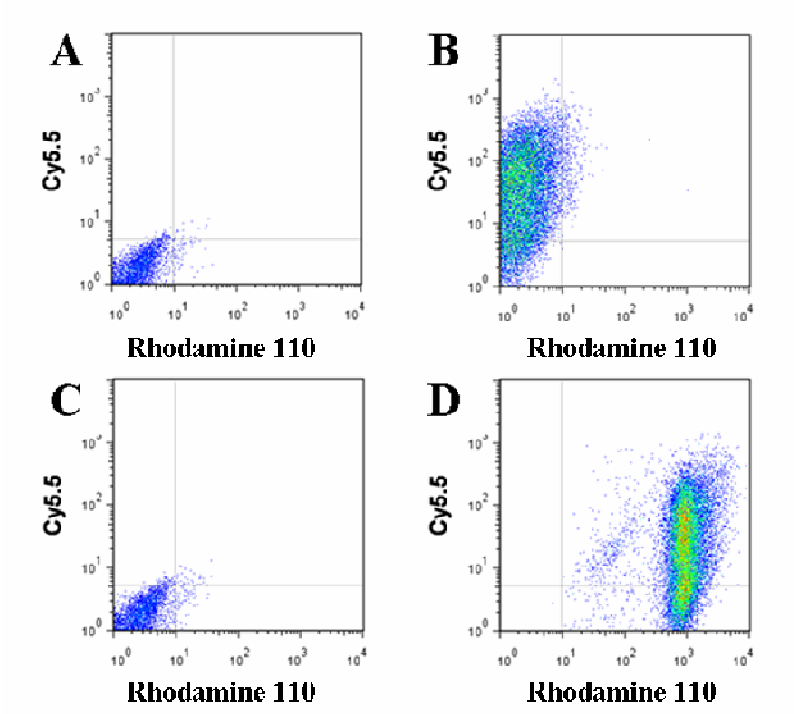

Figure 3.11 *Cytograms showing Pd^0 catalysis of allylcarbamate cleavage: y-axis represents Cy5.5 fluorescence intensity (band pass emission filter: 780/60nm) and the x-axis the FITC-like intensity of the cell (band pass emission filter: 530/30nm). (**A**) Untreated cell control. (**B**) Cells after 24h incubation with Cy5.5-Pd^0-microspheres. (**C**) Cells after 24h incubation with reagent **28**. (**D**) Pd^0-microsphere loaded cells after 24h incubation with reagent **28**.*

In addition, **Figure 3.12a** to **3.12d**, showed cytograms and histograms the uptake of Cy5.5-labelled Pd^0-microspheres (780/60 emission band pass filter) and the deprotection of **27** (530/30 emission band pass filter) in HeLa cells.

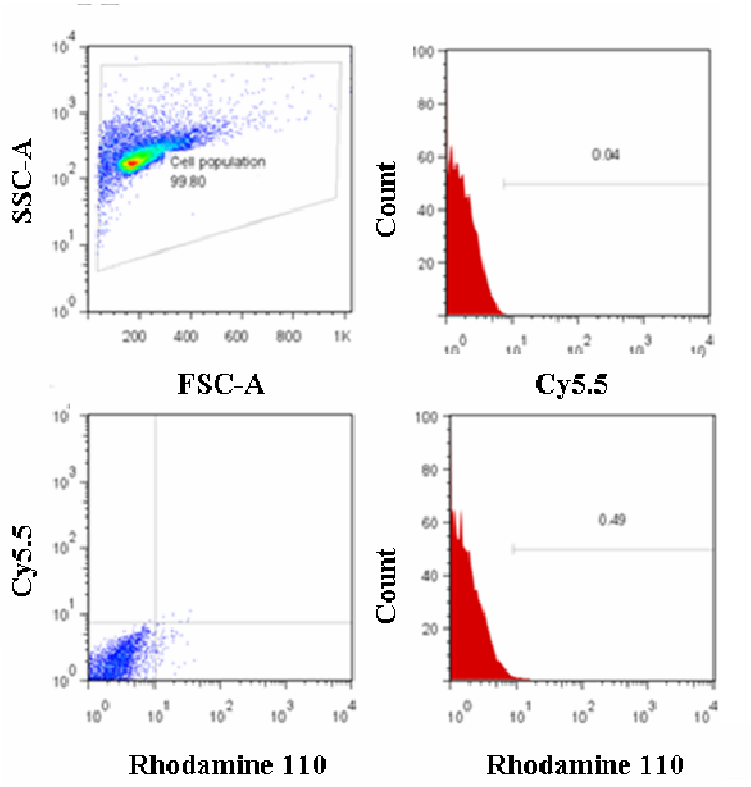

Figure 3.12a *Untreated HeLa cells.*

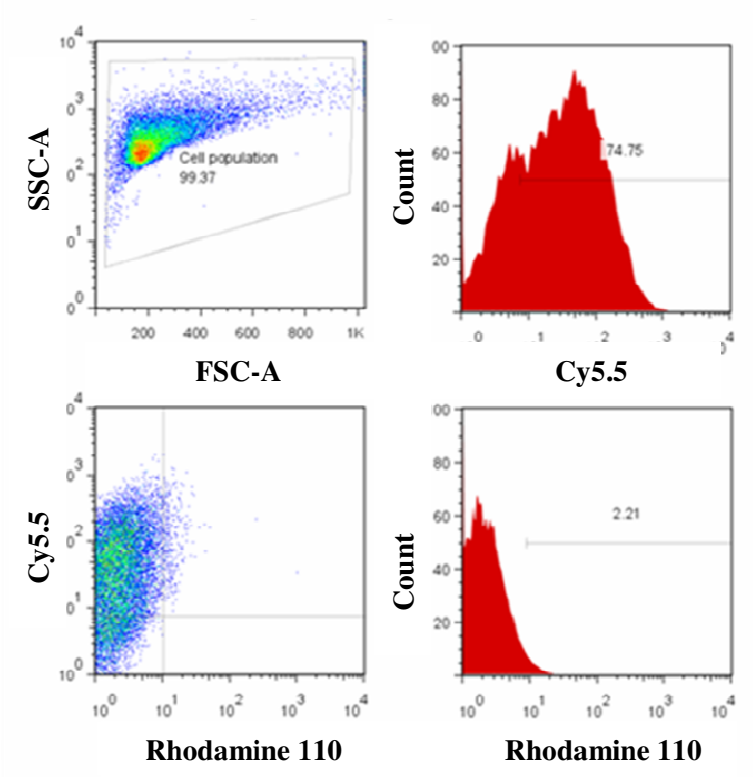

Figure 3.12b *Cells treated with Cy5.5-labelled Pd^0-microspheres.*

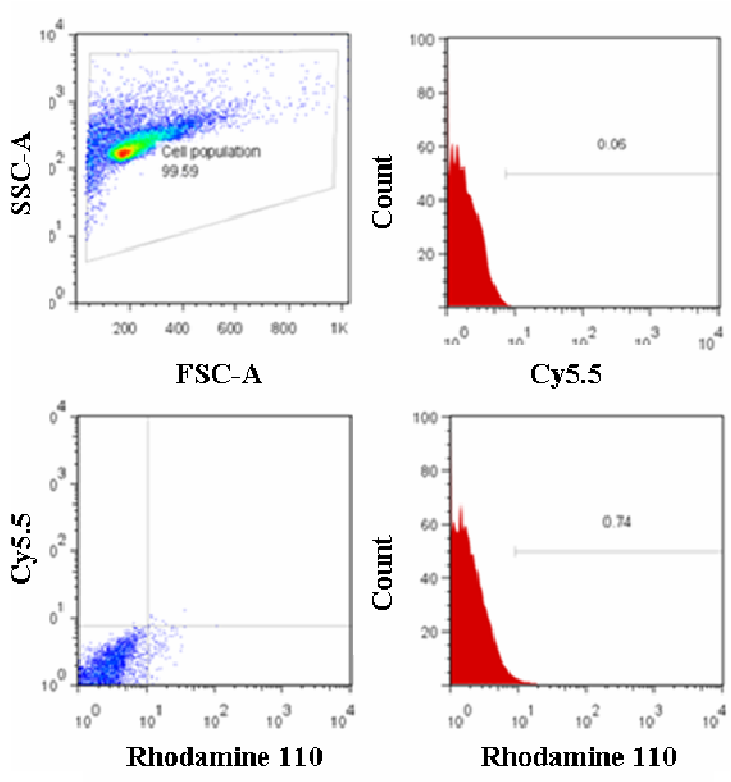

Figure 3.12c *Cells treated with reagent* ***28*** *(30 μM).*

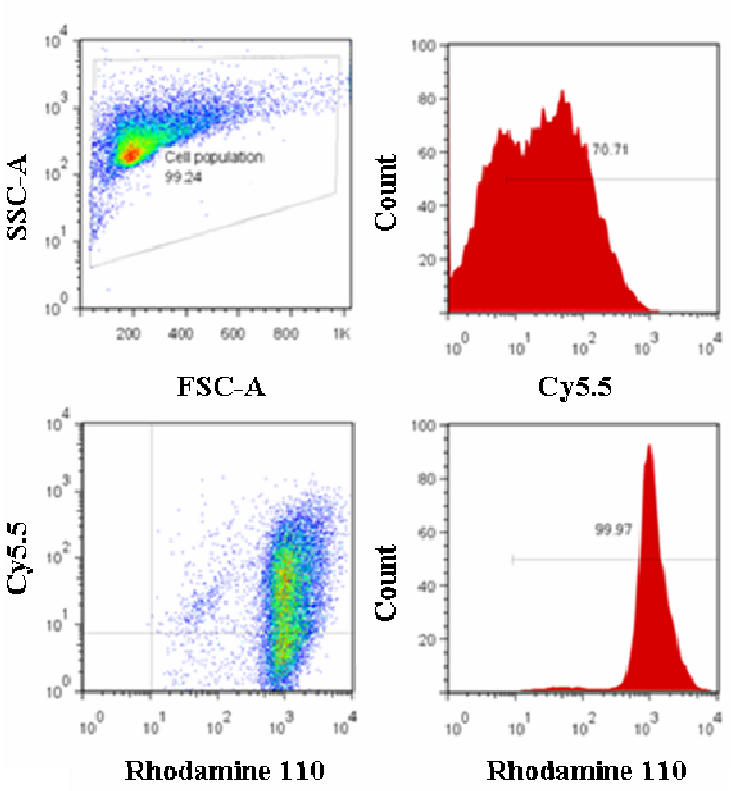

Figure 3.12d *Cells treated with Cy5.5-labelled* Pd^0*-microspheres and reagent* ***28*** *(30 μM).*

3.9.3 Analysis by Confocal Microscopy

The intracellular presence of Pd^0-microspheres and the fluorescent compound **27** was further corroborated by confocal imaging. After reaction, cells were washed and fixed with 4% formaldehyde in PBS for 30 min at room temperature.[168] During fixing the whole contents of the cell essentially become "locked in place" due to extensive cross-linking between free amino groups. Nuclei were stained with Hoeschst 33342. As shown in **Figure 3.13**, confocal microscopy verified the simultaneous presence of fluorescently-labelled Pd^0-microspheres and intracellular compound **27**.

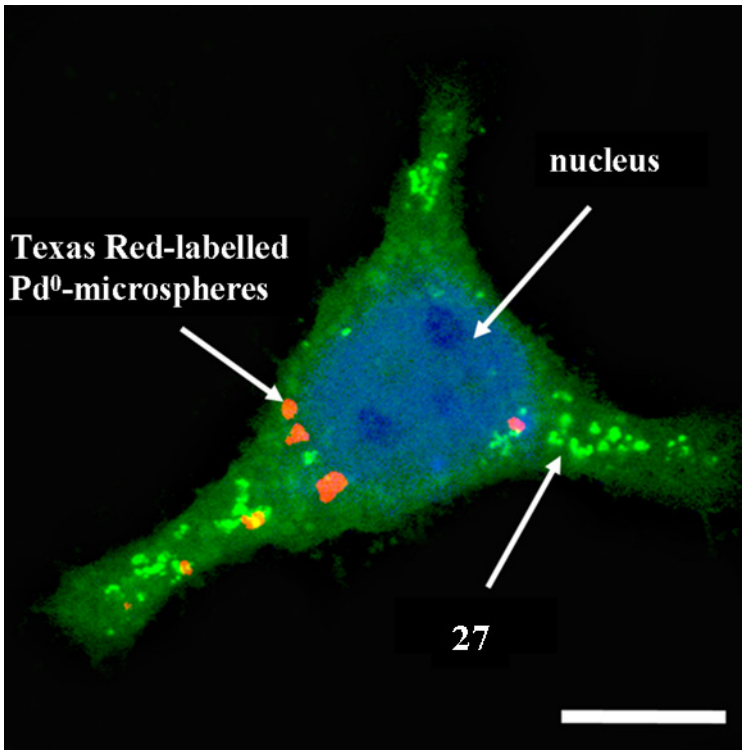

Figure 3.13 *Merged confocal image of a single HeLa cell showing a Hoechst 33342-stained nucleus (blue), Texas Red-labelled Pd^0-microspheres (red) and deprotected compound **27** (green). Microscope settings: excitation laser lines at 488, 543 and 595nm, with emission filters of 385–470nm for Hoechst 33342, 505–530nm for Rhodamine 110 and 595–615nm for Texas Red. Scale bar: 10 µm.*

3.9.4 *In-vitro* Study

The presence of thiophenol on cleavage efficiency was investigated since it is known to increase the conversion of allyl carbamate cleavage.[150] The presence of biomolecules (e.g. cell lysate or glutathione) on the efficiency of allylcarbamate cleavage was also explored (**Table 3.2**). Glutathione was also evaluated as it is naturally present in all mammalian cells.[169] A range of solvents were also used. The catalytic activity of the Pd^0-microspheres was clearly enhanced by the presence of glutathione (5mM), with turnover numbers per-palladium atom up to 30 in the presence of cell extract and glutathione. Meanwhile, the addition of PhSH (entry 17-20) or GSH (entry 21-24) and the combination of GSH and PhSH (entry 25-28) did not show any increase of **27**.

Table 3.2 *Allylcarbamate cleavage experiment in different conditions for 24 hours.*

Entry	Solvent	Reagent **28** (500 μM)	Pd^0-microspheres (10μL, 3.4μM Pd^0)	GSH (5mM)	PhSH (5mM)	Yield of **27** (%)
1	PBS	-	-	-	-	n/a
2	RPMI	-	-	-	-	n/a
3	Cell extract	-	-	-	-	n/a
4	DMF	-	-	-	-	n/a
5	PBS	+	-	-	-	0
6	RPMI	+	-	-	-	0
7	Cell extract	+	-	-	-	0
8	DMF	+	-	-	-	0
9	PBS	+	-	+	-	0
10	RPMI	+	-	+	-	0
11	Cell extract	+	-	+	-	0
12	DMF	+	-	+	-	0
13	PBS	+	+	-	-	3
14	RPMI	+	+	-	-	3
15	Cell extract	+	+	-	-	3
16	DMF	+	+	-	-	3
17	PBS	+	+	-	+	3
18	RPMI	+	+	-	+	3
19	Cell extract	+	+	-	+	3
20	DMF	+	+	-	+	3

21	PBS	+	+	+	-	21
22	RPMI	+	+	+	-	21
23	Cell extract	+	+	+	-	22
24	DMF	+	+	+	-	21
25	PBS	+	+	+	+	21
26	RPMI	+	+	+	+	21
27	Cell extract	+	+	+	+	21
28	DMF	+	+	+	+	21

3.9.5 Recycling Test of Pd^0-microspheres

Recycled microspheres from within the cells (after a reaction) were tested in solution to determine that they were still catalytically active. Pd^0-microspheres were collected from the cell lysate after a catalytic reaction had occurred. The beads were washed with water (3 times), DMF (3 times) and methanol (3 times) then collected by centrifugation at 13000 rpm for 3 minutes. The Pd^0-microspheres were used for an *in vitro* experiment of allylcarbamate cleavage. As shown in **Table 3.3**, the recycled Pd^0-microspheres showed a slightly lower conversion relative to freshly prepared Pd^0-microspheres, however this can be explained by some loss of Pd^0-microspheres during the recovery process from the cells.

Table 3.3 *In vitro experiments of allylcarbamate cleavage: freshly-prepared Pd^0-microspheres (entry 1-4) vs. recycled Pd^0-microspheres (entry 5-8).*

Entry	Solvent	**28** (0.5 mM)	Pd^0-ms (10μL, 3.4 μM Pd^0)	Recycled Pd^0-ms (~3.4 μM Pd^0)	GSH (5mM)	Yield of **27** (%)
1	PBS	+	+	-	+	21
2	RPMI	+	+	-	+	21
3	Cell extract	+	+	-	+	22
4	DMF	+	+	-	+	21
5	PBS	+	-	+	+	16
6	RPMI	+	-	+	+	15
7	Cell extract	+	-	+	+	19
8	DMF	+	-	+	+	17

3.9.6 LC-MS and HPLC Analysis of Allylcarbamate Cleavage in HeLa Cells

The characterization of the reaction products formed in cells were determined by the purification and analysis of the cell lysate which quantitatively confirmed chemical identities via LC-MS and HPLC. In order to have enough **27** to be analysed by MS and HPLC, the reaction was carried out on 3 million HeLa cells. After reaction, the cells were washed extensively with PBS to remove any extra cellular material, the cells were detached with Trypsin-EDTA, lysed with water and by subsequent sonication and the lysate was centrifuged for 5 min at 13,000 rpm. The supernatant was collected and passed through a DSC-18LT column which had been pre-washed with water. The column was washed with water to remove salts and proteins from the cell lysate, and acetonitrile was used to elute the desired product **27** from the column.

The residue was dissolved in methanol and analysed by LCMS in positive ionization mode. LCMS suggested the presence of rhodamine 110 (**27**) with the mass found 331.0 (**Figure 3.14**). In addition, HPLC analysis of the cell lysate showed a retention times with a sample standard of **27** at around 3.2 minutes (**Figure 3.15**).

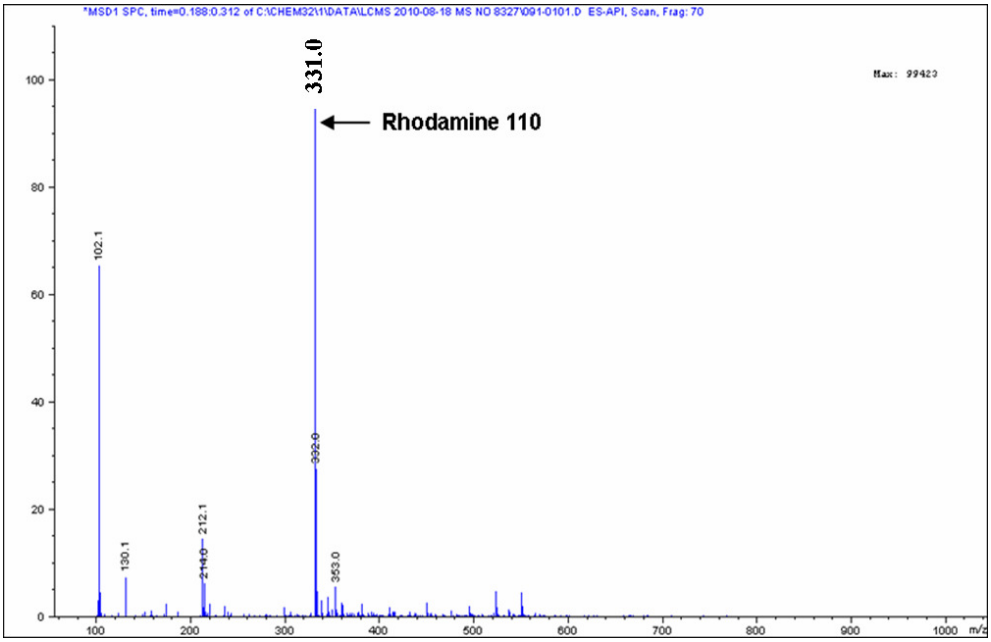

Figure 3.14 *LCMS analysis from the cell lysate confirming the presence of rhodamine 110,* ***27****.*

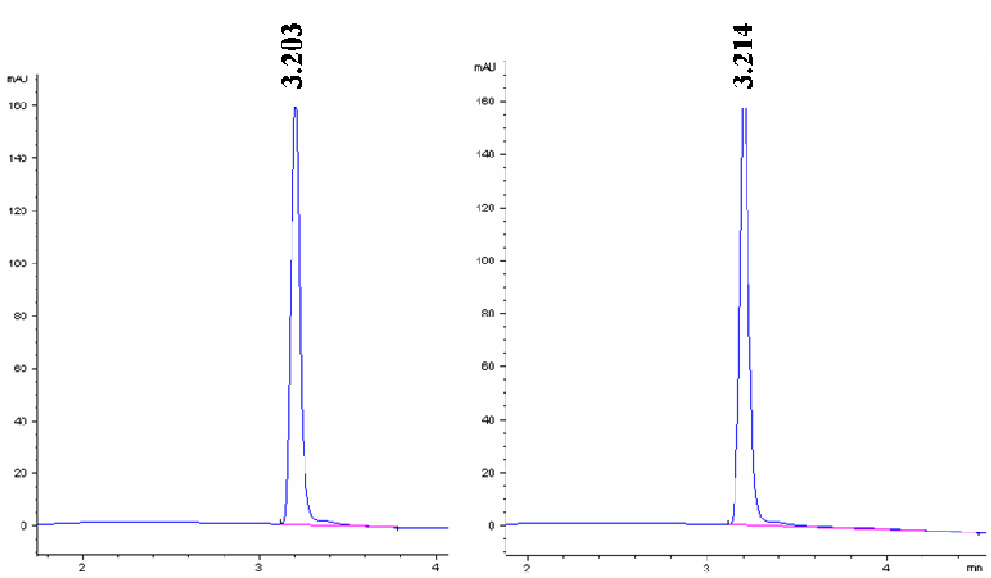

Figure 3.15 *HPLC analysis of standard rhodamine 110 (left) absorbance at 495nm was compared with cell lysate (right).*

3.10 Making C–C Bonds within Cells

Encouraged by the allylcarbamate cleavage in a living cell, research was expanded to a more challenging reaction. The Suzuki-Miyaura cross-coupling of arylboronates or esters with aryl halides (or triflates) in the presence of Pd^0 permits ready access to a spectacular range of biaryls.[129, 130] To explore the intracellular formation of a carbon-carbon cross-coupled product, an unambiguous fluorescence-detectable cell-based experiment was designed, based on palladium mediated synthesis of a fluorescent dye (anthofluorescein, **3**)[73] via an aryl-aryl cross-coupling reaction (**Scheme 3.6**).

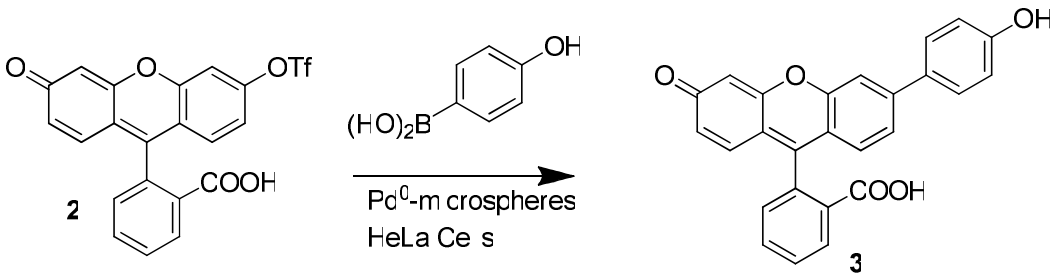

Scheme 3.6 *Anthofluorescein (**3**) was synthesised via palladium-catalyzed cross-coupling between 3'-(trifluoromethanesulfonyl)fluorescein (**2**) and p-hydroxyphenylboronic acid.*

3.10.1 Synthesis Anthofluorescein in Living Cells

Suzuki palladium-catalyzed cross-coupling of fluorescein mono-triflate (**2**) with *p*-hydroxyphenylboronic acid was expected to give anthofluorescein within the cells. However, a preliminary study found the existence of a high background due to the 3'-(trifluoromethanesulfonyl)fluorescein, **2** (λex = 488nm, λem = 510nm), which made cell analysis by confocal microscopy or FACS analysis difficult (overlapping with anthofluorescein).

To address this problem, a non-fluorescent mono-triflate (**29**) was synthesized. A methyl group was introduced into 6'- position of 3'-(trifluoromethanesulfonyl)fluorescein to lock the fluoran polycycle into the lactone. The installation of the methyl group forced the generation of the ring closed, colorless and nonfluorecent lactone form **29**, therefore eliminating any fluorescent background (**Scheme 3.7**). This was synthesised by alkylation of **2** with methyl iodide at 150°C for 60 minutes resulting colorless compound **29**.

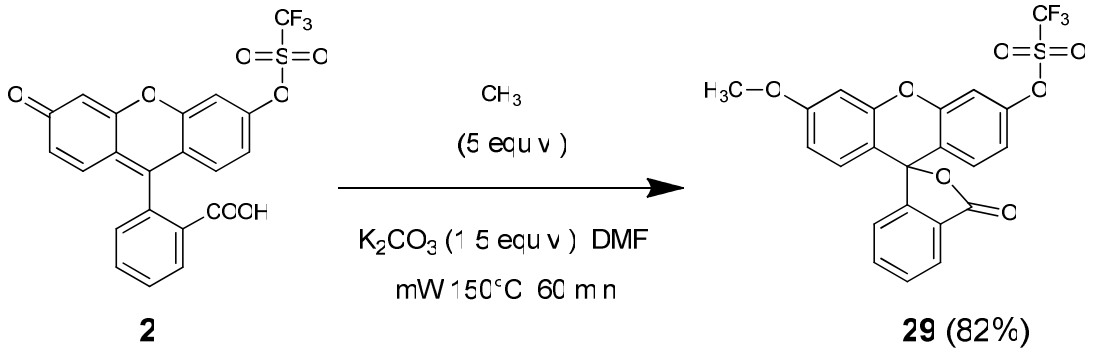

Scheme 3.7 *Synthesis of 6'-methyl-3'-(trifluoromethanesulfonyl)fluorescein (**29**).*[139]

3.10.2 Designing Fluorescent Small Molecule that Target the Mitochondria

One of the main problems in designing small molecule/reagents for intracellular catalysis is the ability for them to stay within the cell over time and a general procedure for quantification either by flow cytometry or confocal microscopy. Leaching out of cross-coupled products from the cells may cause difficulties during

cell analysis. In addition, a turn-on emission increase or shift in excitation/emission profiles is preferred over a turn-off emission-quenching response.[51]

The presence of the triphenylphosphonium moiety (a lipophilic cation) is known to promote direct accumulation several hundred-fold within mitochondria.[170] Molecules were designed both to turn-on fluorescence after reaction and target the mitochondria by introducing a triphenylphosphonium moiety (**30**) in the boronic acid (**31**) to form compound **32** (**Scheme 3.8**).

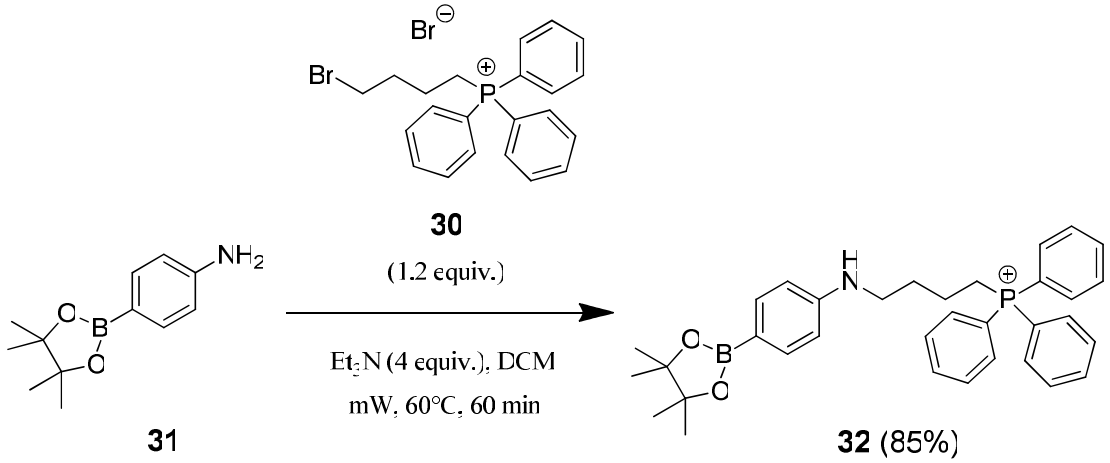

Scheme 3.8 *Synthesis of Synthesis of (4-(4'-(pinacolatoboron)phenylamino]butyl)-triphenyl phosphonium bromide (**32**).*

3.10.3 Synthesis of (4-(4'-(3''-methoxyfluoran-6''-yl)phenylamino]butyl)triphenyl phosphonium bromide (33)

In vitro synthesis of compound **33** was carried out to allow an investigation of its fluorescent and localisation properties (**Scheme 3.9**). The cross-coupling of non-fluorescent mono-triflate **29** and the alkylaminophenylboronate **32** should "unlock" the disrupted conjugation of the fluoran polycycle **29** by opening of the lactone, resulting in colored and fluorescent product **33.**

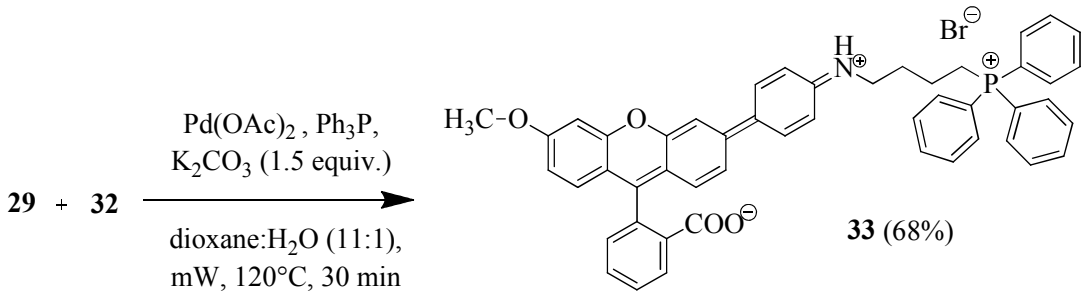

Scheme 3.9 *Synthesis of (4-(4'-(3''-methoxyfluoran-6''-yl)phenylamino] butyl)triphenyl phosphonium bromide,* ***33.***

3.10.4 Study of the Fluorescent Properties of Dye 33

Optical properties of dye **33** were investigated by spectrophotometric analysis. The quantum yield of compound **33** was calculated as 0.32. Spectrophotometric analysis showed that absorbance of **33** (10 μM) (**Figure 3.16**). Meanwhile, emission spectra of compound **33** (λem = 520 – 540nm) has a broad and slightly red-shift emission (**Figure 3.17**), which will partially overlap with the Texas-Red emission spectra.

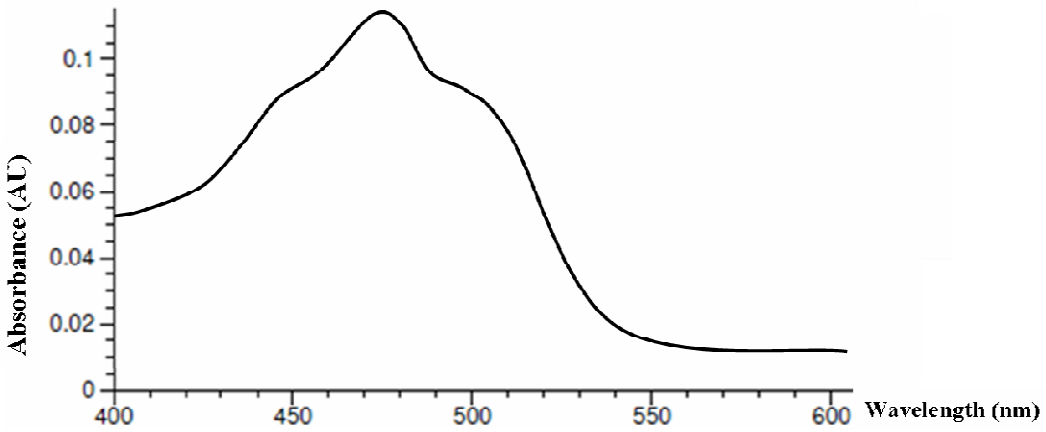

Figure 3.16 *Absorption spectra of 10μM solution of* ***33*** *(20% glycerol in water).*

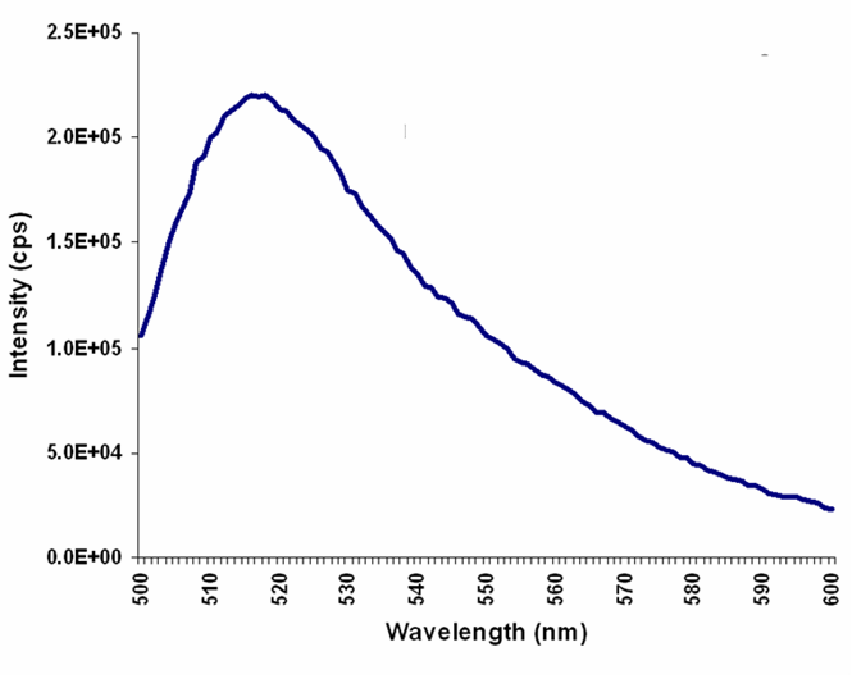

Figure 3.17 *Emission spectra of* ***33*** *with excitation at 480nm (1 μM, 20% glycerol in water);* E_x/E_m *= 480/520nm.*

3.10.5 Hydrolytically Stable Compound 29

Hydrolytically stable of **29** was further investigated by synthesising the hydrolysed product, 6'-methylfluorescein **34** (**Scheme 3.10**).

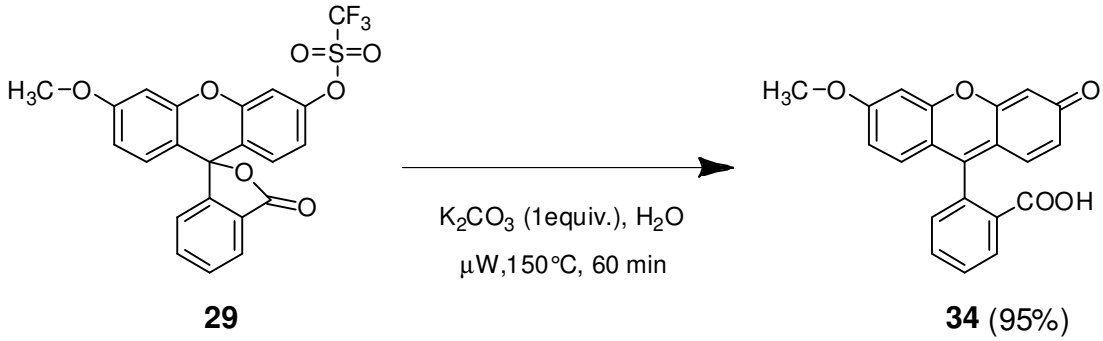

29 **34** (95%)

Scheme 3.10 *Synthesis of hydrolysed product, 6'-(methyl)fluorescein* ***34****.*

In order to investigate the hydrolytic stability of **29**, compound **29** was stirred in PBS at 37°C for 48. After reaction, the formation of **34** was analysed using HPLC. The result showed a retention times corresponded to compound **29** at around 3.7

minutes. In contrast, no formation of **34** was observed where the retention time at around 4.2 minutes (**section 4.3.4.4**), suggesting compound **29 is** hydrolytically stable in the experiment condition used (**Figure 3.18**). Meanwhile, cell based experiment in different conditions were carried out to investigate hydrolytic stable of **29** (**section 3.10.6.1**, **3.10.7** and **3.10.8**).

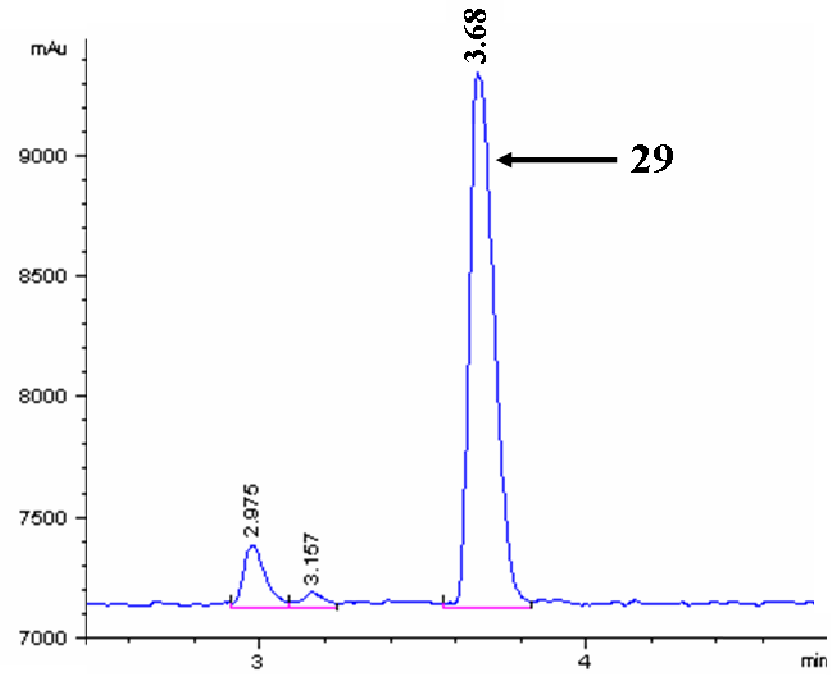

Figure 3.18 *HPLC analysis showed the peak of compound* ***29*** *at 3.7 minutes, while absence of* ***34*** *(4.2 minutes), at absorbance at 495nm.*

3.10.6 Pd^0-mediated Intracellular Synthesis in HeLa Cells

HeLa cells Pre-loaded with Cy5.5-labelled Pd^0-microspheres were incubated with 20 μM of cell permeable compound **29** and **32**. After 48 hours, cross-coupling of these compounds catalysed by Pd^0 would form dye **33** and at the same time localising into the mitochondria (**Scheme 3.11**).

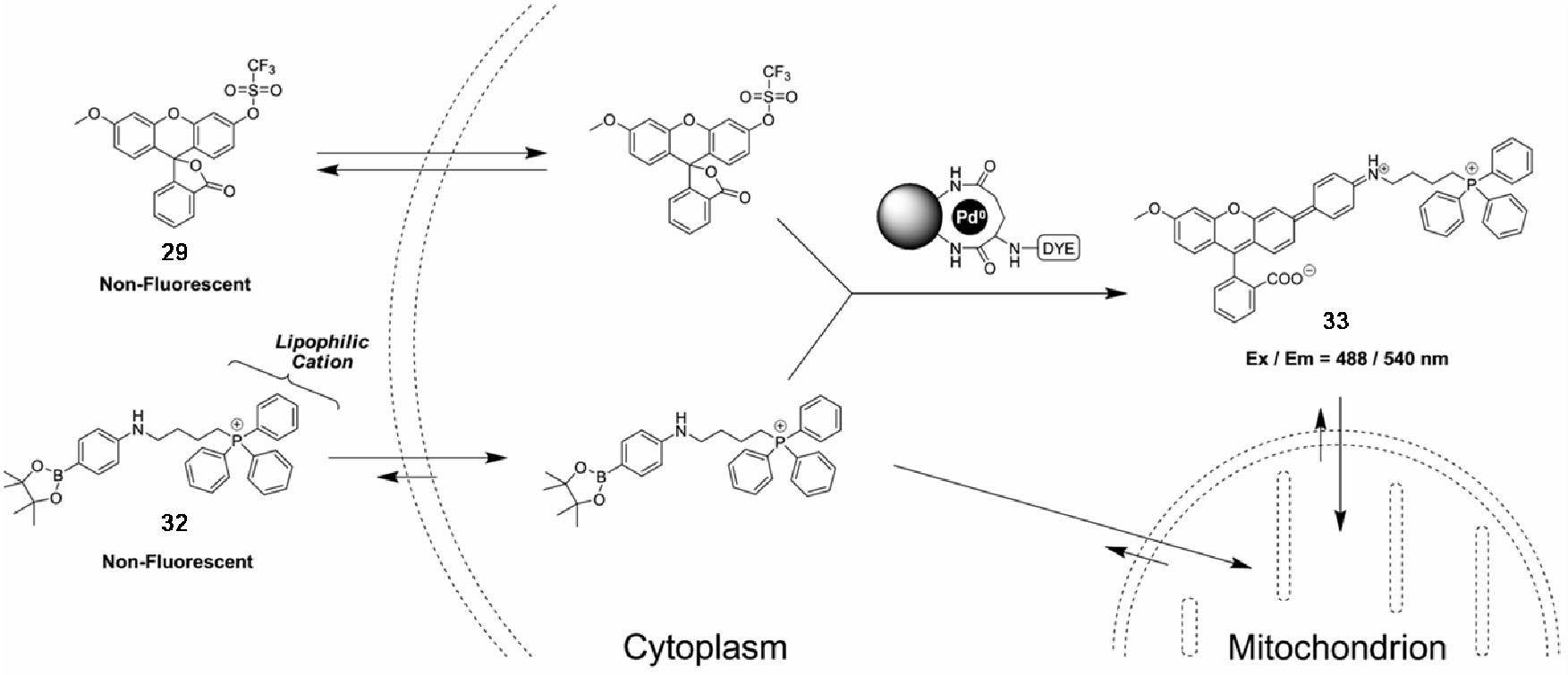

Scheme 3.11 *The idea behind intracellular Pd^0-mediated Suzuki-Miyaura cross-coupled dye synthesis. Pd^0-microspheres were loaded into HeLa cells prior to incubation for 48 hours with reagents 29 and 32.*

3.10.6.1 Flow cytometry analysis

After incubation, cells were washed twice with PBS, harvested with trypsin/EDTA and resuspended in 2% FCS in PBS buffer. The intracellular presence of Cy5.5-labelled Pd^0-microspheres and compound **33** was determined by flow cytometry under different band pass emission filters (780/60 and 576/26, respectively). As shown in **Figure 3.19**, only the cells treated with Cy5.5-labelled Pd^0-microspheres, reagent **29** and **32** were fluorescent under both emission filters, indicating the Pd-mediated synthesis of compound **33**. **Figure 3.20a** to **3.20d** showed cytograms and histograms showing the uptake of Cy5.5-labelled Pd^0-microspheres (780/60 emission band pass filter) and the synthesis of the Suzuki cross-coupled dye **33** (576/26 emission band pass filter) in HeLa cells (**section 4.3.4.6**).

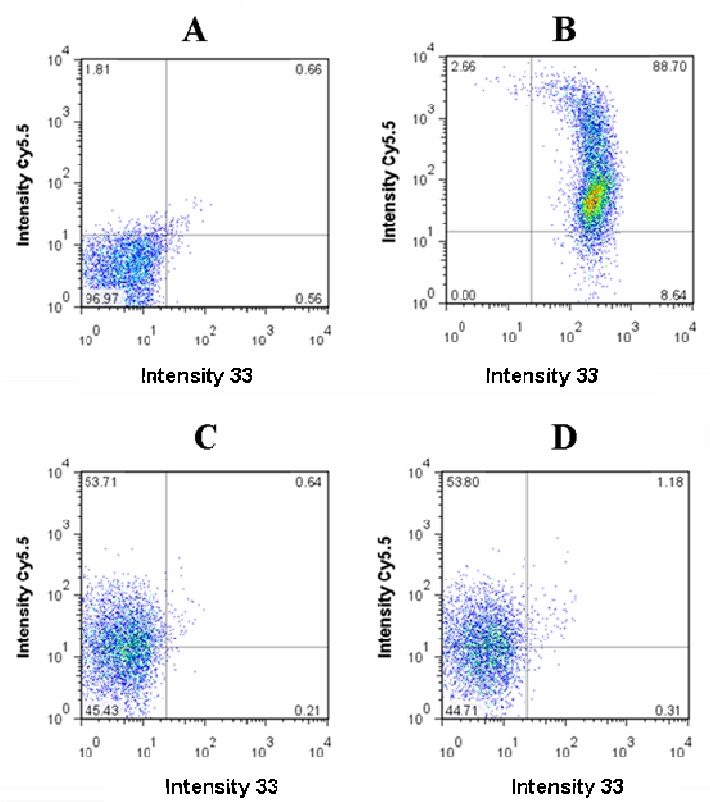

Figure 3.19 *Cytograms showing the uptake of Cy5.5-labelled Pd^0-microspheres, (**A**) Untreated cells, (**B**) Cell treated with Pd^0-microspheres and reagents **29** and **32**, (**C**) Cell treated with Pd^0-microspheres, (**D**) Cells treated with Pd^0-microspheres and **29**.*

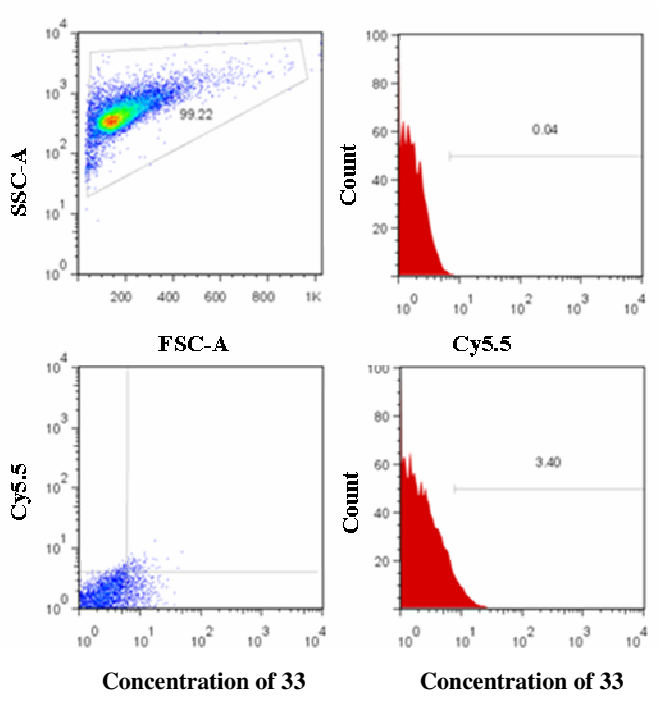

Figure 3.20a *Untreated HeLa cells.*

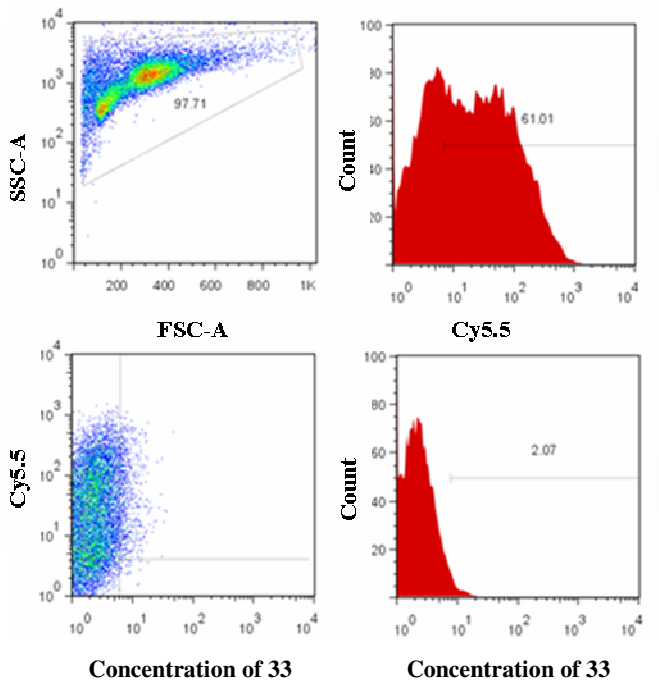

Figure 3.20b *Cells treated with Cy5.5-labelled Pd^0-microspheres.*

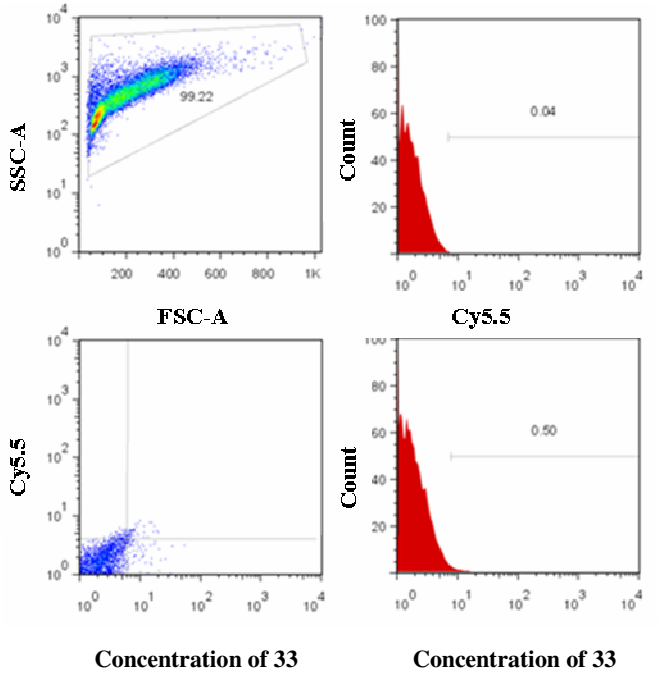

Figure 3.20c *Cells treated with reagent* ***29*** *(20 μM) and* ***32*** *(20 μM).*

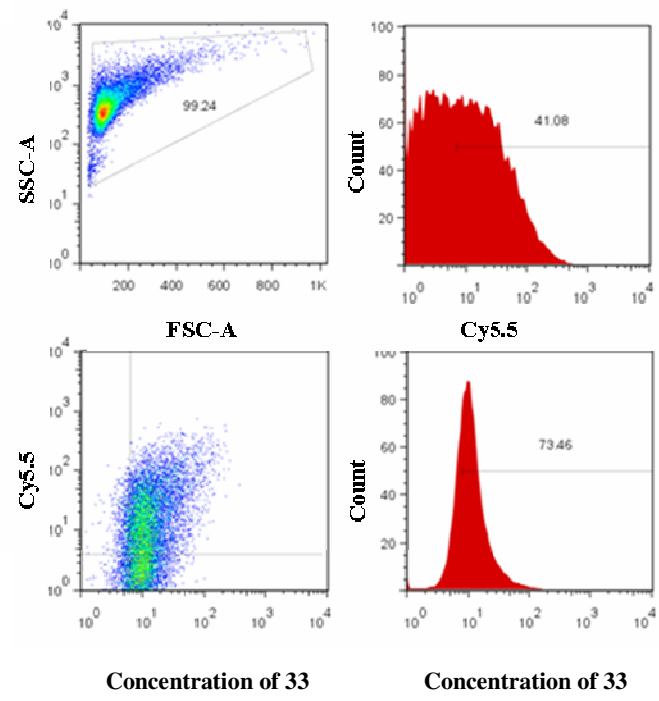

Figure 3.20d *Cells treated with* Pd^0*-microspheres labelled with Texas red, reagents* ***29*** *(20 μM) and* ***32*** *(20 μM).*

These results showed that the Pd^0 beads and both reagents (**29** and **32**) are needed in order to generate the new product **33** (x-axis). Controls were carried out, both in solution and in cell experiments, to rule out the possibility of any fluorescence seen being the result of hydrolysed mono-triflate (**34**), indeed mono-triflate was remarkably robust surviving changed in the presence of the Pd^0-microspheres for over 48 hours.

3.10.6.2 Confocal microscopy

Flow cytometry studies were corroborated with confocal microscopy (**section 4.3.4.7**). After reaction, the cell were washed with PBS and stained with Hoechst 33342 as well as with a mitochondria stain in order to prove accumulation dye **33** in the mitochondria. **Figure 3.21** shows deconvolved confocal images of a single cell under different filters.

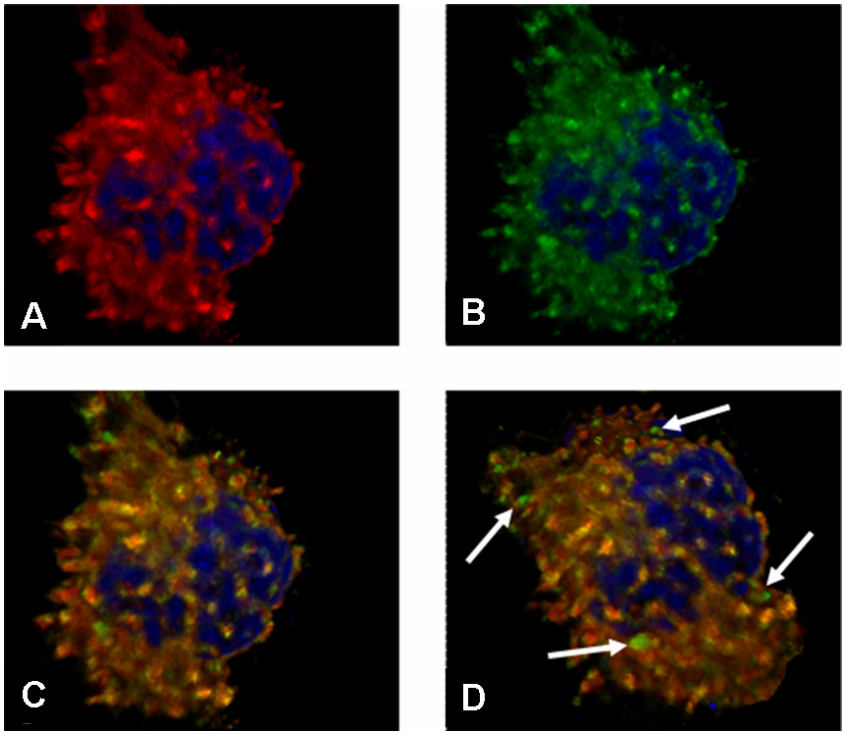

Figure 3.21 *Deconvolved confocal image of a single cell. (**A**) Cell nucleus (blue) and mitochondria (red). (**B**) Cell nucleus (blue) and in cellulo synthesised compound **33** (green). (**C**) Merged (orange indicates colocalization). (**D**) Merged image of the same cell observed from a different angle. White arrow indicates the presence of a Pd^0-microsphere, which was imaged under 550/20 emission filter along with compound **33** and did not localize within mitochondria.*

Due to the broad excitation/emission spectra of Texas Red, both the Suzuki-Miyaura product **33** and the Texas Red-labelled were imaged under the same fluorescent channel. The Pd^0-microspheres could be identified as they did not co-localize with the mitochondria tracker dye or the nucleus stain, thus corroborating their cytoplasmatic location (**Figure 3.22**). As expected, cellular experiments verified that, compound **33** exclusively localised within the mitochondria.

Since Texas red has a very broad emission spectra it was possible to image Texas red labelled Pd^0-microspheres both with the emission filter 540-560 and 595-615nm. Due to partial overlap between compound **33** and Texas Red emission spectra, both **33** and Pd^0-microspheres were imaged under the 540-560nm emission filter (**Figure 3.22b**). Under the emission filter 595-615nm the Pd^0-microspheres were imaged while compound **33** was not, enabling us to distinguish fluorescence originating between Pd^0-microspheres and compound **33** (**Figure 3.22a**).

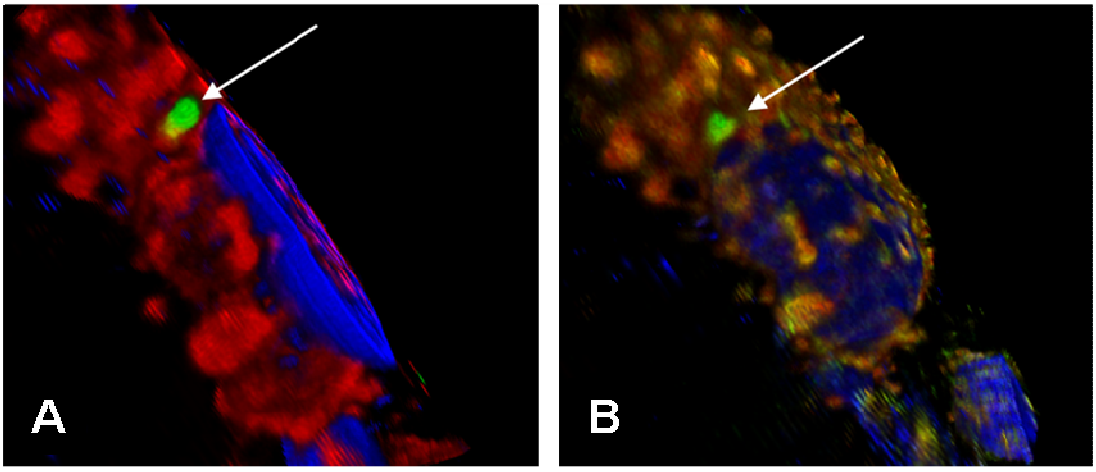

Figure 3.22 *Showing 3D deconvolved image of the same cell after processing the confocal pictures. (**A**) Texas Red –labelled Pd^0-microspheres in the emission channel (green), cell nucleus (blue), and fluorescently-stained mitochondria (red). (**B**) Merged images showed Texas Red-labelled Pd^0-microspheres did not localise with the mitochondria tracker dye or the nuclei dye, thus corroborating their cytoplasmatic location. Images were processed with the AutoQuant X software.*

3.10.7 *In Vitro* Experiments

In vitro experiments of the Suzuki-Miyaura cross-coupling (**Table 3.4**) were carried out in PBS, DMF and cell extract. There was no visible conversion of compound **29** to 6'-methylfluorescein (**34**) in the presence or absence of Pd^0 under a variety of conditions. On the other hand, the presence of Pd^0 showed the formation of **33** due to the cross-coupling between **29** and **32** (entries 17 – 20).

Table 3.4 *In vitro experiments of Suzuki reaction in different conditions for 48 hours.*

Entry	Solvent	Reagent **29** (0.8mM)	Reagent **32** (0.8mM)	Pd^0-ms (10 μL 3.4 μM pd^0)	Yield of **33 (%)**
1	PBS	-	-	-	n/a
2	RPMI	-	-	-	n/a
3	Cell extract	-	-	-	n/a
4	DMF	-	-	-	n/a
5	PBS	+	-	-	n/a
6	RPMI	+	-	-	n/a
7	Cell extract	+	-	-	n/a
8	DMF	+	-	-	n/a
9	PBS	+	+	-	0
10	RPMI	+	+	-	0
11	Cell extract	+	+	-	0
12	DMF	+	+	-	0
13	PBS	+	-	+	n/a
14	RPMI	+	-	+	n/a
15	Cell extract	+	-	+	n/a
16	DMF	+	-	+	n/a
17	PBS	+	+	+	22
18	RPMI	+	+	+	21
19	Cell extract	+	+	+	22
20	DMF	+	+	+	24

3.10.8 LC-MS and HPLC Analysis of Suzuki Product (33) in HeLa Cells

The characterization of the reaction products formed in cells was carried out by the purification and analysis of the cell lysate which quantitatively confirmed chemical identities via MS and HPLC. The cells lysate was prepared as previous described (**section 3.9.6**). A DSC-18LT column was used to flush the non-desired products from the column, and the product eluted with 10% MeOH in DCM. The residue was analysed by LC-MS (**Figure 3.23**) gave the mass 738.2 corresponding to **33** and the

mass of compound **32** was found 536.2, which is known to be able to accumulate directly into mitochondria without undergoing reaction. While it was not possible to determine the overall quantity of unreacted boronate **32**, the identification of compound **32** in the extracts suggests that **32** was in excess in the mitochondria. Compound **29** or its hydrolysed derivative **34** were not detected.

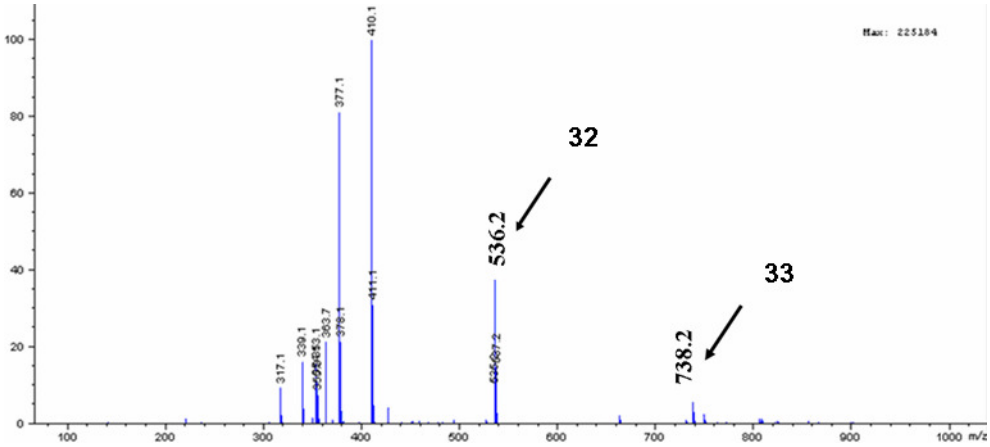

Figure 3.23 *LCMS analysis from cell lysate confirming the presence compound* ***33.***

This result was corroborated by HPLC analysis confirmed the retention time peaks of dye **33** and cells lysate at around 3.8 minutes (**Figure 3.24**).

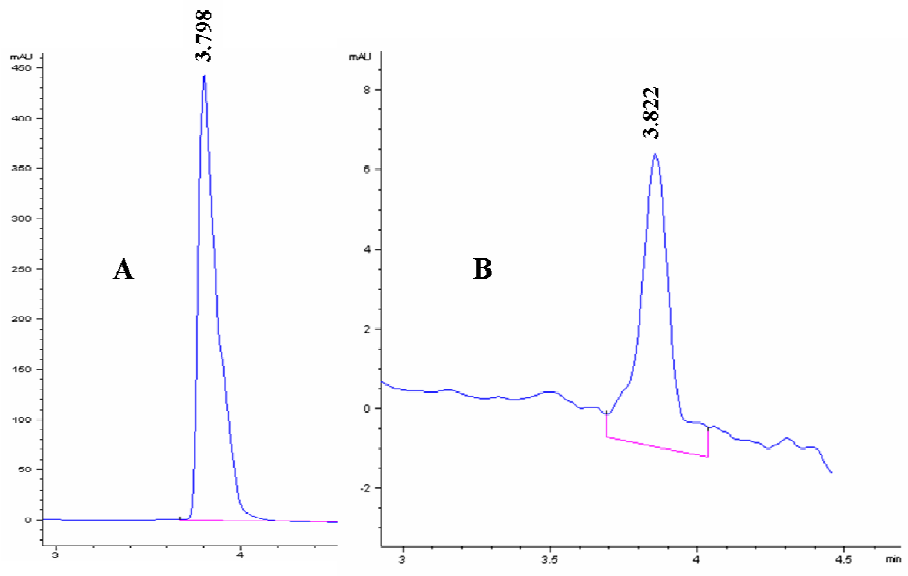

Figure 3.24 *HPLC analysis of (**A**) compound **33** and (**B**) cell lysate.*

3.11 Conclusion

In conclusion, the first Pd^0-based heterogeneous catalyst with the ability to cross cell membranes, stay harmlessly within the cytoplasm for days, and carry out for the first time artificial chemistry has been described. The Pd^0-microsphere catalyst was successfully prepared by immobilising Pd^0 nanoparticles in the microspheres through electronic interactions between the electron-rich of the aryl rings of microspheres and Pd^{2+} atoms followed by extensive cross-linking with the bis acid chloride of racemic Fmoc-Glutamate. Pd^{2+} were reduced to Pd^0 with 10% hydrazine hydrate in methanol gave Pd^0-microspheres.

As expected, Pd^0-microspheres are catalytically active based on Alloc deprotection in solution with and without presence of thiophenol. Furthermore, the Pd^0-microspheres are able to penetrate the cell membrane after 24 hours incubated with HeLa cells. Meanwhile cytotoxicity tests indicated low levels of toxicity (<4%) and good cell viability (>90%) after 48 hours of contact with the Pd^0-microspheres.

This engineered "pseudo-organelle" demonstrated intracellular catalytic activity of an unnatural metal towards exogenous materials. Pd^0-microspheres were successfully used to perform intracellular catalysis both deprotection and C-C formation, such as the Alloc deprotection and a Suzuki–Miyaura cross-coupling reaction (fluorophore synthesis).

This investigation provides the basis for the customization of heterogeneous unnatural catalysts as tools for creative applications in chemical biology (such as *in situ* labelling of cellular structures), pharmacology (for example, *in cellulo* pro-drug activation of hydrophilic molecules with low cell penetrability for functional screening in cellular disease models) and, potentially, in medicine (for example, the systemic administration of a pro-drug with local activation via implant-captured catalysts as well as intracellular drug synthesis).

CHAPTER 4:
EXPERIMENTAL

4.1 General Information

4.1.1 Chemicals

All solvents and reagents were obtained from commercial suppliers and used without purification, unless otherwise stated.

4.1.2 Equipments

^{1}H and **^{13}C NMR** spectra were recorded on a Bruker ava-500 (500 and 75 MHz, respectively) in the solvents indicated at 298 K. Chemical shifts are reported on the δ scale in ppm using the residual non-deuterated solvent as the internal standard or the ^{13}C natural abundance of the deuterated solvent. Coupling constants (*J*) are reported in Hz. **Low Resolution Mass Spectra (LRMS)** were obtained using a Hewlett Packard LCMS 1100 ChemStation with a G1946B mass detector, equipped with an electrospray ion source. **High Resolution Mass Spectra (HRMS)** was performed using Bruker 3.0 T Apex II Spectrometer. **Thin layer chromatography (TLC)** was performed using Alugram SIL G/UV/254 precoated plates. **UV/Vis** measurement was performing on an Agilent 8453 spectrophotometer. **Column chromatography** was performed on silica gel using Keiselgel 60, 230-400 mesh (Merck). **Infrared** (IR) spectra were obtained on a Fourier transform IR Bruker Tensor 27 Spectrometer. All samples were run neat and frequencies are reported in cm^{-1}. Only frequencies corresponding to significant functional groups are reported. **Reverse phase analytical HPLC (RP HPLC)** was performed using an Agilent 1100 Chemstation, and compounds were detected using an ELSD detector. All solvents used were HPLC grade. **Preparative reverse phase-HPLC** purifications were performed on an Agilent Technologies HP1100 Chemstation eluting with (A) H_2O/0.1% TFA and (B) CH_3CN/0.1% TFA on a Waters X-Terra C-18 preparative

column (150 mm x 19 mm, 5 μm), at a flow rate of 5 mL/min. The following gradient was used: 100% (A) to 40% (B) over 5 min, 40% to 70% (B) over 20 min, 70% to 100% (B) over 4 min, with detection by UV at 214, 254 and 440 nm. **Microwave** assisted heating was carried out by irradiating the mixture in a Biotage Initiator at 2.45 GHz. **Scanning Electron Microscopy (SEM)** images were obtained on a Philips XL30CP SEM with a X-ray analysis and HKL channel Electron Backscatter Diffraction (EBSD) system on samples coated with a thin layer of gold, to a depth of approximately 20 nm, under vacuum. **High Resolution Transmission Electron Microscopy (HR-TEM)** analyses were conducted on a JEM-2011 (JEOL, 200Kv) at the Electron Microscopy Laboratory in the School of Chemistry, EastChem University of St Andrews. **X-ray powder diffraction (XRD)** spectra were taken on a Philips PW1800. **Inductively coupled plasma atomic emission spectrometry (ICP-OES)** was obtained on a Perkin Elmer Optima 5300 DV ICPOES sensitive between 0.0002-1000ppm. **Fluorescence spectra** were recorded on a Jobin Yvon SPEX Fluoromax, using 1cm path length fused silica cuvettes. Live HeLa cells were monitored using an x20 objective **Leica fluorescence microscope** under brightlight and 488nm excitation. **Flow cytometry analysis** was carried out on a Becton Dickinson (BD) FACS Aria^{TM} using FACSDivaTM or FlowJo software. The absorbance of 96-well plates was read on a Benchmark Bio-Rad **microplate reader** at 570nm using the Microplate manager 4.0 software. **Confocal** images were taken on a Leica SP5 confocal microscope and Zeiss 510 Meta software was used for digital acquisition. Deconvolution was carried out using **AutoQuant X** software**.**

4.1.3 Biological Section

Media, sera and antibiotics were purchased from Gibco or Sigma-Aldrich. Cell culture was performed in a 5% CO_2 atmosphere at 37°C in a SteriCult 200 (Hucoa-Erloss) incubator. HeLa cells were cultured in RPMI media supplemented with 10% fetal bovine serum (FBS), glutamine (4 mM) and antibiotics (penicillin and streptomycin, 100 units/mL). The day before the assay, cells were washed with phosphate buffered saline (PBS), detached with trypsin/EDTA, counted, and diluted with media to the appropriate concentration.

4.2 Experimental for Chapter 2

4.2.1 Synthesis of 3´-(trifluoromethanesulfonyl)fluorescein (2)[73]

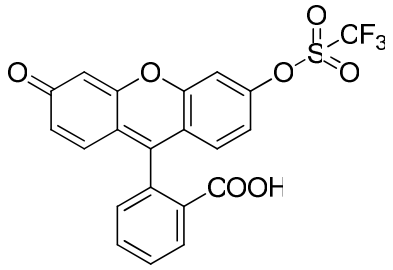

Fluoroscein **1** (536 mg, 1.6 mmol), *N*-phenyl-bis(trifluoromethanesulfonimide) (644 mg, 1.80 mmol) and potassium carbonate (322 mg, 2.40 mmol) were stirred in dry DMF (16 mL) and microwave-irradiated at 80 °C for 20 minutes. The reaction mixture was partitioned between EtOAc (120 mL) and 1M HCl (80 mL), the aqueous layer was extracted with EtOAc (2 x 30 mL), and the combined organics dried ($MgSO_4$) and reduced *in vacuo*. Purification of the residue via chromatography on silica gel (4:1 Hex:EtOAc) afforded 3´-(trifluoromethanesulfonyl)fluorescein as an off-white solid (453 mg, 0.98 mmol, 61%). M.p.: 160-162°C; IR: ν= cm^{-1}: 3385.08, 1735, 1609, 1420, 1207, 1206, 1137, 1106; ^{1}H NMR (500 MHz, DMSO-d_6) δ 10.33 (1H, s, OH), 8.07 (1H, d, *J* 7.1 Hz, ArH), 7.87-7.74 (2H, m, ArH), 7.72 (1H, d, *J* 2.5 Hz, ArH), 7.39 (1H, d, *J* 7.3 Hz, ArH), 7.26 (1H, dd, *J* 8.8 Hz, 2.6 Hz, ArH), 7.04 (1H, d, *J* 8.9 Hz, ArH), 6.78 (1H, s, ArH), 6.66 (2H, s, ArH). ^{13}C NMR (75 MHz, DMSO-d_6) δ 168.01 (C=O), 159.49 (C), 151.74 (C), 151.14 (C), 150.77 (C), 149.18 (C), 135.61 (CH), 130.24 (CH x2), 128.74 (CH), 125.23 (C), 124.59 (CH), 123.69 (CH), 119.55 (C), 116.78 (CH), 113.20 (CH), 110.28 (CH), 108.35 (C), 101.93 (CH), 80.83 (C); MS (ES^+): m/z 465.0 [100, $(M+H)^+$]; HRMS calcd for $C_{21}H_{11}F_3O_7S$: 464.0178, found: 464.0192 ; RP HPLC t_R = 4.9 minutes (100% purity, ELSD); E_x/E_m: 477/510nm.

4.2.2 Synthesis of 3´-hydroxy-6´-(p-hydroxyphenyl)fluoran, (3)[73]

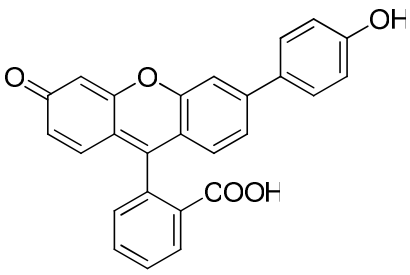

3´-(trifluoromethanesulfonyl)fluorescein (186 mg, 0.40 mmol), 4-hydroxyphenyl boronic acid (66 mg, 0.48 mmol), palladium acetate (5 mg, 0.02 mmol) and triphenylphosphine (21 mg, 0.08 mmol) were stirred in degassed dioxane (10 mL). Potassium carbonate (83 mg, 0.60 mmol) in water (1 mL) was added and the resulting mixture was microwave irradiated at 120 °C for 30 minutes. For heterogeneous catalysis using polystyrene resin captured palladium (XL-RC Pd^0).

3´-(trifluoromethanesulfonyl)fluorescein (186 mg, 0.40 mmol), 4-hydroxyphenyl boronic acid (66 mg, 0.48 mmol), potassium carbonate (83 mg, 0.60 mmol) and XL-RC Pd^0 (180 mg, 5%mmol) were stirred in water (2mL) microwave irradiated at 120 °C for 10 minutes. The reaction mixture was partitioned between EtOAc (50 mL) and 1 M HCl (40 mL), the aqueous layer was extracted with EtOAc (2 x 20 mL) and the combined organics dried ($MgSO_4$) and concentrated *in vacuo*. Purification of the residue via chromatography on silica gel (4:1 Hex:EtOAc) afforded the anthofluorescein as a dark red solid (127 mg, 0.31 mmol, 78%). M.p.: 133-135°C; IR: ν= cm^{-1}: 3438, 2971, 1759, 1599, 1420, 1199, 1100; ^1H NMR (500 MHz, CD_3OD) δ 8.03-8.00 (1H, m, ArH), 7.79-7.66 (2H, m, ArH), 7.51-7.47 (3H, m, ArH), 7.21 (1H, dd, *J* 8.3 Hz, 1.9 Hz, ArH), 7.17-7.14 (1H, m, ArH), 6.79 (2H, d, *J* 8.7 Hz, ArH), 6.70 (1H, d, *J* 8.3 Hz, ArH), 6.65 (1H, d, *J* 2.3 Hz, ArH), 6.56-6.45 (2H, m, ArH); ^{13}C NMR (75 MHz, CD_3OD) δ 171.54 (C=O), 161.25 (C=O), 159.08 (C), 154.62 (C), 154.01 (C), 153.08 (C), 145.24 (C), 136.68 (CH), 131.91 (C), 131.19 (CH), 130.18 (CH), 129.33 (CH), 129.28 (CH), 127.92 (C), 125.87 (CH), 125.27 (CH), 123.04 (CH), 118.15 (C), 116.82 (CH), 116.70 (C), 115.30 (CH), 113.65 (CH), 111.08 (CH), 103.67 (C); MS (ES^+): m/z 409.1 [100, $(M+H)^+$]; HRMS calcd for $C_{26}H_{16}O_5$: 408.0998, found: 408.1358; RP HPLC t_R = 4.7 minutes (100% purity, ELSD); Φ: 0.30 (pH 8, 20% glycerol); E_x/E_m: 530/570nm.

4.2.3 Synthesis of 3´-acetyloxy-6´-(p-acetyloxyphenyl)fluoran (4)[73]

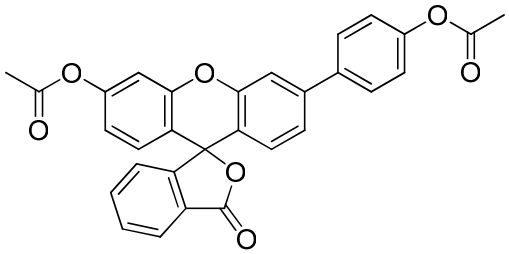

3´-hydroxy-6´-(*p*-hydroxyphenyl)fluoran (30 mg, 0.07 mmol) was stirred in acetic anhydride:pyridine (1:1, 2 mL) for 16 hours. The solvent was reduced *in vacuo* and the residue was partitioned between EtOAc (10 mL) and 1M HCl (5 mL). The organic layer was dried ($MgSO_4$) and reduced *in vacuo*. Purification of the residue via chromatography on silica gel (5:1 Hex:EtOAc) afforded 3´-acetyloxy-6´-(*p*-acetyloxyphenyl)fluoran as a white solid (30 mg, 0.061 mmol, 87%). M.p.: 158-160^{o}C; IR: ν= cm^{-1}: 3205, 3053, 1728, 1605, 1428, 1251, 1111; ^{1}H NMR (500 MHz, CD_3OD) δ 8.06-8.03 (1H, m, ArH), 7.78-7.67 (2H, m, ArH), 7.66-7.62 (2H, m, ArH), 7.54 (1H, d, *J* 1.8 Hz, ArH), 7.32 (1H, dd, *J* 8.3 Hz, 1.8 Hz, ArH), 7.18-7.15 (4H, m, ArH), 6.87-6.83 (3H, m, ArH), 2.28 (3H, s, CH_3), 2.25 (3H, s, CH_3); ^{13}C NMR (75 Hz, CD_3OD) δ 171.10 (C=O), 171.0 (C=O), 170.50 (C=O), 154.50 (C), 153.80 (C), 153.00 (C), 152.60 (C), 152.40 (C), 144.40 (C), 138.10 (C), 136.90 (CH), 131.50 (CH), 130.00 (CH), 129.50 (CH), 129.20 (CH), 127.30 (C), 126.10 (CH), 125.10 (CH), 123.90 (CH), 123.30 (CH), 119.10 (CH), 118.90 (C), 117.70 (C), 116.20 (CH), 111.60 (CH), 83.50 (C), 20.90 (CH_3), 20.97 (CH_3); MS (ES^+): m/z 493.1 [100, $(M+H)^+$]; HRMS calcd for $C_{30}H_{20}O_7$: 492.1209, found: 492.1201; RP HPLC t_R = 4.4 minutes (100% purity, ELSD).

4.2.4 Cell Labelling/viability Assay

35 µL of a 0.25 mM solution of compound **3** (PBS:DMSO, 99:1 v/v) were added to the corresponding well containing HeLa cells (total volume = 350 µL, final concentration of 3´-acetyloxy-6´-(*p*-acetyloxyphenyl)fluoran (25 µM) and incubated for 2h (37°C and 5% CO_2). The culture medium was removed, the cells were washed twice with PBS and phenol red-free media added. HeLa cells were imaged using a

x20 objective (Leica fluorescence microscope) under brightlight and 488nm excitation.

4.2.5 Toxicity Studies

Cytotoxicity tests were carried out on HeLa cells in triplicate for 2, 4 and 8 hours. Cells were plated in a 24-well plate at a density of 10,000 cells/well and left to grow for 24 hours. Aliquots of the compound under investigation (25 μM) were added and cells monitored under a fluorescent microscope. After incubation (2 hr, 4 hr and 8 hr) media was replaced with 360 μL of fresh media (phenol red free) along with 40 μL of 3-(4,5-dimethylthiozol-2-yl)2,5-diphenyl tetrazolium bromide), MTT (5 mg/mL) and the cells incubated for 3 hours at 37°C. After the incubation the resulting formazan crystals were dissolved by adding 300 μL of MTT solubilisation solution. The absorbance was measured spectrophotometrically at a wavelength of 570 nm and results compared to untreated cells.

4.2.6 Absorbance Studies

Absorption spectra were recorded on a Varian Cary-300 spectrometer using 1cm pathlength fused silica cuvettes. The spectral bandwidth was 2nm. Fluorescence spectra were recorded on a SPEX Fluoromax, using 1cm pathlength fused silica cuvettes. The excitation and emission slits were 7nm.

4.2.7 Excitation/Emission Analysis

Fluorescence spectra were recorded on a SPEX Fluoromax, using 1cm pathlength fused silica cuvettes.

4.2.8 Synthesis of Anthofluorescein Derivative

General protocol for synthesising anthofluorescein derivatives is outlined as below:

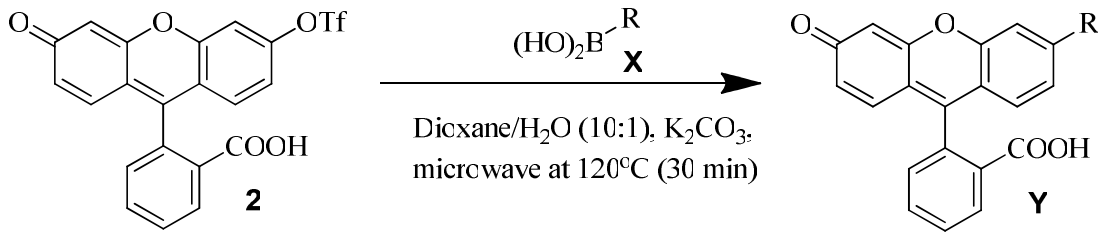

3´-(Trifluoromethanesulfonyl)fluorescein, **2,** (186 mg, 0.40 mmol), boronic acid, **X** (0.48 mmol), palladium acetate (4.5 mg, 0.02 mmol) and triphenylphosphine (21 mg, 0.08 mmol) were stirred in degassed dioxane (10 mL). Potassium carbonate (83 mg, 0.60 mmol) in water (1 mL) was added and the resulting mixture was microwave irradiated at 120 °C for 30 minutes. The reaction mixture was partitioned between EtOAc (50 mL) and 1 M HCl (40 mL), the aqueous layer was extracted with EtOAc (2 x 20 mL) and the combined organics dried ($MgSO_4$) and concentrated *in vacuo*. Purification of the residue via chromatography on silica gel (4:1 Hex:EtOAc) or (1:9 MeOH:DCM) for compounds **19** and **20**.

4.2.8.1 Synthesis of 2-(3-(benzo[d][1,3]dioxol-5-yl)-6-oxo-6H-xanthen-9-yl)benzoate (5)

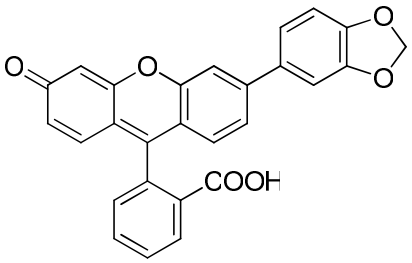

X = (3,4-Methylenedioxyphenyl)boronic acid, afforded **5** as dark red solid (135 mg, 0.31 mmol, 78%). M.p.: 145-148°C; IR: ν= cm^{-1}: 3213, 2923, 2358, 1728, 1606, 1405, 1200,1112; ^1H NMR (500 MHz, CD_3OD): δ = 8.09-8.07(1H, m, ArH), 7.85-7.81 (2H, m, ArH), 7.61 (1H, dd, *J* 8.3 Hz, 1.8 Hz, ArH), 7.37-7.32 (3H, m, ArH), 7.24-7.21 (1H, m, ArH), 7.02 (1H, d, *J* 8.2 Hz, ArH), 6.79 (2H, d, *J* 8.6 Hz, ArH),

6.63 (2H, d, *J* 2.3 Hz, ArH), 6.50-6.01 (2H, m, ArH); ^{13}C NMR (75 MHz, CD_3OD) δ 170.28 (C=O), 168.56 (C=O), 159.62 (C), 152.41 (C), 151.70 (C), 150.91 (C), 148.24 (C), 135.58 (CH), 131.91 (C), 131.19 (CH), 130.18 (CH), 129.33 (CH), 129.28 (CH), 127.92 (C), 125.87 (CH), 125.27 (CH), 123.04 (CH), 118.15 (C), 116.82 (CH), 116.70 (C), 115.30 (CH), 113.65 (CH), 111.08 (CH), 100.64 (C), 82.23 (CH_2); MS (ES^+): m/z 437.1 [100, $(M+H)^+$]; HRMS calcd for $C_{27}H_{16}O_6$: 437.0947, found: 437.1027 ; RP HPLC t_R = 3.8 minutes (100% purity, ELSD); Φ: 0.51; E_x/E_m: 480/532nm.

4.2.8.2 Synthesise 2-(3-(2,3-dihydrobenzo[b][1,4]dioxin-6-yl)-6-oxo-6H-xanthen-9-yl)benzoic acid (6)

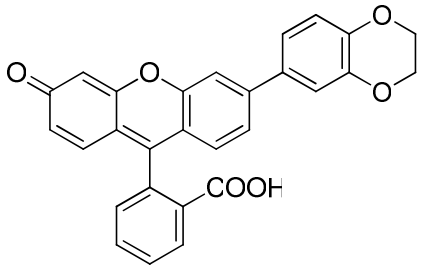

X = 1,4-Benzodioxane-6-boronic acid, afforded **6** as dark red solid (131 mg, 0.29 mmol, 73%). M.p.: 134-136^{o}C; IR: ν= cm^{-1}: 3308, 3021, 1760, 1559, 1430, 1110; ^{1}H NMR (500 MHz, CD_3OD): δ = 8.04-8.03 (1H, m, ArH), 7.81-7.74 (2H, m, ArH), 7.59-7.23 (3H, m, ArH), 7.23 (1H, dd, *J* 8.3 Hz, 1.8 Hz, ArH), 7.17-7.14 (1H, m, ArH), 6.78 (1H, d, *J* 8.7 Hz, ArH), 6.70 (1H, d, *J* 8.5 Hz, ArH), 6.65 (1H, d, *J* 2.3 Hz, ArH), 6.56-6.45 (2H, m, ArH), 4.28 (4H, s, ArH); ^{13}C NMR (75 MHz, CD_3OD) δ 171.54 (C=O), 165.25 (C=O), 159.60 (C), 154.39 (C), 152.01 (C), 149.08 (C), 145.24 (C), 135.65 (CH), 132.91 (C), 131.19 (CH), 130.18 (CH), 129.33 (CH), 129.28 (CH), 127.92 (C), 125.87 (CH), 125.27 (CH), 123.04 (CH), 118.15 (C), 116.82 (CH), 116.70 (C), 115.30 (CH), 113.65 (CH), 111.08 (CH), 103.67 (C), 64.11 (CH_2), 64.00 (CH_2); MS (ES^+): m/z 451.1 [100, $(M+H)^+$]; HRMS calcd for $C_{28}H_{18}O_6$: 450.1103, found: 450.1111; RP HPLC t_R = 4.3 minutes (100% purity, ELSD); Φ: 0.50; E_x/E_m: 480/536nm.

4.2.8.3 Synthesis (3-(2,3-dihydrobenzofuran-6-yl)-6-oxo-6H- xanthen-9-yl) benzoic acid (7)

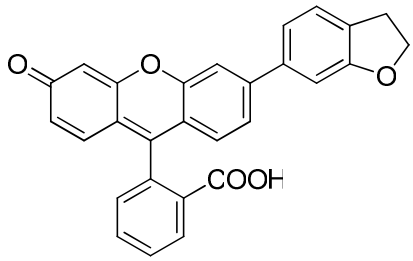

X = 2,3-Dihydrobenzofuran-5-boronic acid, afforded **7** as dark red solid (131 mg, 0.30 mmol, 75%). M.p.: 127-131^{o}C; IR: ν= cm^{-1}: 3361, 2957, 1755, 1594, 1450, 1216, 1100; ^{1}H NMR (500 MHz, CD_3OD): δ = 8.04-8.01 (1H, m, ArH), 7.79-7.66 (2H, m, ArH), 7.51-7.47 (3H, m, ArH), 7.21 (1H, dd, *J* 8.3 Hz, 1.9 Hz, ArH), 7.17-7.14 (1H, m, ArH), 6.79 (2H, d, *J* 8.7 Hz, ArH), 6.70 (1H, d, *J* 8.3 Hz, ArH), 6.65 (1H, d, *J* 2.3 Hz, ArH), 6.56-6.45 (2H, m, ArH), 4.13 (t, J = 6.3 Hz, 4H, OCH_2CH_2); ^{13}C NMR (75 MHz, CD_3OD) δ 171.24 (C=O), 164.24 (C=O), 159.08 (C), 154.62 (C), 154.01 (C), 153.08 (C), 145.24 (C), 136.68 (CH), 131.91 (C), 131.19 (CH), 130.18 (CH), 129.33 (CH), 129.28 (CH), 127.92 (C), 125.87 (CH), 125.27 (CH), 123.04 (CH), 118.15 (C), 116.82 (CH), 116.70 (C), 115.30 (CH), 113.65 (CH), 111.08 (CH), 103.67 (C), 64.14 (CH_2), 60.03 (CH_2); MS (ES^+): m/z 435.1 [100, $(M+H)^+$]; HRMS calcd for $C_{28}H_{18}O_5$: 434.1154, found: 434.1163; RP HPLC t_R = 4.5 minutes (100% purity, ELSD); Φ: 0.49; E_x/E_m: 482/528nm.

4.2.8.4 Synthesis of 2-(3-(1H-indol-6-yl)-6-oxo-6H-xanthen-9-yl)benzoic acid (8)

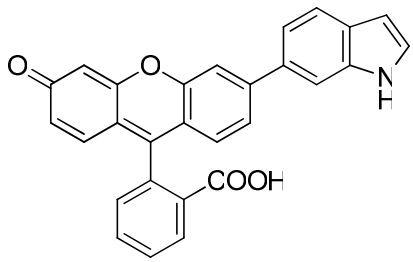

X = 5-Indolylboronic acid, afforded **8** as dark red solid (121 mg, 0.28 mmol, 70%). M.p.: 130-133^{o}C; IR: ν= cm^{-1}: 3338, 2961, 1760, 1559, 1430, 1178, 1110; ^{1}H NMR (500 MHz, CD_3OD): δ = 8.04-8.08 (1H, m, ArH), 7.81-7.64 (2H, m, ArH), 7.51-7.47 (3H, m, ArH), 7.21 (1H, dd, *J* 8.3 Hz, 1.9 Hz, ArH), 7.17-7.14 (1H, m, ArH), 6.79

(2H, d, *J* 8.7 Hz, ArH), 6.70 (1H, d, *J* 8.3 Hz, ArH), 6.68 (1H, d, *J* 2.3 Hz, ArH), 6.56-6.45 (2H, m, ArH); ^{13}C NMR (75 MHz, CD_3OD) δ 171.54 (C=O), 161.25 (C=O), 159.08 (C), 154.62 (C), 154.01 (C), 153.08 (C), 145.24 (C), 136.68 (CH), 131.91 (C), 131.19 (CH), 130.18 (CH), 129.33 (CH), 129.28 (CH), 127.92 (C), 125.87 (CH), 125.27 (CH), 123.04 (CH), 118.15 (C), 116.82 (CH), 116.70 (C), 115.30 (CH), 113.65 (CH), 111.08 (CH), 103.67 (C); MS (ES^+): m/z 432.1 [100, $(M+H)^+$]; HRMS calcd for $C_{28}H_{17}NO_4$: 431.1158, found: 431.1241 ; RP HPLC t_R = 3.6 minutes (100% purity, ELSD); Φ: 0.47; E_x/E_m: 480/531nm.

4.2.8.5 Synthesis of 2-(3-(1-methyl-1H-indol-5-yl)-6-oxo-6H-xanthen-9-yl)benzoate (9)

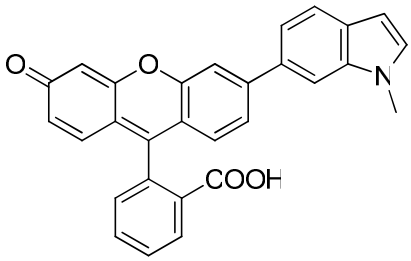

X = 1-Methyl-1H-indole-5-boronic acid, afforded **9** as dark red solid (138 mg, 0.31 mmol, 78%). M.p.: 140-142^{o}C; IR: ν= cm^{-1}: 3265, 3012, 1746, 1559, 1380, 1189, 1090; ^{1}H NMR (500 MHz, CD_3OD): δ = 8.03-8.01 (1H, m, ArH), 7.79-7.66 (2H, m, ArH), 7.51-7.47 (3H, m, ArH), 7.21 (1H, dd, *J* 8.3 Hz, 1.9 Hz, ArH), 7.17-7.14 (1H, m, ArH), 6.79 (2H, d, *J* 8.7 Hz, ArH), 6.70 (1H, d, *J* 8.3 Hz, ArH), 6.59 (1H, d, *J* 2.3 Hz, ArH), 6.56-6.45 (2H, m, ArH), 3.75 (CH_3); ^{13}C NMR (75 MHz, CD_3OD) δ 171.34 (C=O), 162.25 (C=O), 159.08 (C), 154.62 (C), 154.01 (C), 153.08 (C), 145.24 (C), 136.68 (CH), 131.91 (C), 131.19 (CH), 130.18 (CH), 129.33 (CH), 129.28 (CH), 127.92 (C), 125.87 (CH), 125.27 (CH), 123.04 (CH), 118.15 (C), 116.82 (CH), 116.70 (C), 115.30 (CH), 113.65 (CH), 111.08 (CH), 103.67 (C), 52.32 (CH_3); MS (ES^+): m/z 446.1 [100, $(M+H)^+$]; HRMS calcd for $C_{29}H_{19}NO_4$: 445.1314, found: 445.1298 RP HPLC t_R = 4.3 minutes (100% purity, ELSD); Φ: 0.56; E_x/E_m: 480/537nm.

4.2.8.6 Synthesis of 2-(3-(furan-2-yl)-6-oxo-6H-xanthen-9-yl)benzoic acid (10)

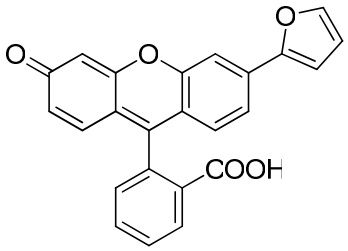

X = 2-Furanylboronic acid, afforded **10** as orange solid (96 mg, 0.25 mmol, 63%). M.p.: 137-141^{o}C; IR: ν= cm^{-1}: 3230, 3092, 1720, 1605, 1390, 1120, 1100; ^{1}H NMR (500 MHz, CD_3OD): δ = 8.04-8.02 (1H, m, ArH), 7.82-7.78 (2H, m, ArH), 7.51-7.47 (3H, m, ArH), 7.31 (1H, dd, *J* 8.2 Hz, 1.8 Hz, ArH), 7.27-7.13 (1H, m, ArH), 6.79 (2H, d, *J* 8.7 Hz, ArH), 6.70 (1H, d, *J* 8.3 Hz, ArH), 6.56-6.45 (2H, m, ArH); ^{13}C NMR (75 MHz, CD_3OD) δ 170.44 (C=O), 165.24 (C=O), 159.08 (C), 154.62 (C), 154.01 (C), 153.08 (C), 145.24 (C), 136.68 (CH), 131.91 (C), 131.19 (CH), 130.18 (CH), 129.33 (CH), 129.28 (CH), 127.92 (C), 125.87 (CH), 125.27 (CH), 123.04 (CH), 118.15 (C), 116.82 (CH), 116.70 (C), 115.30 (CH), 113.65 (CH), 111.08 (CH); MS (ES^{+}): m/z 383.1 [100, (M+H)$^{+}$]; HRMS calcd for $C_{24}H_{14}O_5$: 382.0841, found 382.1205; RP HPLC t_R = 3.7 minutes (100% purity, ELSD); Φ: 0.45; E_x/E_m: 482/533nm.

4.2.8.7 Synthesis of 2-(3-oxo-6-(thiophen-2-yl)-3H-xanthen-9-yl)benzoic acid (11)

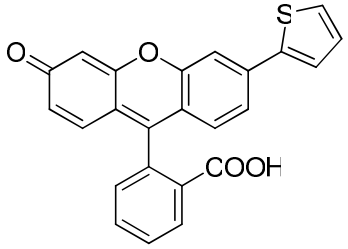

X = 2-Thienylboronic acid, afforded **11** as yellow solid (140 mg, 0.35 mmol, 88%). M.p.: 126-130^{o}C; IR: ν= cm^{-1}: 3280, 3010, 1760, 1559, 1430, 1178, 1110; ^{1}H NMR (500 MHz, CD_3OD): δ = 8.03-8.00 (1H, m, ArH), 7.92-7.79 (2H, m, ArH), 7.41-7.45 (3H, m, ArH), 7.31 (1H, dd, *J* 8.2 Hz, 1.8 Hz, ArH), 7.24-7.13 (1H, m, ArH), 6.79

(2H, d, *J* 8.6 Hz, ArH), 6.70 (1H, d, *J* 8.3 Hz, ArH), 6.56-6.45 (2H, m, ArH); ^{13}C NMR (75 MHz, CD_3OD) δ 170.44 (C=O), 165.24 (C=O), 159.08 (C), 154.62 (C), 154.01 (C), 153.08 (C), 145.24 (C), 136.68 (CH), 131.91 (C), 131.19 (CH), 130.18 (CH), 129.33 (CH), 129.28 (CH), 127.92 (C), 125.87 (CH), 125.27 (CH), 123.04 (CH), 118.15 (C), 116.82 (CH), 116.70 (C), 115.30 (CH), 113.65 (CH), 111.08 (CH); MS (ES^+): m/z 399.1 [100, $(M+H)^+$]; HRMS calcd for $C_{24}H_{14}O_4S$: 398.0613, found 398.0454; RP HPLC t_R = 4.1 minutes (100% purity, ELSD); Φ: 0.46; E_x/E_m: 477/528nm.

4.2.8.8 Synthesis of 2-(3-(benzofuran-2-yl)-6-oxo-6H-xanthen-9-yl)benzoic acid (12)

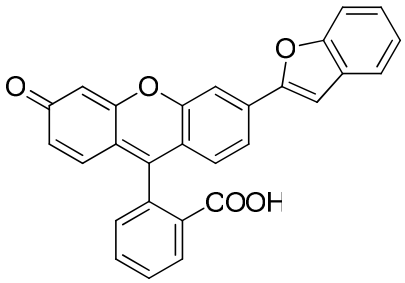

X = 2-Benzofuranylboronic acid, afforded **12** as pale orange solid (139 mg, 0.32 mmol, 80%). M.p.: 155-157^{o}C; IR: ν= cm^{-1}: 3338, 2990, 1730, 1590, 1430, 1178, 1110; ^{1}H NMR (500 MHz, CD_3OD): δ = 8.04-8.00 (1H, m, ArH), 7.82-7.76 (2H, m, ArH), 7.51-7.47 (3H, m, ArH), 7.31 (1H, dd, *J* 8.3 Hz, 1.8 Hz, ArH), 7.37-7.14 (1H, m, ArH), 6.83 (2H, d, *J* 8.6 Hz, ArH), 6.86 (1H, d, *J* 8.3 Hz, ArH), 6.65 (1H, d, *J* 2.3 Hz, ArH), 6.46-6.41 (2H, m, ArH); ^{13}C NMR (75 MHz, CD_3OD) δ 170.64 (C=O), 164.23 (C=O), 159.08 (C), 154.62 (C), 154.01 (C), 153.58 (C), 145.24 (C), 138.68 (CH), 136.91 (C), 135.19 (CH), 133.18 (CH), 132.33 (CH), 131.28 (CH), 128.92 (C), 127.87 (CH), 126.27 (CH), 124.04 (CH), 119.15 (C), 118.82 (CH), 117.70 (C), 116.30 (CH), 115.65 (CH), 109.08 (CH), 100.67 (C); MS (ES^+): m/z 433.1 [100, $(M+H)^+$]; HRMS calcd for $C_{28}H_{16}O_5$: 432.0998, found: 432.1025; RP HPLC t_R = 4.9 minutes (100% purity, ELSD); Φ: 0.42; E_x/E_m: 480/536nm.

4.2.8.9 Synthesis of 2-(3-(benzo[b]thiophen-2-yl)-6-oxo-6H-xanthen-9-yl)benzoic acid (13)

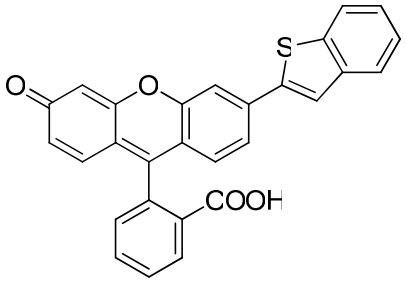

X = Benzo[b]thien-2-ylboronic acid, afforded **13** as pale orange solid (140 mg, 0.31 mmol, 78%). M.p.: 157-160^{o}C; IR: ν= cm^{-1}: 3305, 3010, 1760, 1570, 1395, 1170, 1020; ^{1}H NMR (500 MHz, CD_3OD): δ = 8.03-8.00 (1H, m, ArH), 7.92-7.88 (2H, m, ArH), 7.51-7.47 (3H, m, ArH), 7.31 (1H, dd, *J* 8.3 Hz, 1.8 Hz, ArH), 7.37-7.14 (1H, m, ArH), 6.83 (2H, d, *J* 8.6 Hz, ArH), 6.86 (1H, d, *J* 8.3 Hz, ArH), 6.70 (1H, d, *J* 2.3 Hz, ArH), 6.46-6.41 (2H, m, ArH); ^{13}C NMR (75 MHz, CD_3OD) δ 171.94 (C=O), 163.93 (C=O), 159.08 (C), 154.62 (C), 154.01 (C), 153.58 (C), 145.24 (C), 138.68 (CH), 136.91 (C), 135.19 (CH), 133.18 (CH), 132.33 (CH), 131.28 (CH), 128.92 (C), 127.87 (CH), 126.27 (CH), 124.04 (CH), 119.15 (C), 118.82 (CH), 117.70 (C), 116.30 (CH), 115.65 (CH), 112.08 (CH), 101.67 (C); MS (ES^{+}): m/z 449.1 [100, (M+H)$^{+}$]; HRMS calcd for $C_{28}H_{16}O_4S$: 448.0769, found: 448.1325; RP HPLC t_R = 3.7 minutes (100% purity, ELSD); Φ: 0.40; E_x/E_m: 479/538nm.

4.2.8.10 Synthesis of 2-(3-oxo-6-phenyl-3H-xanthen-9-yl)benzoic acid (14)

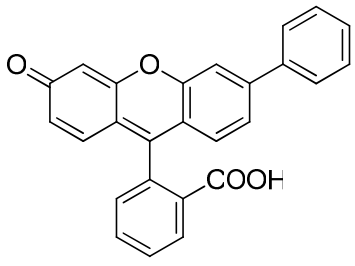

X = 4-phenylboronic acid, afforded **14** as pale yellow (106 mg, 0.27 mmol, 68%). M.p.: 150-153^{o}C; IR: ν= cm^{-1}: 3284, 2950, 1778, 1540, 1380, 1178, 1126; ^{1}H NMR (500 MHz, CD_3OD): δ = 8.03-8.00 (1H, m, ArH), 7.79-7.66 (2H, m, ArH), 7.51-7.47 (3H, m, ArH), 7.21 (1H, dd, *J* 8.3 Hz, 1.9 Hz, ArH), 7.17-7.14 (1H, m, ArH), 6.79

(2H, d, *J* 8.7 Hz, ArH), 6.70 (1H, d, *J* 8.3 Hz, ArH), 6.62 (1H, d, *J* 2.3 Hz, ArH), 6.56-6.45 (2H, m, ArH); ^{13}C NMR (75 MHz, CD_3OD) δ 171.54 (C=O), 161.25 (C=O), 159.08 (C), 154.62 (C), 154.01 (C), 153.08 (C), 145.24 (C), 136.68 (CH), 131.91 (C), 131.19 (CH), 130.18 (CH), 129.33 (CH), 129.28 (CH), 127.92 (C), 125.87 (CH), 125.27 (CH), 123.04 (CH), 118.15 (C), 116.82 (CH), 116.70 (C), 115.30 (CH), 113.65 (CH), 111.08 (CH), 108.67 (C); MS (ES^+): m/z 393.0 [100, $(M+H)^+$]; HRMS calcd for $C_{26}H_{16}O_4$: 392.1049, found: 392.1052; RP HPLC t_R = 3.9 minutes (100% purity, ELSD); Φ: 0.30; E_x/E_m: 470/535nm.

4.2.8.11 Synthesis of 2-(3-oxo-6-(pyren-2-yl)-3H-xanthen-9-yl)benzoic acid (15)

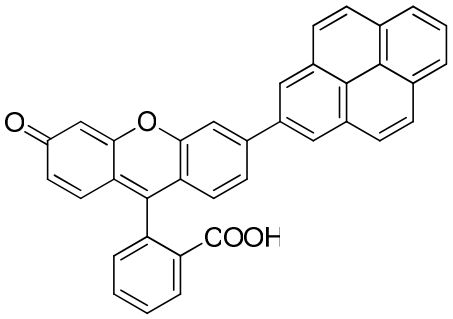

X = Pyrene-1-boronic acid, afforded **15** as pink solid (129 mg, 0.25 mmol, 63%). M.p.: 145-148°C; IR: ν= cm^{-1}: 3338, 2960, 1760, 1559, 1430, 1178, 1110; ^{1}H NMR (500 MHz, CD_3OD): δ = 8.26-8.24 (2H, m, ArH), 8.19-8.18 (1H, m, ArH), 8.12-7.96 (7H, m, ArH), 7.84-7.81 (1H, dd, *J* 8.3 Hz, 1.9 Hz, ArH), 7.76-7.73 (1H, m, ArH), 7.55-7.54 (1H, m, ArH), 7.34 (2H, d, *J* 8.7 Hz, ArH), 6.97 (1H, d, *J* 8.3 Hz, ArH), 6.77 (1H, d, *J* 2.3 Hz, ArH), 6.70 (1H, d, *J* 2.3 Hz, ArH) 6.61 (1H, d, *J* 2.3 Hz, ArH); ^{13}C NMR (75 MHz, CD_3OD) δ 171.54 (C=O), 161.25 (C=O), 159.08 (C), 154.62 (C), 154.01 (C), 153.08 (C), 145.24 (C), 136.68 (CH), 131.91 (C), 130.08 (C), 129.62 (C), 128.01 (C), 127.08 (C), 125.24 (C), 124.19 (CH), 124.14 (CH), 123.33 (CH), 122.28 (CH), 121.92 (C), 119.87 (CH), 118.27 (CH), 117.04 (CH), 115.15 (C), 114.82 (CH), 113.70 (C), 112.30 (CH), 110.65 (CH), 108.08 (CH), 103.68 (C); MS (ES^+): m/z 515.0 [100, $(M+H)^+$]; HRMS calcd for $C_{36}H_{20}O_4$: 516.1362, found, 516.1235; RP HPLC t_R = 4.4 minutes (100% purity, ELSD); Φ: 0.32; E_x/E_m: 477/525nm.

4.2.8.12 Synthesis of 2-(3-(4-(dimethylamino)phenyl)-6-oxo-6H-xanthen-9-yl)benzoic acid (16)

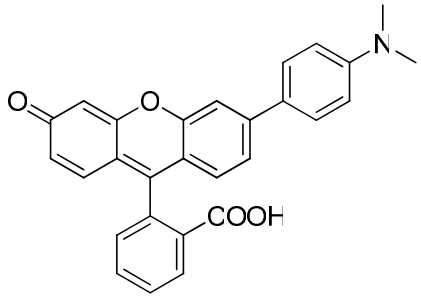

X = 4-(Dimethylamino)phenylboronic acid, afforded **16** as purple solid (136 mg, 0.30 mmol, 75%). M.p.: 160-163°C; IR: ν= cm^{-1}: 3238, 3068, 1760, 1559, 1430, 1170, 1110; ^{1}H NMR (500 MHz, CD_3OD): δ = 8.03-8.00 (1H, m, ArH), 7.79-7.66 (2H, m, ArH), 7.51-7.47 (3H, m, ArH), 7.21 (1H, dd, *J* 8.3 Hz, 1.9 Hz, ArH), 7.17-7.14 (1H, m, ArH), 6.79 (2H, d, *J* 8.7 Hz, ArH), 6.70 (1H, d, *J* 8.3 Hz, ArH), 6.65 (1H, d, *J* 2.3 Hz, ArH), 6.56-6.45 (2H, m, ArH), 3.75 (CH_3), 3.71 (CH_3) ; ^{13}C NMR (75 MHz, CD_3OD) δ 171.54 (C=O), 161.25 (C=O), 159.08 (C), 154.62 (C), 154.01 (C), 153.08 (C), 145.24 (C), 136.68 (CH), 131.91 (C), 131.19 (CH), 130.18 (CH), 129.33 (CH), 129.28 (CH), 127.92 (C), 125.87 (CH), 125.27 (CH), 123.04 (CH), 118.15 (C), 116.82 (CH), 116.70 (C), 115.30 (CH), 113.65 (CH), 111.08 (CH), 103.67 (C), 54.23 (CH_3), 52.45 (CH_3); MS (ES^+): m/z 452.1 [100, $(M+H)^+$]; HRMS calcd for $C_{28}H_{21}NO_4$: 435.1471, found: 435.1487; RP HPLC t_R = 3.9 minutes (100% purity, ELSD); Φ: 0.30; E_x/E_m: 475/530nm.

4.2.8.13 Synthesis of 2-(3-(4-methoxyphenyl)-6-oxo-6H-xanthen-9-yl)benzoic acid (17)

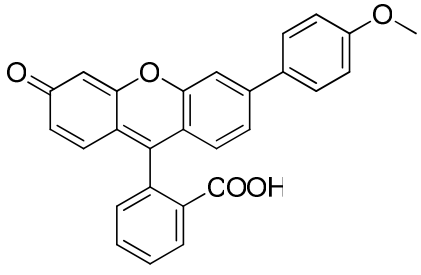

X = 4-(Dimethylamino)phenylboronic acid, afforded **17** as pale yellow solid (140 mg, 0.33 mmol, 83%). M.p.: 152-155^{o}C; IR: ν= cm^{-1}: 3330, 2966, 1760, 1559, 1430, 1178, 1110; ^{1}H NMR (500 MHz, CD_3OD): δ = 8.05-8.01 (1H, m, ArH), 7.89-7.74 (2H, m, ArH), 7.61-7.58 (3H, m, ArH), 7.21 (1H, dd, *J* 8.3 Hz, 1.9 Hz, ArH), 7.17-7.14 (1H, m, ArH), 6.79 (2H, d, *J* 8.7 Hz, ArH), 6.70 (1H, d, *J* 8.3 Hz, ArH), 6.65 (1H, d, *J* 2.3 Hz, ArH), 6.56-6.45 (2H, m, ArH), 3.26 (CH_3); ^{13}C NMR (75 MHz, CD_3OD) δ 173.54 (C=O), 164.25 (C=O), 159.08 (C), 154.62 (C), 154.01 (C), 153.08 (C), 145.24 (C), 136.68 (CH), 131.91 (C), 131.19 (CH), 130.18 (CH), 129.33 (CH), 129.28 (CH), 127.92 (C), 125.87 (CH), 125.27 (CH), 123.04 (CH), 118.15 (C), 116.82 (CH), 116.70 (C), 115.30 (CH), 113.65 (CH), 111.08 (CH), 103.67 (C), 55.34 (CH_3); MS (ES^+): m/z 423.1 [100, $(M+H)^+$]; HRMS calcd for $C_{27}H_{18}O_5$: 422.1154, found: 422.1023; RP HPLC t_R = 3.8 minutes (100% purity, ELSD); Φ: 0.23; E_x/E_m: 470/532nm.

4.2.8.14 Synthesis of 2-(3-(3-methoxyphenyl)-6-oxo-6H-xanthen-9-yl)benzoic acid (18)

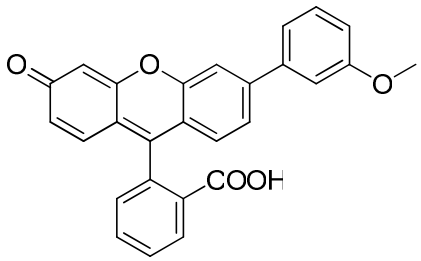

X = 3-(Dimethylamino)phenylboronic acid, afforded **18** as pale yellow solid (131 mg, 0.31 mmol, 78%). M.p.: 143-137^{o}C; IR: ν= cm^{-1}: 3274, 2998, 1706, 1502, 1422, 1178, 1158; ^{1}H NMR (500 MHz, CD_3OD): δ = 8.03-8.00 (1H, m, ArH), 7.89-7.74 (2H, m, ArH), 7.61-7.58 (3H, m, ArH), 7.21 (1H, dd, *J* 8.3 Hz, 1.9 Hz, ArH), 7.17-7.14 (1H, m, ArH), 6.79 (2H, d, *J* 8.7 Hz, ArH), 6.70 (1H, d, *J* 8.3 Hz, ArH), 6.65 (1H, d, *J* 2.3 Hz, ArH), 6.56-6.45 (2H, m, ArH), 3.24 (CH_3); ^{13}C NMR (75 MHz, CD_3OD) δ 173.54 (C=O), 164.25 (C=O), 159.08 (C), 154.62 (C), 154.01 (C), 153.08 (C), 145.24 (C), 136.68 (CH), 131.91 (C), 131.19 (CH), 130.18 (CH), 129.33 (CH), 129.28 (CH), 127.92 (C), 125.87 (CH), 125.27 (CH), 123.04 (CH), 118.15 (C), 116.82 (CH), 116.70 (C), 115.30 (CH), 113.65 (CH), 111.08 (CH), 103.67 (C), 54.21 (CH_3); MS (ES^+): m/z 423.0 [100, $(M+H)^+$]; HRMS calcd for $C_{27}H_{18}O_5$: 422.1154,

found: 422.1025; RP HPLC t_R = 3.8 minutes (100% purity, ELSD); Φ: 0.22; E_x/E_m: 478/533nm.

4.2.8.15 Synthesis of 2-(3-(4-carboxyphenyl)-6-oxo-6H-xanthen-9-yl)benzoic acid (19)

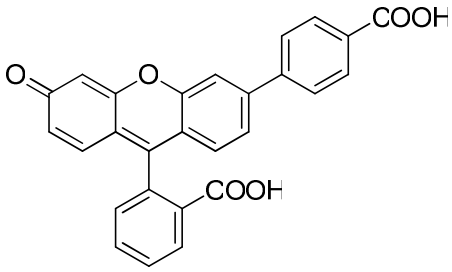

X = 4-Carboxyphenylboronic acid, afforded **19** as yellow solid (149 mg, 0.34 mmol, 85%). M.p.: 162-164°C; IR: ν= cm^{-1}: 3338, 2961, 1760, 1559, 1430, 1178, 1110; ^1H NMR (500 MHz, CD_3OD): δ = 8.12-8.09 (1H, m, ArH), 7.69-7.56 (2H, m, ArH), 7.51-7.47 (3H, m, ArH), 7.21 (1H, dd, *J* 8.3 Hz, 1.9 Hz, ArH), 7.17-7.14 (1H, m, ArH), 6.79 (2H, d, *J* 8.7 Hz, ArH), 6.75 (1H, d, *J* 8.3 Hz, ArH), 6.71 (1H, d, *J* 2.3 Hz, ArH), 6.56-6.45 (2H, m, ArH); ^{13}C NMR (75 MHz, CD_3OD) δ 171.54 (C=O), 161.25 (C=O), 159.08 (C), 154.62 (C), 154.01 (C), 153.08 (C), 145.24 (C), 136.68 (CH), 131.91 (C), 131.19 (CH), 130.18 (CH), 129.33 (CH), 129.28 (CH), 127.92 (C), 125.87 (CH), 125.27 (CH), 123.04 (CH), 118.15 (C), 116.82 (CH), 116.70 (C), 115.30 (CH), 113.65 (CH), 111.08 (CH), 104.64 (C); MS (ES^+): m/z 437.0 [100, $(M+H)^+$]; HRMS calcd for $C_{27}H_{16}O_6$: 436.0947, found: 436.1221; RP HPLC t_R = 4.3 minutes (100% purity, ELSD); Φ: 0.29; E_x/E_m: 480/532nm.

4.2.8.16 Synthesis of 2-(3-(3-carboxyphenyl)-6-oxo-6H-xanthen-9-yl)benzoic acid (20)

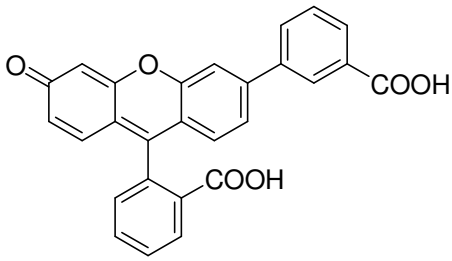

X = 3-Carboxyphenylboronic acid, afforded **20** as yellow solid (139 mg, 0.32 mmol, 80%). M.p.: 129-133°C; IR: ν= cm^{-1}: 3305, 3012, 1762, 1548, 1430, 1207, 1165; ^1H

NMR (500 MHz, CD_3OD): δ = 8.03-8.00 (1H, m, ArH), 7.79-7.66 (2H, m, ArH), 7.51-7.47 (3H, m, ArH), 7.21 (1H, dd, *J* 8.3 Hz, 1.9 Hz, ArH), 7.17-7.14 (1H, m, ArH), 6.79 (2H, d, *J* 8.7 Hz, ArH), 6.70 (1H, d, *J* 8.3 Hz, ArH), 6.65 (1H, d, *J* 2.3 Hz, ArH), 6.56-6.45 (2H, m, ArH); ^{13}C NMR (75 MHz, CD_3OD) δ 170.34 (C=O), 161.25 (C=O), 159.08 (C), 154.62 (C), 154.01 (C), 153.08 (C), 145.24 (C), 136.68 (CH), 131.91 (C), 131.19 (CH), 130.18 (CH), 129.33 (CH), 129.28 (CH), 127.92 (C), 125.87 (CH), 125.27 (CH), 123.04 (CH), 118.15 (C), 116.82 (CH), 116.70 (C), 115.30 (CH), 113.65 (CH), 111.08 (CH), 103.67 (C); MS (ES^+): m/z 437.1 [100, $(M+H)^+$]; HRMS calcd for $C_{27}H_{16}O_6$: 436.0947, found: 436.0956; RP HPLC t_R = 3.7 minutes (100% purity, ELSD); Φ: 0.29; E_x/E_m: 480/530nm.

4.2.8.17 Synthesis of 2-(3-oxo-6-(4-(trifluoromethyl)phenyl)-3H-xanthen-9-yl)benzoic acid (21)

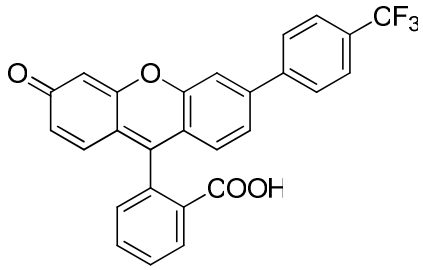

X = 4-(trifluoromethyl)phenylboronic acid, afforded **21** as pale yellow solid (124 mg, 0.27 mmol, 68%). M.p.: 130-134°C; IR: ν= cm^{-1}: 3338, 2961, 1760, 1559, 1430, 1178, 1110; ^1H NMR (500 MHz, CD_3OD): δ = 8.07-8.04 (1H, m, ArH), 7.79-7.66 (2H, m, ArH), 7.51-7.44 (3H, m, ArH), 7.21 (1H, dd, *J* 8.4 Hz, 1.9 Hz, ArH), 7.14-7.12 (1H, m, ArH), 6.79 (2H, d, *J* 8.7 Hz, ArH), 6.70 (1H, d, *J* 8.3 Hz, ArH), 6.60 (1H, d, *J* 2.3 Hz, ArH), 6.56-6.45 (2H, m, ArH); ^{13}C NMR (75 MHz, CD_3OD) δ 171.50 (C=O), 165.75 (C=O), 159.08 (C), 154.62 (C), 154.01 (C), 153.08 (C), 145.24 (C), 136.68 (CH), 131.91 (C), 131.19 (CH), 130.18 (CH), 129.33 (CH), 129.28 (CH), 127.92 (C), 125.87 (CH), 125.27 (CH), 123.04 (CH), 118.15 (C), 116.82 (CH), 116.70 (C), 115.30 (CH), 113.65 (CH), 111.08 (CH), 103.67 (C); MS (ES^+): m/z 461.1 [100, $(M+H)^+$]; HRMS calcd for $C_{27}H_{15}F_3O_4$: 460.0922, found: 460.1021; RP HPLC t_R = 4.3 minutes (100% purity, ELSD); Φ: 0.19; E_x/E_m: 480/533nm.

4.2.8.18 Synthesis of 2-(3-oxo-6-p-tolyl-3H-xanthen-9-yl)benzoic acid (22)

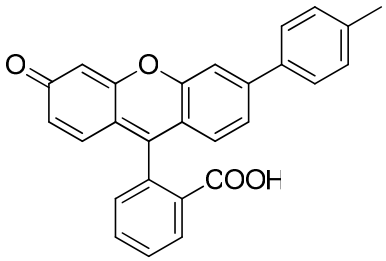

X = 4-methylphenylboronic acid, afforded **22** as orange solid (126 mg, 0.31 mmol, 78%). M.p.: 138-143°C; IR: ν= cm^{-1}: 3280, 2998, 1728, 1570, 1421, 1125, 1106; ^{1}H NMR (500 MHz, CD_3OD): δ = 8.09-8.06 (1H, m, ArH), 7.83-7.68 (2H, m, ArH), 7.63-7.52 (3H, m, ArH), 7.31 (1H, dd, *J* 8.3 Hz, 1.9 Hz, ArH), 7.14-7.09 (1H, m, ArH), 6.79 (2H, d, *J* 8.7 Hz, ArH), 6.70 (1H, d, *J* 8.3 Hz, ArH), 6.65 (1H, d, *J* 2.3 Hz, ArH), 6.56-6.45 (2H, m, ArH), 2.25 (CH_3); ^{13}C NMR (75 MHz, CD_3OD) δ 171.54 (C=O), 161.25 (C=O), 159.08 (C), 154.62 (C), 154.01 (C), 153.08 (C), 145.24 (C), 136.68 (CH), 131.91 (C), 131.19 (CH), 130.18 (CH), 129.33 (CH), 129.28 (CH), 127.92 (C), 125.87 (CH), 125.27 (CH), 123.04 (CH), 118.15 (C), 116.82 (CH), 116.70 (C), 115.30 (CH), 113.65 (CH), 111.08 (CH), 109.67 (C), 53.45 (CH_3); MS (ES^+): m/z 407.1 [100, $(M+H)^+$]; HRMS calcd for $C_{27}H_{18}O_4$: 406.1205, found: 406.1001; RP HPLC t_R = 3.9 minutes (100% purity, ELSD); Φ: 0.27; E_x/E_m: 478/529nm.

4.2.8.19 Synthesis of 2-(3-(4-nitrophenyl)-6-oxo-6H-xanthen-9-yl)benzoic acid (23)

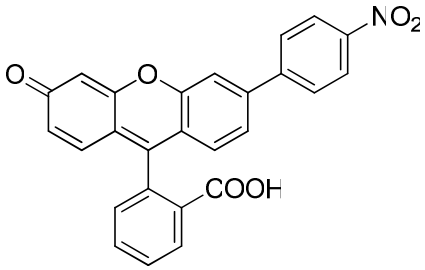

X = 4-nitrophenylboronic acid, afforded **23** as yellow solid (140 mg, 0.32 mmol, 80%). M.p.: 158-160°C; IR: ν= cm^{-1}: 3301, 3008, 1702, 1530, 1178, 1098; ^{1}H NMR (500 MHz, CD_3OD): δ = 8.03-8.00 (1H, m, ArH), 7.79-7.66 (2H, m, ArH), 7.51-7.47

(3H, m, ArH), 7.21 (1H, dd, *J* 8.3 Hz, 1.9 Hz, ArH), 7.17-7.14 (1H, m, ArH), 6.79 (2H, d, *J* 8.7 Hz, ArH), 6.70 (1H, d, *J* 8.3 Hz, ArH), 6.68 (1H, d, *J* 2.3 Hz, ArH), 6.56-6.45 (2H, m, ArH); ^{13}C NMR (75 MHz, CD_3OD) δ 170.86 (C=O), 164.66 (C=O), 158.70 (C), 153.62 (C), 152.71 (C), 152.08 (C), 145.24 (C), 136.68 (CH), 131.91 (C), 131.19 (CH), 130.18 (CH), 129.33 (CH), 129.28 (CH), 127.92 (C), 125.87 (CH), 125.27 (CH), 123.04 (CH), 120.15 (C), 118.82 (CH), 118.70 (C), 117.30 (CH), 115.65 (CH), 114.08 (CH), 108.44 (C); MS (ES^+): m/z 438.0 [100, $(M+H)^+$]; HRMS calcd for $C_{26}H_{15}NO_6$: 437.0899, found: 437.1041; RP HPLC t_R = 3.5 minutes (100% purity, ELSD); Φ: 0.21; E_x/E_m: 482/531nm.

4.2.8.20 Synthesis of 2-(3-(4-cyanophenyl)-6-oxo-6H-xanthen-9-yl)benzoic acid (24)

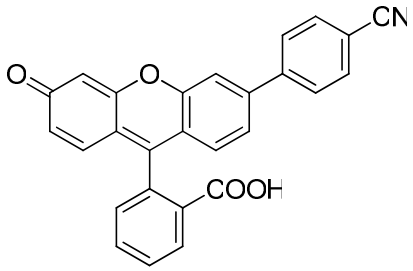

X = 4-Cyanophenylboronic acid, afforded **24** as pale yellow solid (125 mg, 0.30 mmol, 75%). M.p.: 124-127^{o}C; IR: ν= cm^{-1}: 3338, 2961, 2242, 1760, 1430, 1178, 1110; ^{1}H NMR (500 MHz, CD_3OD): δ = 8.10-8.08 (1H, m, ArH), 7.86-7.80 (2H, m, ArH), 7.85-7.67 (3H, m, ArH), 7.44 (1H, dd, *J* 8.3 Hz, 1.9 Hz, ArH), 7.44-7.13 (1H, m, ArH), 6.79 (2H, d, *J* 8.7 Hz, ArH), 6.70 (1H, d, *J* 8.3 Hz, ArH), 6.65 (1H, d, *J* 2.3 Hz, ArH), 6.56-6.45 (2H, m, ArH); ^{13}C NMR (75 MHz, CD_3OD) δ 170.47 (C=O), 162.24 (C=O), 160.21 (C), 155.62 (C), 154.01 (C), 153.08 (C), 145.24 (C), 136.68 (CH), 131.91 (C), 131.19 (CH), 130.18 (CH), 129.33 (CH), 129.28 (CH), 127.92 (C), 125.87 (CH), 125.27 (CH), 123.04 (CH), 118.15 (C), 116.82 (CH), 116.70 (C), 115.30 (CH), 114.44 (CH), 112.08 (CH), 107.07(C); MS (ES^+): m/z 418.1 [100, $(M+H)^+$]; HRMS calcd for $C_{27}H_{15}NO_4$: 417.1001, found 417.1132; RP HPLC t_R = 3.2 minutes (100% purity, ELSD); Φ: 0.18; E_x/E_m: 480/534nm.

4.2.8.21 Synthesis of 2-(3-(4-chlorophenyl)-6-oxo-6H-xanthen-9-yl)benzoic acid (25)

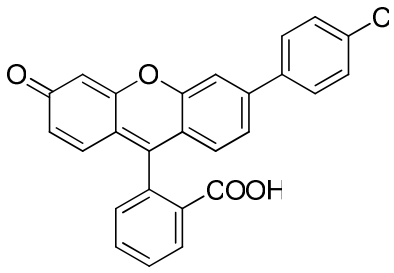

X = 4-Chlorophenylboronic acid, afforded **25** as pale yellow solid (111 mg, 0.26 mmol, 65%). M.p.: 164-167^{o}C; IR: ν= cm^{-1}: 3238, 3061, 1720, 1495, 1430, 1178, 830; ^{1}H NMR (500 MHz, CD_3OD): δ = 8.09-8.06 (1H, m, ArH), 7.86-7.80 (2H, m, ArH), 7.85-7.67 (3H, m, ArH), 7.44 (1H, dd, *J* 8.3 Hz, 1.9 Hz, ArH), 7.44-7.13 (1H, m, ArH), 6.79 (2H, d, *J* 8.7 Hz, ArH), 6.70 (1H, d, *J* 8.3 Hz, ArH), 6.65 (1H, d, *J* 2.3 Hz, ArH), 6.56-6.45 (2H, m, ArH); ^{13}C NMR (75 MHz, CD_3OD) δ 171.47 (C=O), 162.24 (C=O), 160.21 (C), 155.62 (C), 154.01 (C), 153.08 (C), 145.24 (C), 136.68 (CH), 131.91 (C), 131.19 (CH), 130.18 (CH), 129.33 (CH), 129.28 (CH), 127.92 (C), 125.87 (CH), 125.27 (CH), 123.04 (CH), 118.15 (C), 116.82 (CH), 116.70 (C), 115.30 (CH), 114.44 (CH), 112.13 (CH), 105.22(C); MS (ES^{+}): m/z 427.0 [100, (M+H)$^{+}$]; HRMS calcd for $C_{26}H_{15}ClO_4$: 426.0659, found 426.0854; RP HPLC t_R = 3.9 minutes (100% purity, ELSD); Φ: 0.13; E_x/E_m: 470/535nm.

4.2.8.22 Synthesis of 2-(3-(4-aminophenyl)-6-oxo-6H-xanthen-9-yl)benzoic acid (26)

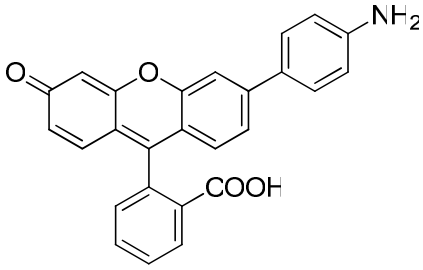

X = 4-aminoyphenyl boronic acid, afforded **26** as yellow solid (118 mg, 0.29 mmol, 73%). M.p.: 156-160^{o}C; IR: ν= cm^{-1}: 3320, 3052, 1698, 1547, 1430, 1110; ^{1}H NMR (500 MHz, CD_3OD) δ 8.03-8.00 (1H, m, ArH), 7.79-7.66 (2H, m, ArH), 7.51-7.47 (3H, m, ArH), 7.21 (1H, dd, *J* 8.3 Hz, 1.9 Hz, ArH), 7.17-7.14 (1H, m, ArH), 6.79

(2H, d, *J* 8.7 Hz, ArH), 6.70 (1H, d, *J* 8.3 Hz, ArH), 6.65 (1H, d, *J* 2.3 Hz, ArH), 6.56-6.45 (2H, m, ArH); ^{13}C NMR (75 MHz, CD_3OD) δ 170.36(C=O), 161.35 (C=O), 158.68 (C), 154.62 (C), 154.01 (C), 153.08 (C), 145.24 (C), 136.68 (CH), 131.91 (C), 131.19 (CH), 130.18 (CH), 129.33 (CH), 129.28 (CH), 127.92 (C), 125.87 (CH), 125.27 (CH), 124.04 (CH), 118.15 (C), 116.82 (CH), 116.70 (C), 115.30 (CH), 113.65 (CH), 111.08 (CH), 105.65 (C); MS (ES^+): m/z 409.1 ; HRMS calcd for $C_{26}H_{17}NO_4$: 407.1158, found: 407.0981; RP HPLC t_R = 4.5 minutes (100% purity, ELSD); Φ: 0.26; E_x/E_m: 476/532nm.

4.2.9 Cell labelling/viability Assay Compound 9

Solution of compound **9** (PBS: DMSO, 99:1 v/v) were added to the well containing HeLa cells (total concentration 5 μM) and incubated for 2h (37°C and 5% CO_2). The culture medium was removed, the cells were washed twice with PBS. HeLa cells were imaged using a x20 objective (Leica fluorescence microscope) under brightlight and 488nm excitation.

4.3 Experimental for Chapter 3

4.3.1 Synthesis and Characterization of Pd^0-microspheres[139]

4.3.1.1 Synthesis of Fmoc-Glu(Cl)-Cl

DMF (186μL, 2.7 mmol) and thionyl chloride (360 μL, 5.4 mmol) were added to a suspension of Fmoc-Glu(OH)-OH (1.00 g, 2.7 mmol) in DCM (10 mL). The reaction mixture was stirred and heated at reflux for 8h, then the reaction was cooled to room temperature and the solvents removed under reduced pressure to afford the corresponding acid chloride (1.10g crude) which was used immediately for the next step.

4.3.1.2 Cross-linked Pd^0-microspheres

1.0 mL of aminomethyl polystyrene microspheres (0.5 μm, 0.08 mmol/g, 4% SC) was placed in an eppendorf and the solvent (water) removed by centrifugation at

13,000 rpm for 5 minutes and subsequently washed with DMF (1 mL) and Toluene (2 x 1 mL). Palladium acetate (0.2 mg) in toluene (0.5 mL) was added to the beads. The eppendorf was placed in an oven (80°C) for 2 minutes and then sonicated, this procedure was repeated 5 times, and then shaken at room temperature for 2 hours to give a light-brown mixture. The beads were washed with toluene (3 x 1 mL) and methanol (1 mL) to ensure excess palladium acetate was removed. The cross-linking agent mixture (10mg of Fmoc-Glu(Cl)-Cl) and 11 μL triethylamine in 1.0 mL of dry DMF) was added to the Pd^{2+}-microsperes and shaken at room temperature for 1 hour. This step was repeated to afford 100% cross-linking. Following washing with methanol (3 x 0.5 mL) and water (3 x 0.5 mL) the microspheres gave a negative ninhydrin test (indicating full coupling of the microsphere amino groups with the cross-linking agent). Hydrazine in Methanol (10 %) was added to the Pd^{2+}-microspheres and shaken at room temperature for 30 min to reduce Pd^{2+} to Pd^{0}. The Pd^{0}-microspheres were washed with methanol (2 x 1 mL) and stored in water as a grey suspension.

4.3.1.3 Preparation of Pd^{0}-microspheres labelled with Texas Red

Fmoc deprotection was carried out using 20% piperidine in MeOH (1h) and the resulting amine-free Pd^{0}-microspheres washed with DMF (3 x 1 mL). Subsequently, a solution of Texas Red in DMF (0.5 mg (5 equiv.) 1 mL) and diisopropylethylamine (DIPEA, 1 μL, 10 equiv.) were sequentially added and the resulting mixture shaken for 24 hours. The labelled Pd^{0}-microspheres were washed with MeOH (3 x 1 mL) and water (3 x 1 mL), and a ninhydrin test carried out. If the test was positive, the procedure was repeated.

4.3.1.4 Preparation of Pd^{0}-microspheres labelled with Cy5.5

Cy5.5-$(CH_2)_5$COOH (2 mg, 3.4 μmol) and *N*-hydroxysuccinimide (0.6 mg, 5.2 μmol) were dissolved in DMF (1 mL), DIC (2 μL, 19 μmol) and DMAP (catalytic amounts) were added and the mixture was stirred overnight. The reaction mixture was added to the Fmoc deprotected Pd^{0}-microspheres (0.5 mL) and stirred overnight. The beads were washed with DMF (3x 1 mL), MeOH (3x 1 mL) and water (3x 1 mL).

4.3.2 Cellular Uptake Studies

Cellular uptake of Pd^0-microspheres was evaluated on HeLa cells by incubation of fluorescently-labelled Pd^0-microspheres for 24 hours, with intracellular fluorescence investigated by confocal microscopy and flow cytometry. Texas Red-labelled Pd^0-microspheres were used for the confocal microscopy studies, while Cy5.5-labelled Pd^0-microspheres were used for the flow cytometry analysis.

4.3.2.1 Confocal microscopy study

After incubation, cells were washed twice with PBS then the HeLa cells were fixed with 4% formaldehyde in PBS for 30 minutes. Nuclei and cellular membrane were stained using a 10 μg/mL solution of HOECHST 33342 in media (5 min at 37°C) and a 1 nM of 1,1′-dioctadecyl-3,3,3′,3′-tetramethylindocarbocyanine perchlorate (DilC 18) in Hank's Buffered Salt Solution (HBSS) (30 min), respectively.

4.3.2.2 Flow Cytometry study

After incubation, cells were washed twice with PBS, harvested with trypsin/EDTA and resuspended in 2% FCS in PBS buffer. The internalization of labelled-microspheres was analyzed by flow cytometry of Cy5.5 signals detected under the 780/60 band pass filter.

4.3.2.3 Cytotoxicity of Pd^0-microspheres (MTT assay)

Cytotoxicity tests were carried out on HeLa cell line. Cells were plated in a 96-well plate with a density of 5,000 cells/well and left to grow for 24 hours. Two concentrations of Pd^0-microspheres were studied (0.25 μL/100 μL (C1, $1.53x10^9$ beads/mL) and 0.5 μL/100 μL (C2 $3.06x10^9$ beads/mL)). Pd^0-microspheres were added to the well and incubated with the cells for 24 hours. Each condition was carried out in triplicate, with cells growth monitored under a microscope.

4.3.2.4 Counting and replating

HeLa cells were diluted in RPMI-CM (1 mL) at a density of 40,000 cells/well, plated in a 12 well plate and grown for 24 hours. Pd^0-microspheres (Texas red or Cy5.5 labelled) in media were added to the well plates and incubated for another 36 hours.

The media was removed, the cells were washed with PBS (10 mM) and then detached with trypsin (2.5% in EDTA) for 5 min at 37°C .The cells were diluted with 1 mL of media, counted by phase contrast microscopy using trypan blue, and then replated for 1 h. The number of cells in the suspension after 1 hour was quantified by phase contrast microscopy using trypan blue (in triplicate).

4.3.3 Pd^0-mediated Allyl-carbamate Cleavage in Living Cells

4.3.3.1 Synthesis of bis-allyloxycarbonyl-protected rhodamine 110 (28)[150]

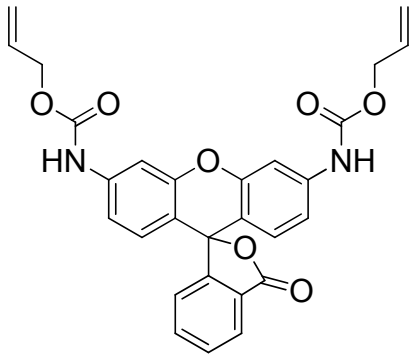

Bis-allyloxycarbonyl-protected Rhodamine 110, **28**, was synthesised from rhodamine 110 (**27**), as previously described.[150] The resulting product (Rf = 0.35 using hexane/ethyl acetate (2:1)) was isolated as a white solid (150 mg, 30%). M.p.: 178-180°C; ^{1}H NMR (250 MHz, DMSO-d_6) δ (ppm) 10.08 (s, 2H), 8.03 (d, J = 7.5 Hz, 1H), 7.79 (td, J = 7.4, 1.2 Hz, 1H), 7.71 (td, J = 7.4, 1.0 Hz, 1H), 7.56 (d, J = 2.0 Hz, 2H), 7.27 (d, J = 7.5 Hz, 1H), 7.14 (dd, J = 8.7, 2.1 Hz, 2H), 6.72 (d, J = 8.7 Hz, 2H), 5.98 (m, 2H), 5.36 (ddt, J = 17.2, 1.7, 1.6 Hz, 2H), 5.22 (ddt, J = 10.5, 1.6, 1.4 Hz, 2H), 4.62 (dt, J = 5.5, 1.4 Hz, 4H). ^{13}C NMR (125 MHz, DMSO-d_6) δ (ppm) 168.6, 153.1, 152.5, 150.9, 141.4, 135.7, 132.9, 130.1, 128.5, 125.7, 124.7, 123.9, 117.8, 114.4, 112.4, 105.1, 81.9, 64.9. IR (thin film) ν (cm^{-1}) = 3306, 2926, 1750, 1614, 1552, 1526, 1424, 1351, 1285, 1219, 1108, 1058, 992, 871, 763. HPLC (GE10CM5A, λ=254) 100% pure, retention time 3.9. LRMS (ES+) Calc. for $C_{22}H_{14}F_3O_7S$ $[M+H]^+$ = 498.14, found: $[M+H]^+$ 499.0.

4.3.3.2 Alloc deprotection of Bis-allyloxycarbonyl-protected Rhodamine 110 in solution

Negative control.

25 µL of a 20 mM solution of compound **28** in DMSO (0.5 µmol) was diluted with 1.0 mL of water and was used as a negative control **(Figure 3.6A)**.

Allylcarbamate deprotection of compound 28 in solution

25 µL of a 20 mM solution of compound **28** in DMSO (0.5 µmol) was diluted with 975 µL of water to give a final concentration of 0.5 mM. Un-labelled Pd^0-microspheres (8.0 µmol, 100 µL) were added and the reaction shaken at 300 rpm for 24 hour at 37°C **(Figure 3.6B)**. Reaction progress was monitored by TLC.

Allylcarbamate deprotection of compound 28 in solution with thiophenol

25 µL of a 20 mM solution of compound **28** in DMSO (0.5 µmol) was diluted with 975 µL of water to give a final concentration of 0.5 mM., followed by 35 µL of a thiophenol solution (100 mM in DMSO). Un-labelled Pd^0-microspheres (8.0 µmol, 100 µL) were added and the reaction shaken at 300 rpm for 24 hour at 37°C **(Figure 3.6C)**. Reaction progress was monitored by TLC.

4.3.3.3 Alloc deprotection - flow cytometry

HeLa cells were plated in RPMI-CM (1 mL) in 12-well microplates with a density of 40,000 cells/well and cells were grown for 24 hours. Thereafter Cy5.5-labelled Pd^0-microspheres (1 µL/1 mL RPMI-CM, 6.11 x 10^8 beads/mL) (0.17 µM Pd^0) in 1000 µL media were added and incubated for another 24 hour. The media of the cells was removed and cells washed with PBS (3 x) to eliminate extracellular Pd^0-microspheres. Protected Rhodamine 110, **28** (20 mM in DMSO) was added to a final concentration of 30µM and incubated at 37°C and 5% CO_2 for 24 hours. After the incubation time, cells were washed twice with PBS, harvested with trypsin/EDTA and resuspended in 2% FCS in PBS buffer.

4.3.3.4 Alloc deprotection - confocal microscopy

For the confocal microscopy study, HeLa cells were cultured on sterilised cover slips (24 mm) coated with 0.01% poly-lysine in water for 5 minutes at room temperature. The cover slips were washed with PBS (3x). The cover slips were placed in 6-well plates and seeded with 90,000 cells/well in 1600 μL RPMI-CM and incubated overnight. Texas Red-labelled Pd^0-microspheres (1 μL/1 mL RPMI-CM, 6.11 x 10^8 beads/mL) (0.17 μM Pd^0) were added to the cells and incubated for another 24 hours. The media of the cells was removed and extracellular Pd^0-microspheres removed by intensive washing with PBS (3x). Protected Rhodamine 110 (**28**) (20 mM in DMSO) was added to a final concentration of 30 μM and incubated at 37°C and 5% CO_2 for 24 hours. After incubation, cells were washed twice with PBS and the cells were fixed with 4% formaldehyde in PBS for 15 minutes. Nuclei were stained by incubation with a 10 μg/mL solution of HOECHST 33342 in media for 5 minutes at 37°C, then washed with PBS, and the membrane stained by incubation with 1 nM of 1,1′-dioctadecyl-3,3,3′,3′- tetramethylindocarbocyanine perchlorate (DilC 18) in Hank's Buffered Salt Solution (HBSS) for 30 minutes at room temperature. Cells were imaged using a Leica SP5 Confocal. Microscope lasers setting were: excitation laser lines at 488 nm, 543 nm, 595 and 633 nm with emission filters of 385-470nm for HOECHST 33342 (nuclei stain), 505-530nm for Rhodamine 110 (**27**), 670-690nm for DilC 18 (membrane stain), 595-615nm for Texas Red (Pd^0-microspheres).

4.3.3.5 *In vitro* study

Conversion studies of allylcarbamate cleavage were carried out in PBS, DMF, RPMI media and cell extracts, with the reaction carried out at 37°C for 30 hours. Fluorescence due to Rhodamine 110 formation was measured on a SPEX Fluoromax and its concentration calculated by comparison to a standard curve (**Figure 4.1**).

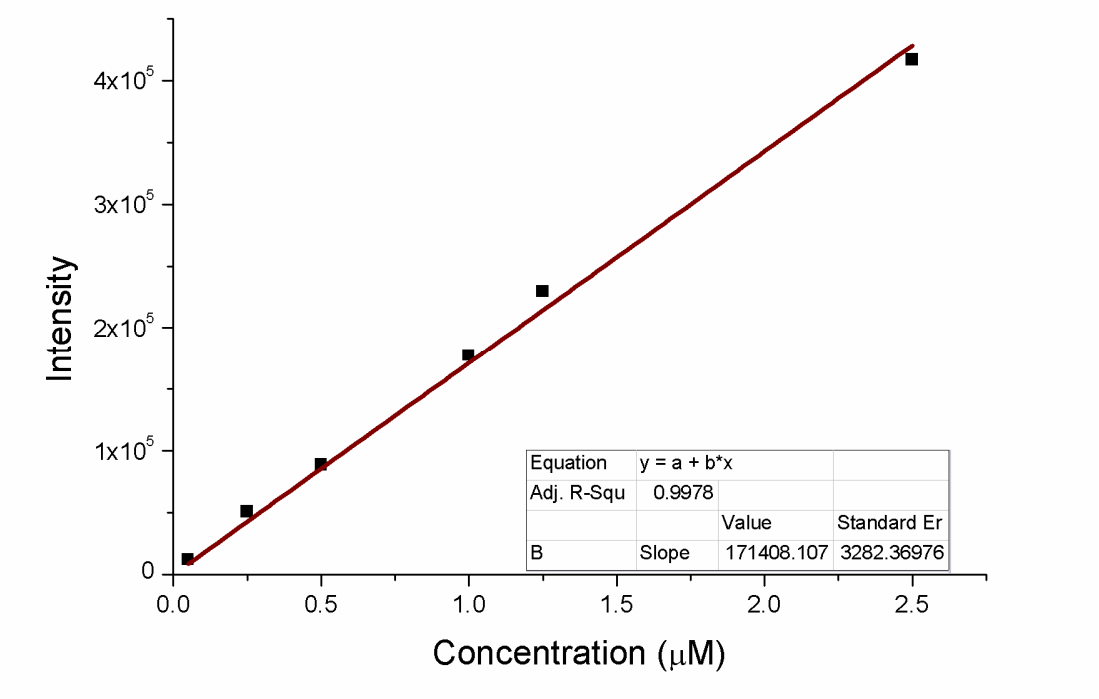

Figure 4.1 *Standard curve of Rhodamine 110 (**27**) on six data-points at emission 520nm. The excitation and emission slits were 2nm.*

4.3.4 Making C–C Bonds within Cells

4.3.4.1 Synthesis of 6'-methyl-3'-(trifluoromethanesulfonyl)fluorescein (29)[139]

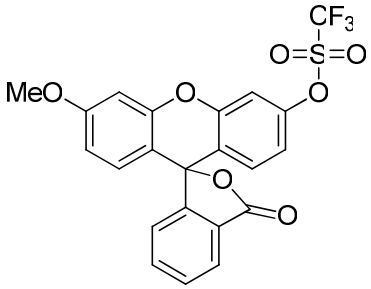

3′-(trifluoromethanesulfonyl)fluorescein, **2**, (0.4 mmol, 186 mg), methyl iodide (2.0 mmol, 125μL) and potassium carbonate (0.6 mmol, 83 mg) were stirred in dry DMF (10 mL) and microwave-irradiated at 150°C for 60 minutes. The reaction mixture was partitioned between EtOAc (120 mL) and 1 M HCl (80 mL), the aqueous layer was extracted with EtOAc (2 x 30 mL), and the combined organics dried ($MgSO_4$) and reduced *in vacuo*. Purification of the residue via column chromatography on silica gel (2:1 Hexane:EtOAc, Rf: 0.4) afforded compound **29** as a colourless solid

(157 mg, 0.33 mmol, 82%); M.p.: 120°C-124°C; ^{1}H NMR (500 MHz, DMSO-d_6) δ = 8.07 (1H, d, *J* 7.1 Hz, ArH), 7.87-7.74 (2H, m, ArH), 7.72 (1H, d, *J* 2.5 Hz, ArH), 7.39 (1H, d, *J* 7.3 Hz, ArH), 7.26 (1H, dd, *J* 8.8 Hz, 2.6 Hz, ArH), 7.04 (1H, d, *J* 8.9 Hz, ArH), 6.78 (1H, s, ArH), 6.66 (2H, s, ArH), 3.75 (CH_3); ^{13}C NMR (75 MHz, DMSO-d_6) δ 170.69 (C=O), 163.23 (C), 153.97 (C), 153.32 (C), 153.18 (C), 151.45 (C), 136.90 (CH), 131.54 (CH x2), 129.98 (CH), 127.41 (C), 126.14 (CH), 125.07 (CH), 121.84 (C), 118.31 (CH), 113.55 (CH), 111.72 (CH), 111.68 (C), 102.05 (CH), 80.83 (C), 56.21 (CH_3O); MS (ES^+): m/z 479.0 [100, $(M+H)^+$]; HRMS calcd for $C_{22}H_{14}F_3O_7S$ $[M+H]^+$ = 478.0334, found: 478.0356 ; RP HPLC t_R = 3.7 minutes (100% purity, ELSD).

4.3.4.2 Synthesis of (4-[4'-(pinacolatoboron)phenylamino]butyl)triphenyl phosphonium bromide (32)[139]

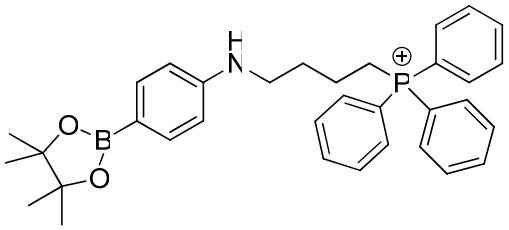

4-Aminophenylboronic acid pinacol ester, **31**, (0.5 mmol, 110 mg) and (4-bromo butyl)triphenylphosphonium bromide, **30**, (0.6 mmol, 287 mg) were dissolved in 10 ml DCM. Subsequently, triethylamine (2.0 mmol, 278 µL) was added and the reaction was microwave-irradiated for 60 min at 60°C. The solvent was removed under reduced pressure to give a pink solid which was purified by column chromatography on silica gel (DCM/MeOH 98:2) to yield **32** as a colourless solid (227 mg, 0.43 mmol, 85%); M.p.: 129°C-133°C; ^{1}H NMR (500 MHz, DMSO-d_6) δ = 7.90-7.72(15H, m, PPhH), 7.47 (2H, d *J*=8.4 Hz, ArH), 6.54 (2H, d, J=8.4 Hz, ArH), 3.66-3.22 (4H, m, CH), 2.06-2.03 (2H, m, CH), 1.89-1.77 (4H, m, CH), 1.30 (12H, s, CH_3); ^{13}C NMR (75 MHz, CH_3OD) δ 165.69 (C=O), 162.22 (C), 152.92 (C), 151.12 (C), 150.18 (C), 149.49 (C), 136.90 (CH), 131.54 (CH x2), 129.98 (CH), 127.41 (C), 126.14 (CH), 125.07 (CH), 121.84 (C), 118.31 (CH), 113.55 (CH), 111.72 (CH), 111.68 (C), 102.05 (CH), 101.83 (C), 56.3.13 ($4CH_3$); MS (ES^+): m/z 536.3 [100,

$(M+H)^+$]; HRMS calcd for $C_{34}H_{40}BNO_2$ [M+ H]$^+$: 537.2884, found: 537.2964; RP HPLC t_R = 3.9 minutes (100% purity, ELSD).

4.3.4.3 Synthesis of (4-[4'-(3''-methoxyfluoran-6''-yl)phenylamino]butyl)triphenyl phosphonium bromide (33)[139]

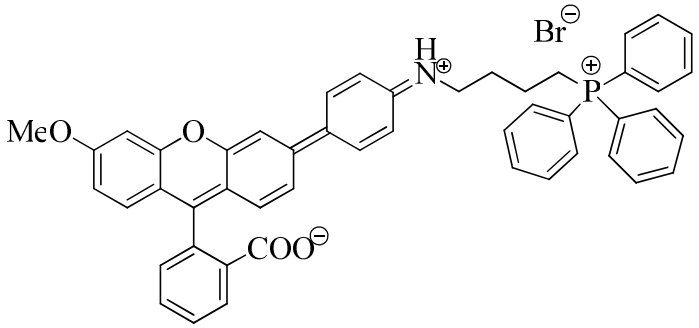

Compound **29** (0.4 mmol, 192 mg), compound **32** (0.5 mmol, 268 mg), palladium acetate (4.5 mg, 0.02 mmol) and triphenylphosphine (21 mg, 0.08 mmol) were added in a microwave vial followed of 10 mL of degassed dioxane. Subsequently, potassium carbonate (83 mg, 0.6 mmol) in water (1 mL) was added and the resulting mixture was stirred and microwave irradiated at 120°C for 30 min. The reaction mixture was partitioned between EtOAc (50 mL) and 1 M HCl (40 mL), the aqueous layer was extracted with EtOAc (2 x 20mL) and the combined organic phases were dried over $MgSO_4$, and filtered off. The solvent was removed under reduced pressure to give a dark red solid which was purified by column chromatography on silica gel (DCM/MeOH 9:1) to yield **33** as a red solid (201mg, 0.27mmol, 68%); M.p.: 160-163^{o}C; ^{1}H NMR (400 MHz, CH_3OD) δ= 8.07-6.74 (29H, m, ArH), 3.99-3.86 (5H, m, OCH_3, CH_2) 3.40-3.30 (2H, m, CH_2), 2.03-1.96 (2H, m, CH_2), 1.75-1.72 (2H, m, CH_2); ^{13}C NMR (75 MHz, CH_3OD) δ 164.45 (C=O), 163.23 (C), 153.97 (C), 153.22 (C), 152.18 (C), 150.45 (C), 136.90 (CH), 131.54 (CH x2), 128.96 (CH), 127.41 (C), 125.15 (CH), 124.04 (CH), 120.80 (C), 117.31 (CH), 114.55 (CH), 111.72 (CH), 111.68 (C), 102.05 (CH), 80.83 (C), 56.21 (CH_3); MS (ES^+): m/z 737.3 [100, $(M+H)^+$]; HRMS calcd for $C_{49}H_{40}NO_4P$ [M+ H]$^+$: 738.2762, found: 738.2768; RP HPLC t_R = 3.8 minutes (100% purity, ELSD); Φ: 0.32; E_x/E_m: 488/540 nm.

4.3.4.4 Synthesis of 6'-methylfluorescein (34)[139]

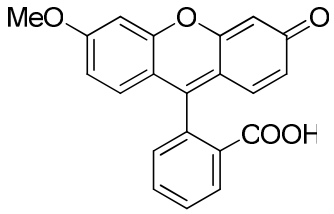

6'-methyl-3'-(trifluoromethanesulfonyl)fluorescein, **29**, (0.4 mmol, 186 mg) and potassium carbonate (0.6 mmol, 83 mg) were stirred in water (10 ml) and microwave-irradiated at 150°C for 1 hour The reaction mixture was partitioned between EtOAc (120 mL) and 1 M HCl (80 mL), the aqueous layer was extracted with EtOAc (2 x 30 mL), and the combined organics dried ($MgSO_4$) and reduced *in vacuo*. Purification of the residue via column chromatography on silica gel (1:1 Hexane:EtOAc, Rf: 0.2) afforded compound **34** as an orange solid (131mg, 0.38 mmol, 95%); M.p.: 130-133^oC; ^1H NMR (500 MHz, CH_3OD) δ = 8.29 (1H, d, *J* 7.1 Hz, ArH), 7.85-7.78 (2H, m, ArH), 7.42 (1H, d, *J* 2.5 Hz, ArH), 7.01 (1H, d, *J* 7.3 Hz, ArH), 7.00 (1H, dd, *J* 8.8 Hz, 2.6 Hz, ArH), 6.75 (1H, d, *J* 8.9 Hz, ArH), 6.70 (1H, s, ArH), 6.68 (2H, s, ArH), 3.61 (CH_3); ^{13}C NMR (125.8 MHz, CH_3OD) δ 188.15 (C=O), 166.23 (C), 166.98 (C), 160.87 (C), 154.01 (C), 153.27 (C), 135.01 (CH), 134.50 (CH x2), 132.78 (CH), 132.49 (C), 131.97 (CH), 131.66 (CH), 131.45 (C), 131.23 (CH), 122.71 (CH), 121.56 (CH), 119.29 (C), 106.56 (CH), 80.83 (C), 52.99 (CH_3O); MS (ES^+): m/z 347.0 [100, $(M+H)^+$]; HRMS calcd for $C_{21}H_{14}O_5$ $[M+H]^+$:; RP HPLC t_R = 4.2 minutes (100% purity, ELSD); Φ: 0.26; E_x/E_m: 488/518nm.

4.3.4.5 Hydrolytically stable compound 29

1 mM compound **29** was stirred in PBS (1 mL) at 37^oC for 48 hours. The solution was analysed using HPLC with an absorbance at 490nm.

4.3.4.6 Suzuki-Miyaura cross-coupling in HeLa cells - flow cytometry

HeLa cells were plated in 12 well plate (40,000 cells/well) and incubated at 37°C for 24 hours. The media was removed and replaced with 1000 μL media containing Cy5.5-labelled Pd^0-microspheres (1 μL/1 mL RPMI-CM, 6.11 x 10^8 beads/mL) (0.17 μM Pd^0)) and incubated at 37°C for 24 hours. The media of the cells was removed and any excess extracellular Pd^0-microsperes eliminated by subsequent washing with PBS (x3). Compounds **29** and **32** (20 mM) in DMSO were diluted with fresh media to give a final concentration of 20 μM of each reagent, added to the cells and incubated at 37°C for 48 hours. After incubation, cells were washed twice with PBS, harvested with trypsin/EDTA and resuspended in 2% FCS in PBS buffer. The intracellular presence of Cy5.5-labelled Pd^0-microspheres and fluorescent compound **33** were analyzed by flow cytometry under different band pass emission filters (780/60 and 576/26, respectively).

4.3.4.7 Experiments analysed by confocal microscopy

For the confocal microscopy study, HeLa cells were cultured on sterilised cover slips (24 mm) coated with 0.01% poly-lysine in water for 5 minutes at room temperature. The cover slips were washed with PBS (3x). The cover slips were placed in 6-well plates and seeded with 90,000 cells/well in 1600 μL RPMI-CM and incubated overnight. Texas Red-labelled Pd^0-microspheres (1 μL/1 mL RPMI-CM, 6.11 x 10^8 beads/mL) (0.17 μM Pd^0) were added to the cells and incubated for another 24 hours. The media of the cells was removed and extracellular Pd^0-microspheres removed by intensive washing with PBS (3x). Compounds **29** and **32** (20 mM in DMSO) were diluted in fresh media to a final concentration of 20 μM, added to the cells and incubated at 37°C and 5% CO_2 for 48 hours. After the incubation time, the media was removed and mitochondria were stained by addition of 50 nM of MitoTracker® Deep Red in media at 37°C for 30 minutes. Subsequently, cells were washed twice with PBS and the cells were fixed with 4% formaldehyde in PBS for 30 min. Nuclei were stained by incubation with a 10 μg/mL solution of HOECHST 33342 in media for 5 minutes at 37°C. Cells were imaged using a Leica SP5 Confocal. Microscope lasers setting were: excitation laser lines at 488nm, 543nm, 595 and 633nm with

emission filters of 385-470nm for HOECHST 33342 (nuclei stain), 540-560nm for compound **33**, 650-670nm for MitoTracker® Deep Red (mitochondria stain), 595-615nm for Texas Red (Pd^0-microspheres).

4.3.4.8 Standard curve

Using the same way of making standard curve for rhodamine 110, standard curve of compound **33** spectra was establish (**see section 4.3.3.5**).

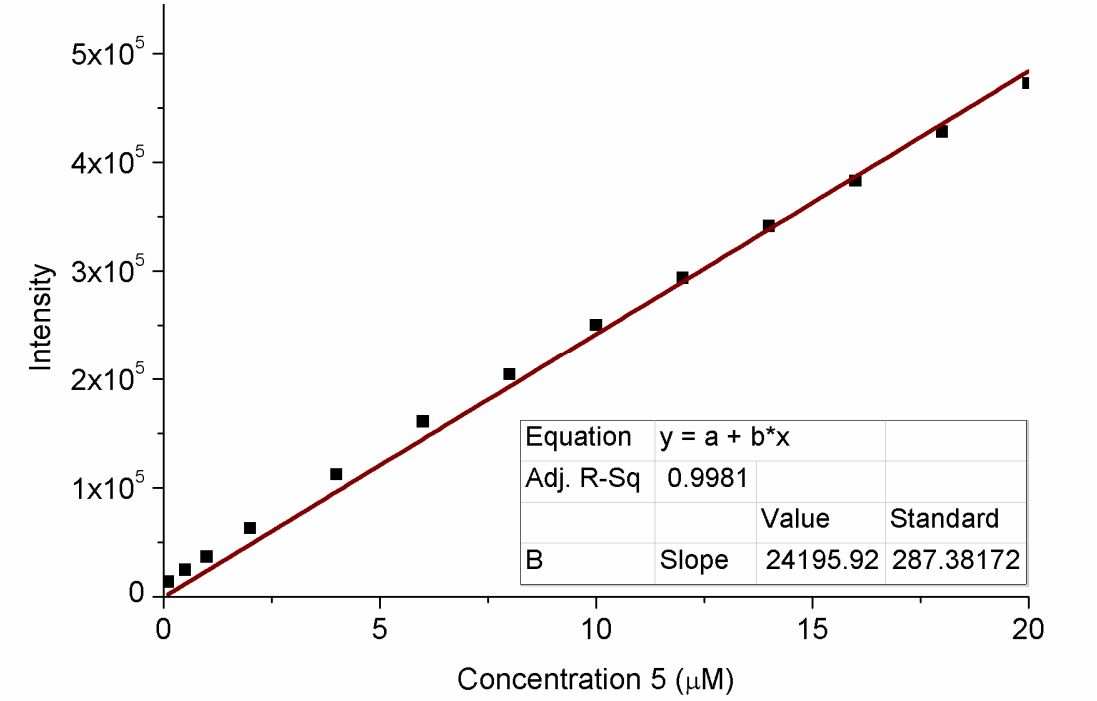

Figure 4.2 *Standard curves of compound* ***33*** *at emission 520nm (emission at 488nm). The excitation and emission slits were 5nm.*

REFERENCE LIST

1. Negishi, E. I., *Handbook of Organopalladium Chemistry for Organic Synthesis* Wiley-Interscience: New York, 2002; Vol. 1, p 3424.

2. Tsuji, J., *Palladium Reagents and Catalysts: New Perspectives for the 21st Century*. Wiley: Chichester, 2004; p 670.

3. Buchwald, S. L.; Mauger, C.; Mignani, G.; Scholz, U., Industrial-Scale Palladium-Catalyzed Coupling of Aryl Halides and Amines –A Personal Account. *Advanced Synthesis & Catalysis* **2006,** 348, (1-2), 23-39.

4. King, A. O.; Yasuda, N., Palladium-Catalyzed Cross-Coupling Reactions in the Synthesis of Pharmaceuticals. In *Organometallics in Process Chemistry*, Springer: Heidelberg, 2004; Vol. 6, pp 205-245.

5. Wu, X.-F.; Anbarasan, P.; Neumann, H.; Beller, M., From Noble Metal to Nobel Prize: Palladium-Catalyzed Coupling Reactions as Key Methods in Organic Synthesis. *Angewandte Chemie International Edition* **2010,** 49, (48), 9047-9050.

6. Carey, J. S.; Laffan, D.; Thomson, C.; Williams, M. T., Analysis of the reactions used for the preparation of drug candidate molecules. *Organic & Biomolecular Chemistry* **2006,** 4, (12), 2337-2347.

7. Antler, The Development and Application of Palladium Contact Materials *Platinum Metals Review* **1987,** 31 (1), 13.

8. Christine M.; Detlef K., I. M. *Environmental Health Criteria 226*; Fraunhofer Institute for Toxicology and Aerosol Research: Hanover, 2002; pp 1-222.

9. Mayer, A.; Sharma, S. K.; Tolner, B.; Minton, N. P.; Purdy, D.; Amlot, P.; Tharakan, G.; Begent, R. H. J.; Chester, K. A., Modifying an immunogenic epitope on a therapeutic protein: a step towards an improved system for antibody-directed enzyme prodrug therapy (ADEPT). *British Journal of Cancer* **2004,** 90, (12), 2402-2410.

10. Bownes, P.; Flynn, A., Prostate brachytherapy: a review of current practice. *Journal of Radiotherapy in Practice* **2004,** 4, (2-3), 86-101.

11. Caires, A. C. F., Recent Advances Involving Palladium (II) Complexes for the Cancer Therapy. *Anti-Cancer Agents in Medicinal Chemistry* **2007,** 7, (5), 484-891.

12. Sobjerg, L. S.; Gauthier, D.; Lindhardt, A. T.; Bunge, M.; Finster, K.; Meyer, R. L.; Skrydstrup, T., Bio-supported palladium nanoparticles as a catalyst for Suzuki-Miyaura and Mizoroki-Heck reactions. *Green Chemistry* **2009,** 11, (12), 2041-2046.

13. Durand, J.; Teuma, E.; Gómez, M., An Overview of Palladium Nanocatalysts: Surface and Molecular Reactivity. *European Journal of Inorganic Chemistry* **2008,** 2008, (23), 3577-3586.

14. Mitsudome, T.; Nose, K.; Mori, K.; Mizugaki, T.; Ebitani, K.; Jitsukawa, K.; Kaneda, K., Montmorillonite-Entrapped Sub-nanoordered Pd Clusters as a Heterogeneous Catalyst for Allylic Substitution Reactions. *Angewandte Chemie International Edition* **2007,** 46, (18), 3288-3290.

15. Choi, M.; Lee, D.-H.; Na, K.; Yu, B.-W.; Ryoo, R., High Catalytic Activity of Palladium(II)-Exchanged Mesoporous Sodalite and NaA Zeolite for Bulky Aryl Coupling Reactions: Reusability under Aerobic Conditions. *Angewandte Chemie International Edition* **2009,** 48, (20), 3673-3676.

16. Cho, J. K.; Najman, R.; Dean, T. W.; Ichihara, O.; Muller, C.; Bradley, M., Captured and Cross-Linked Palladium Nanoparticles. *Journal of the American Chemical Society* **2006,** 128, (19), 6276-6277.

17. Baxter-Plant, V. S.; Mikheenko, I. P.; Macaskie, L. E., Sulphate-reducing bacteria, palladium and the reductive dehalogenation of chlorinated aromatic compounds. *Biodegradation* **2003,** 14, (2), 83-90.

18. Najman, R.; Cho, J. K.; Coffey, A. F.; Davies, J. W.; Bradley, M., Entangled palladium nanoparticles in resin plugs. *Chemical Communications* **2007**, (47), 5031-5033.

19. Astruc, D.; Lu, F.; Aranzaes, J. R.; Ruiz, Nanoparticles as Recyclable Catalysts: The Frontier between Homogeneous and Heterogeneous Catalysis. *Angewandte Chemie International Edition* **2005,** 44, (48), 7852-7872.

20. Astruc, D., Palladium Nanoparticles as Efficient Green Homogeneous and Heterogeneous Carbon-Carbon Coupling Precatalysts: A Unifying View. *Inorganic Chemistry* **2007,** 46, (6), 1884-1894.

21. Burda, C.; Chen, X.; Narayanan, R.; El-Sayed, M. A.; A., M., Chemistry and Properties of Nanocrystals of Different Shapes. *Chemical Reviews* **2005,** 105, (4), 1025-1102.

22. Panigrahi; Basu, S.; Praharaj, S.; Pande, S.; Surojit Jana, S. P.; Ghosh, A.; Pal, S. K.; Tarasankar, Synthesis and Size-Selective Catalysis by Supported Gold Nanoparticles: Study on Heterogeneous and Homogeneous Catalytic Process. *The Journal of Physical Chemistry C* **2007,** 111, (12), 4596-4605.

23. Tew, M.; Miller, W.; T., J.; Bokhoven, V.; A., J., Particle Size Effect of Hydride Formation and Surface Hydrogen Adsorption of Nanosized Palladium Catalysts: L3 Edge vs K Edge X-ray Absorption Spectroscopy. *The Journal of Physical Chemistry C* **2009,** 113, (34), 15140-15147.

24. Reetz; T., M.; Elke, W., Phosphane-Free Palladium-Catalyzed Coupling Reactions: The Decisive Role of Pd Nanoparticles. *Angewandte Chemie International Edition* **2000,** 39, (1), 165-168.

25. Shin, J. Y. L.; Jung, B. S.; Kim, Y.; Lee, S. J.; Gi, S., Palladium nanoparticles captured onto spherical silica particles using a urea cross-linked imidazolium molecular band. *Chemical Communications* **2007**, (48), 5238-5240.

26. Lang, H. M.; Iversen, R. A., Dendrimer-Encapsulated Nanoparticle Precursors to Supported Platinum Catalysts. *Journal of the American Chemical Society* **2003,** 125, (48), 14832-14836.

27. Schauermann, S.; Hoffmann, J.; Johánek, V.; Hartmann, J.; Libuda, J.; Freund, H.-J., Catalytic Activity and Poisoning of Specific Sites on Supported Metal Nanoparticles. *Angewandte Chemie International Edition* **2002,** 41, (14), 2532-2535.

28. Choudary, B. M.; Madhi, S.; Chowdari, N. S.; Kantam, M. L.; Sreedhar, B., Layered Double Hydroxide Supported Nanopalladium Catalyst for Heck-, Suzuki-, Sonogashira-, and Stille-Type Coupling Reactions of Chloroarenes. *Journal of the American Chemical Society* **2002,** 124, (47), 14127-14136.

29. Riahi, G.; Guillemot, D.; Polisset-Thfoin; Khodadadi, M.; A. A. Fraissard, J., Preparation, characterization and catalytic activity of gold-based nanoparticles on HY zeolites. *Catalysis Today* **2002,** 72, (1-2), 115-121.

30. Price; McQuade, K. E.; Tyler, D., A cross-linked reverse micelle-encapsulated palladium catalyst. *Chemical Communications* **2005**, (13), 1714-1716.

31. Kobayashi, S.; Nagayama, S., A Microencapsulated Lewis Acid. A New Type of Polymer-Supported Lewis Acid Catalyst of Wide Utility in Organic Synthesis. *Journal of the American Chemical Society* **1998,** 120, (12), 2985-2986.

32. Kobayashi, S.; Endo, M.; Nagayama, S., Catalytic Asymmetric Dihydroxylation of Olefins Using a Recoverable and Reusable Polymer-Supported Osmium Catalyst. *Journal of the American Chemical Society* **1999,** 121, (48), 11229-11230.

33. Akiyama, R.; Kobayashi, S., The Polymer Incarcerated Method for the Preparation of Highly Active Heterogeneous Palladium Catalysts. *Journal of the American Chemical Society* **2003,** 125, (12), 3412-3413.

34. Okamoto, K.; Akiyama, R.; Yoshida, H.; Yoshida, T.; Kobayashi, S., Formation of Nanoarchitectures Including Subnanometer Palladium Clusters and Their Use as Highly Active Catalysts. *Journal of the American Chemical Society* **2005,** 127, (7), 2125-2135.

35. Yoo, W.-J.; Miyamura, H.; Kobayashi, S., Polymer-Incarcerated Gold-Palladium Nanoclusters with Boron on Carbon: A Mild and Efficient Catalyst for the Sequential Aerobic Oxidation-Michael Addition of 1,3-Dicarbonyl Compounds to Allylic Alcohols. *Journal of the American Chemical Society* **2011**,133, (9), 3095-3103.

36. Ramarao, C.; Ley, S. V.; Smith, S. C.; Shirley, I. M.; DeAlmeida, N., Encapsulation of palladium in polyurea microcapsules. *Chemical Communications* **2002**, (10), 1132-1133.

37. Lee, C. K. Y.; Holmes, A. B.; Ley, S. V.; McConvey, I. F.; Al-Duri, B.; Leeke, G. A.; Santos, R. C. D.; Seville, J. P. K., Efficient batch and continuous flow Suzuki cross-coupling reactions under mild conditions, catalysed by polyurea-encapsulated palladium (ii) acetate and tetra-n-butylammonium salts. *Chemical Communications* **2005**, (16), 2175-2177.

38. Ley, S. V.; Mitchell, C.; Pears, D.; Ramarao, C.; Yu, J.-Q.; Zhou, W., Recyclable Polyurea-Microencapsulated Pd(0) Nanoparticles: An Efficient Catalyst for Hydrogenolysis of Epoxides. *Organic Letters* **2003,** 5, (24), 4665-4668.

39. Bremeyer, N.; Ley, S. V.; Ramarao, C.; Shirley, I. M.; Smith, S. C., Palladium acetate in polyurea microcapsules: a recoverable and reusable catalyst for hydrogenations. *SYNLETT* **2002**, (11), 1843-1844.

40. Ley, S. V.; Ramarao, C.; Lee, A.-L.; Smith, S. C.; Shirley, I. M., Microencapsulation of Osmium Tetroxide in Polyurea. *Organic Letters* **2002,** 5, (2), 185-187.

41. Yuryev, R.; Liese, A., Biocatalysis: The Outcast. *ChemCatChem* **2010,** 2, (1), 103-107.

42. Bartholomew, C. H.; Farrauto, R. J., *Fundamentals of industrial catalytic processes*. 2nd ed.; Wiley: Hoboken, 2005; p 996.

43. Cornils, B.; Herrmann, W. A., *Applied Homogeneous Catalysis with Organometallic Compounds: A Comprehensive Handbook*. Wiley-VCH: Weinheim, 2000; p 1-26.

44. Brunner, H., Dendrizymes: Expanded ligands for enantioselective catalysis. *Journal of Organometallic Chemistry* **1995,** 500, (1-2), 39-46.

45. Beigi, M.; Roller, S.; Haag, R.; Liese, A., Polyglycerol-Supported Co- and Mn-salen Complexes as Efficient and Recyclable Homogeneous Catalysts for the Hydrolytic Kinetic Resolution of Terminal Epoxides and Asymmetric Olefin Epoxidation. *European Journal of Organic Chemistry* **2008,** 2008, (12), 2135-2141.

46. Ash, C.; Stone, R., A Question of Dose. *Science* **2003,** 300, (5621), 925-.

47. Finney, L. A.; O'Halloran, T. V., Transition Metal Speciation in the Cell: Insights from the Chemistry of Metal Ion Receptors. *Science* **2003,** 300, (5621), 931-936.

48. Morrison, K. L.; Weiss, G. A., The origins of chemical biology. *Nature Chemical Biology* **2006,** 2, (1), 3-6.

49. Editorial, Metals in chemical biology. *Nature Chemical Biology* **2008,** 4, (3), 143-143.

50. Frederickson, C. J.; John, R. S. a. R. J. B., Neurobiology of Zinc and Zinc-Containing Neurons. In *International Review of Neurobiology*, Academic Press: 1989; Vol. Volume 31, pp 145-238.

51. Domaille, D. W.; Que, E. L.; Chang, C. J., Synthetic fluorescent sensors for studying the cell biology of metals. *Nature Chemical Biology* **2008,** 4, (3), 168-175.

52. Hentze, M. W.; Muckenthaler, M. U.; Andrews, N. C., Balancing Acts: Molecular Control of Mammalian Iron Metabolism. *Cell* **2004,** 117, (3), 285-297.

53. Barnham, K. J.; Masters, C. L.; Bush, A. I., Neurodegenerative diseases and oxidative stress. *Nature Reviews Drug Discovery* **2004,** 3, (3), 205-214.

54. Thompson, R. B., Studying zinc biology with fluorescence: ain't we got fun? *Current Opinion in Chemical Biology* **2005,** 9, (5), 526-532.

55. Domaille, D. W.; Zeng, L.; Chang, C. J., Visualizing Ascorbate-Triggered Release of Labile Copper within Living Cells using a Ratiometric Fluorescent Sensor. *Journal of the American Chemical Society* **2010,** 132, (4), 1194-1195.

56. Kaufman; S., T.; Rúveda; A., E., The Quest for Quinine: Those Who Won the Battles and Those Who Won the War. *Angewandte Chemie International Edition* **2005,** 44, (6), 854-885.

57. Stokes, G. G., On the Change of Refrangibility of Light. *Philosophical Transactions of the Royal Society of London* **1852,** 142, 463-562.

58. Baeyer, A., Ueber eine neue Klasse von Farbstoffen. *Berichte der deutschen chemischen Gesellschaft* **1871,** 4, (2), 555-558.

59. Lavis, L. D.; Raines, R. T., Bright Ideas for Chemical Biology. *ACS Chemical Biology* **2008,** 3, (3), 142-155.

60. Lakowicz, J. R., *Principles of Fluorescence Spectroscopy*. Springer: Maryland, 2006; Vol. 3, p 1255.

61. Tsien Roger, Y., Fluorescent and Photochemical Probes of Dynamic Biochemical Signals inside Living Cells. In *Fluorescent Chemosensors for*

Ion and Molecule Recognition, American Chemical Society: 1993; Vol. 538, pp 130-146.

62. Zhang, J. C., Robert E. Ting, Alice Y. Tsien, Roger Y., Creating new fluorescent probes for cell biology. *Nature Reviews Molecular Cell Biology* **2002,** 3, (12), 906-918.

63. Phillips, G. J., Green fluorescent protein – a bright idea for the study of bacterial protein localization. *FEMS Microbiology Letters* **2001,** 204, (1), 9-18.

64. Prescher, J. A.; Bertozzi, C. R., Chemistry in living systems. *Nature Chemical Biology* **2005,** 1, (1), 13-21.

65. Tsien, R. Y., The Green Fluorescent Protein. *Annual Review of Biochemistry* **1998,** 67, (1), 509-544.

66. Goldys, E. M., *Fluorescence and it Application in Biotechnology and Life Sciences*. Wiley: New Jersey, 2009; p 367

67. Giepmans, B. N. G.; Adams, S. R.; Ellisman, M. H.; Tsien, R. Y., The Fluorescent Toolbox for Assessing Protein Location and Function. *Science* **2006,** 312, (5771), 217-224.

68. Chalfie, M.; Tu, Y.; Euskirchen, G.; Ward, W. W.; Prasher, D. C., Green fluorescent protein as a marker for gene expression. *Science* **1994,** 263, 802.

69. Pinton, P.; Rimessi, A.; Romagnoli, A.; Prandini, A.; Rizzuto, R., Biosensors for the detection of calcium and pH. *Methods Cell Biol.* **2007,** 80, 297.

70. Han, J.; Burgess, K., Fluorescent Indicators for Intracellular pH. *Chemical Reviews* **2009,** 110, (5), 2709-2728.

71. Cheng; Soetjipto, J.; Hoffmann, C.; R., M., Confocal Fluorescence Microscopy of the Morphology and Composition of Interstitial Fluids in Freezing Electrolyte Solutions. *The Journal of Physical Chemistry Letters* **2009,** 1, (1), 374-378.

72. Sun, W. C.; Gee, K. R.; Klaubert, D. H.; Haugland, R. P., Synthesis of Fluorinated Fluoresceins. *The Journal of Organic Chemistry* **1997,** 62, (19), 6469-6475.

73. Unciti-Broceta, A.; Rahimi Yusop, M.; Richardson, P. R.; Walton, J. G. A.; Bradley, M., A fluorescein-derived anthocyanidin-inspired pH sensor. *Tetrahedron Letters* **2009,** 50, (26), 3713-3715.

74. Haidekker, M.; Theodorakis, E., Environment-sensitive behavior of fluorescent molecular rotors. *Journal of Biological Engineering* **2010,** 4, (1), 11-14.

75. Santra, M.; Ko, S.-K.; Shin, I.; Ahn, K. H., Fluorescent detection of palladium species with an O-propargylated fluorescein. *Chemical Communications* **2010,** 46, (22), 3964-3966.

76. Charier, S.; Ruel, O.; Baudin, J.-B.; Alcor, D.; Allemand, J.-F.; Meglio, A.; Jullien, L., An Efficient Fluorescent Probe for Ratiometric pH Measurements in Aqueous Solutions. *Angewandte Chemie International Edition* **2004,** 43, (36), 4785-4788.

77. Wong, L. S.; Birembaut, F.; Brocklesby, W. S.; Frey, J. G.; Bradley, M., Resin Bead Micro UV-Visible Absorption Spectroscopy. *Analytical Chemistry* **2005,** 77, (7), 2247-2251.

78. Cho, J. K.; Wong, L. S.; Dean, T. W.; Ichihara, O.; Muller, C.; Bradley, M., pH Indicating resins. *Chemical Communications* **2004**, (13), 1470-1471.

79. Cho, J. K.; White, P. D.; Klute, W.; Dean, T. W.; Bradley, M., Self-Indicating Resins: Sensor Beads and in Situ Reaction Monitoring. *Journal of Combinatorial Chemistry* **2003,** 5, (5), 632-636.

80. Wong, L. S.; Brocklesby, W. S.; Bradley, M., Fibre optic pH sensors employing tethered non-fluorescent indicators on macroporous glass. *Sensors and Actuators B: Chemical* **2005,** 107, (2), 957-962.

81. Bradley, M.; Alexander, L.; Duncan, K.; Chennaoui, M.; Jones, A. C.; Sanchez-Martin, R. M., pH sensing in living cells using fluorescent microspheres. *Bioorganic & Medicinal Chemistry Letters* **2008,** 18, (1), 313-317.

82. Vasylevska, A.; Karasyov, A.; Borisov, S.; Krause, C., Novel coumarin-based fluorescent pH indicators, probes and membranes covering a broad pH range. *Analytical and Bioanalytical Chemistry* **2007,** 387, (6), 2131-2141.

83. Lavis, L. D.; Rutkoski, T. J.; Raines, R. T., Tuning the pKa of Fluorescein to Optimize Binding Assays. *Analytical Chemistry* **2007,** 79, (17), 6775-6782.

84. Smith, J. P. D., L. R. , Modulation of Monocarboxylic Acid Transporter-1 Kinetic Function by the cAMP Signaling Pathway in Rat Brain Endothelial Cells. *Journal Biological Chemistry* **2006**, (281), 2053–2060.

85. Srivastava, J.; Barber, D. L.; Jacobson, M. P., Intracellular pH Sensors: Design Principles and Functional Significance. *Physiology* **2007,** 22, (1), 30-39.

86. Roos, A.; Boron, W. F., Intracellular pH. *Physiol. Rev.* **1981,** 61, 296.

87. Kotyk, A.; Slavik, J., *Intracellular pH and Its Measurement*. CRC Press: Florida, 1989; Vol. 1, p 192.

88. Gottlieb, R. A.; Dosanjh, A., Apoptosis induced in Jurkat cells by several agents is preceded by intracellular acidification. *Proceedings of the National Academy of Sciences . U.S.A.* **1996,** 93, (2), 654–658.

89. Perez-Sala, D.; Collado-Escobar, D.; Mollinedo, F., Intracellular Alkalinization Suppresses Lovastatin-induced Apoptosis in HL-60 Cells through the Inactivation of a pH-dependent Endonuclease. *Journal Biological Chemistry* **1995,** 270, (17), 6235-6242.

90. Liang, E.; Liu, P.; Dinh, S., Use of a pH-sensitive fluorescent probe for measuring intracellular pH of Caco-2 cells. *International Journal of Pharmaceutics* **2007,** 338, (1), 104-109.

91. Walker, N. M.; Simpson, J. E.; Levitt, R. C.; Boyle, K. T.; Clarke, L. L., Talniflumate increases survival in a cystic fibrosis mouse model of distal intestinal obstructive syndrome. *Journal of Pharmacology and Experimental Therapeutics* **2006,** 317, (1), 275-283.

92. Varadi, A.; Rutter, G. A., Ca2+-induced Ca2+ release in pancreatic islet beta.-cells: Critical evaluation of the use of endoplasmic reticulum-targeted "cameleons". *Endocrinology* **2004,** 145, (10), 4540.

93. Chin, E. R.; Allen, D. G., The contribution of pH-dependent mechanisms to fatigue at different intensities in mammalian single muscle fibers. *Journal of Physiology* **1998,** 512, (3), 831-840.

94. Miksa, M.; Komura, H.; Wu, R.; Shah, K. G.; Wang, P., A novel method to determine the engulfment of apoptotic cells by macrophages using pHrodo succinimidyl ester. *Journal of Immunological Methods* **2009,** 342, (1), 71-77.

95. Schindler, M.; Grabski, S.; Hoff, E.; Simon, S., Defective pH Regulation of Acidic Compartments in Human Breast Cancer Cells (MCF-7) Is Normalized in Adriamycin-Resistant Cells (MCF-7adr). *Biochemistry* **1996,** 35, (9), 2811-2817.

96. Izumi, H.; Torigoe, T.; Ishiguchi, H.; Uramoto, H.; Yoshida, Y.; Tanabe, M.; Ise, T.; Murakami, T.; Yoshida, T.; Nomoto, M.; Kohno, K., Cellular pH regulators: potentially promising molecular targets for cancer chemotherapy. *Cancer Treatment Reviews* **2003,** 29, (6), 541-549.

97. Davies, T. A.; Fine, R. E.; Johnson, R. J.; Levesque, C. A.; Rathbun, W. H.; Seetoo, K. F.; Smith, S. J.; Strohmeier, G.; Volicer, L., Non-age related differences in thrombin responses by platelets from male patients with advanced Alzheimer's disease. *Biochemistry Biophysical Researsh Communication* **1993,** 194, (1), 537-543.

98. O'Connor, N.; Silver, R. B.; Greenfield Sluder and David, E. W., Ratio Imaging: Practical Considerations for Measuring Intracellular Ca2+ and pH

in Living Cells. In *Methods in Cell Biology*, Academic Press: 2007; Vol. Volume 81, pp 415-433.

99. Bright, G. R.; Fisher, G. W.; Rogowska, J.; Taylor, D. L., Fluorescence ratio imaging microscopy *Methods Cell Biology* **1989,** 30, (92), 157-162.

100. Rink, T. J.; Tsien, R. Y.; Pozzan, T., Cytoplasmic pH and free magnesium^{2+} in lymphocytes. *The Journal of Cell Biolgy* **1982,** 95, (1), 189-196.

101. Varadi, A.; Rutter, G. A., Ca2+-induced Ca2+ release in pancreatic islet beta.-cells: Critical evaluation of the use of endoplasmic reticulum-targeted "cameleons". *Endocrinology* **2004,** 145, (null), 4540.

102. Hille, C.; Walz, B., Characterisation of neurotransmitter-induced electrolyte transport in cockroach salivary glands by intracellular Ca2+, Na+ and pH measurements in duct cells. *Journal of Experimental Biology* **2008,** 211, (4), 568-576.

103. Hille, C.; Berg, M.; Bressel, L.; Munzke, D.; Primus, P.; Loehmannsroeben, H. G.; Dosche, C., Time-domain fluorescence lifetime imaging for intracellular pH sensing in living tissues. *Analytical and Bioanalytical Chemistry* **2008,** 391, (5), 1871-1879.

104. Donoso, P.; Beltran, M.; Hidalgo, C., Luminal pH Regulates Calcium Release Kinetics In Sarcoplasmic Reticulum Vesicles. *Biochemistry* **1996,** 35, (41), 13419-13425.

105. Martinez, G. M.; Gollahon, L. S.; Shafer, K.; Oomman, S. K.; Busch, C.; Martinez-Zaguilan, R. In *Fluorescent pH probes, fluorescent proteins, and intrinsic cellular fluorochromes are tools to study cytosolic pH (pH[sup cyt]) in mammalian cells*, Biomarkers and Biological Spectral Imaging, San Jose, CA, USA, 2001; SPIE: San Jose, CA, USA, 2001; pp 144-156.

106. Liu, J.; Diwu, Z.; Klaubert, D. H., Fluorescent molecular probes III. 2',7'-Bis-(3-carboxypropyl)-5-(and-6)-carboxyfluorescein (BCPCF): a new polar dual-excitation and dual-emission pH indicator with a pKa of 7.0. *Bioorganic & Medicinal Chemistry Letters* **1997,** 7, (23), 3069-3072.

107. Jiao, G. S.; Han, J. W.; Burgess, K., Syntheses of regioisomerically pure 5- or 6-halogenated fluoresceins. *The Journal of Organic Chemistry* **2003,** 68, (21), 8264-8467.

108. Grabowski, J.; Ke-Cheng, H.; Baker, P. R.; Bornman, C. H., Fluorogenic compound hydrolysis as a measure of toxicity-induced cytoplasmic viscosity and pH changes. *Environmental Pollution* **1997,** 98, (1), 1-5.

109. Graber, M. L.; DiLillo, D. C.; Friedman, B. L.; Pastoriza-Munoz, E., Characteristics of fluoroprobes for measuring intracellular pH. *Analytical Biochemistry* **1986,** 156, (1), 202-212.

110. Fischer, D.; Theodorakis, E. A.; Haidekker, M. A., Synthesis and use of an in-solution ratiometric fluorescent viscosity sensor. *Nature Protocols* **2007,** 2, (1), 227-236.

111. Haidekker, M. A.; Brady, T. P.; Lichlyter, D.; Theodorakis, E. A., Effects of solvent polarity and solvent viscosity on the fluorescent properties of molecular rotors and related probes. *Bioorganic Chemistry* **2005,** 33, (6), 415-425.

112. Haidekker, M. A.; Brady, T. P.; Lichlyter, D.; Theodorakis, E. A., A Ratiometric Fluorescent Viscosity Sensor. *Journal of the American Chemical Society* **2005,** 128, (2), 398-399.

113. Haidekker, M. A.; Ling, T.; Anglo, M.; Stevens, H. Y.; Frangos, J. A.; Theodorakis, E. A., New fluorescent probes for the measurement of cell membrane viscosity. *Chemistry & Biology* **2001,** 8, (2), 123-131.

114. Loutfy, R. O.; Arnold, B., Fluorescence probes for polymer free-volume. *The Journal of Physical Chemistry* **1982,** 86, (9), 4205-4209.

115. Kung, C. E.; Reed, J. K., Microviscosity measurements of phospholipid bilayers using fluorescent dyes that undergo torsional relaxation. *Biochemistry* **1986,** 25, (20), 6114-6121.

116. Haidekker, M. A.; L'Heureux, N.; Frangos, J. A., Fluid shear stress increases membrane fluidity in endothelial cells: a study with DCVJ fluorescence. *American Journal of Physiology - Heart and Circulatory Physiology* **2000,** 278, (4), 1401-1406.

117. Urano, Y.; Kamiya, M.; Kanda, K.; Ueno, T.; Hirose, K.; Nagano, T., Evolution of fluorescein as a platform for finely tunable fluorescence probes. *Journal of the American Chemical Society* **2005,** 127, (13), 4888-94.

118. Haugland, R. P., *A Guide to Fluorescent Probes and Labeling Technologies*. 10 ed.; Molecular Probes: Eugene, 2005.

119. Waggoner, A., Fluorescent labels for proteomics and genomics. *Current Opinion in Chemical Biology* **2006,** 10, (1), 62-66.

120. McHedlov-Petrossyan, N. O.; Rubtsov, M. I.; Lukatskaya, L. L., Ionization and Tautomerism of Chloro-Derivatives of Fluorescein in Water and Aqueous Acetone. *Dyes and Pigments* **1992,** 18, (3), 179-198.

121. Sparano, B. A.; Shahi, S. P.; Koide, K., Effect of Binding and Conformation on Fluorescence Quenching in New 2',7'-Dichlorofluorescein Derivatives. *Organic Letters* **2004,** 6, (12), 1947-1949.

122. Sun, W.-C.; Gee, K. R.; Klaubert, D. H.; Haugland, R. P., Synthesis of Fluorinated Fluoresceins. *The Journal of Organic Chemistry* **1997,** 62, (19), 6469-6475.

123. Lin, H.-J.; Szmacinski, H.; Lakowicz, J. R., Lifetime-Based pH Sensors: Indicators for Acidic Environments. *Analytical Biochemistry* **1999,** 269, (1), 162-167.

124. Huang, Z.; Wang, Q.; Ly, H. D.; Gorvindarajan, A.; Scheigetz, J.; Zamboni, R.; Desmarais, S.; Ramachandran, C., 3,6-Fluorescein Diphosphate: A Sensitive Fluorogenic and Chromogenic Substrate for Protein Tyrosine Phosphatases. *Journal of Biomolecular Screening* **1999,** 4, (6), 327-334.

125. Zaikova, T. O.; Rukavishnikov, A. V.; Birrell, G. B.; Griffith, O. H.; Keana, J. F. W., Synthesis of Fluorogenic Substrates for Continuous Assay of Phosphatidylinositol-Specific Phospholipase C. *Bioconjugate Chemistry* **2001,** 12, (2), 307-313.

126. Rotman, B., Zderic, J. A., and Edelstein, M. , Fluorogenic substrates for ß-D-galactosidases and phosphatases derived from fluorescein (3,6-dihydroxyfluoran) and its monomethylether. *Proceedings of the National Academy of Science U.S.A.* **1963,** 50, (3), 581-585.

127. Castaneda-Ovando, A.; Pacheco-Hernandez, M. d. L.; Paez-Hernandez, M. E.; Rodriguez, J. A.; Galan-Vidal, C. A., Chemical studies of anthocyanins: A review. *Food Chemistry* **2009,** 113, (4), 859-871.

128. Miller, E. W.; Albers, A. E.; Pralle, A.; Isacoff, E. Y.; Chang, C. J., Boronate-Based Fluorescent Probes for Imaging Cellular Hydrogen Peroxide. *Journal of the American Chemical Society* **2005,** 127, (47), 16652-16659.

129. Miyaura, N.; Suzuki, A., Palladium-Catalyzed Cross-Coupling Reactions of Organoboron Compounds. *Chemical Reviews* **1995,** 95, (7), 2457-2483.

130. Alonso, F.; Beletskaya, I. P.; Yus, M., Non-conventional methodologies for transition-metal catalysed carbon-carbon coupling: a critical overview. Part 2: The Suzuki reaction. *Tetrahedron* **2008,** 64, (14), 3047-3101.

131. Jurd, L.; Geissman, T. A., Anthocyanins and Related Compounds. II. Structural Transformations of Some Anhydro Bases. *The Journal of Organic Chemistry* **1963,** 28, (9), 2394-2397.

132. Williams, A. T. R.; Winfield, S. A.; Miller, J. N., Relative fluorescence quantum yields using a computer-controlled luminescence spectrometer. *Analyst* **1983,** 108, (1290), 1067-1071.

133. Daniels, B. R.; Masi, B. C.; Wirtz, D., Probing Single-Cell Micromechanics In Vivo: The Microrheology of C. elegans Developing Embryos. *Biophysical Journal* **2006,** 90, (12), 4712-4719.

134. Arbeloa, I. L.; Rohatgi-Mukherjee, K. K., Solvent effects on the photophysics of the molecular forms of rhodamine B. Internal conversion mechanism. *Chemical Physics Letters* **1986,** 129, (6), 607-614.

135. Meallier, P.; Guittonneau, S.; Emmelin, C.; Konstantinova, T., Photochemistry of fluorescein and eosin derivatives. *Dyes and Pigments* **1999,** 40, (2-3), 95-98.

136. Haidekker, M. A.; Brady, T. P.; Lichlyter, D.; Theodorakis, E. A., A ratiometric fluorescent viscosity sensor. *J. Am. Chem. Soc.* **2006,** 128, 398-399.

137. Haidekker, M. A.; Theodorakis, E. A., Molecular rotors-fluorescent biosensors for viscosity and flow. *Organic & Biomolecular Chemistry* **2007,** 5, (11), 1669-1678.

138. Dean, J. A., *Lange's Handbook of Chemistry*. McGraw-Hill: New York, 1992.

139. Yusop, R. M.; Unciti-Broceta, A.; Johansson, E. M. V.; Sanchez-Martin, R. M.; Bradley, M., Palladium-mediated intracellular chemistry. *Nature Chemistry* **2011,** 3, (3), 241-245.

140. Silverman, R. E., *The Organic Chemistry of Enzyme-Catalyzed Reactions*. 2nd ed.; Academic Press, London: 2002

141. Bugg, T., *Introduction to Enzyme and Coenzyme Chemistry*. 2nd ed.; Wiley-Blackwell: Oxford, 2004.

142. Lippard, S. J. B., J. M. , *Principles of Bioinorganic Chemistry*. University Science Books: California, 1994.

143. Claudia Andreini, I. B., Gabriele Cavallaro, Gemma L. Holliday and Janet M. Thornton, Metal ions in biological catalysis: from enzyme databases to general principles *Journal of Biological Inorganic Chemistry* **2008,** 13, 1205-1218.

144. Xie, X. S.; Yu, J.; Yang, W. Y., Living Cells as Test Tubes. *Science* **2006,** 312, (5771), 228-230.

145. Jewett, J. C.; Bertozzi, C. R., Cu-free click cycloaddition reactions in chemical biology. *Chemical Society Reviews* **2010,** 39, (4), 1272-1279.

146. Baskin, J. M.; Bertozzi, C. R., Bioorthogonal Click Chemistry: Covalent Labeling in Living Systems. *QSAR & Combinatorial Science* **2007,** 26, (11-12), 1211-1219.

147. Salic, A.; Mitchison, T. J., A chemical method for fast and sensitive detection of DNA synthesis in vivo. *Proceedings of the National Academy of Sciences* **2008,** 105, (7), 2415-2420.

148. Soares, E. V., Kristel Hebbelinck, and Helena MVM Soares, Toxic effects caused by heavy metals in the yeast Saccharomyces cerevisiae: a comparative study. *Canadian Journal of Microbiology* **2003,** 49, (5), 336-343.

149. Chen, Z.; Meng, H.; Xing, G.; Chen, C.; Zhao, Y.; Jia, G.; Wang, T.; Yuan, H.; Ye, C.; Zhao, F.; Chai, Z.; Zhu, C.; Fang, X.; Ma, B.; Wan, L., Acute toxicological effects of copper nanoparticles in vivo. *Toxicology Letters* **2006,** 163, (2), 109-120.

150. Craig, S.; Eric, M., Ruthenium-Induced Allylcarbamate Cleavage in Living Cells13. *Angewandte Chemie International Edition* **2006,** 45, (34), 5645-5648.

151. Johnsson, N.; Johnsson, K., Chemical Tools for Biomolecular Imaging. *ACS Chemical Biology* **2007,** 2, (1), 31-38.

152. Waldron, K. J.; Rutherford, J. C.; Ford, D.; Robinson, N. J., Metalloproteins and metal sensing. *Nature* **2009,** 460, (7257), 823-830.

153. Liang, G.; Ren, H.; Rao, J., A biocompatible condensation reaction for controlled assembly of nanostructures in living cells. *Nature Chemistry* **2010,** 2, (1), 54-60.

154. Abu-Surrah; Adnan S.; Kettunen, M., Platinum Group Antitumor Chemistry: Design and development of New Anticancer Drugs Complementary to Cisplatin. *Current Medicinal Chemistry* **2006,** 13, 1337-1357.

155. Bruijnincx, P. C. A.; Sadler, P. J., New trends for metal complexes with anticancer activity. *Current Opinion in Chemical Biology* **2008,** 12, (2), 197-206.

156. Liu, T. Z.; Lee, S. D.; Bhatnagar, R. S., Toxicity of palladium. *Toxicology Letters* **1979,** 4, (6), 469-473.

157. Liu, T. Z.; Chou, L. Y.; Humphreys, M. H., Inhibition of intestinal alkaline phosphatase by palladium. *Toxicology Letters* **1979,** 4, (6), 433-438.

158. Liu, T. Z.; Lin, T. F.; Chiu, D. T. Y.; Tsai, K.-J.; Stern, A., Palladium or Platinum Exacerbates Hydroxyl Radical Mediated DNA Damage. *Free Radical Biology and Medicine* **1997,** 23, (1), 155-161.

159. Costas, M.; Mehn, M. P.; Jensen, M. P.; Que, L., Jr., Dioxygen Activation at Mononuclear Nonheme Iron Active Sites: Enzymes, Models, and Intermediates. *ChemInform* **2004,** 35, (21), 248.

160. Sanchez-Martin, R. M.; Lois, A.; Mathilde, M.; Juan, M. C.-M.; Anestis, T.; Joshua, M. B.; Mark, B., Microsphere-Mediated Protein Delivery into Cells. *ChemBioChem* **2009,** 10, (9), 1453-1456.

161. Sanchez-Martin, R. M.; Mathilde, M.; Nutcha, C.; Siew Eng, H.; Stifun, M.; Mark, B., Bead-Based Cellular Analysis, Sorting and Multiplexing. *ChemBioChem* **2005,** 6, (8), 1341-1345.

162. Alexander, L. M.; Sanchez-Martin, R. M.; Bradley, M., Knocking (Anti)-Sense into Cells: The Microsphere Approach to Gene Silencing. *Bioconjugate Chemistry* **2009,** 20, (3), 422-426.

163. Alexander, L. M.; Pernagallo, S.; Livigni, A.; Sanchez-Martin, R. M.; Brickman, J. M.; Bradley, M., Investigation of microsphere-mediated cellular delivery by chemical, microscopic and gene expression analysis. *Molecular BioSystems* **2010**, (6), 399-409.

164. Sanchez-Martin, R. M.; Matt, C.; Stifun, M.; Mark, B., Microsphere-Based Real-Time Calcium Sensing. *Angewandte Chemie International Edition* **2006,** 118, (33), 5598-5600.

165. Shen, C. M.; Su, Y. K.; Yang, H. T.; Yang, T. Z.; Gao, H. J., Synthesis and characterization of n-octadecayl mercaptan-protected palladium nanoparticles. *Chemical Physics Letters* **2003,** 373, (1-2), 39-45.

166. Mosmann, T., Rapid colorimetric assay for cellular growth and survival: Application to proliferation and cytotoxicity assays. *Journal of Immunological Methods* **1983,** 65, (1-2), 55-63.

167. Rossignol, P.; Vranckx, R.; Bouton, M.-C.; Meilhac, O.; Lijnen, H. R.; Guillin, M.-C.; Michel, J.-B., Protease Nexin-1 Inhibits Plasminogen Activation-induced Apoptosis of Adherent Cells. *The Journal of Biological* **2004,** 279, (11), 10346-10356.

168. Harlow, E.; Lane, D., Fixing Attached Cells in Paraformaldehyde. *Cold Spring Harbour Protocols* **2006,** 2006, (3), 4294-4296.

169. Kaplowitz, N.; Aw, T. Y.; Ookhtens, M., The Regulation of Hepatic Glutathione. *Annual Review of Pharmacology and Toxicology* **1985,** 25, (1), 715-744.

170. Smith, R. A. J.; Porteous, C. M.; Gane, A. M.; Murphy, M. P., Delivery of bioactive molecules to mitochondria invivo. *Proceedings of the National Academy of Sciences of the United States of America* **2003,** 100, (9), 5407-5412.

APPENDIX

(I) EMISSION SPECTRA COMPOUND 5–26

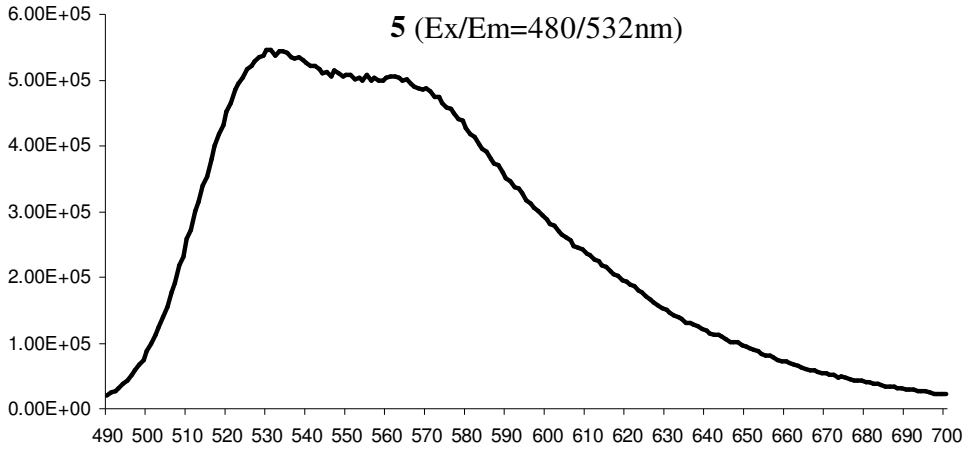

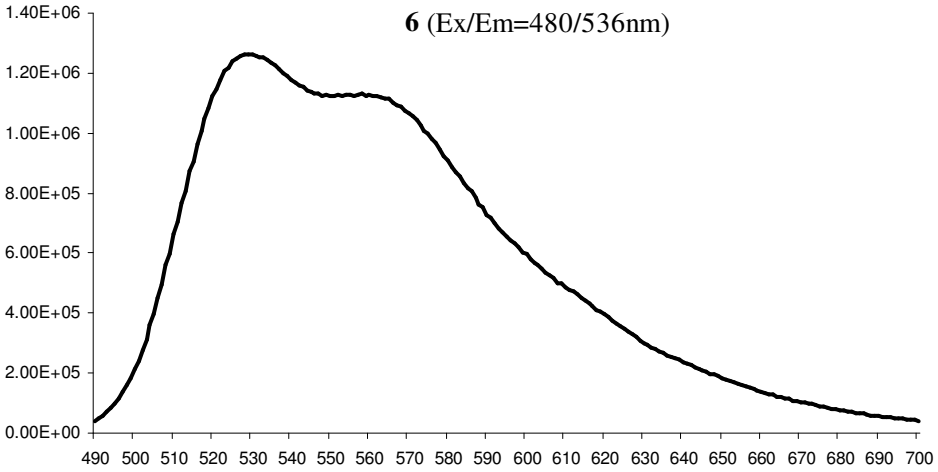

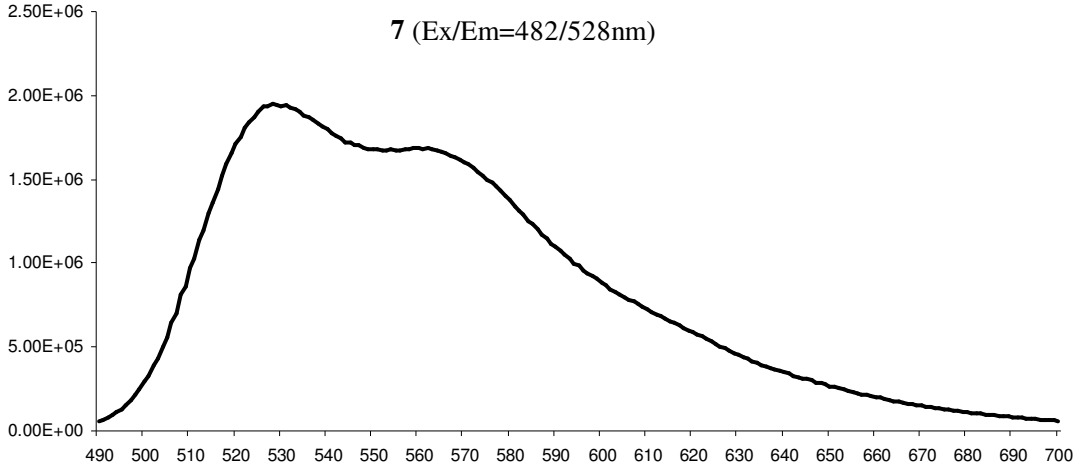

7 (Ex/Em=482/528nm)

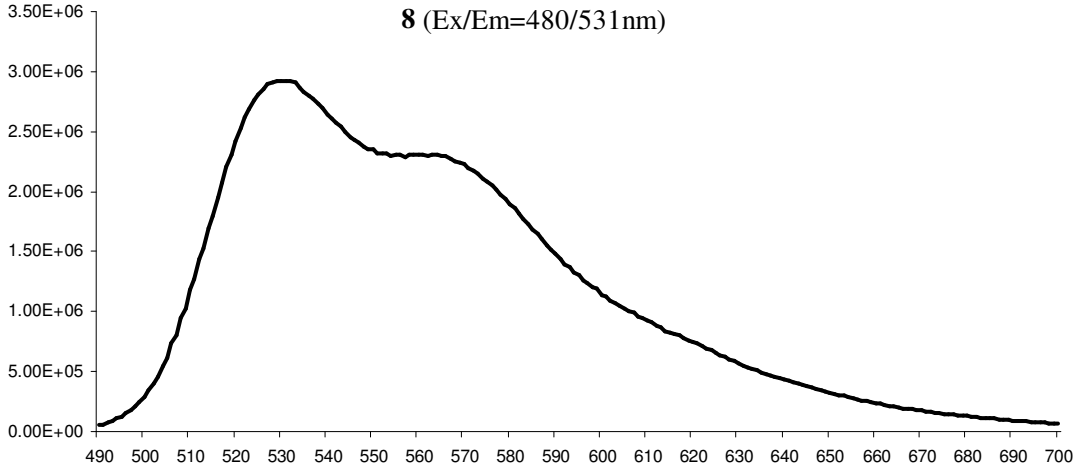

8 (Ex/Em=480/531nm)

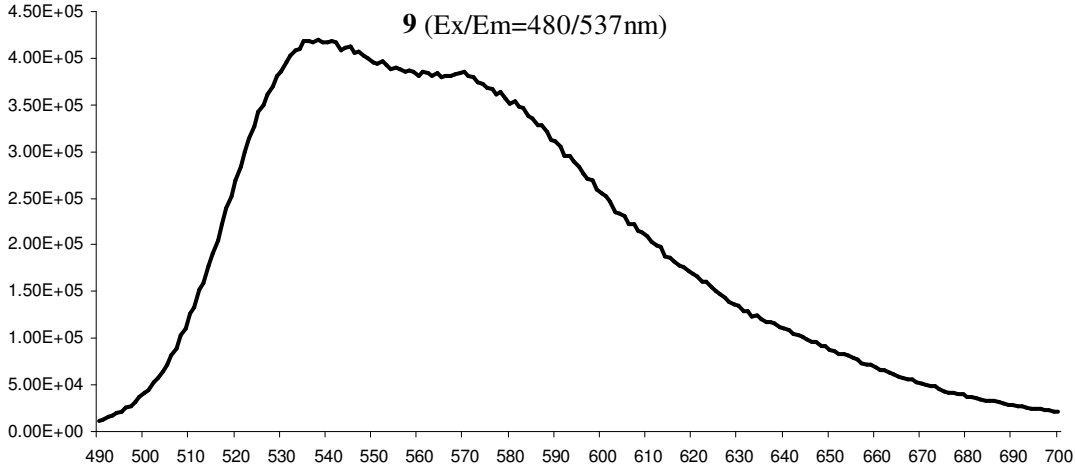

9 (Ex/Em=480/537nm)

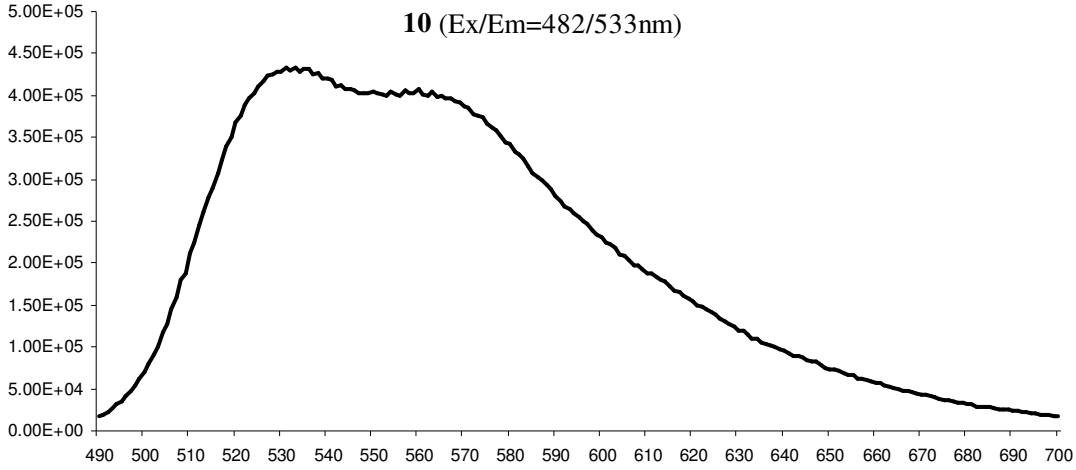

10 (Ex/Em=482/533nm)

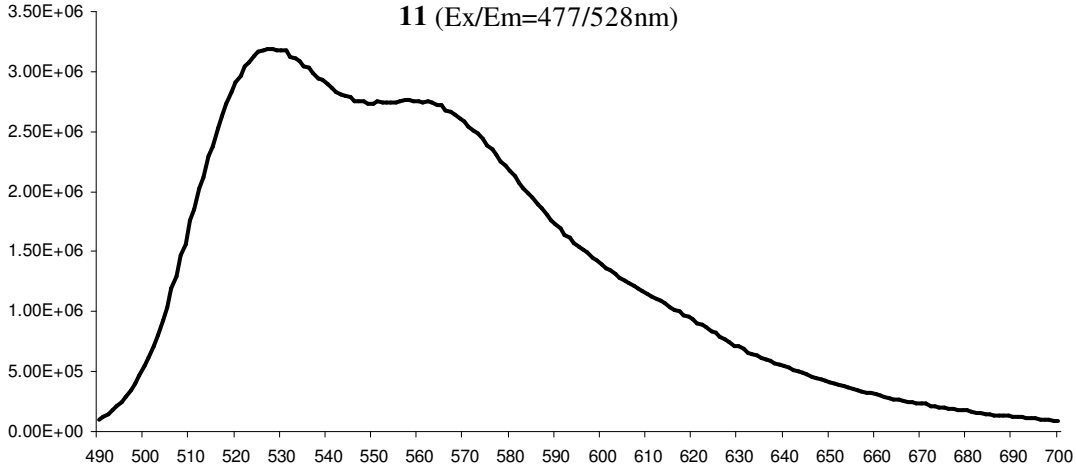

11 (Ex/Em=477/528nm)

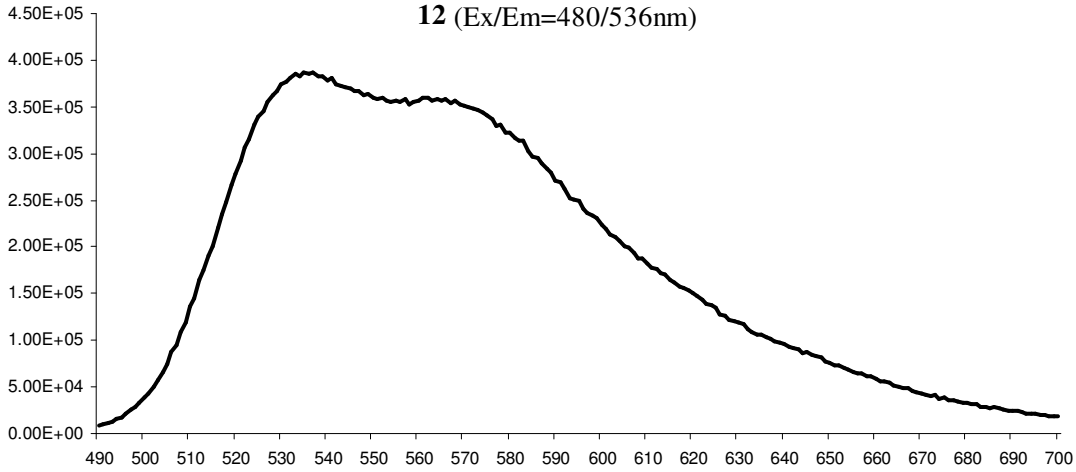

12 (Ex/Em=480/536nm)

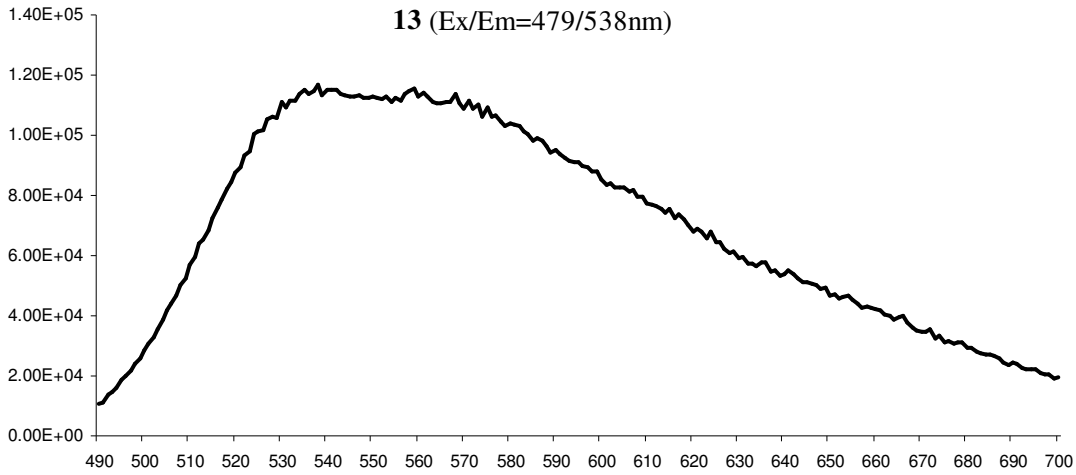
13 (Ex/Em=479/538nm)
1.40E+05
1.20E+05
1.00E+05
8.00E+04
6.00E+04
4.00E+04
2.00E+04
0.00E+00
490 500 510 520 530 540 550 560 570 580 590 600 610 620 630 640 650 660 670 680 690 700

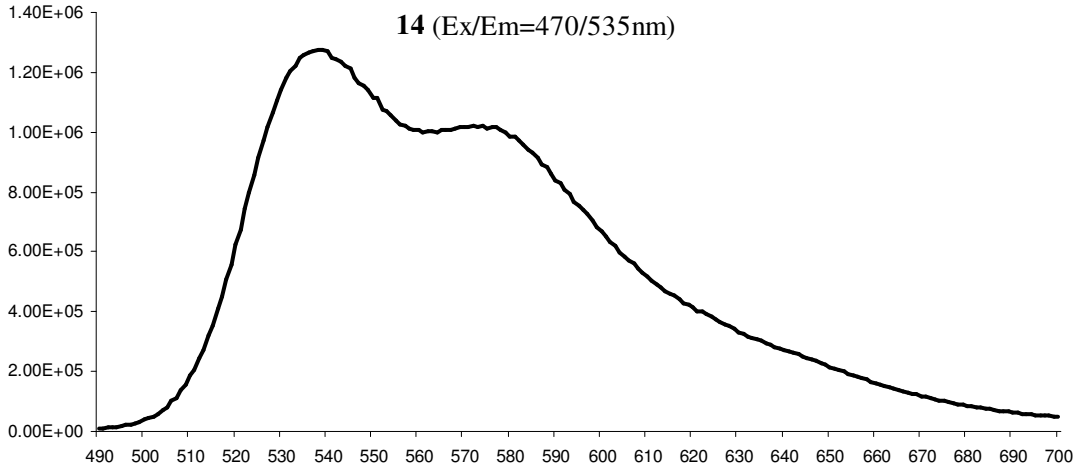
14 (Ex/Em=470/535nm)
1.40E+06
1.20E+06
1.00E+06
8.00E+05
6.00E+05
4.00E+05
2.00E+05
0.00E+00
490 500 510 520 530 540 550 560 570 580 590 600 610 620 630 640 650 660 670 680 690 700

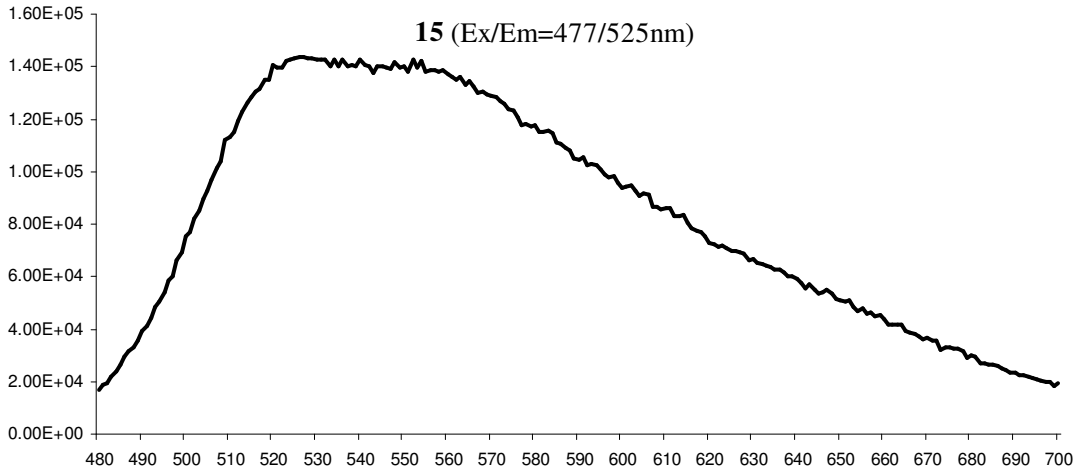
15 (Ex/Em=477/525nm)
1.60E+05
1.40E+05
1.20E+05
1.00E+05
8.00E+04
6.00E+04
4.00E+04
2.00E+04
0.00E+00
480 490 500 510 520 530 540 550 560 570 580 590 600 610 620 630 640 650 660 670 680 690 700

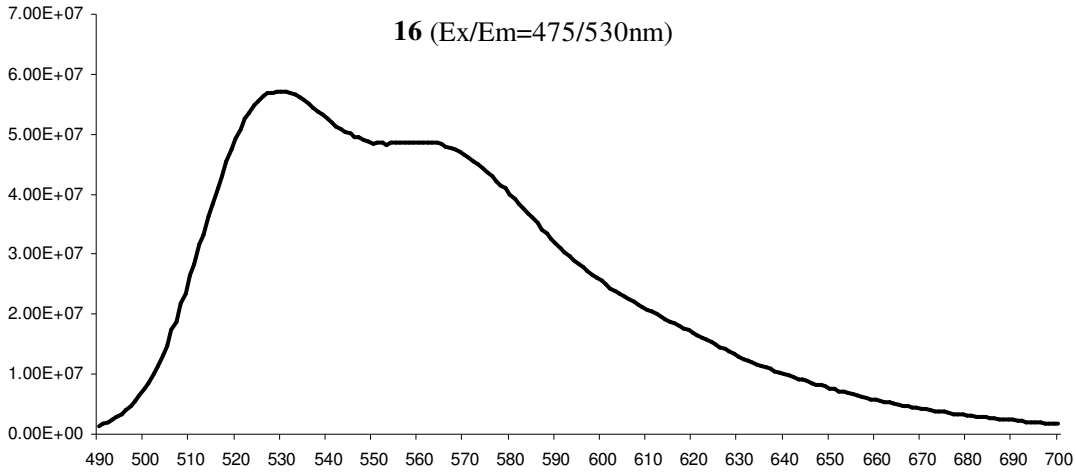

16 (Ex/Em=475/530nm)

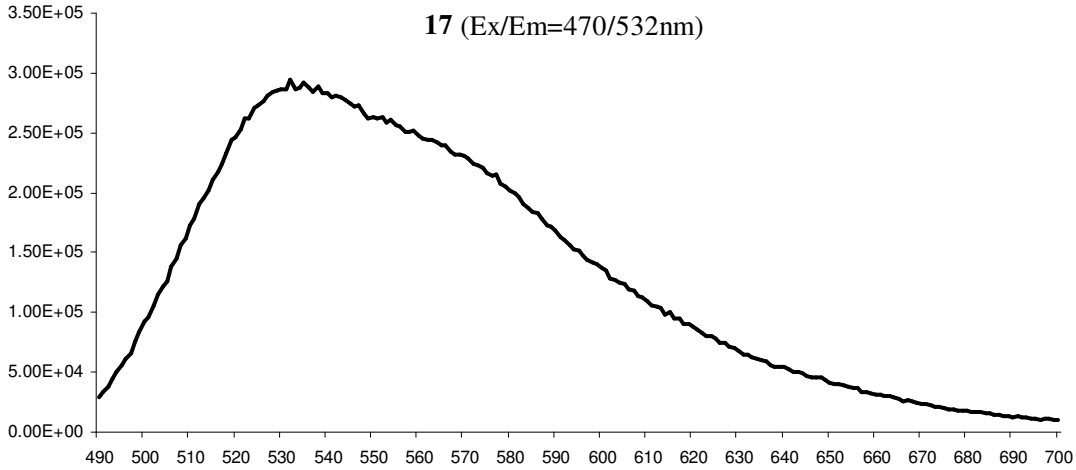

17 (Ex/Em=470/532nm)

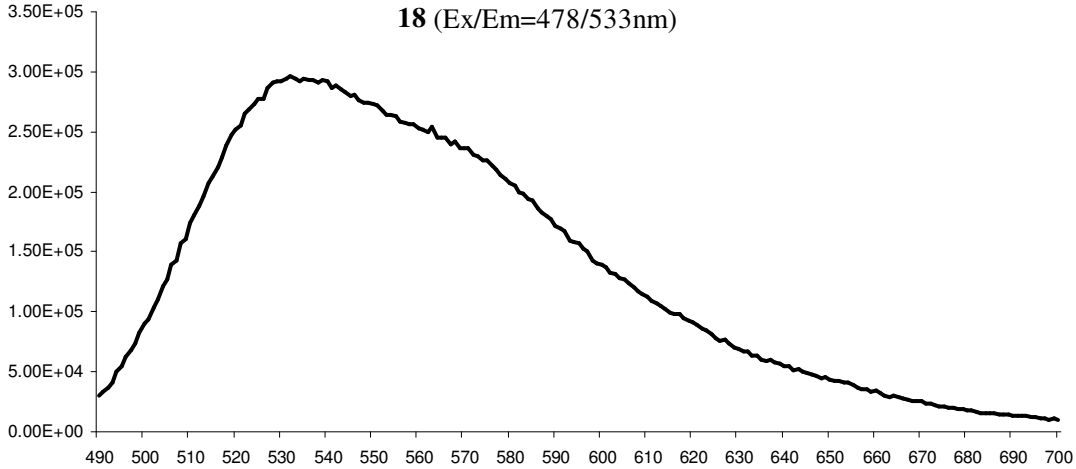

18 (Ex/Em=478/533nm)

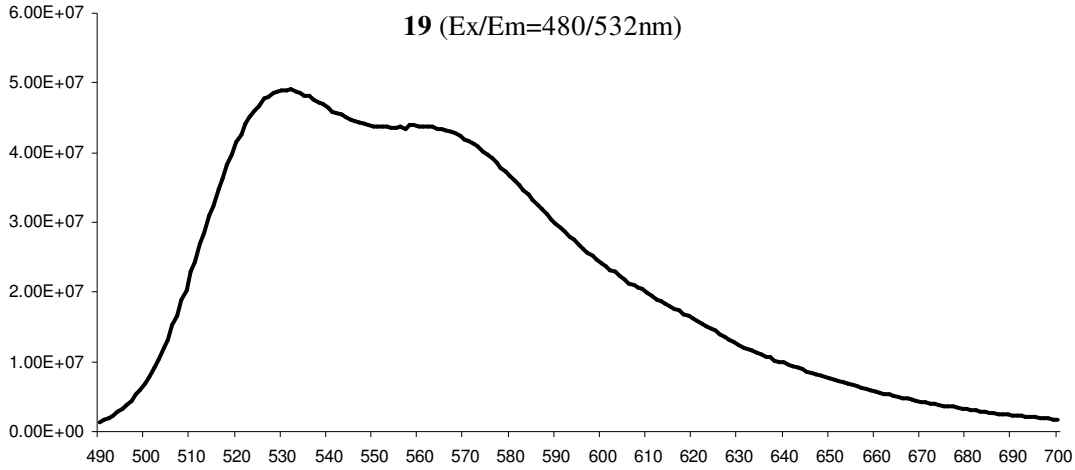

19 (Ex/Em=480/532nm)

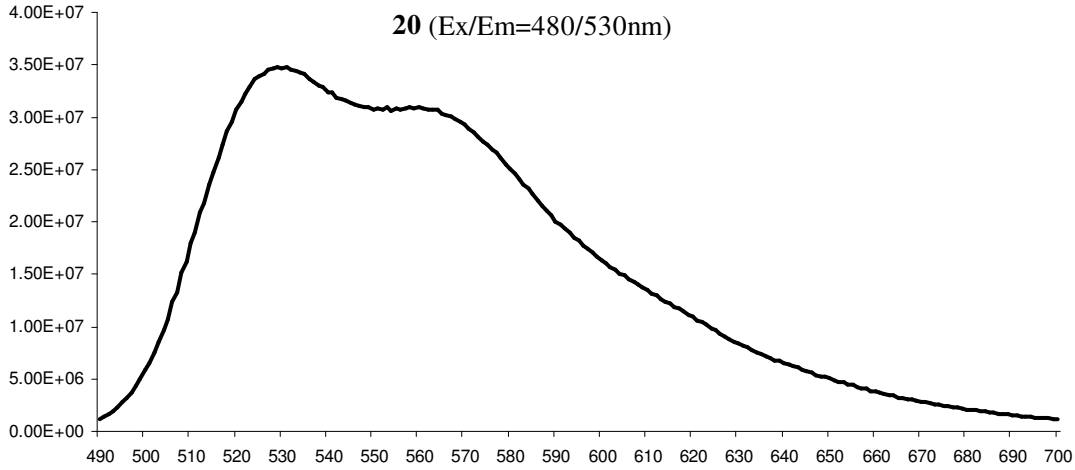

20 (Ex/Em=480/530nm)

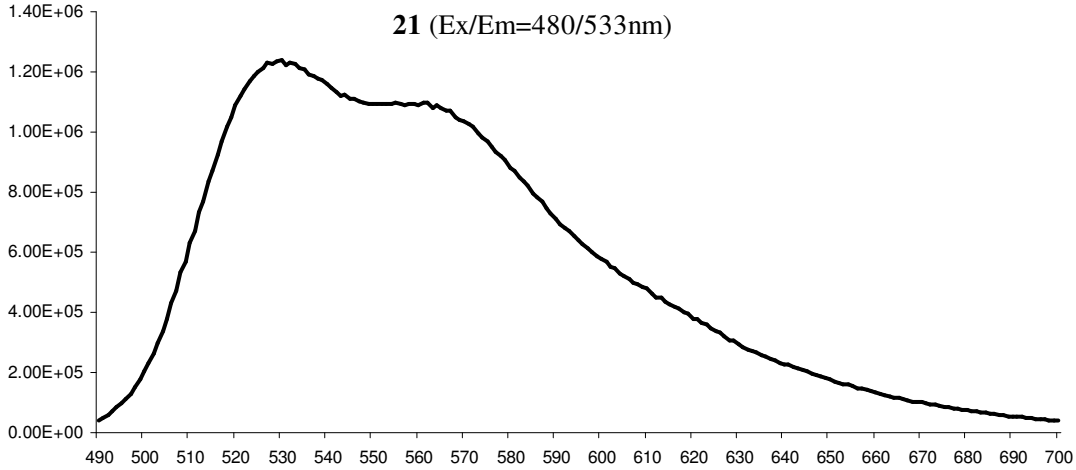

21 (Ex/Em=480/533nm)

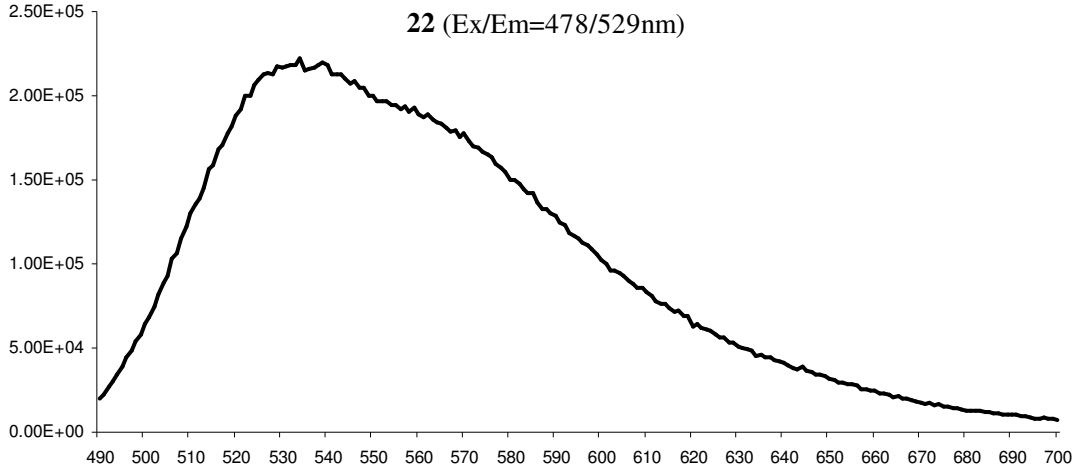

22 (Ex/Em=478/529nm)

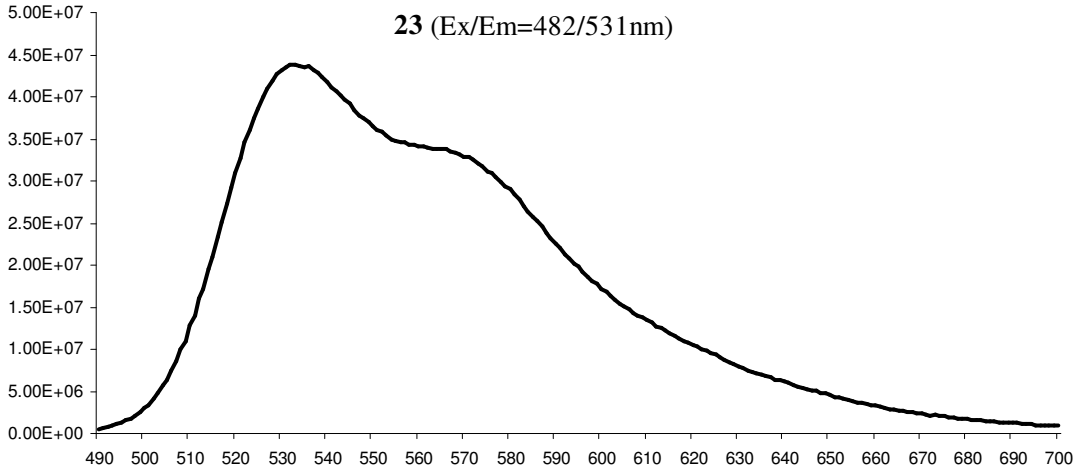

23 (Ex/Em=482/531nm)

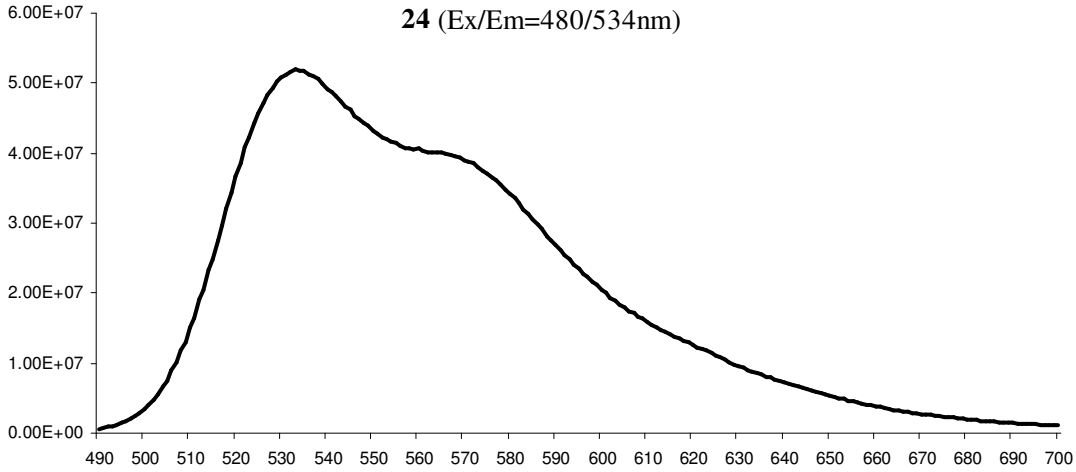

24 (Ex/Em=480/534nm)

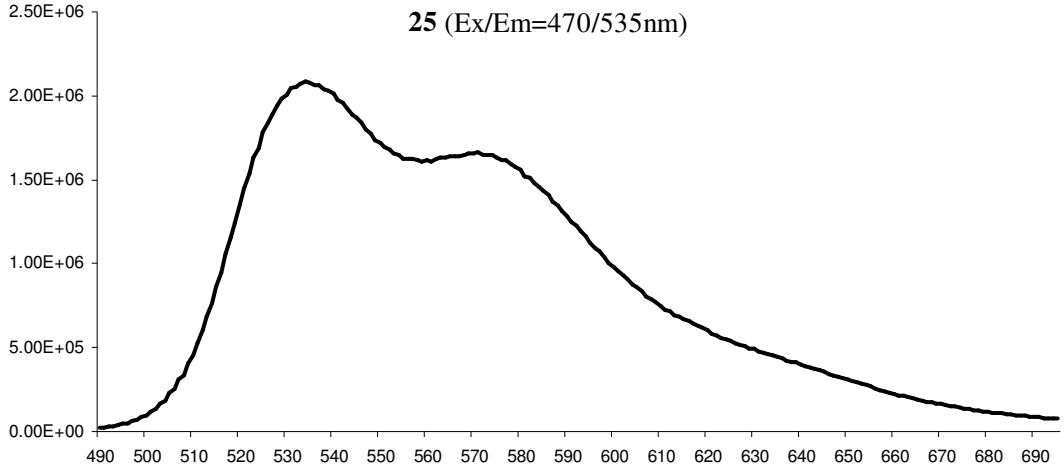

25 (Ex/Em=470/535nm)

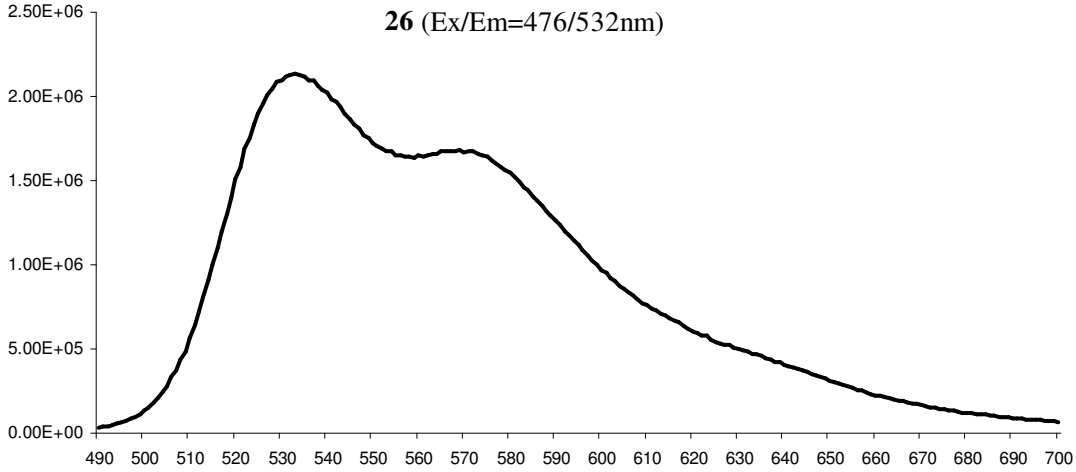

26 (Ex/Em=476/532nm)

(II) PATENT AND PUBLICATIONS

Edinburgh Research and Innovation

THE UNIVERSITY of EDINBURGH

A novel family of intracellular dyes for measurement of *in vitro* properties

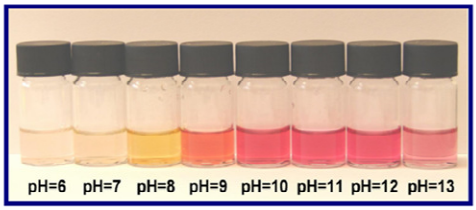

Anthofluorescein dye undergoes a pH-mediated colour change

The University of Edinburgh has created a new family of fluorescein-based dyes in the visible range. They provide end users with the ability to measure intracellular pH, viscosity and temperature.

Measuring the effect of external parameters (eg. drugs) or internal cellular changes (eg. aberrant gene expression) on multiple intracellular properties is of interest to most biologists. This new family of fluorescein analogues have improved stability and can measure multiple intracellular properties. Anthofluorescein has a highly sensitive absorption and fluorescence emission in the pH range from 7 to 10 (*see figure*) and is proven to have the necessary sensitivity required for optical measurements of intracellular pH inside living cells.

The versatility of the analogues allows the properties of the compounds to be optimised for measurement of other intracellular properties such as temperature and viscosity as well as specific targeting of intracellular organelles. A mitochondrial tag derivative has confirmed that the dyes can be used to successfully label intracellular organelles of choice.

A diacetylated derivative of Anthofluorescein has been demonstrated to be cell permeable and to successfully label living cells. This derivative has applications for cell phenotyping (cancer cells are more acidic), pathology and confocal imaging.

The compound family could be extended to cover the entire spectrum of visible range dyes from yellow to far-red and to allow rapid labelling of bio-molecules (antibodies, proteins, DNA, etc).

Publication Details

Unciti-Broceta *et al* "A fluorescein-derived anthocyanidin-inspired pH sensor". Tetrahedron Letters (2009) 50: 3713–3715

Han and Burgess "Fluorescent indicators for intracellular pH" Chemical Reviews (2009) doi: 10.1021/cr900249z

Key Benefits

- Visible pH dependent colour change in physiological range (pH7-10)
- In cells, dyes have low extracellular background, with excellent signal to noise ratio
- Uniquely multifunctional probes also capable of measuring temperature and viscosity and specific organelle tagging
- Simple synthetic method for the development of further multicolour fluorescence dyes from yellow to far-red

Applications

- Studies of intracellular biological systems by tagging specific organelles with a different dye
- Visual imaging of cellular and tissue samples with applications for phenotyping and pathology (eg. cancer / necrotic cells)
- Tools to measure intracellular properties such as pH, temperature and viscosity
- Bio-molecule labelling system with customised colour

Materials available

Three different compounds are currently available:

- Mitochondrial tag that stains the mitochondria that can be used in co-localisation studies
- pH sensor that stains cells
- A diacetylated derivative that is cell permeable and stains all intracellular organelles

Commercial Opportunity

The University of Edinburgh is looking to license the fluorophores to a company to manufacture and sell.

Further Information

For further information on this opportunity with the University of Edinburgh, please contact:

Dr Keith Finlayson
School of Chemistry
The University of Edinburgh
Joseph Black Building
King's Buildings
Edinburgh EH9 3JJ
Scotland, UK.

Telephone: +44 (0)131 650 4826
Email: **Keith.Finlayson@ed.ac.uk**

Tetrahedron Letters 50 (2009) 3713–3715

Contents lists available at ScienceDirect

Tetrahedron Letters

journal homepage: www.elsevier.com/locate/tetlet

A fluorescein-derived anthocyanidin-inspired pH sensor

Asier Unciti-Broceta, M. Rahimi Yusop †, Patricia R. Richardson †, Jeffrey G. A. Walton, Mark Bradley *

School of Chemistry, University of Edinburgh, West Mains Road, Edinburgh EH9 3JJ, UK

ARTICLE INFO

Article history:
Received 19 January 2009
Revised 26 March 2009
Accepted 31 March 2009
Available online 17 April 2009

ABSTRACT

A new multicolor pH-dependent fluorophore was synthesized via Pd-mediated cross-coupling chemistry of the mono-triflate of fluorescein with *p*-hydroxyphenylboronic acid. The novel indicator, named anthofluorescein, is highly sensitive to pH changes between 7 and 10 and displays a green to red fluorescence shift, making it a valuable candidate for biological studies.

The direct visualization of general biochemical events, specific molecular targets, or defined biochemical processes are indispensable for both in vitro[1–4] and, increasingly, in vivo applications.[3–6] These applications, because of the remarkable advances in imaging techniques, have begun to use a multitude of different fluorescent labels, probes, and sensors in multi-channel multiplex studies[7–9] which include the real-time analysis of cells and whole organisms.[10–13]

Due to the particular needs of each and every study, fluorescent dyes and probes with a myriad of defined optical, chemical, and biological properties are in high demand. Much effort has been focused on the development of optical pH chemosensors,[14–18] with specific attention paid to highly sensitive indicators within the physiological pH range.[19,20] In this area fluorescein and its derivatives are perhaps the most widely used fluorescent pH probes,[21,22] due in part to their excellent spectral and physical properties.

Anthocyanidins are the chromophores of a well-known family of natural dyes and are characterized by their broad spectral window, which is controlled by the various substituents on the benzopyrylium core and the pH.[23] Inspired by the general structures of the anthocyanidins **1**, the work described herein focuses on the modification of fluorescein **2** via substitution of one of its phenolic groups with *p*-hydroxyphenyl (see Fig. 1), a feature found in many anthocyanidins.[23] Due to its extended conjugation, compound **3** (which has been named anthofluorescein) was expected to display optical properties similar to both fluorescein and the anthocyanidins, but without the chemical instability of the latter.[23,24]

To assess the usefulness of the sensor prior to synthesis, the potential bathochromic shift in the excitation/emission wavelength of the different prototropic forms of derivative **3** was calculated via a series of configuration interaction singles, CIS/6-31g(d,p) calculations. These predicted that the 4″-oxo dianion form (D-I in the Supplementary data) would display a maximum absorbance at 530 nm and emission at 570 nm, the emission being red shifted by over 50 nm relative to fluorescein (see Supplementary data). In contrast, the 3′-oxo dianion form (D-II in the Supplementary data) should keep the original spectroscopic properties of fluorescein, with absorption maximum at 480 nm and emission maximum at 513 nm. These dianionic forms were predicted to have significant oscillator strengths. Due to the different pK_a values of the two phenolic OH groups, we envisaged that we would observe a dual-color performance tuned by the pH of the solution.

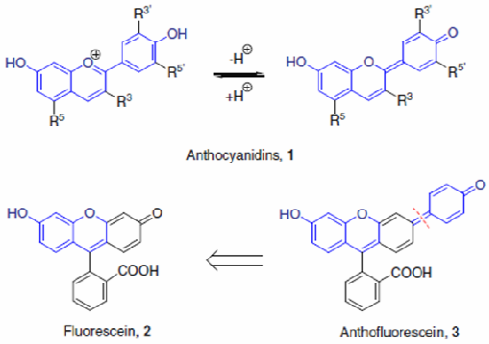

Figure 1. Structures of anthocyanidins, fluorescein (quinoid form), and anthofluorescein (quinoid form). Similarities in the structures are highlighted in blue.

Compound **3** was synthesized via sequential microwave-assisted mono-triflation of fluorescein **2** using one equivalent of *N*-phenylbis(trifluoromethanesulfonimide)[25] (a mild triflation reagent) followed by Suzuki aryl palladium-catalyzed cross-coupling of **4** with *p*-hydroxyphenylboronic acid (see Scheme 1) to give rise to anthofluorescein **3**. Heterogeneous catalysis using polystyrene resin captured palladium was successful but lower yields were obtained in this case (41%).[26]

* Corresponding author. Tel.: +44 131 650 4820; fax: +44 131 777 0334.
E-mail address: mark.bradley@ed.ac.uk (Mark Bradley).
† These authors contributed equally to this work.

0040-4039/$ - see front matter © 2009 Elsevier Ltd. All rights reserved.
doi:10.1016/j.tetlet.2009.03.223

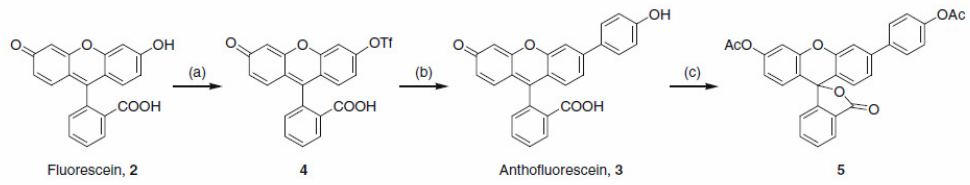

Scheme 1. Reagents and conditions: (a) $PhN(Tf)_2$, K_2CO_3, DMF, μω 80 °C, 20 min, 61%; (b) *p*-hydroxyphenylboronic acid, $Pd(OAc)_2$, K_2CO_3, PPh_3, H_2O:dioxane (1:9), μω 120 °C, 30 min, 78%; (c) Ac_2O:Pyr (1:1), 16 h, 87%.

A study of the absorptivity and the fluorescent properties of the novel dye confirmed that the optical properties of anthofluorescein were quite different from those of fluorescein, with both the absorption and emission spectra highly influenced by pH (as is also observed for the anthocyanidins). Spectrophotometric analysis of anthofluorescein solutions (50 μM) at distinct pH values (Fig. 2) showed that absorbance increased with pH, with the largest impact being observed between pH 7 and 10 (see Fig. 2 for the apparent colors of the solution), with a maximum absorptivity at pH 11 ($\varepsilon = 25{,}000\ M^{-1}\ cm^{-1}$). Absorptivity greatly decayed at pH 13, indicating a large change in the prototropic composition of the solution.

We attribute the changes seen in the fluorescence emission spectra between pH 7 and pH 13 (see Fig. 3) as being predominantly due to the prototropic equilibrium existing between the two dianionic forms of the molecule (for a more detailed explanation see Supplementary data). The experimental quantum yield[27] of the dye at pH 8, where maximal emission was observed, was very low (0.02), which in practice would limit applicability for cell assays. However, further analysis indicated that the quantum yield was highly influenced by the viscosity of the solution, with the quantum yield rising to 0.3 at pH 8 in 20% glycerol, presumably due to a decrease in the rate of internal conversion mediated by the *p*-hydroxyphenyl group torsional motion, similar to that ascribed to the diethylamino torsional motion in Rhodamine B.[28] It would be expected that the changes in emission intensity and quantum yield would be mirrored by changes in fluorescence lifetime and, as such, the molecule could find application as a, potentially, very sensitive probe of local temperature and viscosity in fluorescence lifetime imaging microscopy.

A non-fluorescent derivative of anthofluorescein **3**, diacetylated derivative **5**, was synthesized (see Scheme 1) in order to enhance the cellular penetrability of anthofluorescein and to reduce extracellular background. Compound **5** was incubated with HeLa cells for 2 h and then imaged using a 488/20 excitation filter (in the absence of an emission filter). As expected, intracellular deacetylation led to the formation of anthofluorescein **3**, which was identified by fluorescently yellow cells (Fig. 4), highlighting the viability of the cells. Due to the higher viscosity of the cell cytoplasm (expected to be more akin to glycerol than water)[29] the anthofluorescein dye was strongly emissive within the cells, confirming the previous viscosity observations.

In conclusion a new pH-sensitive dye synthesized from fluorescein using a straightforward microwave-assisted two-step proce-

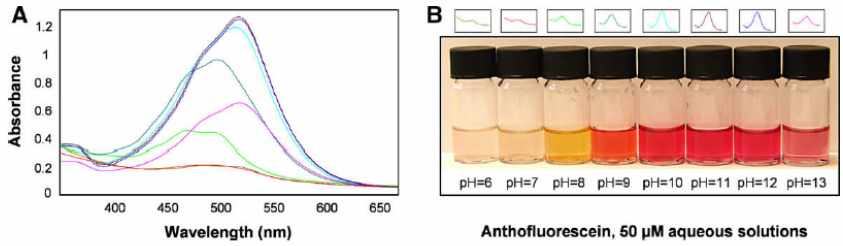

Figure 2. (A) Absorption spectra of 50 μM solutions of anthofluorescein **3** at pH 6–13. (B) Images of the dye solutions at various pH values.

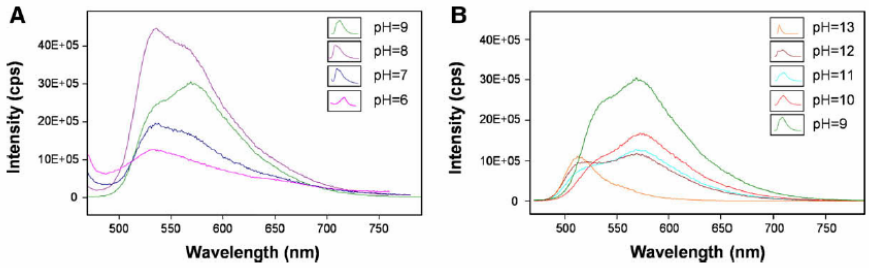

Figure 3. Emission spectra of anthofluorescein **3**, with excitation at 450 nm: (A) pH 6–9 and (B) pH 9–13.

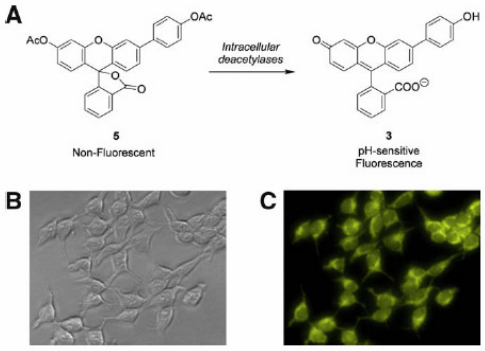

Figure 4. (A) Intracellular deacetylation of compound **5** to give anthofluorescein **3**. HeLa cells were incubated for 2 h with a 25 μM solution of diacetylated anthofluorescein **5**. (B) Brightfield. (C) Fluorescent image with 488 nm excitation and no emission filter.

dure consisting of mono-triflation and subsequent Suzuki aryl cross-coupling with *p*-hydroxyphenylboronic acid has been developed. The new dye, named anthofluorescein, was characterized by a highly sensitive absorption and fluorescence emission particularly in the pH range from 7 to 10. A diacetylated derivative of anthofluorescein successfully labeled living HeLa cells, which indicates that it might become a valuable tool for cell labeling and viability studies and, with the assistance of advanced microscopy techniques, for uses such as a ratiometric reporter of pH, viscosity, and/or temperature. Finally, the synthetic method provides a facile route to the development of new multicolor fluorescence dyes with red-shifted absorption and emission, which are in high demand as fluorescence probes.

Acknowledgments

We thank the MRC, the Government of Malaysia (MRY) and edikt2 (PRR) for funding. Computational resources were provided by the EaStCHEM research computing facility.

Supplementary data

Supplementary data associated with this article can be found, in the online version, at doi:10.1016/j.tetlet.2009.03.223.

References and notes

1. Johnsson, N.; Johnsson, K. *ACS Chem. Biol.* **2007**, *2*, 31–38.
2. Unciti-Broceta, A.; Díaz-Mochón, J.; Mizomoto, H.; Bradley, M. *J. Comb. Chem.* **2008**, *10*, 179–184.
3. Domaille, D. W.; Que, E. L.; Chang, C. J. *Nat. Chem. Biol.* **2008**, *4*, 168–175.
4. Giepmans, B. N.; Adams, S. R.; Ellisman, M. H.; Tsien, R. Y. *Science* **2006**, *312*, 217–224.
5. Weissleder, R.; Ntziachristos, V. *Nat. Med.* **2003**, *9*, 123–128.
6. Zhang, J.; Campbell, R. E.; Ting, A. Y.; Tsien, R. Y. *Nat. Rev. Mol. Cell Biol.* **2002**, *3*, 906–918.
7. Díaz-Mochón, J. J.; Tourniaire, G.; Bradley, M. *Chem. Soc. Rev.* **2007**, *36*, 449–457.
8. Pemagallo, S.; Unciti-Broceta, A.; Díaz-Mochón, J. J.; Bradley, M. *Biomed. Mater.* **2008**, *3*, Art. No. 034112 (6pp).
9. Unciti-Broceta, A.; Diezmann, F.; Ou-Yang, C. Y.; Fara, M. A.; Bradley, M. *Bioorg. Med. Chem.* **2009**, *17*, 959–966.
10. Lavis, L. D.; Raines, R. T. *ACS Chem. Biol.* **2008**, *3*, 142–155.
11. Hell, S. W. *Nat. Biotechnol.* **2003**, *11*, 1347–1355.
12. Weissleder, R. *Science* **2006**, *312*, 1168–1171.
13. Alexander, L.; Dhaliwal, K.; Simpson, J.; Bradley, M. *Chem. Commun.* **2008**, 3507–3509.
14. Charier, S.; Ruel, O.; Baudin, J.-B.; Alcor, D.; Allemand, J.-F.; Meglio, A.; Jullien, L. *Angew. Chem., Int. Ed.* **2004**, *43*, 4785–4788.
15. Wong, L. S.; Birembaut, F.; Bocklesby, W. S.; Frey, J. G.; Bradley, M. *Anal. Chem.* **2005**, *77*, 2247–2251.
16. Cho, J. K.; Wong, L. S.; Dean, T. W.; Ichihara, O.; Muller, C.; Bradley, M. *Chem. Commun.* **2004**, 1470–1471.
17. Cho, J. K.; White, P. D.; Klute, W.; Dean, T. W.; Bradley, M. *J. Comb. Chem.* **2003**, *5*, 632–636.
18. Wong, L. S.; Brocklesby, W. S.; Bradley, M. *Sens. Actuators B-Chem.* **2005**, *107*, 957–962.
19. Bradley, M.; Alexander, L.; Duncan, K.; Chennaoui, M.; Jones, A. C.; Sanchez-Martin, R. M. *Bioorg. Med. Chem. Lett.* **2008**, *18*, 313–317.
20. Vasylevska, A. S.; Karasyov, A. A.; Borisov, S. M.; Krause, C. *Anal. Bioanal. Chem.* **2007**, *387*, 2131–2141.
21. Lavis, L. D.; Rutkoski, T. J.; Raines, R. T. *Anal. Chem.* **2007**, *79*, 6775–6782.
22. Smith, J. P.; Drewes, L. R. *J. Biol. Chem.* **2006**, *281*, 2053–2060.
23. Castañeda-Ovando, A.; Pacheco-Hernández, M. L.; Páez-Hernández, M. E.; Rodríguez, J. A.; Galán-Vidal, C. A. *Food Chem.* **2009**, *113*, 859–871.
24. Jurd, L.; Geissman, T. A. *J. Org. Chem.* **1963**, *28*, 2394–2397.
25. Miller, E. W.; Albers, A. E.; Pralle, A.; Isacoff, E. Y.; Chang, C. J. *J. Am. Chem. Soc.* **2005**, *127*, 16652–16659.
26. Cho, J. K.; Najman, R.; Dean, T. W.; Ichihara, O.; Muller, C.; Bradley, M. *J. Am. Chem. Soc.* **2006**, *128*, 6276–6277.
27. Williams, A. T. R.; Winfield, S. A.; Miller, J. N. *Analyst* **1983**, *108*, 1067.
28. Lopez Arbeloa, I.; Rohatgi-Mukherjee, K. K. *Chem. Phys. Lett.* **1986**, *129*, 607–614.
29. Daniels, B. R.; Masi, B. C.; Wirtz, D. *Biophys. J.* **2006**, *90*, 4712–4719.

nature chemistry

ARTICLES

PUBLISHED ONLINE: 6 FEBRUARY 2011 | DOI: 10.1038/NCHEM.981

Palladium-mediated intracellular chemistry

Rahimi M. Yusop[1,2], Asier Unciti-Broceta[1†], Emma M. V. Johansson[1], Rosario M. Sánchez-Martín[1] and Mark Bradley[1]*

Many important intracellular biochemical reactions are modulated by transition metals, typically in the form of metalloproteins. The ability to carry out selective transformations inside a cell would allow researchers to manipulate or interrogate innumerable biological processes. Here, we show that palladium nanoparticles trapped within polystyrene microspheres can enter cells and mediate a variety of Pd^0-catalysed reactions, such as allylcarbamate cleavage and Suzuki–Miyaura cross-coupling. The work provides the basis for the customization of heterogeneous unnatural catalysts as tools to carry out artificial chemistries within cells. Such *in cellulo* synthesis has potential for a plethora of applications ranging from cellular labelling to synthesis of modulators or inhibitors of cell function.

Cellular biochemistry is governed by a wide range of enzymatic entities, with the complex cellular machinery engineered to perform a myriad of diverse chemical reactions[1,2]. Many of these reactions are catalysed by transition metals, typically in the form of metalloproteins[3–5], which modulate a wide variety of transformations, from highly selective oxidations to the efficient formation, lysis or isomerization of multifarious chemical bonds[1,2]. In this context, many groups have taken advantage of the properties of these proteins with the generation of bio-inspired devices, based on coordination complexes aimed at mimicking biological function[6–11]. Bioorganometallic chemistry has therefore evolved as a fascinating field, full of possibilities and creative applications, ranging from highly selective chemistries to the manipulation and *in situ* interrogation of innumerable biological processes[12–16]. A fluorogenic chemosensor for the *in vivo* detection of Pd^{2+} species has recently been described[17], but the use of Pd^0 catalysts to synthesize exogenous materials in cells has never been explored.

Of significant relevance is the work of Meggers, who described a water-soluble ruthenium complex that rapidly enters cells and performs an allylcarbamate cleavage from *bis*-*N*,*N*′-allyloxycarbonyl rhodamine 110 (**1**) (ref. 18), and proving to be non-toxic to cells during the short duration of the experiment. We reasoned that the use of a purely heterogeneous catalyst in the form of an 'artificial organelle' would allow the long-term cytoplasmic presence of metals with minimal leakage and toxicity (many transition metals, including palladium[19], trigger cell death[20]). This would then allow the exploration of challenging metal-catalysed reactions inside a cell.

Results and discussion

Encouraged by the vast possibilities and applications of palladium chemistry[21], the preparation of a bio-friendly internalizable Pd^0-based heterogeneous catalyst was undertaken. This was achieved through the application of two technologies. First, a microsphere (500 nm) mediated delivery system was used that had previously been applied in both cellular labelling and intracellular delivery of biomaterials, showing remarkable cellular biocompatibility and exonuclear localization[22–26]. The second technology involved the application of palladium nanoparticles entrapped within crosslinked resin beads, which have been shown to operate catalytically in a truly heterogeneous manner[27].

This innovative catalyst-loaded delivery system was synthesized as shown in Fig. 1. Amino-functionalized polystyrene microspheres (500 nm) were synthesized by dispersion polymerization from styrene-based monomers as previously described[22] and subsequently mixed with $Pd(OAc)_2$. The electron-rich microsphere network binds Pd^{2+} by coordination to the free amino groups and aromatic rings, while reduction of Pd^{2+} to Pd^0 leads to aggregation and the generation of Pd^0 nanoparticles (Fig. 1). Extensive crosslinking of the available amino groups on the particles means that the stable Pd^0 nanoparticles are permanently entangled and trapped within the microsphere. Finally, Pd^0 microspheres were fluorescently labelled to allow intracellular tracking of the catalysts (Supplementary Sections S2 and S3). Two different dyes were used for analytical reasons: Cy5.5-labelled Pd^0 microspheres were used for flow cytometry analyses and Texas Red-labelled Pd^0 microspheres were used for the confocal studies.

Analysis of the resulting microspheres by transmission electron microscopy (TEM) showed palladium nanoparticles evenly distributed on the microsphere (Fig. 1b,c), with the presence of the Pd^0 confirmed by powder X-ray diffraction (XRD) analysis (Fig. 1d). To demonstrate the catalytic activity of the microsphere-captured Pd^0 nanoparticles, the *bis*-*N*,*N*′-allyloxycarbonyl rhodamine 110 (**1**) used by Meggers[18] was incubated with Pd^0 microspheres under different conditions (Supplementary Tables S3–S5). The Pd^0 catalyst mediated the effective deprotection of the allyloxycarbonyl group, resulting in the liberation of the strongly fluorescent rhodamine 110 (**2**). Interestingly, the catalytic activity of the Pd^0 microspheres was clearly enhanced by the presence of glutathione (5 mM), with turnover numbers up to 30 in the presence of cell extract and glutathione.

Although the microspheres have shown remarkable cellular compatibility and have been widely used as a highly efficient cellular delivery vehicle for a variety of materials[22–26], the presence of Pd^0 on the beads required an investigation of their biological compatibility. Pd^0 microspheres were therefore incubated with HeLa cells and uptake and toxicity evaluated. After 24 h, the intracellular presence of fluorescently labelled Pd^0 microspheres was determined by flow cytometry, demonstrating that more than 75% of cells had taken up one or more of the Pd^0 microspheres, uptake that was further corroborated by confocal imaging (Supplementary Figs S6 and

[1]School of Chemistry, University of Edinburgh, West Mains Road, Edinburgh EH9 3JJ, UK, [2]School of Chemical Sciences and Food Technology, Faculty of Science and Technology, Universiti Kebangsaan Malaysia, 43600 UKM, Bangi, Selangor Darul Ehsan, Malaysia, †Present address: Edinburgh Cancer Research UK Centre, Institute of Genetics and Molecular Medicine, University of Edinburgh, Crewe Road, Edinburgh EH4 2XR, UK. *e-mail: mark.bradley@ed.ac.uk

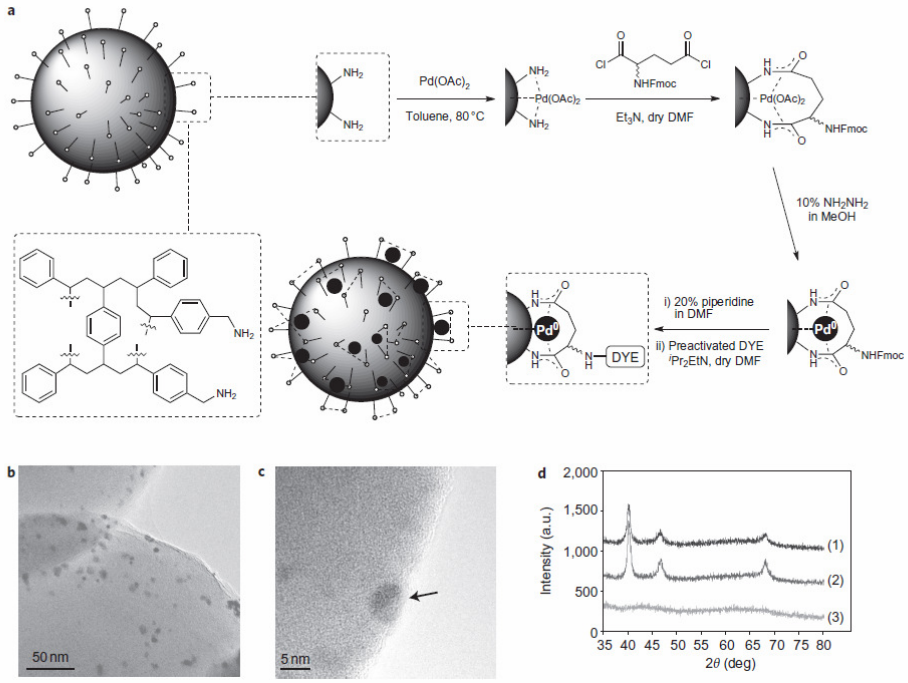

Figure 1 | Synthesis and characterization of Pd^0 microspheres. a, Synthesis of fluorescently labelled Pd^0 microspheres. Amino-functionalized polystyrene microspheres[22] were treated with $Pd(OAc)_2$ for 3 h to ensure uptake and interaction with the beads. The coordinated Pd^{2+} was subsequently trapped by extensive crosslinking with the *bis* acid chloride of racemic Fmoc-glutamic acid (generated *in situ*). Hydrazine in methanol was used to reduce Pd^{2+} to Pd^0. Labelling of the Pd^0 microspheres was carried out by deprotection of the Fmoc group and subsequent treatment with an activated dye under basic conditions. **b**,**c**, TEM of Pd^0 nanoparticles within microspheres at two different magnifications: image of Pd^0 nanoparticles physically captured and entrapped on the microspheres (**b**); image of a single microsphere-captured Pd^0 nanoparticle (arrow, **c**). Average diameter of nanoparticles: 5 ± 2.5 nm. **d**, Powder XRD patterns of (1) Pd^0 microspheres, (2) commercial Pd^0 powder, and (3) naked microspheres.

S7). Cytotoxicity associated with the Pd^0 microspheres, determined using both (3-(4,5-dimethylthiazol-2-yl)-2,5-diphenyltetrazolium bromide (MTT) and propidium iodide assays, indicated low levels of necrosis (<4%) and good cell viability (>91%) after 48 h of contact with the Pd^0 microspheres (Supplementary Figs S8 and S9, Tables S1 and S2).

Pd^0-mediated allylcarbamate cleavage within cells. The catalytic activity of the Pd^0 microspheres was investigated within living cells, using HeLa cells as a model system. Cells were loaded with fluorescently labelled Pd^0 microspheres, washed to eliminate extracellular Pd^0 microspheres, then fresh media containing 30 μM *bis*-*N*,*N*′-allyloxycarbonyl rhodamine 110 (**1**) was added. The lipophilic nature of non-fluorescent compound **1** allows its cellular internalization, whereas upon allylcarbamate cleavage most of the resulting fluorescent compound **2** is retained within the cell (Fig. 2a). As observed in Fig. 2, flow cytometry analysis of an untreated cell control (Fig. 2b), a control treated with only the Cy5.5-labelled Pd^0 microspheres (Fig. 2c) or incubated just with reagent **1** (Fig. 2d) showed no fluorescence under the FITC emission filter (530/35 nm). In contrast, Cy5.5-labelled Pd^0 microsphere-loaded HeLa cells incubated with reagent **1** showed fluorescence emission under both Cy5.5 (indicating the presence of the Pd^0 microspheres) and FITC-like bandpass filters (associated with the deprotection of dye **2**) (Fig. 2e), showing Pd^0-mediated catalysis inside a cell for the first time. As shown in Fig. 2f, confocal microscopy verified the simultaneous presence of Texas Red-labelled Pd^0 microspheres and intracellular compound **2**.

To expand the scope of the *in cellulo* deprotection method, a preliminary cytotoxicity study based on an allylcarbamate-protected derivative of amsacrine (a commercially available antineoplastic agent[28]) was performed (Supplementary Fig. S22). Alloc protection led to a measurable reduction in the cytotoxic properties of this chemically modified derivative relative to free amsacrine, a fact that was used to investigate if amsacrine could be released *in situ* by the catalytic activity of cell-containing Pd^0 microspheres. Cells incubated with alloc-protected amsacrine showed up to a sevenfold increment of cytotoxicity in cell cultures preloaded with Pd^0 microspheres.

Making C–C bonds within cells. The Suzuki–Miyaura cross-coupling of arylboronates or esters with aryl halides (or triflates) in the presence of Pd^0 permits ready access to a spectacular range of biaryls[29,30]. To explore the intracellular formation of a carbon–carbon cross-coupled product, an unambiguous fluorescence-detectable cell-based experiment was designed, based on the palladium-mediated synthesis of a fluorescent dye (anthofluorescein[31]) via an aryl–aryl cross-coupling reaction (Fig. 3a). The lipophilic non-fluorescent mono-triflate **3**, containing a fluoran-based pro-fluorophore, and the alkylaminophenylboronate **4** were therefore synthesized. Cross-coupling of these two components would restore the π-electron

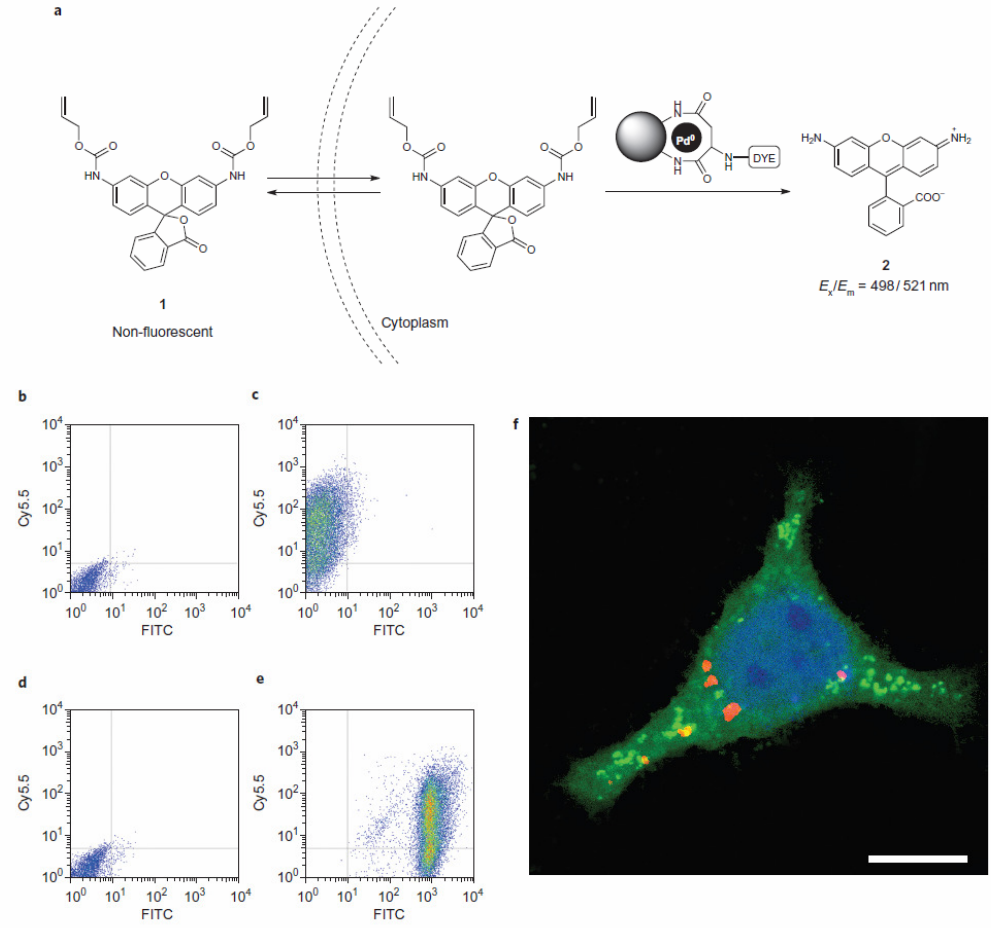

Figure 2 | Pd^0-mediated allylcarbamate cleavage within HeLa cells. a, Pd^0-catalysed intracellular deprotection of reagent **1** generates fluorescent compound **2**. **b**–**e**, Flow cytometry analysis of HeLa cells showing intracellular Pd^0 catalysis of allylcarbamate cleavage. The *y*-axis represents Cy5.5 fluorescence intensity due to the Cy5.5-labelled Pd^0 microspheres (bandpass emission filter, 780/60 nm) and the *x*-axis the FITC-like intensity of the cell due to compound **2** (bandpass emission filter, 530/30 nm). **b**, Untreated cell control (no fluorescence emission). **c**, Cells after 24 h incubation with Cy5.5-labelled Pd^0 microspheres (positive fluorescence emission from Cy5.5 channel). **d**, Cells after 24 h incubation with reagent **1** (no fluorescence emission). **e**, Cy5.5-labelled Pd^0 microsphere-loaded cells after 24 h incubation with reagent **1**, showing fluorescence emission under both Cy5.5 (indicating the presence of the Pd^0 microspheres) and FITC-like bandpass filters (confirming the synthesis of deprotected dye **2**). **f**, Merged confocal image of a single HeLa cell (fixed with paraformaldehyde) showing a Hoechst 33342-stained nucleus (blue) with Texas Red-labelled Pd^0 microspheres (red) and deprotected compound **2** (green). Scale bar, 10 μm.

conjugation of the fluoran polycycle **3** by opening of the lactone, resulting in molecular fluorescence while at the same time localizing the product **5** to the mitochondria due to the presence of a triphenylphosphonium moiety (lipophilic cations direct accumulation of several hundredfold within mitochondria[32]).

Suzuki–Miyaura dye *in cellulo* synthesis was initiated by the incubation of fluorescently labelled Pd^0 microspheres with HeLa cells for 24 h, followed by intensive washing of the cells to eliminate extracellular Pd^0 microspheres before the addition of the two reagents **3** (20 μM) and **4** (20 μM). After 48 h incubation, cellular fluorescence was investigated by confocal microscopy with mitochondria labelled with a far-red dye (MitoTracker Deep Red, $E_x/E_m \approx 640/662$ nm). Fixed cells were labelled with Hoechst 33342 (nuclei stain), imaged by confocal microscopy and the images processed for three-dimensional analysis. As shown in Fig. 3b, confocal images showed co-localization of both Pd^0-synthesized dye and MitoTracker, demonstrating the unambiguous identification of the Suzuki–Miyaura product **5**, with *in cellulo* synthesis confirmed by flow cytometry analysis (Supplementary Fig. S15). Controls were carried out, both in solution and in cell experiments, to rule out the possibility of any fluorescence being the result of hydrolysed mono-triflate **3** (Supplementary Figs S15,

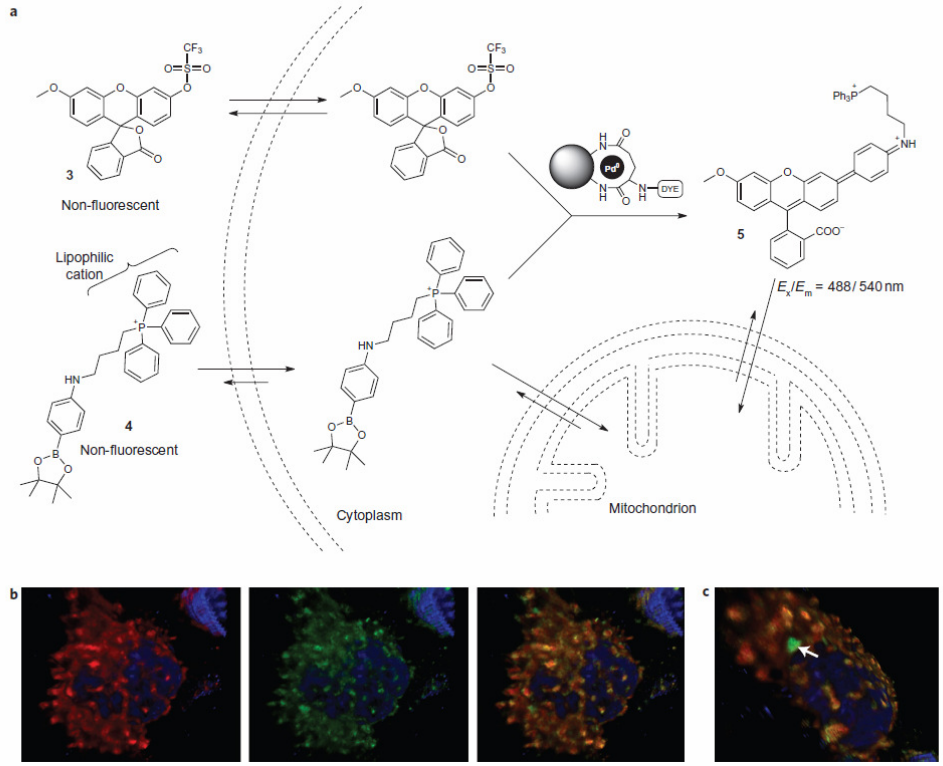

Figure 3 | Pd^0-mediated Suzuki–Miyaura cross-coupling within HeLa cells. a, Pd^0-catalysed intracellular cross-coupling of reagents **3** and **4** generates the mitochondria-localized fluorescent compound **5**. **b**,**c**, HeLa cells were loaded with Pd^0 microspheres, washed to eliminate extracellular Pd^0 microspheres, and subsequently incubated for 48 h with reagents **3** and **4**. Cells were incubated for 30 min with MitoTracker Deep Red (mitochondrial stain), fixed with paraformaldehyde, incubated with Hoechst 33342 (nuclei stain) and imaged by confocal microscopy. Deconvolved confocal images (**b**) of a single cell showing co-localization of MitoTracker-labelled mitochondria and Suzuki–Miyaura product **5**. Left panel: cell nucleus (blue) and mitochondria (red). Centre panel: cell nucleus (blue) and *in cellulo* synthesized compound **5** (green). Right panel: merged image (orange indicates co-localization). Merged image (**c**) of the same cell observed from a different angle. White arrow indicates the presence of a Texas Red-labelled Pd^0 microsphere (not localized within the mitochondria), which was imaged using a 550/20 nm emission filter together with compound **5**.

S19 and S20, Table S5). Indeed, mono-triflate was remarkably robust, surviving unchanged in the presence of Pd^0 for over 48 h. Compound **5** was also extracted from the cells and its identity confirmed by high-performance liquid chromatography (HPLC) and mass spectrometry (MS) studies, confirming intracellular synthesis. Owing to the broad excitation/emission spectra of Texas Red, both the Suzuki–Miyaura product **5** and the Texas Red-labelled Pd^0 microspheres were imaged under the same fluorescent channel. The Pd^0 microspheres could be identified, because they did not co-localize with the mitochondria tracker dye or the nucleus stain, thus corroborating their cytoplasmatic location (Fig. 3c; Supplementary Figs S16 and S17). This experiment represents the first non-enzymatic aryl–aryl bond formation ever achieved within living cells.

In conclusion, the first Pd^0-based heterogeneous catalyst with the ability to cross cell membranes, stay harmlessly within the cytoplasm for days, and carry out artificial chemistry has been described. This engineered pseudo-organelle demonstrated intracellular catalytic activity towards exogenous materials, allowing chemistry never before achieved within cells to be performed, such as the Suzuki–Miyaura cross-coupling reaction. This investigation provides the basis for the customization of heterogeneous unnatural catalysts as tools for creative applications in chemical biology (such as *in situ* labelling of cellular structures), pharmacology (for example, *in cellulo* pro-drug activation of hydrophilic molecules with low cell penetrability for functional screening in cellular disease models) and, potentially, in medicine (for example, the systemic administration of a pro-drug with local activation via implant-captured catalysts).

Methods

Pd^0 microsphere synthesis. Aminomethyl polystyrene microspheres were prepared as previously described[22]. Microspheres (1 ml, aminomethyl polystyrene microsphere, 0.5 μm, 0.08 mmol g^{-1}, 4% solid content (SC)) were placed in a 1 ml eppendorf tube and the water removed after centrifugation at 13,000 r.p.m. for 5 min. The beads were subsequently washed with toluene (2 × 1 ml). A volume of 0.2 ml of a 0.4 mg ml^{-1} palladium acetate solution in toluene was added and heated to 80 °C and sonicated every 2 min (5×). Subsequently, the reaction mixture was shaken at room temperature for 2 h to give a light-brown coloured mixture. The bead mixture was washed with toluene (3 × 1 ml) to ensure excess of palladium acetate was removed. Cross-coupling reagent (10 mg, Fmoc-Glu(Cl)-Cl) was freshly

prepared and dissolved in 1 ml of dry dimethylformamide (DMF) together with triethylamine (11 µl, 0.08 mmol). Subsequently, 0.5 ml of this coupling solution was added to the beads and shaken for 1 h at room temperature to afford 100% crosslinked beads. The resulting microspheres were washed with methanol (3 × 0.5 ml) and water (3 × 0.5 ml). The Pd^0 microspheres were stored in water as a light-grey suspension. The Fmoc group was deprotected using 20% piperidine in DMF, and the Pd^0 microspheres were washed with DMF (3 × 1 ml), then treated with pre-activated dye (5 equiv. Cy5.5 or Texas Red, 0.5 mg ml^{-1} in DMF) and diisopropylethylamine (DIPEA) (10 equiv.). The resulting mixture was shaken for 24 h at room temperature. The fluorescently labelled Pd^0 microspheres were washed with MeOH (3 × 1 ml) and water (3 × 1 ml) and stored in water in the dark. Cy5.5-labelled Pd^0 microspheres were used for the flow cytometry analysis, and Texas Red-labelled Pd^0 microspheres were used for the confocal microscopy studies.

Pd^0-mediated allylcarbamate cleavage in HeLa cells. For flow cytometry analysis, HeLa cells were plated in Roswell Park Memorial Institute (RPMI) supplemented with serum and antibiotics (RPMI Complete Media (RPMI-CM)) in a 12-well plate with a density of 40,000 cells per well and the cells were grown for 24 h. Thereafter, 1.0 µl of Pd^0 microspheres per ml (Cy5.5 labelled for flow cytometry analysis and Texas Red labelled for confocal analysis) were added and incubated with the cells for 24 h. Excess Pd^0 microspheres were removed by washing with phosphate buffered saline (PBS) (3×). Protected Rhodamine 110 (**1**) was added (30 µM in RPMI-CM) and incubated with the cells at 37 °C and in 5% CO_2 for 24 h. After incubation, cells were washed twice with PBS, harvested with trypsin/ethylenediaminetetraacetic acid (EDTA), washed again with PBS and resuspended in 2% fetal calf serum (FCS) in PBS buffer. Cell fluorescence was analysed by flow cytometry using a FACS Aria flow cytometer (Becton Dickinson). A total of 10,000 events per sample were analysed. A 530/30 nm bandpass filter (FITC) was used for Rhodamine 110 (**2**) and 780/60 nm for Cy5.5 detection. For the confocal microscopy study, HeLa cells were cultured on sterilized circular glass slide cover slips (24 mm), which were coated with 0.01% polylysine in water for 5 min at room temperature. The cover slips were washed with PBS (3×) before use. The glass cover slips were placed in six-well plates with 90,000 cells per well and incubated overnight following the procedure described above. HeLa cells were then fixed with 4% formaldehyde in PBS for 30 min at room temperature. Nuclei were stained by incubation with a 10 µg ml^{-1} solution of Hoeschst 33342 in media for 5 min at 37 °C before analysis. Microscope settings: excitation laser lines at 488, 543 and 595 nm, with emission filters of 385–470 nm for Hoechst 33342, 505–530 nm for Rhodamine 110 and 595–615 nm for Texas Red.

Pd^0-mediated Suzuki cross-coupling in HeLa cells. HeLa cells were plated on sterilized glass cover slips (24 mm) placed in a six-well plate (90,000 cells per well) and incubated at 37 °C for 24 h. Media were removed and replaced with fresh media containing Texas Red-labelled Pd^0 microspheres (2 µl, 1.52×10^{10} beads per well) and incubated at 37 °C for 24 h. Excess of extracellular Pd^0 microspheres was removed by washing with PBS (3×). Compounds **3** and **4** (20 mM in dimethyl sulfoxide (DMSO)) were diluted in fresh media to give a final concentration of 20 µM and incubated at 37 °C and in 5% CO_2 for 48 h. Subsequently, mitochondria were stained by 30 min incubation with 50 nM of MitoTracker Deep Red in RPMI-CM at 37 °C. HeLa cells were then fixed with 4% formaldehyde in PBS (30 min at room temperature), and nuclei were stained by the addition of a 10 µg ml^{-1} solution of Hoechst 33342 (5 min). Microscope settings: excitation laser lines at 488 nm, 595 nm and 633 nm, with emission filters of 385–470 nm for Hoechst 33342, 540–560 nm for compound 5 and 650–670 nm for MitoTracker Deep Red.

Received 23 September 2010; accepted 16 December 2010; published online 6 February 2011

References

1. Silverman, R. E. *Organic Chemistry of Enzyme-Catalyzed Reactions* 2nd edn (Academic Press, 2002).
2. Bugg, T. *Introduction to Enzyme and Coenzyme Chemistry* 2nd edn (Wiley-Blackwell, 2004).
3. Lippard, S. J. & Berg, J. M. *Principles of Bioinorganic Chemistry* (University Science Books, 1994).
4. Andreini, C., Bertini, I., Cavallaro, G., Holliday, G. L. & Thornton, J. M. Metal ions in biological catalysis: from enzyme databases to general principles. *J. Biol. Inorg. Chem.* **13**, 1205–1218 (2008).
5. Waldron, K. J., Rutherford, J. C., Ford, D. & Robinson, N. J. Metalloproteins and metal sensing. *Nature* **460**, 823–830 (2009).
6. Costas, M., Mehn, M. P., Jensen, M. P. & Que, L Jr. Dioxygen activation at mononuclear nonheme iron active sites: enzymes, models, and intermediates. *Chem. Rev.* **104**, 939–986 (2004).
7. Tshuva, E. Y. & Lippard, S. J. Synthetic models for non-heme carboxylate-bridged diiron metalloproteins: strategies and tactics. *Chem. Rev.* **104**, 987–1012 (2004).
8. Lippard, S. J. The inorganic side of chemical biology. *Nat. Chem. Biol.* **2**, 504–507 (2006).
9. Tolman, W. B. & Spencer, D. J. E. New advances in ligand design for synthetic modeling of metalloprotein active sites. *Curr. Opin. Chem. Biol.* **5**, 188–195 (2001).
10. Xing, G. & DeRose, V. J. Designing metal–peptide models for protein structure and function. *Curr. Opin. Chem. Biol.* **5**, 196–200 (2001).
11. Baltzer, L. & Nilsson, J. Emerging principles of *de novo* catalyst design. *Curr. Opin. Biotech.* **12**, 355–360 (2001).
12. Lu, Y. Biosynthetic inorganic chemistry. *Angew. Chem. Int. Ed.* **45**, 5588–5601 (2006).
13. Haas, K. L. & Franz, K. J. Application of metal coordination chemistry to explore and manipulate cell biology. *Chem. Rev.* **109**, 4921–4960 (2009).
14. Domaille, D. W., Que, E. L. & Chang, C. J. Synthetic fluorescent sensors for studying the cell biology of metals. *Nat. Chem. Biol.* **4**, 168–175 (2008).
15. McRae, R., Bagchi, P., Sumalekshmy, S. & Fahrni, C. J. *In situ* imaging of metals in cells and tissues. *Chem. Rev.* **109**, 4780–4827 (2009).
16. Liang, G., Ren, H. & Rao, J. A biocompatible condensation reaction for controlled assembly of nanostructures in living cells. *Nature Chem.* **2**, 54–60 (2010).
17. Santra, M., Ko, S.-K., Shin, I. & Ahn, K. H. Fluorescent detection of palladium species with an *O*-propargylated fluorescein. *Chem. Commun.* **46**, 3964–3966 (2010).
18. Streu, C. & Meggers, E. Ruthenium-induced allylcarbamate cleavage in living cells. *Angew. Chem. Int. Ed.* **45**, 5645–5648 (2006).
19. Bruijnincx, P. C. A. & Sadler, P. J. New trends for metal complexes with anticancer activity. *Curr. Opin. Chem. Biol.* **12**, 197–206 (2008).
20. Abu-Surrah, A. S. & Kettunen, M. Platinum group antitumor chemistry: design and development of new anticancer drugs complementary to cisplatin. *Curr. Med. Chem.* **13**, 1337–1357 (2006).
21. Negishi, E. I. *Handbook of Organopalladium Chemistry for Organic Synthesis* (Wiley-Interscience, 2002).
22. Sanchez-Martin, R. M. *et al.* Bead-based cellular analysis, sorting and multiplexing. *ChemBioChem* **6**, 1341–1345 (2005).
23. Sanchez-Martin, R. M., Cuttle, M., Mittoo, S. & Bradley, M. Microsphere-based real-time calcium sensing. *Angew. Chem. Int. Ed.* **45**, 5472–5474 (2006).
24. Alexander, L. M., Sanchez-Martin, R. M. & Bradley M. Knocking (anti)-sense into cells: the microsphere approach to gene silencing. *Bioconjug. Chem.* **20**, 422–426 (2009).
25. Sanchez-Martin, R. M. *et al.* Microsphere-mediated protein delivery into cells. *ChemBioChem* **10**, 1453–1456 (2009).
26. Alexander, L. M. *et al.* Investigation of microsphere-mediated cellular delivery by chemical, microscopic and gene expression analysis. *Mol. BioSyst.* **6**, 399–409 (2010).
27. Cho, J. K. *et al.* Captured and cross-linked palladium nanoparticles. *J. Am. Chem. Soc.* **128**, 6276–6277 (2006).
28. Horstmann, M. A. *et al.* Amsacrine combined with etoposide and high-dose methylprednisolone as salvage therapy in acute lymphoblastic leukemia in children. *Haematologica* **95**, 1701–1703 (2005).
29. Miyaura, N. & Suzuki, A. Palladium-catalyzed cross-coupling reactions of organoboron compounds. *Chem. Rev.* **95**, 2457–2483 (1995).
30. Alonso, F., Beletskaya, I. P. & Yus, M. Non-conventional methodologies for transition-metal catalysed carbonecarbon coupling: a critical overview. Part 2: The Suzuki reaction. *Tetrahedron* **64**, 3047–3101 (2008).
31. Unciti-Broceta, A., Yusop, M. R., Richardson, P., Walton, J. & Bradley, M. A fluorescein-derived anthocyanidin-inspired pH sensor. *Tetrahedron Lett.* **50**, 3713–3715 (2009).
32. Smith, R. A., Porteous, C. M., Gane, A. M. & Murphy, M. P. Delivery of bioactive molecules to mitochondria *in vivo*. *Proc. Natl Acad. Sci. USA* **100**, 5407–5412 (2003).

Acknowledgements

This work was supported financially by the Government of Malaysia (R.M.Y.), the Swiss National Science Foundation (E.M.V.J.) and the Engineering and Physical Sciences Research Council. R.M.S.M. thanks the Royal Society for a Dorothy Hodgkin Fellowship. The authors thank D. Kelly for his help with the confocal microscopy studies.

Author contributions

R.M.Y. synthesized materials, performed cell-based experiments and analysed the data. A.U.B. designed and supervised the research, analysed the data and co-wrote the paper. E.M.V.J. synthesized materials, performed experiments and analysed the data. R.M.S.M. designed and supervised the experiments and analysed the data. M.B. came up with the concept, designed the research, analysed the data and co-wrote the paper.

Additional information

The authors declare no competing financial interests. Supplementary information and chemical compound information accompany this paper at www.nature.com/naturechemistry. Reprints and permission information is available online at http://npg.nature.com/reprintsandpermissions/. Correspondence and requests for materials should be addressed to M.B.

(III) SYNTHESISED COMPOUNDS

Name	Structure	Number
3´-(trifluoromethanesulfonyl) fluorescein	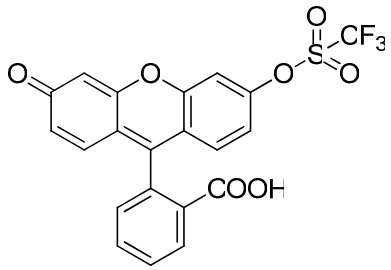	**2**
3´-hydroxy-6´-(p-hydroxyphenyl)fluoran	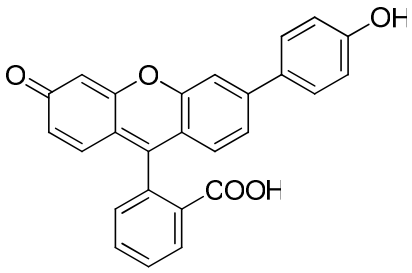	**3**
3´-acetyloxy-6´-(p-acetyloxyphenyl)fluoran	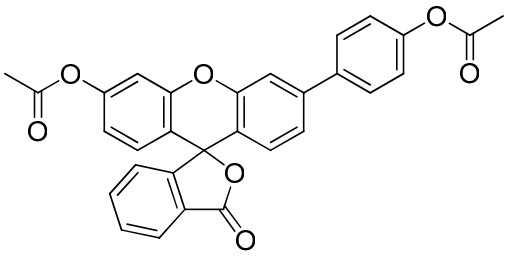	**4**
2-(3-(benzo[d][1,3]dioxol-5-yl)-6-oxo-6H-xanthen-9-yl)benzoate	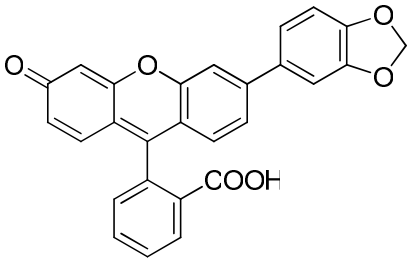	**5**
2-(3-(2,3-dihydrobenzo[b][1,4]dioxin-6-yl)-6-oxo-6H-xanthen-9-yl)benzoic acid	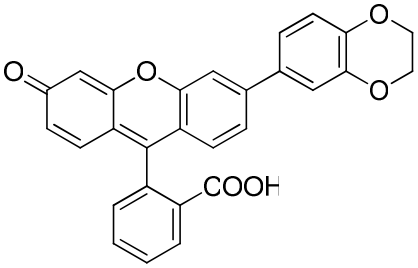	**6**

3 (3-(2,3-dihydrobenzofuran-6-yl)-6-oxo-6H-xanthen-9-yl)benzoic acid	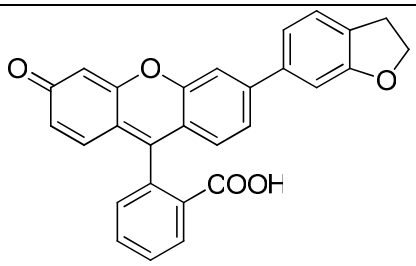	**7**
2-(3-(1H-indol-6-yl)-6-oxo-6H-xanthen-9-yl)benzoic acid	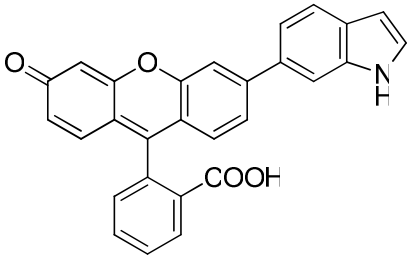	**8**
2-(3-(1-methyl-1H-indol-5-yl)-6-oxo-6H-xanthen-9-yl)benzoate	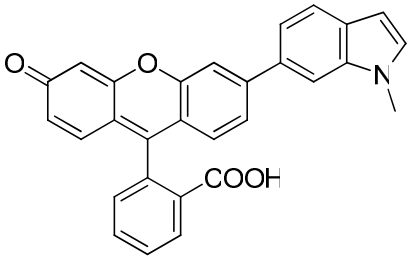	**9**
2-(3-(furan-2-yl)-6-oxo-6H-xanthen-9-yl)benzoic acid	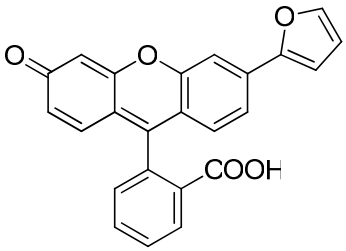	**10**
2-(3-oxo-6-(thiophen-2-yl)-3H-xanthen-9-yl)benzoic acid	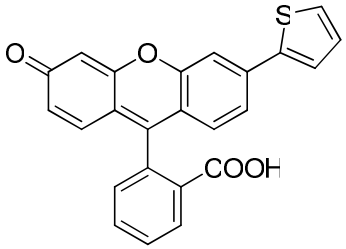	**11**
2-(3-(benzofuran-2-yl)-6-oxo-6H-xanthen-9-yl)benzoic acid	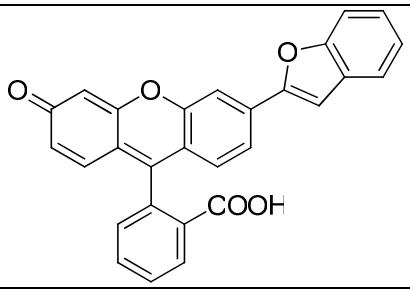	**12**

of 2-(3-(benzo[b]thiophen-2-yl)-6-oxo-6H-xanthen-9-yl)benzoic acid	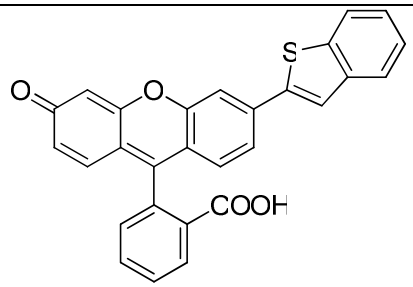	**13**
2-(3-oxo-6-phenyl-3H-xanthen-9-yl)benzoic acid	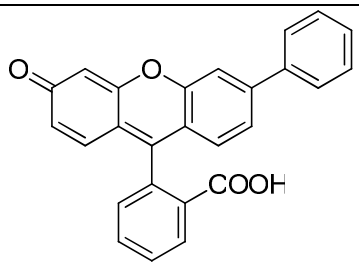	**14**
2-(3-oxo-6-(pyren-2-yl)-3H-xanthen-9-yl)benzoic acid	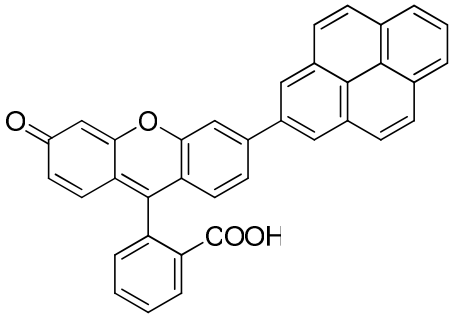	**15**
2-(3-(4-(dimethylamino)phenyl)-6-oxo-6H-xanthen-9-yl)benzoic acid	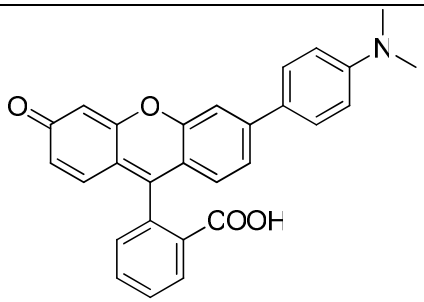	**16**
2-(3-(4-methoxyphenyl)-6-oxo-6H-xanthen-9-yl)benzoic acid	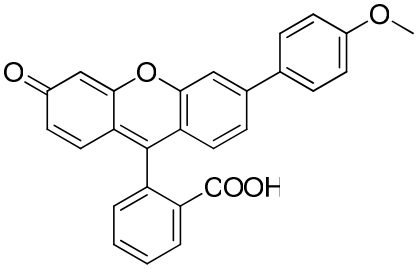	**17**
2-(3-(3-methoxyphenyl)-6-oxo-6H-xanthen-9-yl)benzoic acid	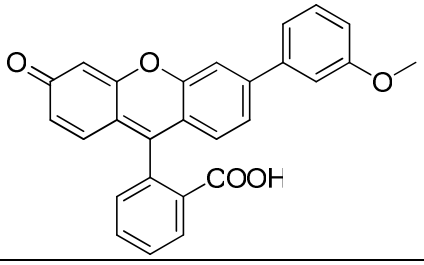	**18**

2-(3-(4-carboxyphenyl)-6-oxo-6H-xanthen-9-yl)benzoic acid	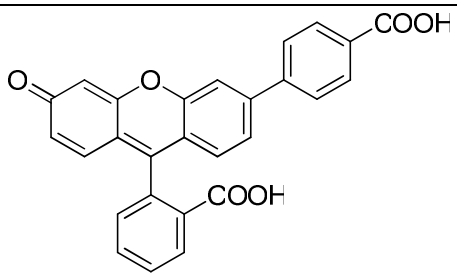	**19**
2-(3-(3-carboxyphenyl)-6-oxo-6H-xanthen-9-yl)benzoic acid	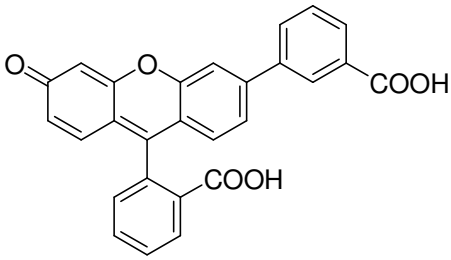	**20**
of 2-(3-oxo-6-(4-(trifluoromethyl)phenyl)-3H-xanthen-9-yl)benzoic acid	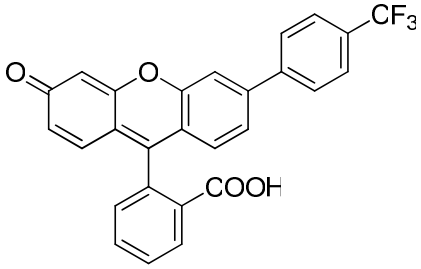	**21**
2-(3-oxo-6-p-tolyl-3H-xanthen-9-yl)benzoic acid	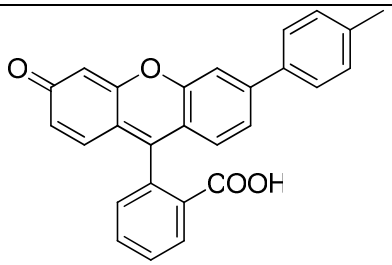	**22**
2-(3-(4-nitrophenyl)-6-oxo-6H-xanthen-9-yl)benzoic acid	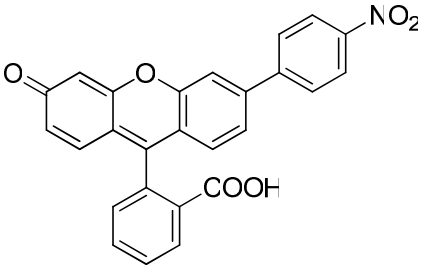	**23**
2-(3-(4-cyanophenyl)-6-oxo-6H-xanthen-9-yl)benzoic acid	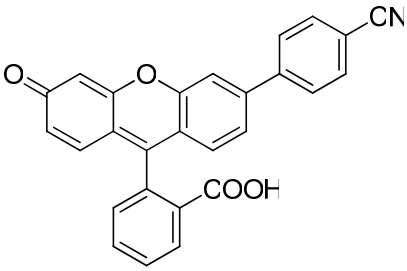	**24**

of 2-(3-(4-chlorophenyl)-6-oxo-6H-xanthen-9-yl)benzoic acid	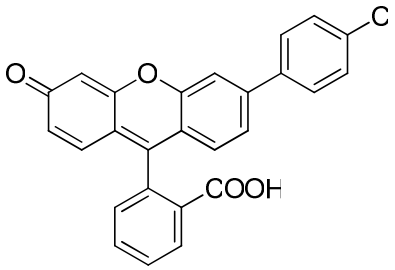	**25**
2-(3-(4-aminophenyl)-6-oxo-6H-xanthen-9-yl)benzoic acid	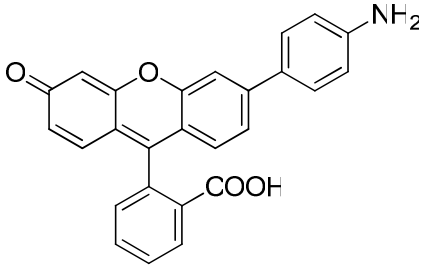	**26**
bis-allyloxycarbonyl-protected rhodamine 110	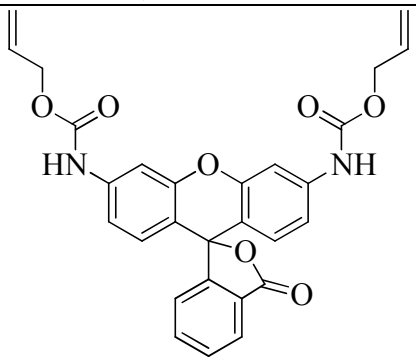	**28**
6'-methyl-3'-(trifluoromethanesulfonyl) fluorescein	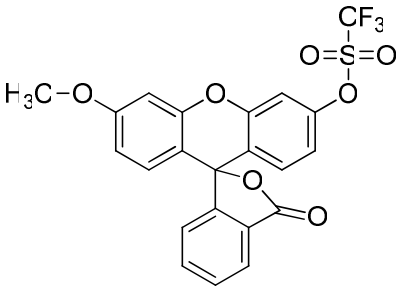	**29**
(4-[4'-(pinacolatoboron)phenylamino] butyl)triphenyl phosphonium bromide	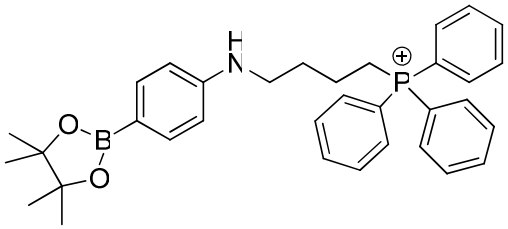	**32**

(4-[4'-(3''-methoxyfluoran-6''-yl)phenylamino]butyl) triphenyl phosphonium bromide	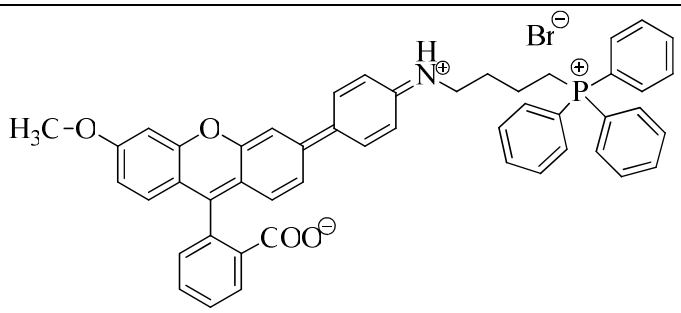	**33**
6'-methylfluorescein	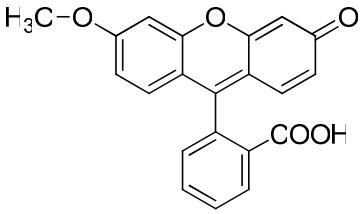	**34**